ANTI-VASCULAR ENDOTHELIAL GROWTH FACTOR THERAPY IN MOUSE MODELS OF VASCULAR DYSPLASIA AND CHRONIC COLITIS

by

DANIELA SIMONA ARDELEAN

A THESIS SUBMITTED IN CONFORMITY WITH
THE REQUIREMENTS FOR THE DEGREE OF
DOCTOR OF PHILOSOPHY

in

GRADUATE DEPARTMENT OF IMMUNOLOGY
UNIVERSITY OF TORONTO

Abstract

ANTI-VASCULAR ENDOTHELIAL GROWTH FACTOR THERAPY

IN MOUSE MODELS OF VASCULAR DYSPLASIA AND CHRONIC COLITIS

Daniela Simona Ardelean, Doctor of Philosophy,

Department of Immunology, University of Toronto, 2014

Hereditary hemorrhagic telangiectasia (HHT) and inflammatory bowel disease (IBD) are associated with pathological angiogenesis. Vascular endothelial growth factor, VEGF, is a major angiogenic modulator implicated in HHT and IBD. Hence, we hypothesized that VEGF-targeted therapy might be beneficial in these disorders.

HHT is an inherited vascular dysplasia characterized by arteriovenous malformations in organs leading to severe complications. HHT is caused by mutations in *Endoglin* (*ENG;* HHT1) or *Activin receptor-like kinase 1* (*ALK1;* HHT2) genes, coding for transforming growth factor β (TGF-β) superfamily receptors. We studied the angiogenic phenotype of *Endoglin* and *Alk1* heterozygous mice and determined their response to anti-VEGF therapy. We demonstrated that lungs, but not liver, heart or colon, showed dysregulated angiogenesis, characterized by reduction in peripheral microvessel density (MVD). An increase in angiostatic thrombospondin-1 (TSP-1) and vascular destabilizing factor angiopoietin-2 (Ang-2), was associated with reduced MVD in $Eng^{+/-}$ and $Alk1^{+/-}$ lungs respectively. Surprisingly, anti-VEGF treatment increased peripheral pulmonary MVD and normalized levels of TSP-1 and Ang-2, suggesting that the treatment restored the angiogenic balance by distinct pathways in HHT1 and HHT2 models.

IBD is characterized by severe, relapsing gut inflammation, leading to multiple complications. Pathological angiogenesis in chronic colitis is persistent, excessive and abnormal. We tested the effect of anti-VEGF therapy in chronic colitis using the $Eng^{+/-}$ mouse model subjected to dextran-sodium sulphate, characterized by severe, chronic intestinal inflammation and pathological angiogenesis. We demonstrated that pathologic angiogenesis is characterized by high colonic MVD and increased *in vivo* microvascular hemodynamics, as assessed by ultrasound. Interestingly, colitic $Eng^{+/-}$ mice showed an inflammation-induced rise in colonic endoglin, several pro-inflammatory cytokines and myeloid chemotactic factors. They had a further increase in G-CSF and amphiregulin, when compared to wild type mice. This suggests that endoglin might have a triple role, as a protective regenerative factor and as a marker of inflammation and angiogenesis in colitis. Importantly, anti-VEGF therapy showed effects associated with resolution of *in vivo* and *in vitro* inflammation and pathological angiogenesis in the $Eng^{+/-}$ model of chronic colitis.

Our findings establish the foundation for future translational studies in patients with vascular dysplastic and chronic inflammatory diseases.

Dedication

To my family for their love, patience, spirit and continuous support

during the training and completion of the requirements for the PhD degree

&

to all teachers and mentors that believed in me

Acknowledgements

First and foremost I want to thank my supervisor, Dr. Michelle Letarte, for the opportunity to work in her laboratory, and for teaching, guidance, help and support. What I have learned from you, Michelle, will remain with me forever. I want to thank my co-supervisor, Dr. Robert Kerbel for his encouragement to look for answers to my burning questions about angiogenesis and the role of anti-angiogenic therapies in chronic inflammatory diseases and for his support. Without his encouragement, I would have not started this journey. A special thanks to Dr. Stuart Foster for the amazing opportunity to work with him and his team. During several months of work on common projects, I have learned a lot about ultrasound in small animals.

I am grateful to Dr. Juan Carlos Zuniga-Plucker and Dr. Stuart Berger of the Department of Immunology for the opportunity to be part of one of the most dedicated, outspoken and interesting team of immunologist trainees. Because of them, I have been admitted in the Graduate Department of Immunology at University of Toronto. I owe special thanks to the members of my graduate committee, Dr. Lisa Robinson and Dr. Shannon Dunn. Your help, support and guidance have been invaluable during these years of training.

I would also like to express my gratitude to Dr. Norman Rosenblum, the Director of the Clinician Investigator Program at University of Toronto for his support and encouragement during these years of training in fundamental science. Your continuous, tremendous commitment to excellence in research training and support for all incoming clinician scientists is unparallel. Dr. Janet Rossant, thank you for your support in transferring from the Master to the PhD program. Many thanks to Dr. Rayfel Schneider,

Ron Laxer and Shirley Tse of Rheumatology, Dr. Denis Daneman, Pediatrician-in Chief, Dr. Bo Ngan of Pathology, Dr. Nicola Jones of Gastroenterology, Dr. Eyal Grunebaum of Immunology, Dr. Etienne Sochett of Endocrinology and Dr. Elena Pope of Dermatology at the Hospital for Sick Children in Toronto, for your support during training in research. A special thanks to a unique teacher, pediatrician and mentor, Dr. Susan Tallett. Because of you and your belief in me, I am here today. Dr. Sarita Verma of University of Toronto, thank you for a great lesson and support. Your encouragement helped me decide to continue on the chosen path.

My graduate experience would not have been the same without the team from the Letarte's laboratory. I want to thank Dr. Mirjana Jerkic for many sessions of teaching and for technical assistance. Madonna, Allison, Valentin, Joyce, Josh, Arvind, thank you for a helping hand, for your smiles and sharing your stories.

Last but not least, I want to thank Melissa Yin from Dr. Stuart Foster's lab for her incredible energy, work ethic and dedication to these two projects presented in the thesis.

Finally, I extend my sincere thanks to the Canadian Institute of Health Research (CIHR), Canadian Association of Gastroenterology, Ministry of Health (MOH), Clinician Investigator Program (CIP) and Postgraduate Graduate Medical Education (PGME) Program of University of Toronto, Department of Pediatrics of the Hospital for Sick Children and the Department of Immunology at the University of Toronto for their generous financial support during this training.

Acknowledgements of Contributions

Dr. Mirjana Jerkic in the Letarte's laboratory

Chapter 2: Supervised and assisted in counting the lung microvasculature. These data were used to generate Fig. 14 a,b. Participated in weighting the hearts; these data were used to generate Fig. 16 b. Supervised and performed the duplicate lung western blots; these data were used to generate Fig. 17 a-e. Supervised and participated in the blood pressure measurements; these data were used to generate Table 7; performed the western blots from the endothelial cells; these data were used to generate Fig. 18 b.

Chapter 3: supervised and participated in colonic multi-analyte cytokine measurements; these data were used to generate Table 8.

Melissa Yin in Dr. Stuart Foster's laboratory

Chapter 2: performed all the ultrasound experiments; these data were used to generate Fig.24 a-h.

Chapter 3: performed all the ultrasound experiments; these data were used to generate Fig.27 a-f; Fig. 28 a-c.

Table of Contents

List of Tables

List of Figures

Abbreviations

ACVR2 : Activin type II receptor

aFGF : Acidic fibroblast growth factor

ALK1 : Activin receptor- like kinase 1 gene (human)

ALK1 : Activin receptor- like kinase 1 protein (human)

$Alk1^{+/+}$: Activin receptor- like kinase 1 wild type mouse

$Alk1^{+/-}$: Activin receptor- like kinase 1 heterozygous mouse

Ang : Angiopoietin

AVMs : Arteriovenous malformations

bFGF : Basic fibroblast growth factor

BMP9 : Bone morphogenic protein 9

CE-US : Contrast-enhanced micro-ultrasound

DC : Dendritic cells

DSS : Dextran sodium sulphate

dTE : Differential targeted enhancement parameter

EC : Endothelial cells

ECM : Extracellular matrix

EG-VEGF : Endocrine-gland vascular endothelial growth factor

ELISA : Enzyme-linked immunosorbent assay

ENG : *ENDOGLIN* gene (human)

$Eng^{+/+}$: Endoglin wild type mouse

$Eng^{+/-}$: Endoglin heterozygous mouse

ERK : Extracellular signal-regulated kinases

FAK : Focal-adhesion kinase

G-CSF : Granulocyte colony stimulating factor

HGF : Hepatocyte growth factor

HHT : Hereditary hemorrhagic telangiectasia

HSPG : Heparan sulphate proteoglycan

IBD : Inflammatory bowel diseases

IL-1 : Interleukin 1 beta

IL-6 : Interleukin 6

MAdCAM-1 : Mucosal addressin cell adhesion molecule

MAPK : Mitogen-activated protein kinases

MBs : Microbubbles

MCP-1 : Monocyte chemoattractant protein-1

MDSCs : Myeloid-derived suppressor cells

MVD : Microvessel density

Nrp : Neuropilin

NK : Natural killer cells

PAH : Pulmonary arterial hypertension

PE : Peak enhancement

PlGF : Placental growth factor

PDGF : Platelet-derived groth factor

PMN : Polymorphonuclear neutrophil

ROI : Region of interest

RTKs : Receptor tyrosine kinases

SDF-1 : Stromal cell-derived factor 1

sEng : soluble endoglin

Smad : Mothers against decapentaplegic homolog

SMC : Smooth muscle cells

TGF-β1 : Transforming growth factor β1

TIC : Time-intensity curve

TNF : Tumor necrosis factors

T reg : Regulatory T

TSP-1 : Thrombospondin-1

VEGF : Vascular endothelial growth factor

VEGFR : Vascular growth factor receptor

WT : Wild type

WiR : Wash-in-rate

Chapter One
Introduction

1.1 Overview

Angiogenesis, the process of new vessel growth from the pre-existing vascular structures, plays a major role in health and disease. Since the pioneer work of Dr. Judath Folkman demonstrated more than 40 years ago that tumorigenesis is angiogenesis-dependent and that targeting angiogenesis could be beneficial in controlling the growth of tumors, the field of angiogenesis and anti-angiogenic therapy has grown considerably[2]. Moreover, the spectrum of "angiogenic diseases" is increasing continuously[2].

Among non-malignant angiogenic diseases, two distinct disorders deserve special consideration: hereditary hemorrhagic telangiectasia (HHT) and inflammatory bowel diseases (IBD). HHT is an inherited systemic vascular dysplastic disease, characterized by the development of arteriovenous malformations (AVMs) in multiple organs, leading to life-long and sometimes life-threatening complications, such as recurrent bleeding, stroke, cardiac failure and even pulmonary arterial hypertension (PAH). It is now known that more than 80% of HHT cases are due to haploinsufficiency in endoglin *(ENG)* and activin receptor- like kinase 1 *(ACVRL1* or *ALK1*) genes, a co-receptor and receptor respectively for the transforming growth factor superfamily of ligands[3]. IBD is a group of chronic inflammatory conditions characterized by severe, relapsing gut inflammation of multifactorial causes, leading to severe complications, including gut perforation, strictures and even cancer[4].

Despite their differences, HHT and IBD have several common characteristics. First, the disruption of the homeostatic vascular angiogenic/angiostatic balance leads to pathological angiogenesis in both diseases. Second, inflammation plays a role in HHT and IBD. In HHT, inflammation may trigger the development of AVM; in IBD, persistent inflammation is the major inducer of abnormal vessel formation in the inflamed gut. Third, several molecules have a crucial role in HHT, IBD, angiogenesis and inflammation: transforming growth factor TGF-β1, endoglin, ALK1 and vascular endothelial growth factor VEGF. TGF-β1 plays both pro- or anti-angiogenic and inflammatory roles, in a context-, cell- and concentration-dependent manner in these two diseases. Endoglin, a co-receptor for TGF-β1, has a regulatory role on TGF-β1-mediated signals and modulates in both positive and negative manners numerous effects after TGF-β1 stimulation. ALK1 is the binding receptor for bone morphogenic protein 9 (BMP9) of the TGF-β superfamily of ligands that has a crucial role in vascular development and remodeling in health and HHT.

VEGF is a major angiogenic factor that has the ability to act upon numerous immune cells and induce their migration, differentiation and functional alterations, therefore exerting indirect immune effects. Moreover, an increase in circulatory and tissue VEGF levels was reported in both HHT and IBD.

Data presented in Chapter Two demonstrate that the angiostatic factor thrombospondin-1 (TSP-1) negatively correlates with endoglin and that Ang2 inversely relates to *Alk1* in HHT. Hence, it appears that these two proteins might contribute to the pathogenesis of dysregulated angiogenesis in HHT. Furthermore, several studies have shown that TSP-1 is a protective factor in IBD, whereas the role of Ang-2 in colitis has not been fully elucidated.

The introduction will summarize briefly our understanding of physiological and pathological angiogenesis, review the pertinent roles of VEGF, TGF-β1, endoglin, ALK1, Ang2, and TSP-1 in angiogenesis and inflammation. I will also highlight the contribution of dysregulated angiogenesis in HHT and IBD and the role of anti-VEGF therapies in these diseases.

1.2. Vessel formation during life span

The vascular system develops through three distinct processes during the life span of an organism: vasculogenesis, angiogenesis and arteriogenesis. During embryonic life, blood vessels are generated mainly through vasculogenesis, whereas in adulthood, angiogenesis is the major process for new vessel formation. Arteriogenesis (collateralization) is a compensatory vascular response to vessel occlusion, leading to formation of collateral bridges between arterial networks[5, 6].

Vasculogenesis or *de novo* formation of blood vessels, comprises two successive steps: a) differentiation of angioblasts from mesoderm and b) migration of angioblasts to form blood islands and the vascular plexus or the primitive endothelial tubular network[7, 8]. During the establishment of blood flow, the vascular plexus is remodeled further into a hierarchical system of vessels, which adopt either an arterial or venous identity[8]. This specification of vessels is one of the first factors to influence the heterogenic tissue response to angiogenic stimuli.

It was long-believed that vasculogenesis is a phenomenon exclusively embryonic. However, recently it was shown the vasculogenesis can also occur postnatally through participation of endothelial precursors cells (EPC) and circulating endothelial cells (EC) to *de novo* vessel formation[9].

1.3. Angiogenesis

1.3.1 Definition and characteristics

Under physiological conditions, blood vessels are kept in a quiescent state. The main role of this network of vascular conduits is to transport oxygen, nutrients, electrolytes, hormones and patrolling immune cells[7]. When stimulated, blood vessels become activated and acquire angiogenic, immune, endocrine and metabolic properties.

Physiological angiogenesis occurs in healthy individuals in response to a local stimulus, during wound healing, in ovaries and uterus during menstrual cycle and pregnancy[10], in testis[11,12] and in hair follicles[13]. The release of local growth factors, such as VEGF, triggers angiogenesis that is amplified by several immune cells, including myeloid cells, through cell-assisted angiogenesis[6]. Moreover, intracellular events, such as sequestration, internalization, degradation of specific receptors or proteins are involved in maintenance of the angiogenic balance[14].

Physiological angiogenesis has two phases: activation and resolution. The activation phase includes a) basement membrane dissolution; b) EC migration towards the angiogenic factors and the invasion of the extracellular matrix (ECM); c) EC proliferation; d) capillary lumen formation. The resolution phase consists of vessel maturation and regression and includes a) inhibition of EC proliferation; b) cessation of EC migration; c) basement membrane reconstitution and completion of vascular coverage with pericytes and smooth muscle cells (SMC)[15, 16]. Importantly, physiological angiogenesis is short-lived and reversible through vessel regression. Vessel regression occurs when a) the angiogenic process is switched from "on to off", and commences

when the angiostatic factors prevail; b) vascular perfusion is inadequate; c) pericyte coverage is established; d) ECM proteolysis is minimal[5, 16].

Whether physiological angiogenesis leads to further vascular proliferation or regression is dictated by the balance of angiogenic and angiostatic factors, or the angiogenic balance.

1.4. Major mediators and regulators of angiogenesis

The microvascular system is designed to remain quiescent. However, vessels can respond rapidly to physiological or pathological demands, such as chronic inflammation and neoplastic conditions[14]. Irrespective of circumstances, the angiogenic fate of the activated vessel depends initially on the tissue amount and gradient of angiogenic and angiostatic factors. This balance will determine and guide the type and duration of vascular responses in various organs.

1.4.1. The angiogenic balance

The angiogenic balance is a tightly regulated, dynamic equipoise between factors that promote and control the rate of vascular growth, the pro-angiogenic mediators, and those that induce the vascular regression, the angiostatic factors. This angiogenic balance is finely tuned so that even a minor loss of the homeostatic distribution of opposing factors will skew the process towards uncontrolled proliferation or excessive inhibition of new vessel formation.

According to Folkman, angiogenic factors are "direct" or "indirect" mediators of neovascular growth, depending on their ability to promote *in vivo* and *in vitro* EC migration and proliferation, two key angiogenic events. Some "direct" angiogenic

factors, such as acidic FGF (aFGF), basic FGF (bFGF) and TGF-α, can stimulate EC migration, proliferation or both. Other angiogenic factors do not target directly the vascular endothelium and have no effect on EC *in vitro*. They likely act on some "indirect" pathways, by a) stimulating macrophages to secrete growth factors; b) activating chemotactic factors for vascular EC or c) releasing intracellular stores of endothelial growth factors[14]. Table 1 lists a few direct and indirect angiogenic mediators.

Several angiogenic mediators and regulators play an important role in angiogenesis, inflammation, vascular and tissue remodeling, and will be reviewed briefly in the next section.

1.4.2.VEGF family

1.4.2.1 Ligands and receptors

The VEGF family of growth factors has a fundamental role in vasculogenesis, angiogenesis, and cardiovascular, haematopoietic and lymphatic development. This family comprises five members, VEGF-A (known as VEGF), placenta growth factor (PlGF), VEGF-B, VEGF-C, VEGF-D and VEGF-E. It also includes several alternate spliced isoforms of the human VEGF-A gene, VEGF-A_{121}, VEGF-A_{145}, VEGF-A_{165}, VEGF-A_{189} and VEGF-A_{206}. Interestingly, the recently discovered VEGF-Axxx isoforms, VEGF-A_{121}b, VEGF-A_{145}b, VEGF-A_{183}b, VEGF-A_{189b}, have anti-angiogenic properties in tumors and in retinal neovascularization in mice[24,31]. For the purpose of this thesis, I will focus on the VEGF-A and its receptors.

Table 1. A partial list of angiogenic mediators

Angiogenic factors	Angiostatic factors	Dual factors (pro- and anti-angiogenic)	Vascular stabilizers and quiescence factors
Growth factors **VEGF-A,** VEGF-B, PlGF, bFGF & aFGF[14]; HGF[17]; PDGF[18] **Hormones** Adrenomedullin[19]; insulin-like growth factor, leptin[17], growth hormone /parathyroid hormone, thyroid-stimulating hormone[20]; human chorionic gonadotropin,lutenizing hormone, follicle-stimulating hormone[10] **Cytokines** TNF-α, IL-8[17]; MCP-1[17]; IL-6, IL-4, M-CSF , G-CSF, IL-17[18] **Other factors** Angiogenin, prostaglandins (PGE1, PGE2), adipocyte lipids, heparin, copper[14]; αvβ3 integrin[17]; collagens I, III, IV and XV, laminin-1 and -8, fibronectin, perlecan and tenascins (after proteolytic degradation)[21]; adenosin, CCL2, endothelin-1, CXCL12, TLR2 ligands[18]	**Growth factors** Pigment epithelial derived factor (PEDF)[22]; VEGF165b[23], VEGF121b, VEGF145b, VEGF183b, VEGF189b[24] **Hormones** Circulating angiostatic steroids[14]; prolactin, IL-4, IL-13[17]; ghrelin, gonadotropin-releasing hormone, somatostatin[20] **Cytokines** IL-4, IL-13[17]; interferon-β[22] **Other factors** Angiostatin, endostatin[14]; **TSP-1**&2, sVEGFR1, alphastatin, arrestin, anti-thrombin III (truncated), canstatin, fibulin, semaphorin 3A, troponin I, TIMP-2, tumstatin, vasostatin[22]; restin[25]; sEng[26]	**TGF-β1**[14] **Endoglin**[27, 28]; TNF-α[17]	**Ang2**, Ang1[29]; BMP9[30]

Note: The angiogenic mediators that will be discussed further in the thesis are highlighted in blue.

VEGF-A is produced by most parenchymal cells and also by EC[32] and has a crucial role in vasculogenesis and angiogenesis. Mice lacking one *Vegf-a* allele die in utero at embryonic day E11-12, due to severe blood-island, angiogenic and developmental defects in heart, large vessels and brain[33]. Conversely, even a two-fold increase in *Vegf-a* leads to embryonic lethality, highlighting the importance of appropriate VEGF gene dosage during development[32]. Extensive work has shown that VEGF induces EC migration, proliferation, survival and vascular permeability[32]. What determines if the vascular angiogenic response is normal or aberrant is the VEGF concentration in the microenvironment, and not the total VEGF tissue level[34]. It was reported in mice with *Vegf-a* gene deletion in EC ($VEGF^{ECKO}$) that VEGF levels in plasma, serum and several organs were similar, indicating that the endothelial VEGF is not a major source of circulating or tissue VEGF levels. Additional experiments showed that both $VEGF^{ECKO}$ mice and wild type controls had similar capillary density, angiogenic response and vascular permeability. These findings indicate that the paracrine VEGF signaling is essential for angiogenesis, proliferation, survival, permeability responses and endothelial differentiation, whereas the autocrine VEGF signaling was needed for survival signals[32]. Moreover, $Vegf^{ECKO}$ mice developed at 40-50 weeks of age a systemic vascular pathology resembling the one seen after long-term use of bevacizumab, an antibody to human VEGF: hemorrhages, intestinal perforations, multiple micro-infarcts and disruption in the elastic lamina of larger vessels. These results demonstrated that long-term blockage of VEGF signaling in EC can alter the vasculature of normal tissues[32].

The role of VEGF in initiation and resolution of inflammation is less understood. Several studies showed that tissue VEGF was increased in chronic inflammatory

diseases such as rheumatoid arthritis, psoriasis and IBD[35]. Moreover, Lee et al demonstrated that *Vegf*^{ECKO} mice with a deletion of endothelial VEGF could survive the embryonic window of lethality, but display a chronic inflammatory state and significant fibrosis in several organs between 8 and 20 weeks of age[32]. These changes were not associated with alterations in *Vegfr2* protein levels, the major signalling receptor for VEGF[32].

The VEGF family signals through three receptor tyrosine kinases, VEGFR1, -2, -3, two co-receptors neuropilin 1 (Nrp-1) and neuropilin 2 (Nrp-2) and through transmembrane heparan sulphate proteoglycan (HSPG) receptors[23], as depicted below in Figure 1.

VEGFR1 (Flt-1) has vasculogenic, pro-inflammatory, and both pro-and anti-anti-angiogenic effects. VEGFR1 is expressed in tissues and in monocytes and macrophages. VEGFR1 binds with high affinity to VEGF, but its kinase activity is low, as demonstrated by the deletion of the *Vegfr1* tyrosine kinase domain in mice, which is compatible with vascular development[23]. In contrast, *Vegfr1*$^{-/-}$ embryos die at E9 of abnormal, disorganized vessels that lack lumen[23]. Thus, VEGFR1 has an important role in vasculogenesis. Moreover, VEGFR1 facilitates migration of monocytes and macrophages, participates in haematopoiesis, recruitment of hematopoietic progenitor cells from the bone marrow, and has a role in vascular permeability[23].

In addition, VEGFR1 negatively regulates VEGFR2 signaling by binding VEGF directly or indirectly, through its product, sFlt-1[36]. Further modulation of VEGF signaling occurs through heterodimerization of VEGFR1-VEGFR2, as well as of VEGFR2-VEGFR3.

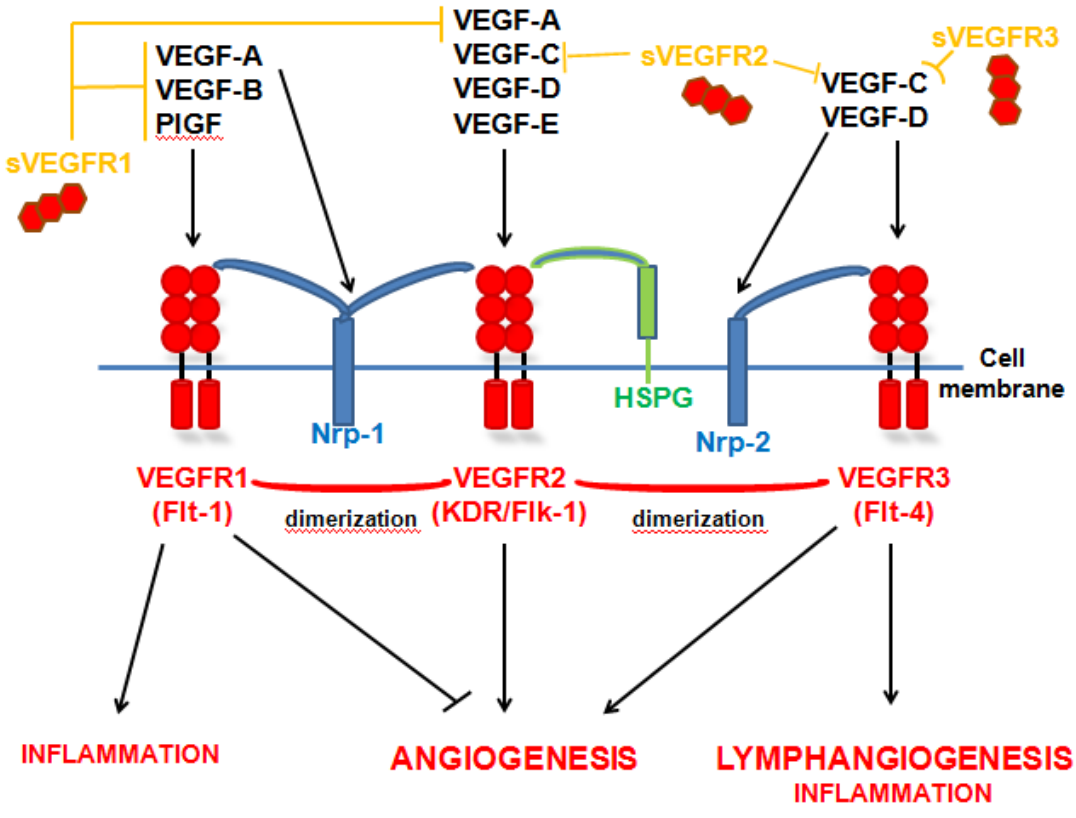

Figure 1. **The VEGF family of ligands, receptors and co-receptors.** VEGF-A, VEGF-B and PlGF bind VEGFR1; VEGFR1 has a dual role in angiogenesis and stimulates the migration of monocytes and macrophages, thus playing a role in inflammation. VEGF-A, -C, -D, -E isoforms bind VEGFR2; VEGFR2 has a major pro-angiogenic effect. The ligands for VEGFR3 are VEGF-C and -D. This receptor plays a major role in lymphangiogenesis and through stimulation of macrophages, might have a role in inflammation. The three corresponding soluble VEGF receptors have different roles: sVEGFR1 binds VEGF-A[37], VEGF-B and PlGF[23] effects via VEGFR1 or VEGFR2 pathways; sVEGFR2[38] inhibits VEGF-C, therefore blocking its effects on VEGFR2 and on lymphangiogenesis; sVEGFR3 sequesters VEGF-C and inhibits lymphangiogenesis and through inhibition of VEGF-C-mediated VEGFR2 phosphorylation, also blocks angiogenesis[39]. Neuropilin 1(Nrp-1) and 2 are co-receptors, and modulate the activity of VEGFR1, R2 and R3, respectively. Heparin-sulphate proteoglycan (HSPG) influences the signaling through VEGFR2[23].

VEGFR2 (KDR/Flk-1) has a vasculogenic and a major pro-angiogenic role. VEGFR2 is the primary transducer of VEGF-A effects on EC differentiation, proliferation, survival, migration, tube formation, and in vascular permeability, even though it binds VEGF-A with ten-fold lower affinity than VEGFR1[36]. This affirmation is supported by the observation that *Vegfr2*$^{-/-}$ mice die at E8.5 from impaired development of hematopoietic cells and EC, similarly to *Vegf-a*$^{-/-}$ mice. Alternative splicing of VEGFR2 leads to formation of soluble VEGFR2 (sVEGFR2), which is present in various tissues (skin, heart, spleen, kidney, ovary) and in plasma[38]. sVEGFR2 binds mostly VEGF-C, hence it inhibits lymphatic EC proliferation[36].

VEGFR3 has a critical lymphangiogenic and possible inflammatory role. VEGFR3 is expressed in vascular and lymphatic ECs and is up-regulated during angiogenesis and lymphangiogenesis. Without *Vegfr3*, mice die at E10-11 because of severe growth and vascular defects. Moreover, VEGFR3 is also expressed on macrophages[36].

Neuropilin (Nrp) Nrp-1 and Nrp-2 lack an intrinsic catalytic function. Nrp-1 appears to act primarily as a co-receptor for VEGFR1/2, modulating receptor signaling particularly during vessel sprouting and branching. Nrp-2 functions as a co-receptor for VEGFR3. During development, Nrp-1 is preferentially expressed in arteries, whereas Nrp-2 is localized on veins and lymphatics. Disruption of *Nrp1* in mice led to embryonic lethality at E12.5-13.5, caused by multiple vascular abnormalities[36]. In contrast, *Nrp2* knockout mice have abnormal development only in capillaries and small lymphatics[36].

Membrane heparan sulphate proteoglycans (HSPGs) mediate VEGF interactions with VEGFR2 in *cis*, inducing cell signaling and subsequent internalization of the

complex or in *trans*, delaying internalization of the signaling complex, trapping the VEGFR2 at the cell surface and enhancing VEGF response[40].

1.4.2.2 Signaling pathways and effects

VEGF-A induces and stimulates EC proliferation through VEGFR2-mediated activation of the RAS/RAF/ERK/p42/44 MAPK pathway. Furthermore, activation of VEGFR2-PI3K leads to membrane recruitment and phosphorylation of AKT, which inhibits the activity of the BCL-2 associated death promoter (BAD) and caspase 9, thus promoting the survival of EC. VEGF-A also triggers the expression of the anti-apoptotic proteins BCL-2 and A1, and of the inhibitors of apoptosis XIAP and survivin, while blocking the terminal effectors caspases 3 and 7, which further enhances the survival of EC. Moreover, VEGF-A is a powerful vascular permeability factor[41].

Some of the pathways that regulate VEGFR2-mediated vascular permeability include Src, eNOS, p38MAPK[23]. However, VEGF-mediated vascular permeability mostly depends on the communication between VEGFR2 and VEGFR1, through their heterodimerization. Furthermore, VEGF-A-induced EC migration via VEGFR2 includes activation of the focal-adhesion kinase (FAK) and its substrate paxillin. These main effects of the VEGF-A signalling are shown below in Figure 2.

Furthermore, modulation of VEGFRs is critical for VEGF signaling. Depending on the binding ligand, VEGFRs can form heterodimers. Dimerization of VEGFRs leads to activation of their receptor kinase activity and auto-phosphorylation of the receptors. Phosphorylated receptors recruit various proteins and induce the activation of diverse downstream signalling pathways.

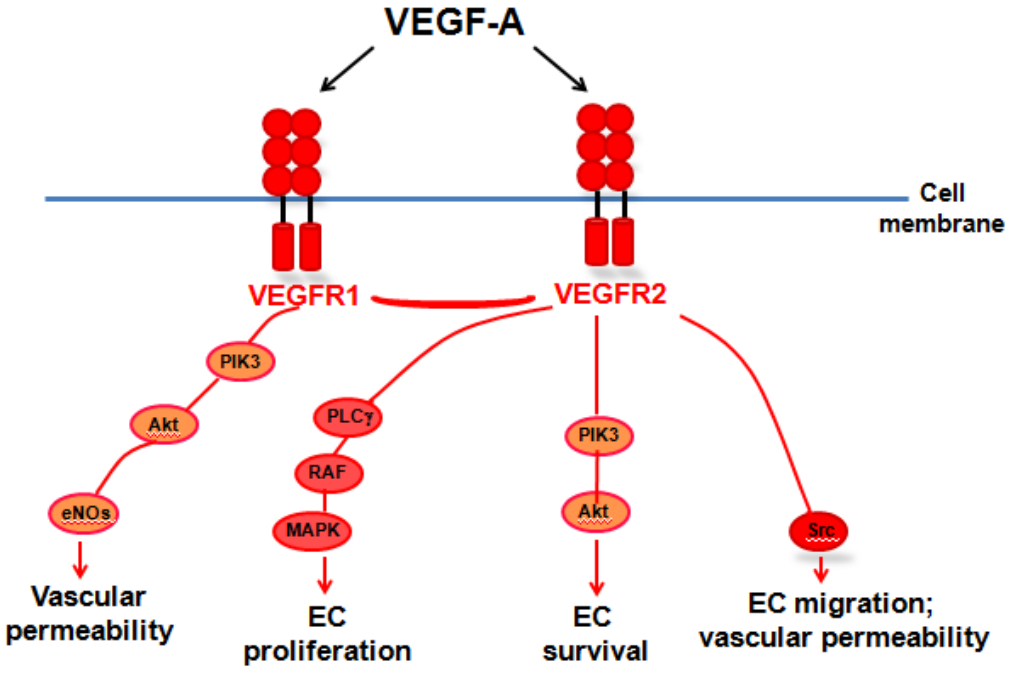

Figure 2. Main VEGF-A signaling pathways. VEGF-A signals through VEGFR1 and VEGFR2. VEGFR2 is mainly responsible for EC proliferation, survival, migration. It also participates in vascular permeability in conjunction with VEGFR1, via heterodimerization (adapted from[42]).

Negative regulation of receptor tyrosine kinases (RTKs) is important for limiting the response of the target cells. This occurs through rapid RTK dephosphorylation, internalization, lysosomal and proteomic degradation[23].

1.4.3. TGF-β family

1.4.3.1 TGF-β and BMP ligands

The transforming growth factor-β (TGF-β) superfamily of ligands has a fundamental role in embryonic development, lineage determination, vasculogenesis, angiogenesis and inflammation[43]. This superfamily has a least 40 members, grouped into TGF-β and bone morphogenic protein (BMP) families. The TGF-β superfamily includes TGF-β isoforms, activins, nodal and myostatin ligands that activate mothers against decapentaplegic homologs Smad2 and Smad3. The BMP family includes BMPs and growth and differentiation factors (GDFs) that activate Smad1, Smad5 and Smad8 molecules.

Among the three TGF-β isoforms, TGF-β1 is the crucial regulator of vasculogenesis, cardiac development and angiogenesis, as shown by the *Tgf-β1* knock-out mice that die in utero due to severe cardiovascular defects[44]. TGF-β1 also modulates several immune and hematopoietic cells, and has a major role in tissue repair mechanisms, including fibrosis[45].

The bone morphogenetic protein (BMP) family has a least 20 members, some of which have been recently involved in angiogenesis[30]. BMP9 (or GDF2) is a factor secreted mainly by the liver that circulates in inactive (40%) and active (60%) forms[46]. The active BMP9 keeps EC in a resting state, hence BMP9 is a vascular quiescence molecule[30]. BMP9 appears to be necessary for post-natal development, as BMP9 cannot

be detected *in utero*, but can be measured during the 3 weeks after birth, after which its levels decrease[30]. Furthermore, BMP9 inhibits[47] or promotes[48] angiogenesis, in a context-dependent manner, further substantiating the complexity and versatily of the angiogenic modulation through this ligand.

1.4.3.2 Endoglin

Endoglin (CD105), a co-receptor for TGF-β1 and TGF-β3, activin-A, BMP9, BMP10, BMP7 and BMP2 ligands, has an important modulatory role in vasculogenesis, angiogenesis, inflammation and fibrosis. Endoglin was first identified, cloned and sequenced in Dr. Michelle Letarte's laboratory[27]. Endoglin is a homodimeric glycoprotein (180kDa) constitutively expressed on all blood vessels**.** It is present on quiescent vascular endothelium and up-regulated on activated vessels in tumors and chronic inflammatory disorders[49,50]. For these reasons, endoglin has been used as a marker of pathological angiogenesis, even though is also present on resting vessels[50]. In addition, endoglin is expressed by erythroid precursors[51], mesenchymal stem cells[52], activated monocytes and macrophages[53], vascular SMC and fibroblasts[54,55] and long-term hematopoietic stem cells[56]. Furthermore, endoglin is expressed on the placental syncytiotrophoblast throughout pregnancy[57] and in extravillous trophoblast cells during first term[58]. Endoglin is also transiently expressed in the mesenchymal endocardium during valve formation[59].

The vital role that endoglin plays in developmental angiogenesis, cardiac organogenesis, early myelopoiesis and erythropoiesis is demonstrated by the *Endoglin* null ($Eng^{-/-}$) mice that die at E10.5 of cardiovascular defects and impaired hematopoiesis[60-62]. Further work revealed that absence of endoglin leads to severe

impairment in myelopoiesis, definitive erythropoiesis and mild impairment of lymphopoiesis[62]. Moreover, endoglin has also a role in early hematopoiesis, contributing to hemangioblast specification and hematopoietic commitment[63]. Lastly, endoglin is required for early patterning of the heart and endocardial to mesenchymal transition during formation of the endocardial cushions. Interestingly, the same study showed that the lack of endoglin does not affect vasculogenesis, but reduces branching ability or angiogenesis[64].

Two isoforms arising by alternate splicing of endoglin, L-endoglin (L, long) and S-endoglin (S, short) that differ in the amino acid composition of their cytoplasmic tails, have been characterized more than 20 years ago. L-endoglin (180kDa) and S-endoglin (170kDa), contain 47 and 14 residues respectively in the cytoplasmic tail. Both isoforms bind TGF-β1 and are co-expressed on myeloid cells, EC and placenta, with L-endoglin being the predominant isoform[65]. L-endoglin stimulates the ALK1-mediated pathway and appears to have a pro-angiogenic role, while S-endoglin promotes ALK5 signalling and might have an anti-angiogenic effect[66].

Recently, it was shown that a soluble form of endoglin, sEng, binds with high affinity to BMP9 and BMP10, and act as an anti-angiogenic factor[26]. A molecular model for the extracellular domain of endoglin has been proposed, but no definite 3D structure has been identified yet[67]. A structural diagram of endoglin is depicted in Figure 3.

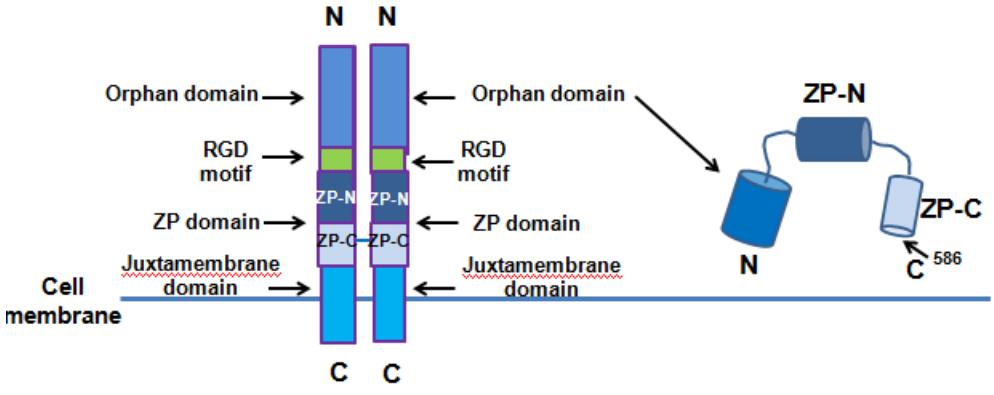

Figure 3. Structure of human endoglin. The N-terminal orphan domain binds TGF-β1, in association with the type II receptor; the arginine-glycine-aspartic acid (RGD) tripeptide is a recognition motif for several integrins; ZP = zona pellucida domains are involved in protein-protein interactions; a single transmembrane domain and the C-terminal cytoplasmic domain, rich in serine/threonine, and interacting with endothelial NO synthase. The molecular model of the extracellular domain of endoglin (1-586) is shown for an endoglin monomer (adapted from[67]).

1.4.3.3 ALK-1 receptor

The HHT2 disease results from haploinsufficiency in the ALK1 receptor. ALK1 can associate with endoglin, responsible for HHT1. Although both ALK1 and endoglin participate in the pathogenesis of HHT, ALK1 differ in several aspects from endoglin.

The ALK1 receptor, expressed almost exclusively in arterial EC[68], binds with high affinity to BMP9 and BMP10; it also binds TGF-β1 in complex with the TGF-β type II receptor and ALK5. It is generally accepted that ALK1 plays an important role in angiogenesis; however, controversies exist about the pro- or anti-angiogenic role of ALK1. Several groups have shown that ALK1 has a pro-angiogenic effect,[45, 69, 70, 71-73]. Other studies noted that *Alk1* has a role in resolution of angiogenesis[70] and that targeting ALK1 leads to retinal hypervascularization in mice[47] or to a sligh increase in number of cerebral EC in mutant zebrafish *vbg*[74]. This indicates that the role of Alk1 in modulating angiogenesis is context- and model-dependent.

In addition, ALK1 is involved in the homeostatic maintenance of mature vessels, since total deletion of the *Alk1* gene in postnatal mice results in AVM formation, severe internal hemorrhaging and lethality[75]. Moreover, *Alk1* homozygous null embryos die at E11.5 due to defective EC and SMC coverage of the primary capillary plexus and AVM formation[69,76], further substantiating the role of *Alk1* in vascular remodeling. These findings were later confirmed in the *ALK1* deficient zebrafish (namely *violet beauregarde*) embryos[77, 74].

However, in the same zebrafish model, an increase in the number of EC in the dilated cranial vessels suggested that *Alk1* might inhibit EC proliferation[77,74]. Similarly, in the early postnatal period, *Alk1* appeared to have an anti-angiogenic role, as inhibition of Alk1 with an ALK1Fc ligand trap resulted in retinal hypervascularization and AVM

formation, by cooperation with the Notch pathway[47]. Yet, it is unknown if this is a tissue-specific effect or a more generalized phenomenon. Potential reasons for these opposing findings could be the context-, cell type- and ligand-specific effects exerted by Alk1 during signaling.

Furthermore, ALK1 expression is increased during wound healing and tumor growth, demonstrating that it plays a role in physiological and pathological angiogenesis. In the *Alk1*$^{+/lacZ}$ mice, arterial Alk1 expression had a specific pattern during wound healing: it started to rise by day 3, culminated on day 10 and was almost completely reduced by day 14 upon wound closure[68]. Moreover, increased Alk1 expression was found in blood vessels of several tumors[68,71]. Importantly, the generation of tumoral vessels was reduced following treatment with a soluble chimeric protein (ALK1-Fc)[72].

1.4.3.4 ALK5 receptor

ALK5 is the type I receptor for the TGF-β1-mediated angiogenic signaling. The ALK5 receptor, expressed ubiquitously in tissues, is detected primarily in vascular SMC, but is present at much lower levels in the endothelium[78,79]. Recent experimental data showed that ALK5 appears to control EC adhesion, mural cell recruitment and remodeling of ECM, promoting the maturation of blood vessels or the late resolution phase of angiogenesis[45].

1.4.3.5 Signaling pathways and effects

TGF-β/BMP signaling is one of the most complex and heterogeneous signaling systems, regulating cell proliferation, differentiation, motility, and apoptosis, in a context-, cell-, receptor- and concentration-dependent manner in health and disease.

Members of the TGF-β superfamily of ligands signal through heteromeric complexes formed by type II (TGFβR2 and BMPR2), type I serine/threonine kinase receptors (ALK1 and ALK5) and the co-receptor endoglin. Upon ligand binding, the constitutively active type II serine/threonine kinase receptors phosphorylate and activate the type I receptors. The activated type I receptors phosphorylate downstream the receptor-regulated Smads (RSmads) proteins, which bind the adaptor protein Smad4 (Co-Smad). Smad2 and Smad3 transduce signals for TGF-β1 and activins, whereas Smad1/5/8 mediate the signaling for BMPs. Smad complexes move into the nucleus and regulate the transcription of specific target genes. In addition, TGF-β/BMP signaling is negatively modulated by intracellular inhibitory Smads (Smad 6 and 7) that compete for Co-Smad binding or cause degradation of RSmads[80], or by extracellular molecules, such as noggin, chordin, cerberus, and gremlin for BMPs or the pseudo-receptor BAMBI, for TGF-β1[80].

Furthermore, TGF-β1 activates two distinct *canonical Smad pathways*: Smad2/3 pathway through ALK5 activation, and the Smad1/5/8 pathway via ALK1 stimulation[70]. Endoglin, by modulating the effects of various ligands, extracellular proteins and transmembrane receptors, can either stimulate or inhibit responses to the TGF-β superfamily ligands. In EC, endoglin generally inhibits the TGF-β1-ALK5 pathway, while promoting the TGF-β1/ALK1 signaling pathway. In addition, ALK1 can indirectly inhibit ALK5-induced Smad-dependent transcriptional responses. Moreover, BMP9 can

interfere with Smad2/3 phosphorylation through activation of BMPR2/ACVR2/ALK1/ALK2 pathways[81]. However, ALK1-ALK5 crosstalk is bidirectional, as ALK5 is required for optimal ALK1 activation[82] and ALK5 phosphorylation of the endoglin cytoplasmic domain regulates Smad1/5/8 signaling[83]. Thus, even though ALK1 and ALK5 have distinct functions during angiogenesis, their balance is crucial for the fine-tuning and control of vasculogenesis and angiogenesis[69]. Moreover, this "lateral" crosstalk between TGF-β1 and BMP9-mediated pathways at the level of ligands, transmembrane receptors and cytoplasmic proteins, allows the system to display a flexible and versatile angiogenic response in the activated endothelium. The effects of TGF-β1/BMP9 stimulation are depicted in Figure 4.

TGF-β1 stimulation can also alter the EC-ECM interface, by enhancing cell-cell adhesion, increasing the expression of some ECM components, such as collagen and fibronectin, the latter enhancing the TGF-β1 and BMP9-induced Smad1/5/8 phosphorylation via endoglin and ALK1[84].

In addition, TGF-β1 signals through several *non-canonical molecules and pathways* which a) are directly stimulated by Smads; b) can directly modify Smad function; c) can directly interact with or become phosphorylated by the TGF-β receptors, without altering the function of Smads[80]. Some of these non-canonical TGF-β1 pathways include ERK/MAPK, JNK and p38 MAPK, RhoA and PI3K/AKT signaling cascades. MAP kinases, including ERK, JNK and p38, can also be activated by BMPs, which increases the need for fine-tuning and regulation of this multi-layered and complex system[80, 85, 86].

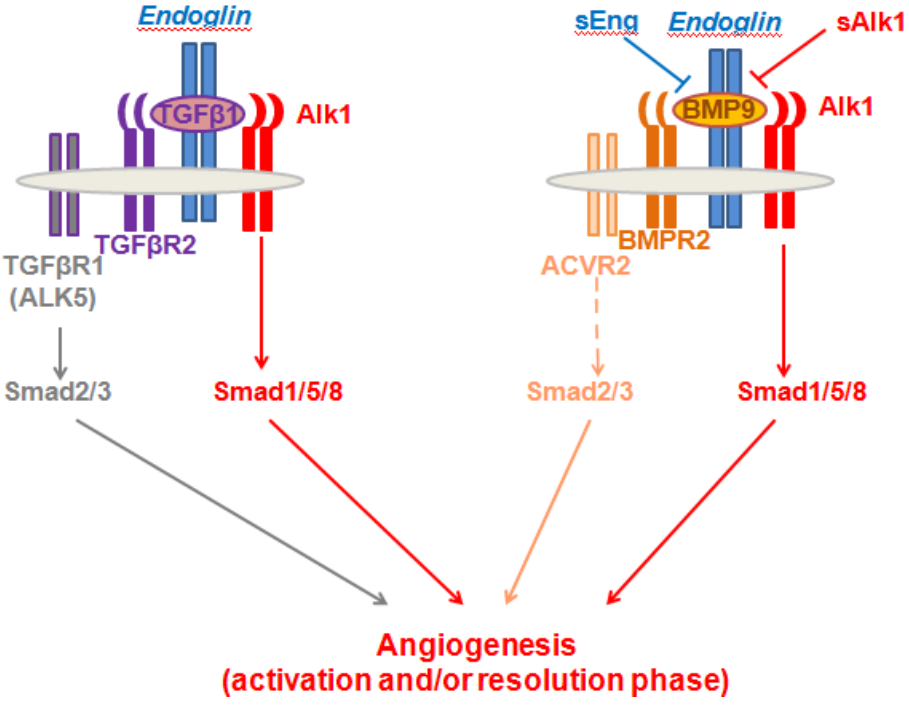

Figure 4. A working model for TGF-β1 and BMP9 signaling. TGF-β1 binds TGFBR2, which subsequently recruits and phosphorylates TGFβR1 (ALK5) or ALK1. Activated ALK5 recruits and phosphorylates Smad2/3, whereas ALK1 induces Smad1/5/8 phosphorylation, resulting in activation of ALK5- and ALK1-specific target genes, respectively. BMP9 binds to ALK1 and BMPR2 and signals via Smad1/5/8 pathway; by stimulating activin type II receptor (ACVR2), BMP9 can also activate the Smad2/3 pathway. sEng and sAlk1 bind with high affinity to BMP9 and exert anti-angiogenic effects. Endoglin modulates all of these pathways in a ligand-, receptor-, cell- and context-dependent manner.

1.4.4. Angiopoietin family

1.4.4.1 Ligands and receptors

The angiopoietin-Tie receptor system is essential for controlling vessel quiescence, vascular maturation and remodelling, processes that are critical for physiological and pathological angiogenesis. The angiopoietin family includes 4 secreted ligands, Ang-1 and Ang-2 being the main ones; Ang-3 (mouse) and Ang-4 (human) are interspecies orthologs[87]. Ang-1 and -2 bind Tie2, a tyrosine kinase receptor.

Even though Tie1 receptor has no known ligand, it can bind Ang-1 when present at high concentration, via integrins[88]. In addition, there are seven newly discovered orphan Ang-like molecules (Angpl1-7) that do not bind to Tie1 or Tie2. Ang-like molecules can regulate the metabolism and Angpl1-4 and Angpl6 can transduce survival and migration signals, thus exerting a pro-angiogenic effect[29]. Moreover, the angiopoietin–Tie2 signaling system is negatively regulated by the EC-specific transmembrane receptor tyrosine phosphatase VE-PTP, also called PTPRb[87]. The complexity of the Ang-Tie signaling is further increased by the presence of four Ang-1 alternatively spliced isoforms, two of which could act as dominant negative molecules[89].

Ang-1 is constitutively expressed in the perivascular region, in SMC, pericytes and fibroblasts. Ang-1 stabilizes the quiescent vasculature and reduces endothelial permeability under basal conditions and after VEGF stimulation. Ang-1 also mediates migration, adhesion and survival of EC, demonstrating a pro-angiogenic effect. *Ang1*-deficient mice, similar to *Tie-2*-deficient mice, die in utero due to severe vascular and cardiac impairment, indicating that Ang-1 is critical for cardiovascular maturation[90].

Ang-2 has a dual role, agonist or antagonist for the angiopoietin-Tie system, in a context-dependent manner. Ang-2 is primarily produced by EC during angiogenic remodeling and can be induced by VEGF, among other factors. Ang-2 is the functional antagonist of Ang-1 and binds to Tie2 without inducing a signal transduction. In fact, the balance of Ang-1 and Ang-2 levels determine Tie2 activity. Moreover, Ang-2 disrupts the connections between the endothelium and perivascular cells and promotes apoptosis and vascular regression, thus exerting an anti-angiogenic effect. Yet, in conjunction with VEGF, Ang2 can promote neo-vascularization. Interestingly, *Ang2*-deficient mice are born apparently normal, implying that the developmental angiogenesis is not affected. However, these mice have a delayed, inflammation-mediated up-regulation of ICAM1 and VCAM1 adhesion molecules after TNFα stimulation, indicating that Ang-2 might play a protective, anti-inflammatory role[29]. These findings support the observation that Ang-2 expression is low in quiescent mature vessels, but markedly increased in inflammatory and angiogenic diseases.

Tie1 and Tie2 are receptor tyrosine kinases (RTKs), which similar to VEGF receptors, are expressed by EC and hematopoietic cells. Recently it was shown that Tie2 is also expressed on neutrophils (PMN) and a subset of monocytes[87, 91]. Several recent studies reported that Tie receptors play an essential role in late vascular and lymphatic development. For example, *Tie1*-deficient mice die between E13.5 and birth due to extensive edema[92,93] and *Tie2*-null mice die earlier at E10.5-12.5 of lack of vascular development beyond the capillary plexus, defective hematopoiesis and cardiac impairment[94].

1.4.4.2 Signaling pathways and effects

Ang-1 binds Tie2. Ang-2 is a weak agonist of Tie2 and can even inhibit Ang-1-mediated Tie-2 activation, in a context-dependent manner. In comparison, Tie1, without a known ligand, is able to heterodimerize with Tie2 and modulate Tie2 signal transduction[87].

Several lines of evidence point to the role of Ang-1 in maintenance of vascular endothelium quiescence[88]. Ang-1-mediated Akt signaling directly inhibits EC apoptosis. Moreover, Ang-1 inhibits Ang-2 expression and secretion. Ang-1 blocks Src and maintains vascular permeability under basal conditions and in response to VEGF[95].

The role of the Ang-1-Ang-2 system in inflammation is controversial. Tie2 activation recruits A20-binding inhibitor of nuclear factor NF-kB (ABIN-2), which inhibits the NF-kB pathway and the inflammatory response. However, it was recently demonstrated that Ang-1 and Ang-2 together can activate the Tie2 receptor on PMN, leading to enhanced neutrophil adhesion, thus acting as pro-inflammatory mediators[91].

Furthermore, Ang-2 and VEGF can cooperate and alter the angiogenic responses. A high ratio of Ang-2 to VEGF levels leads to vessel regression, whereas high VEGF Ang-2 levels results in angiogenesis. Some of the Ang-1 and Ang-2 effects are represented in Figure 5.

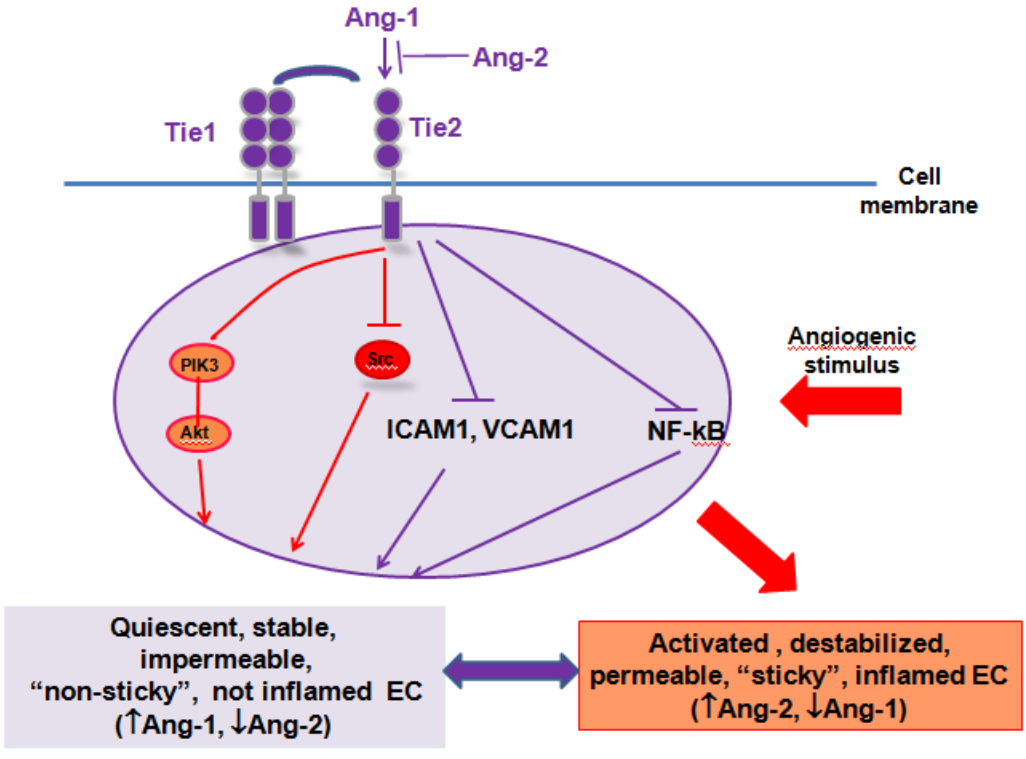

Figure 5. Angiopoietin-Tie signaling effects depend on the ratio of Ang-1 to Ang-2 levels. Ang-1 binds Tie2 and Ang-2 inhibits the Ang-1 stimulation. Tie 1 can dimerize with Tie 2 receptor. Tie2 downstream signaling involves activation of survival Akt pathway and inhibition of Src-mediated vascular permeability. Ang-1 activation decreases the expression of adhesion molecules ICAM1 and VCAM1 and of NF-kB, hence reducing inflammation.

1.4.5. Thrombospondin family

1.4.5.1 Ligands and receptors

The thrombospondin (TSP) family includes several naturally occurring endogenous angiostatic proteins, with major role in angiogenesis, tissue remodeling and inflammation. Among the five members of the TSP family, TSP-1 to TSP-5, TSP-1 is the most studied of all.

TSP-1 is a matrix glycoprotein secreted by platelets, EC, fibroblasts, SMC, monocytes, macrophages and adipocytes[96]. Recently, a soluble form of TSP-1 (sTSP-1) was generated by cleavage of the N-domain of TSP-1[97].

TSP-1 has multiple and often opposite cellular effects, possibly due to the interaction of its domains with an array of receptors and proteins. TSP-1 has direct anti-angiogenic effects, by signaling through its receptors CD36 and CD148. However, by activating the latent TGF-β1 and releasing the VEGF sequestered in the ECM, TSP-1 may exert, in a context-dependent manner, some pro-angiogenic effects. The CD36 receptor is expressed in EC and SMC, whereas CD47 is ubiquitously found, including in T cells and PMN[96]. CD148 (DEP-1/PTPη) is a tyrosine phosphatase receptor expressed in several cell types, including vascular EC, hematopoietic lineages, megakaryocytes and platelets [96].

TSP-1 can also interact with fibronectin, fibrinogen, heparin sulfate proteoglycans (HSPG) and a number of integrins, and therefore can modulate cellular motility and adhesion[97]. Moreover, TSP-1 is involved in maintenance of immune tolerance through signaling via its receptors CD36 and CD47[97].

1.4.5.2 Signaling pathways and effects

In physiological conditions, high TSP-1 expression is restricted to megakaryocytes and platelets. In pathological conditions, TSP-1 is synthesized by many other cell types**,** including EC, SMC, fibroblasts, macrophages, T cells and PMN.

TSP-1 signaling through CD36 is responsible for most of the anti-angiogenic and inflammatory functions[97]. TSP-1 binding to CD36 induces subsequent activation of MAPK and FAS, which results in activation of caspases[98]. TSP-1 also inhibits epithelial and hematopoietic cells, but these effects are less well studied.

Furthermore, TSP-1 binds and activates latent TGF-β1. Activated TGF-β1 can also induce TSP-1 expression, indicating a positive feedback loop in the signalling pathway[97]. Moreover, TSP-1 can release VEGF sequestered in the ECM and modulate phosphorylation of VEGFR2 directly and through complexes formed by CD36, CD47 and VEGFR2. Interestingly, in *Tsp-1*-null mice, VEGF-A-driven vascular permeability is reduced. Moreover, *Tsp-1*-null EC have altered expression or activation of fibronectin, Src, PI3K, Akt and p38MAPK, the additional pathways through which TSP-1 exerts its effects[98].

Soluble thrombospondin-1 (sTSP1) binds to the extracellular segment of CD148 with high affinity and specificity. CD148 dephosphorylates and inhibits several receptors involved in angiogenesis, such as VEGFR2, EGF receptor, hepatocyte growth factor receptor (HGFR), FGF receptor (FGFR), PGDF receptor (PDGFR), thus exerting an anti-angiogenic effect. Growing evidence indicates a prominent role for CD148 in inhibition of cell proliferation and transformation[99]. Some of the TSP-1 complex roles are shown below in Figure 6.

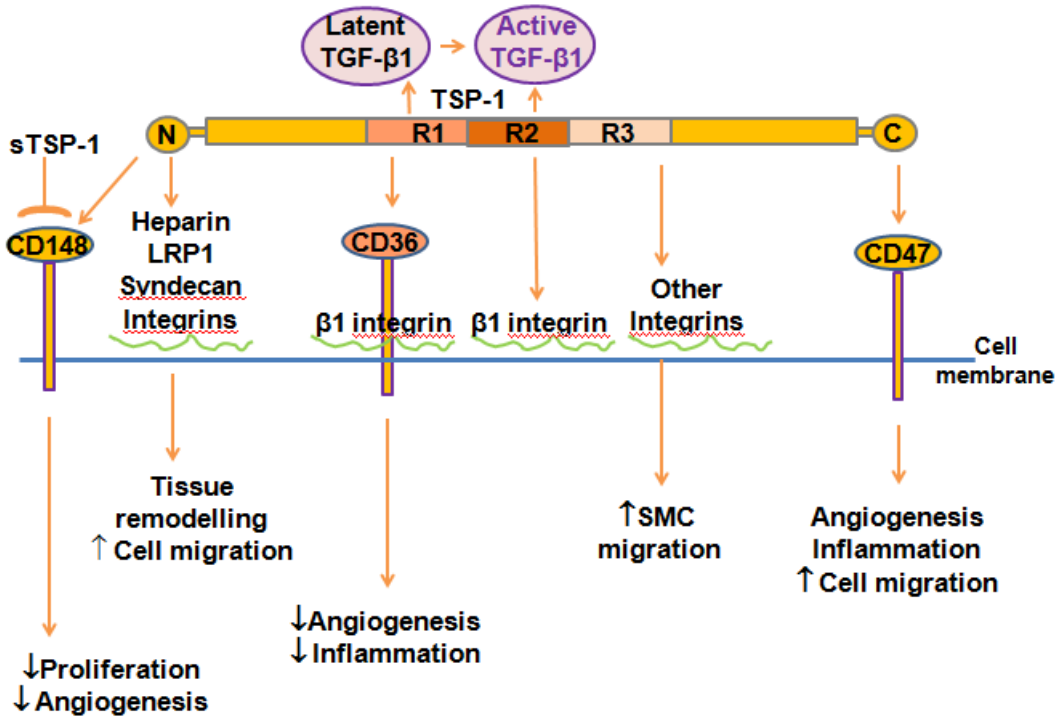

Figure 6. The complexity of the TSP-1 system and its potential roles. N=N-terminal domain; C= C-terminal domain; R1, R2, R3 - type 1, 2, 3 central repeats; SMC = smooth muscle cells. CD36, CD47, CD148 are transmembrane receptors for TSP-1. TSP-1 can bind directly various ECM proteins, including latent TGF-β1, leading to its activation. The angiostatic effects of TSP-1 are transduced mainly by CD36 and CD148. CD47, being ubiquitously expressed on several subsets of immune cells, can induce cell migration, angiogenesis and promote inflammation.

1.5. Pathological angiogenesis

Pathological angiogenesis contributes to progression of tumors, chronic inflammatory and vascular dysplastic disorders.

1.5.1 Definition and characteristics

When angiogenesis becomes defective, it leads to formation of abnormal vessels, different from those observed in steady state. Some of the angiogenic steps that become dsyregulated and the particularities of pathological angiogenic vessels are described in Table 2.

Pathological angiogenesis can occur in one or multiple organs, being systemic in the latter case. Moreover, pathological angiogenesis can be inherited or acquired (often multifactorial). The three major types of pathological angiogenesis, excessive, insufficient and abnormal neovessel formation, are depicted below in Figure 7.

Is pathological angiogenesis "good or bad"? In general, excessive, insufficient or abnormal angiogenesis is bad, because it contributes to disease progression. For example, excessive, abnormal, inflammation-induced pathological angiogenesis is detrimental to patients with chronic inflammatory diseases, such as IBD[100] and arthritis[101]. Similarly, insufficient angiogenesis has been implicated in the pathogenesis of muscular dystrophy[102], preeclampsia[103], myocardial infarction[104], stroke[105] and duodenal ulcers[106].

When dysregulated angiogenesis affects multiple organs, it becomes systemic. Systemic abnormal angiogenesis is present in HHT, an inherited vascular dysplastic disease characterized by AVM development, leading to multiple complications[107].

Table 2. Dysregulated angiogenesis generates pathological angiogenic vessels

Parameter	Characteristics of pathological angiogenic vessels
Excessive or deficient angiogenesis	Too many or too few vessels
Poor vascular quality	Loose/incomplete pericyte coverage; disappearance of basement membrane; fibrotic, occluded, tortuous vessels; thin-walled vessel, without nervous and muscular components[111]
Defective branching/transition between vessels	Disorganized, misguided sprouting; aberrant (direct) communications between vessels (e.g. arteriovenous malformations); lack of hierarchy of arterioles, capillaries and venules in tumors[112]
Dysfunctional vasculature	Increased permeability; altered hemodynamics; impaired vascular tone
Distinct molecular vascular profile	Changes in adhesion molecules, proteins, genes, transcription factors repertoires[111]

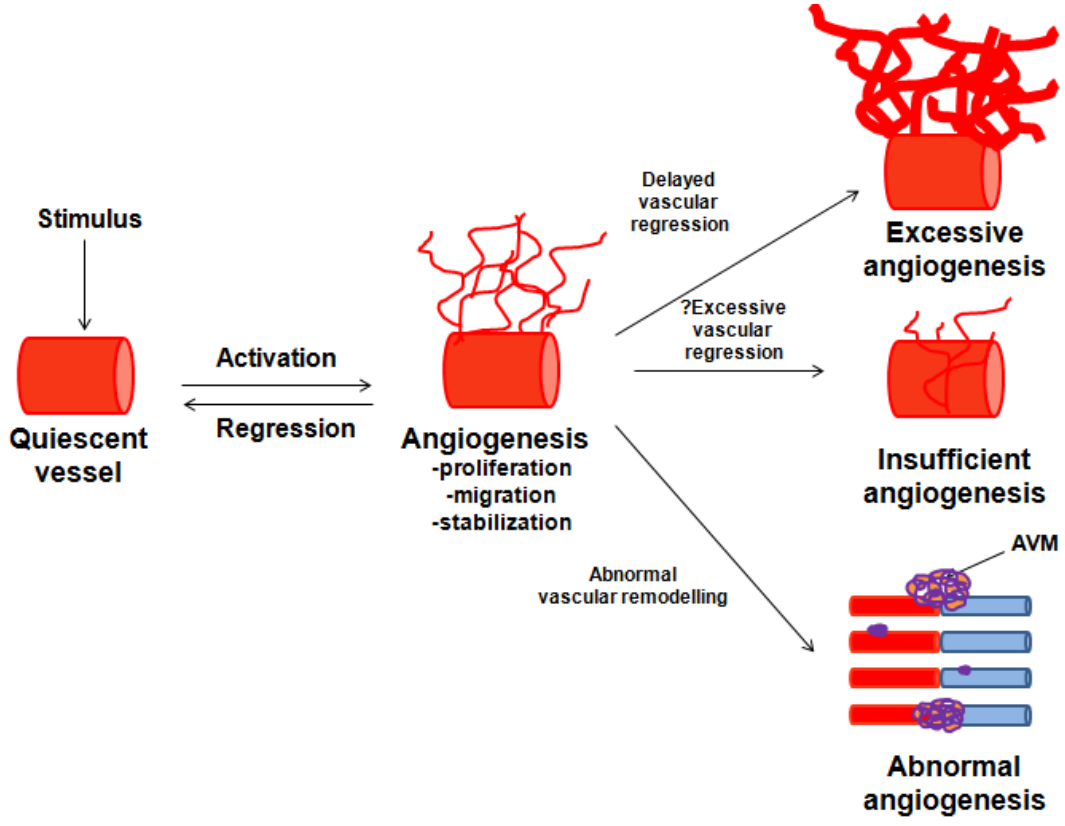

Figure 7. Formation and types of pathological angiogenic vessels. Quiescent vessels, when activated, generate angiogenic vessels. This process is reversible and initiated by the vascular regression towards the end of the healing process. Angiogenic vessels proliferate, migrate and mature. When vascular regression is delayed, excessive angiogenesis occurs. Similarly, exaggerated vascular regression can lead to insufficient angiogenesis, which is pathological. Abnormal vascular remodeling can lead to arteriovenous malformations (AVM), characterized by direct communication between arterial and venous branches, focal vascular ballooning and lastly, development of vascular malformations.

Interestingly, the organ-specific microvascular phenotype of certain "angiogenic diseases"[14] may differ within the spectrum of a given disease. For example, some of the complications of long-standing diabetes can result from deficient (e.g. impaired wound healing, embryonic vasculopathy) or excessive pathological angiogenesis (e.g. diabetic retinopathy and nephropathy)[108]. This suggests that organ-specific factors can alter the angiogenic response in the affected tissues. It is unknown if other angiogenic systemic diseases, such as cancer[25], rheumatic diseases[101], IBD, obesity[109] or atherosclerosis[110] have similar "mixed" pathological angiogenic phenotypes.

Moreover, the timing of angiogenic stimuli can influence organ-specific microvascular manifestations. For example, in retinopathy of prematurity[113], there are two stages of abnormal retinal vascularization: a) incomplete delayed retinal vascular development due to prematurity, followed by b) excessive vaso-proliferation, triggered by oxygen administration in babies delivered prematurely.

Some other factors that influence the pathological angiogenic phenotypes are explored in the next sections.

1.5.2 Angiogenic diseases

The spectrum of "angiogenic diseases" is expanding continuously and consequently, the need for novel therapies is increasing. Several non-malignant angiogenic diseases are listed in Table 3.

To understand the pathogenesis of abnormal vessel formation in angiogenic diseases, we need to elucidate what tissue-specific factors might influence the organ-dependent vascular response to angiogenic stimuli.

Table 3. Examples of several angiogenic diseases

Primary organ	Congenital diseases	Acquired diseases
Central nervous system	Moya Moya angiopathy[116]; Cerebral cavernous malformation[117]; CADASIL[118]; brain AVM in HHT[119]	Stroke[105]; Alzheimer[120]; Parkinson[121]; Multiple sclerosis[122]
Eye	Congenital vascular malformations of the retina and choroid[123]; HHT[124]	Diabetic retinopathy[108]; ROP[125]; Age-related macular degeneration[126]; Choroidal neovascularization[127]
Oral cavity	Telangiectases in HHT[128]	Chronic periodontitis[8]
Heart	Congenital heart diseases[129]; DiGeorge syndrome[130]	Myocardial infarction[104]; Cardiac hypertrophy[131]
Lungs	Primary pulmonary hypertension[132]; AVM in HHT	Asthma[133], nasal polyps
Liver	Polycystic liver disease[134]; telangiectases and AVM in HHT[135]	Portal hypertension, liver cancer, liver regeneration after partial hepatectomy[136]
Gastrointestinal tract	Telangiectases in HHT[107]	Duodenal ulcer[106]; IBD[100]
Musculo-skeletal	Muscular dystrophy[102]	Arthritis[101]
Skin	Cutaneo-mucosal venous malformations[117]; Hemangiomas[106]; HHT	Psoriasis[137]
Adipose tissue	Unknown	Obesity[109]
Kidney	Autosomal dominant polycystic kidney disease[138]	Chronic kidney diseases[139]
Reproductive tract	Unknown	Endometriosis, infertility, ovarian cysts, preeclampsia[140]

CADASIL (cerebral autosomal dominant arteriopathy with subcortical infarcts and leukoencephalopathy; HHT (hereditary hemorrhagic telangiectasia)

1.5.3 Organ-dependent angiogenesis

Blood vessels exist in every tissue. However, their response to angiogenic stimuli is contextual and depends on the presence and concentration of several factors, some of which are organ-specific[16].

First, *the organ-specific angiogenic response is influenced by the tissue-specific vascular signature.* Table 4 shows a few general and tissue-specific characteristics of vessels. For example, liver is an unique organ, with a heterogeneous vasculature, including sinusoidal endothelium, well-adapted to the complex functions of this organ[114], as depicted in Figure 8.

Second, *different types of EC can coexist in the same organ*, which alter the tissue response to angiogenic cues and/or anti-angiogenic therapies. For example, the kidney contains fenestrated EC in the peritubular capillaries, discontinuous EC in the glomerular capillaries and continuous EC in other regions[115].

Third, *cell-assisted angiogenesis* can alter the organ-specific vascular response in pathological conditions. Recently, it was demonstrated that monocytes migrating towards the perivascular space in response to organ-induced VEGF expression can be reprogrammed in the targeted organ to express a short-term pro-angiogenic and pro-arteriogenic phenotype, which contributes to organ-specific angiogenic response[6].

Fourth, *tissue microenvironment,* through specific soluble mediators, adhesion molecules, matrix proteins or local regulatory pathways can influence the vascular angiogenic response. For example, it was reported previously that transplantation of quail brain fragments to chick coelomic cavity resulted in formation of new vessels devoid of blood-brain barrier characteristics, whereas transplantation of quail somites to chick brain ventricles led to formation of vessels whose structures were similar to

Table 4. Some general and tissue-specific characteristics of vessels.

Type of vessel	Characteristics	
Artery	No valves Strong SMC coverage; Specific arterial markers (EphrinB2, Dll4, Alk1, Nrp1, EPAS-1 Hey1/2, Depp); Notch pathway components are highly expressed[141]	
Vein	Valves; Lower SMC coverage; Specific venous markers (EphB4, Nrp2, COUP-TFII); Notch pathway components are poorly expressed[141]	
Capillaries	Organ-specific endothelium	
	Continuous -non-fenestrated (brain, lungs, skin, muscles) -fenestrated (gastrointestinal tract, kidney glomerulus)[142]	*Discontinuous* - liver, bone marrow[142]

ALK1 indicates activin-receptor-like kinase 1; Depp, decidual protein induced by progesterone; Dll4, delta-like 4; EPAS-1, endothelial PAS domain protein 1; Nrp1, neuropilin 1.

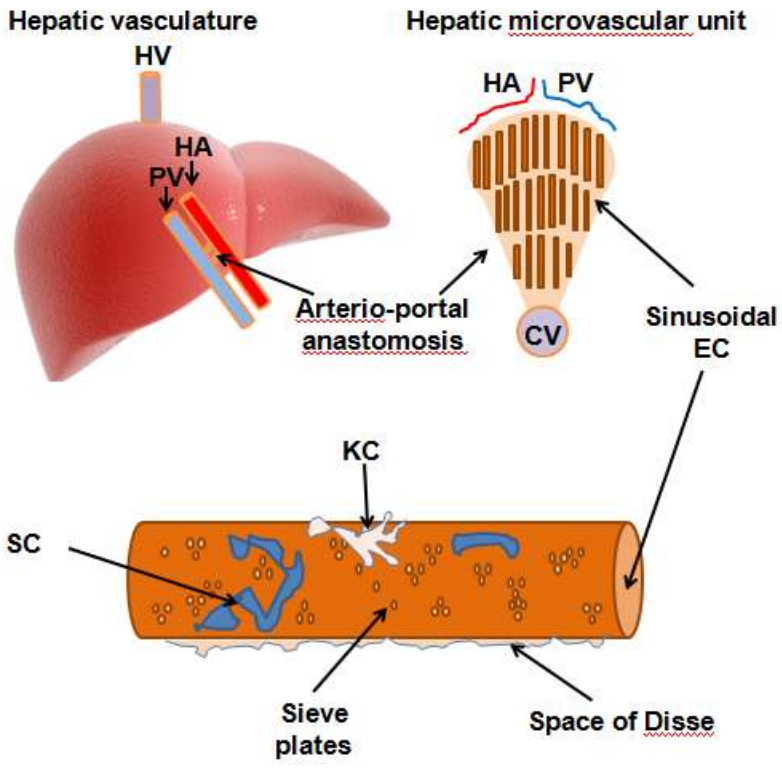

Figure 8. The hepatic macro-and microvasculature. In liver, 80% of blood enters through the portal vein (PV), the remaining 20% coming from the hepatic artery (HA). At the PV-HA anastomotic site, the blood is transported slowly through a network of specialized sinusoidal ECs that normally lack basement membrane and have multiple fenestrations, called "sieve plates". Sieve plates are tightly regulated portals that permit translocation of specific molecules. The Space of Disse (perisinusoidal space) forms between the endothelial lining and the surrounding hepatocytes, because hepatic ECs do not have an organized basement membrane. Stellate cells (SC) are specialized hepatic pericytes; Kupffer cells[52] are embedded in the sinusoidal wall and act as specialized phagocytes (adapted from[114]).

blood-brain barrier EC[143]. Yet, some form of "early" endothelial commitment exists even in the absence of the interaction with the harboring tissue, as demonstrated in the developing brain vessels[115].

Additional new tissue-specific factors that influence the organ-specific vascular responses were detected in several organs. For example, the endocrine-gland VEGF (EG-VEGF) and its receptors, endothelial gland EG-VEGFR1 and EG-VEGFR2, are found exclusively in ovary, testis, adrenal cortex and placenta[140]. Moreover, two anti-angiogenic proteins, chondromodulin-I and tenomodulin, are expressed in the avascular cartilages, ligaments, tendons and specific ocular structures[144]. Thus, these avascular tissues will be resistant to anti-angiogenic therapies. Recently, it was demonstrated that sVEGFR3 isolated so far only from the human and mouse corneas sequesters VEGF-C, inhibits lymphangiogenesis and blocks angiogenesis through inhibition of VEGF-C-induced VEGFR2 phosphorylation[39].

Fifth, *the distribution of common angiogenic and angiostatic factors and/or their receptors differ among organs.* For example, in avascular cornea, the expression of the angiostatic factors TSP-1, TSP-2, angiostatin, and endostatin is increased[17]. Moreover, VEGF receptors have an organ-specific expression[145]. VEGFR1, VEGFR2 and VEGFR3 coexist in the human ocular microvasculature, gastrointestinal mucosa, liver, kidney and lymphoid tissues. In contrast, only VEGFR-1 expression could be detected in the microvasculature of the brain and retina[145]. Furthermore, Ang-2, a vascular destabilizing and remodeling factor, has a high expression in brain, but is barely detectable in skeletal muscle[29].

Sixth, *the organ-specific angiogenic response will depend on the genetic background of the host*, as shown in congenital disorders, such as HHT, muscular dystrophy etc (see Table 3).

Overall, these findings suggest that the organ-specific angiogenic response plays a major role in health and disease and in understanding the effects of vascular-targeted therapies in experimental models and in patients.

1.5.4 Inflammation and angiogenesis

Inflammation is a rapid tissue defensive reaction to trauma, infection or sterile stimuli. Tissue cells release cytokines, which attract leukocytes from the bone marrow, circulation and vascular lumen. The vascular system is a vital participant in both acute and chronic inflammation and immune-mediated diseases. Vessels respond to inflammation through: a) functional alterations that occur first and include activation, vasodilation, increased permeability, extravasation of circulating cells, release of mediators; b) structural changes that lead to angiogenesis. The expansion of the inflamed vascular bed enhances the influx of immune cells, which further augments vessel growth. However, immune and vascular systems influence each other. Several immune cell can display pro-angiogenic properties, and the activated endothelium acquires some immune properties. Therefore, inflammation and angiogenesis are interdependent and coexist. Some of these interchangeable effects of the activated immune and vascular systems are highlighted below.

1.5.4.1 Immune cells and their cytokines have angiogenic effects

A. The role of immune cells in angiogenesis

Most activated immune cells, especially monocytes, macrophages, PMN, platelets, T and B cells, and some progenitors cells can intervene in the angiogenic switch and orchestration of both physiological and pathological angiogenesis[8]. For example, in health, PMN and natural killer cells (NK) cells are involved in cyclic uterine angiogenesis in menstruation, whereas in endometriosis, they contribute to disease pathogenesis.

a**)** *Immune cells secrete known angiogenic mediators*

PMN, myeloid-derived suppressor cells (MDSCs), dendritic cells, natural killer (NK) cells, macrophages, B cells and regulatory T cells[146] can produce angiogenic factors, such as VEGF, placental growth factor (PlGF), platelet-derived growth factor (PDGF), bFGF, Ang2, epidermal growth factor (EGF), TGF-β1, monocyte chemotactic protein (MCP-1) and several proteinases[18]. Interestingly, leukocytes can also secrete anti-angiogenic molecules, such as TSP-1, indicating that immune cells have a role both in the stimulation and inhibition of angiogenesis.

Although the amount of VEGF released by the circulating and tissue-infiltrating PMN is relatively low, the high traffic and turnover of PMN in inflammatory infiltrates may increase their contribution to the tissue VEGF pool. Moreover, PMN-derived elastase, by degrading vascular basement membranes, can facilitate EC migration into the wounded tissues[147].

Moreover, human and mouse $CD4^+CD25^+FOXP3^+$ Treg cells, at steady state and under hypoxic conditions, can secrete VEGF-A, thus having a pro-angiogenic effect. Interestingly, Treg cells also constitutively express Nrp1 and can transport additional

VEGF-A to the affected tissue[148]. Furthermore, it has recently been demonstrated that activated $CD4^+$ T cells can acquire the Nrp-1 receptor from mature DC during their interaction, and become VEGF-A-shuttling cells[18].

b) *Monocytes contribute to the differentiation of endothelial progenitor cells (EPC) into endothelial-like cells*

Activated macrophages can stimulate angiogenesis[14]. Recently, it was demonstrated that monocytes may contribute to EPC that differentiate into endothelial-like cells. For example, acetylated LDL^+ulex-lectin$^+$ monocyte/macrophage-derived EPCs have a low proliferation and endothelial differentiation potential, but are able to secrete growth factors[149]. Moreover, $Ly6C^{high}$ monocytes, known as precursors for mouse macrophages and inflammatory DC and bearing VEGFR1 on their surface, can be recruited by VEGF to sites of inflammation. After entrapment in the target organ, $Ly6C^{high}$ monocytes change their surface markers, transiently populate the inflamed tissue without proliferating or differentiating into persistent macrophages, and disappear by day 7[6]. This constant influx of new monocytes, which will be reprogrammed *in situ,* is required for continuous and efficient neovascularization, and provides a simple mean to terminate the angiogenic response after the VEGF signal ends. However, these monocytes are incapable of direct VEGF signaling[6].

B. Cytokines exert pro-angiogenic effects

Cytokines, mostly known for their pro- or anti-inflammatory properties, can induce EC proliferation, migration or survival, and/or can modulate the expression of pro- or anti-angiogenic factors.

IL-1 can reprogram the function of EC, by triggering the synthesis of some

genes and repressing others[115].

TNF-α has both pro- and anti-angiogenic effects. The pro-angiogenic effect of TNF-α occurs in a dose and time-dependent manner, by inducing the secretion of VEGF, IL-8 and bFGF in EC. It is unclear if TNF-α has direct angiogenic effects[137].

IL-8, produced by PMN, T cells, mast cells, EC and keratinocytes, is a strong pro-angiogenic factor, as it stimulates EC proliferation, migration, survival and tube formation. Importantly, this pro-angiogenic effect is independent of its pro-inflammatory functions, as IL-8 can stimulate angiogenesis in the absence of inflammation[137].

IL-17 is a pro-angiogenic factor, which induces EC proliferation, migration and tube formation and stimulates the expression of pro-angiogenic factors, including VEGF[137].

Stromal-derived factors 1 (SDF-1 or CXCL12) and monocyte chemotactic protein 1 (MCP-1) can also directly stimulate EC[5].

1.5.4.2. The activated vascular endothelium modulates the immune response in inflammation

A. The effects of VEGF and TSP-1 on immune cells

Angiogenic and angiostatic factors can act as a) chemotactic factors; b) functional modulators of immune cells.

a) *VEGF-A regulates a diverse array of immune functions*

VEGF is an important chemotactic factor for $VEGFR1^+$ monocytes/macrophages[5], which can further exert pro-angiogenic and pro-vasculogenic effects. VEGF can also recruit $VEGFR1^+$ hematopoietic progenitor cells to the affected site, facilitating their differentiation into new vascular endothelium[150]. The interaction

between VEGF-A, circulating endothelial progenitor cells (EPC) and monocytes/macrophages is depicted below in Figure 9.

Moreover, VEGF-A can impair DC function and maturation[151]. It is unknown if a similar process occurs in patients with chronic inflammatory diseases. At pathophysiologic concentrations, VEGF-A can also inhibit T cell development and function through the impairment of early hematopoetic progenitor cells[152].

Furthermore, VEGF-A treatment of mouse splenocytes induced T-cell mediated IL-10 production and suppression of interferon-γ (IFNγ) production through an undefined mechanism[18].

b) *TSP-1 has both anti- and pro-inflammatory effects*, likely due to its interactions with multiple receptors or diverse ECM proteins in the injured tissue. TSP-1 is transiently released during acute inflammation, facilitates phagocytosis of the affected cells and promotes resolution of the inflammation. Thus, enhanced production of TSP-1 could be a compensatory mechanism for controlling the immune response and protecting tissues from excessive damage.

TSP-1 mediates macrophage phagocytosis of apoptotic cells via the CD36 receptor co-expressed in macrophages and EC. By activating CD36, TSP-1 also controls blood flow and leukocyte infiltration. The TSP-1 receptor CD47 is expressed in PMN and other immune cells. CD47 activation enhances the expression of TSP-1 in leukocytes, has a role in T cell activation and also activates Treg cells. Moreover, TSP-1 also induces leukocyte apoptosis through the CD47 pathway[96].

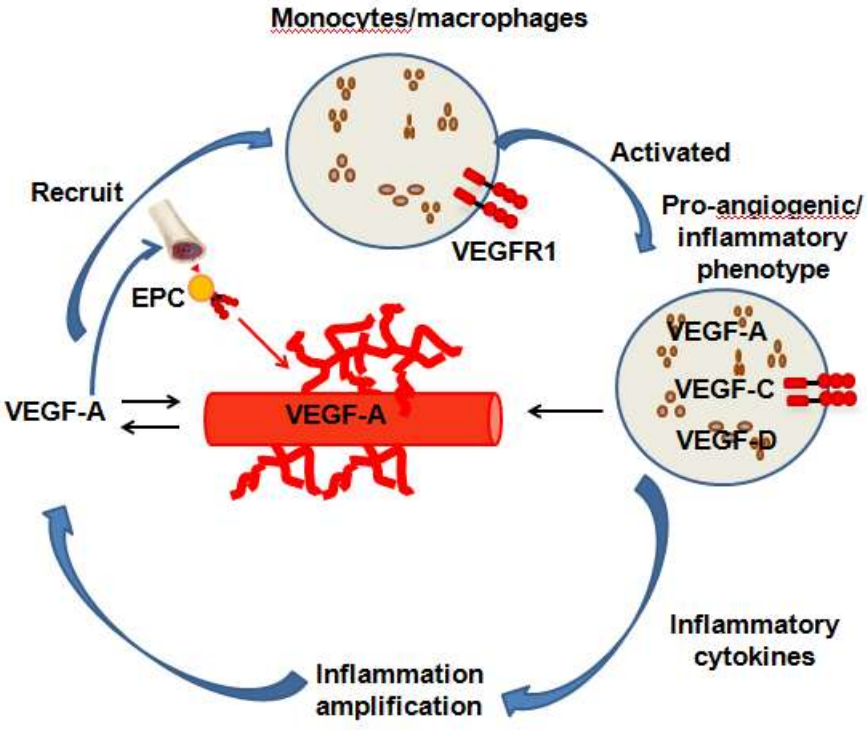

Figure 9. VEGF-induced recruitment and activation of circulating EPC, monocytes and macrophages, and secretion of VEGF from activated monocytes/macrophages. VEGF, secreted from EC and perivascular tissue, stimulates migration of endothelial progenitor cells (EPC) and monocytes/macrophages bearing VEGFR1 on their surface towards the inflamed vessel. Activated monocytes/macrophages secrete VEGF-A, C and D, amplifying the immuno-angiogenic loop.

In the early stages of injury and inflammation, high levels of TSP-1 increase the tolerance of DC to antigens, ending the inflammatory response. TSP-1 can inhibit or enhance IL-10 secretion, thus regulating DC functions. TSP-1 also inhibits APC by decreasing their capacity to sensitize the T cells in the host.

Furthermore, TSP-1 has been shown to decrease immune responses by inhibition of T effector cells, or by directly inducing T-cell apoptosis. In addition, TSP-1 promotes T cell adhesion and chemotaxis[96]. Importantly, TSP-1 also promotes chemotaxis of leukocytes to inflammatory sites. TSP-1 can also provide the co-stimulatory signal for the activation of the autoreactive T cells through interaction with CD36 on APCs and with CD47 on T cells, as shown in the inflamed rheumatoid synovium[153].

B. The immune role of the vascular endothelium

a) The vascular endothelium expresses receptors that mediate immune effects. EC express TLRs in health or under pathological conditions, such as atherosclerosis. Moreover, EC express nucleotide-binding oligomerization domains (NODs) 1 and 2, two regulators of inflammation and sensors for microbial peptides. Furthermore, EC express MHC class I and class II molecules and can potentially act as antigen presenting cells *in vitro.* Lastly, EC also display several accessory molecules that may be involved in direct stimulation of T cells, such as ICOS ligand (ICOSL), CD40, programmed cell death ligand 2 (PD-L2), CD58 (LFA-3), CD80, CD86, CD137[23,154].

b) Activated EC synthesize numerous soluble mediators that suppress immune responses, such as IL-6, IL-10, TGF-β1 and PGE2[23].

c) Endothelial-leukocyte and endothelial-platelet interactions influence T-cell function indirectly[154].

1.5.4.3 Role of TGF-β1 in immunity and inflammation

Among the multiple roles of TGF-β1, the modulation of immune and inflammatory responses is crucial. TGF-β1 controls the initiation and resolution of inflammation by regulating chemotaxis, activation and survival of lymphocytes, NK cells, DC, macrophages, mast cells, and granulocytes. This immune regulatory activity of TGF-β1 is context-, cell-, and concentration-dependent[155].

In general, TGF-β1 exerts an anti-inflammatory effect. It can a) suppress proliferation of all T cell subsets and reduce T cell responses; b) inhibit proliferation and function of B cells; c) decrease NK cells activity; d) modulate cytokine production by immune cells; e) regulate macrophage function. This crucial anti-inflammatory effect of TGF-β1 is demonstrated by the fact that *Tgfb1*-null mice, if surviving to birth, develop by 2-3 weeks of age a lethal systemic inflammatory syndrome[44].

However, TGF-β1 can also exert a pro-inflammatory activity. TGF-β1 is able to recruit both monocytes and PMN at fentomolar concentrations, and is one of the most potent monocytic and PMN chemotactic factors. In addition, TGF-β1 increases the expression of FcγRIII (CD16) on monocytes, influencing their phagocytic activity. It also promotes the monocyte-derived secretion of IL-1, IL-6, TNF-α, PlGF and TGF-β1, maintaining the inflammatory state[156].

Interestingly, TGF-β1 has both inhibitory and stimulatory effects on B cells. It reduces B cell proliferation, induces apoptosis of immature or resting B cells, blocks B cell activation and class switching, except for IgA. Moreover, TGF-β1 suppresses NK cell-derived IFN-γ production and reduces their cytolytic activity. Lastly, TGF-β1 is a strong chemotactic factor for mast cells[155].

1.5.4.4. Role of endoglin in immunity and inflammation

The role of endoglin (CD105) in immunity and inflammation is mostly unexplored. It was shown that endoglin is up-regulated upon differentiation of monocytes into macrophages and in activated monocytes[53]. Moreover, most of the human $CD4^+$ T memory cells and 30% of the naive T-cells constitutively express CD105[157]. In these T-cells, endoglin expression is increased following TCR engagement, which induces phosphorylation of CD105. In contrast to the immunosuppressive effect of TGF-β1 on T cells, endoglin enhances T cell proliferation, by transducing a signal via ERK kinase phosphorylation[157].

Endoglin expression was also found on some human $CD19^+$ (12%) and $CD20^+$ B cells (15%) and a large proportion of Treg cells (69%)[157]. The fact that endoglin is expressed in early B and stromal cells from fetal but not from adult bone marrow, suggests that CD105 might play a role in early B cell differentiation[158].

Up-regulation of endoglin expression in inflammatory conditions, such as inflammatory bowel diseases (IBD)[49], psoriasis[86], is often associated with macrophage and T cell inflammatory infiltrates[49]. However, in fibrotic tissues, high endothelial endoglin expression was seen only in areas of inflammation, in association with inflammatory cells, whereas vessels in the dermal scar had barely detectable endoglin[49].

Recently it was shown that endoglin plays a modulatory role in leukocyte trans-endothelial migration. In $Eng^{+/-}$ mice, the inflammation-induced leukocyte trans-endothelial migration to peritoneum or lungs was significantly lower compared to $Eng^{+/+}$ mice, and reversed by increased endoglin expression. Endothelial endoglin interacts with leukocyte integrin α5β1 via its RGD motif, an interaction stimulated by the inflammatory chemokine CXCL12 (stroma-derived factor 1). Thus, the endoglin RGD

extracellular domain motif might be responsible for the increased leukocyte transmigration[159].

Furthermore, long-term treatment with TNF-α of human dermal microvascular EC reduced by more than 50% the endoglin protein levels, but not the transcriptional levels[160].

1.6 Hereditary hemorrhagic telangiectasia (HHT) and inflammatory bowel diseases (IBD) are angiogenic diseases

1.6.1 Hereditary hemorrhagic telangiectasia (HHT)

1.6.1.1 Contribution of endoglin and ALK1 to HHT pathogenesis

Hereditary hemorrhagic telangiectasia (HHT) is an autosomal dominant vascular disease, characterized by multiple muco-cutaneous telangiectases, recurrent nose bleeding episodes and development of arteriovenous malformation (AVM) in major organs: lungs (~50%), liver (~30%), brain (~10%)[161]. More than 80% of cases of HHT arise from mutations in *ENG* (HHT1) and *ACVRL1* (*ALK1*; HHT2) genes, respectively. A few patients with mutations in *MADH4* (the gene responsible for producing SMAD4) can also develop HHT associated with juvenile polyposis (2% to 3%). Overall, *ENG* mutations are more common (61%) than *ACVRL1* mutations (37%) or *MADH4* (2%)[161]. The rest of patients (~ 20%) have no identifiable mutation. Recently, two new loci have been reported in linkage disequilibrium with HHT: the HHT3 locus, on chromosome 5q31[162] and the HHT4 locus on chromosome 7p14[163].

Several studies have shown that *ENG* or *ALK1* haploinsufficiency is the underlying mechanism of HHT1 and HHT2 respectively. This implies that the lower

level of expression of these two genes rather than specific mutations, is responsible for some of the major phenotypic manifestations. For example, pulmonary and cerebral AVMs are more frequent in HHT1 than in HHT2 patients[3]. In contrast, hepatic AVMs and gastrointestinal teleangiectases are more often found in HHT2 than HHT1 patients. More recently, pulmonary arterial hypertension (PAH) has also been associated with mutations in *ALK1* and *ENG*, with most of the cases attributed to *ALK1* deficiency[161].

1.6.1.2. Dysregulated angiogenesis in HHT

The experimental work done in the last two decades has shown clearly that HHT is an inherited angiogenic disease[107], leading to AVM formation. It is recognized that haploinsufficiency in *ENG* and *ALK1* represents the fundamental mechanism responsible for HHT, leading to vascular malformations. A schematic diagram of how *ENG* and *ALK1* deficiency leads to dysregulated angiogenesis is shown in Figure 10. Confirming this mechanistic concept, *Endoglin*[60] or *Alk1*[69] heterozygous null mice developed AVM. How the targeted deletion leads to anomalies in vessels is still unclear. What is know is that $Eng^{+/-}$ 129/Ola mice developed dilated postcapillary venules in skin, and ~ 70% of them lack SMC. In addition, the perivascular collagen and elastin layers were irregular, adding to the fragility of these vessels[164]. Furthermore, *Alk1*-conditional deletion resulted in enlarged, tortuous vessels with thin walls, loss of capillaries and development of severe AVMs[79].

However, other modifier genes, tissue-specific and environmental factors (such as infections or trauma) might trigger the dysregulated angiogenesis in HHT and cause the heterogeneous HHT manifestations. For example, the $Eng^{+/-}$ 129 strain developed earlier and more severe HHT manifestations than $Eng^{+/-}$ C57BL/6 mice[165], suggesting

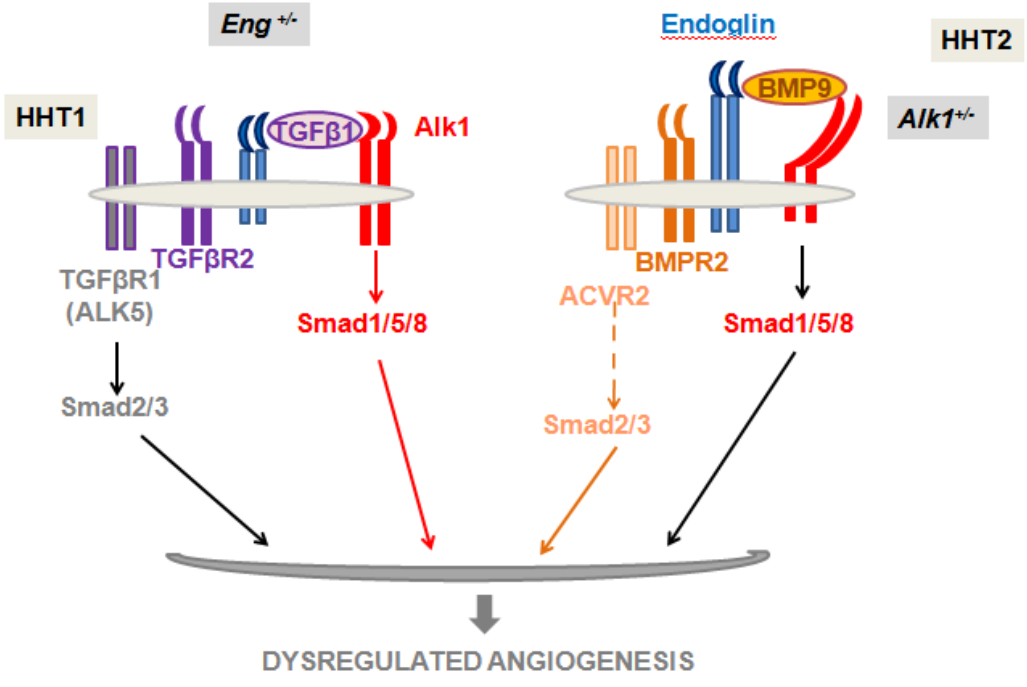

Figure 10. Endoglin and ALK1 haploinsufficiency contribute to dysregulated angiogenesis in HHT. Endoglin and ALK1 bind TGF-β1 and BMP9 and modulate their signaling. *ENG* haploinsufficiency (in HHT1) leads to impairment of the TGF-β1-TGFβR2-TGFβR1(Alk5) downstream signaling and Alk1-mediated pathway. ALK1 deficiency (in HHT2) alters primarily the BMP9-mediated downstream route, and also the TGF-β1-ALK5 pathway. Overall, the outcome in both *ENG* and *ALK1* deficiencies is dysregulated angiogenesis. *ENG* and *ALK1* haploinsufficiency are represented by 50% reduced thickness of the bars, depicting the corresponding dimers.

that perhaps modifier genes, some of which could be tissue-specific, may influence the HHT phenotype. Furthermore, the endoglin/CD31 ratio was similar in pulmonary AVMs and non-affected vessels in HHT1 patients, suggesting that AVMs could not be attributed to a focal loss of endoglin[166]. Recently, a human polymorphic variant of non-receptor tyrosine phosphatase *PTPN14* within the *TGFBM2* locus has been shown to influence the severity of pulmonary AVM in HHT1 and HHT2 patients, by alterations in angiogenic and/or arteriovenous fate in the affected vessels in HHT, via EphrinB2 and ALK1 signaling[167].

It is debatable whether the primary HHT lesions occur in the venous or arterial vascular bed. From the pathologic point of view, the earliest vascular alteration in HHT is the focal dilatation of postcapillary venules, followed by changes in SMC layers and then loss of capillaries[168]. This suggests that a venous defect could be the initiating factor in AVM. However, defective arteries could undergo the primary vascular change in HHT2, as *ALK1* is almost exclusively expressed in arteries, and ALK1 haploinsufficiency leads to HHT2[68].

Furthermore, the perivascular supporting tissue might be defective in HHT. Loss of endoglin in E9.5 $Eng^{-/-}$ yolk sacs caused poor vascular SMC development and arrested endothelial remodeling, demonstrating that endoglin mediates the endothelial-mesenchymal contact that is essential for angiogenesis[169]. Moreover, in a telangiectasia (small AVM) in HHT, pericytes display prominent stress fiber, in contrast to pericytes from normal skin vessels[170].

Moreover, intracellular changes in the organization and structure of the cytoskeleton could precede the development of HHT lesions. For example, it was shown

that blood outgrowth EC obtained from HHT1 patients have a disorganized cytoskeleton and a depolymerized F-actin, which correlated with lower endoglin levels. Thus, endoglin deficiency could lead to abnormal cytoskeleton structure and organization, which may impair the endothelium and vascular strength[171].

It was postulated that a second hit is necessary to activate the abnormal EC to proliferate and develop AVM[69,75]; for example, intracranial VEGF-induced angiogenic stimulation in *Eng* and *Alk1* heterozygous mice led to brain AVM formation[172]. Moreover, the perivascular lymphocytic and monocyte/macrophage infiltrates observed in cutaneous telangiestases might contribute to AVM development[168].

1.6.2 Inflammatory bowel diseases (IBD)

IBD are chronic inflammatory disorders characterized by severe gut inflammation and pathological angiogenesis, leading to multiple life-long complications. Intestinal pathological angiogenesis accompanies and enhances the inflammation, thus plays a pathogenic role in IBD.

1.6.2.1. Angiogenic dysregulation in IBD

In the last decade, the concept of pathological angiogenesis contributing to progression of inflammatory bowel disease has gained more acceptance and interest. It is now recognised that not only the infiltrating immune cells induce a pro-angiogenic vascular response in the inflamed gut, but also that the non-immune vascular and perivascular cells can modulate the immune response in IBD[100,154]. Hence, the bidirectional dysregulated immunity and angiogenesis drive the chronic inflammation in IBD.

IBD is characterized by chronic gut inflammation, ulceration, and regeneration,

accompanied by abnormal vessels. These vessels become activated, leaky, adhesive for leucocytes, pro-coagulant and proliferative, in other words, angiogenic. The recruitment of circulatory leukocytes occurs primarily at the level of postcapillary venules[154]. In IBD, several adhesions molecules show an enhanced expression: selectins, integrins and IgG superfamily molecules (especially ICAM-1, VCAM-1, CD31 and mucosal addressin cell adhesion molecule, MAdCAM-1)[173]. In addition, intestinal EC in IBD also express the CD40 co-stimulatory molecule, which binds to CD40L on T-cells and platelets, increasing their adhesion, thus the influx of these cells towards the inflamed gut[174]. Furthermore, previous work by Burgio et al. showed that monocytes, macrophages, $CD19^+$ B and naive T cells were preferentially recruited to the chronically inflamed intestine in IBD[175]. It also appeared that the perivascular extravasate of naive T cells underwent local activation and induction to express the memory phenotype after further cell-cell interaction[175]. Figure 11 depicts the interaction between an inflamed, angiogenic vessel and several immune cells.

Furthermore, several studies confirmed *in vivo* that the intestine of patients with IBD has an increased number of abnormal vessels in the inflamed gut areas, suggesting that active angiogenesis has occurred[176, 177].

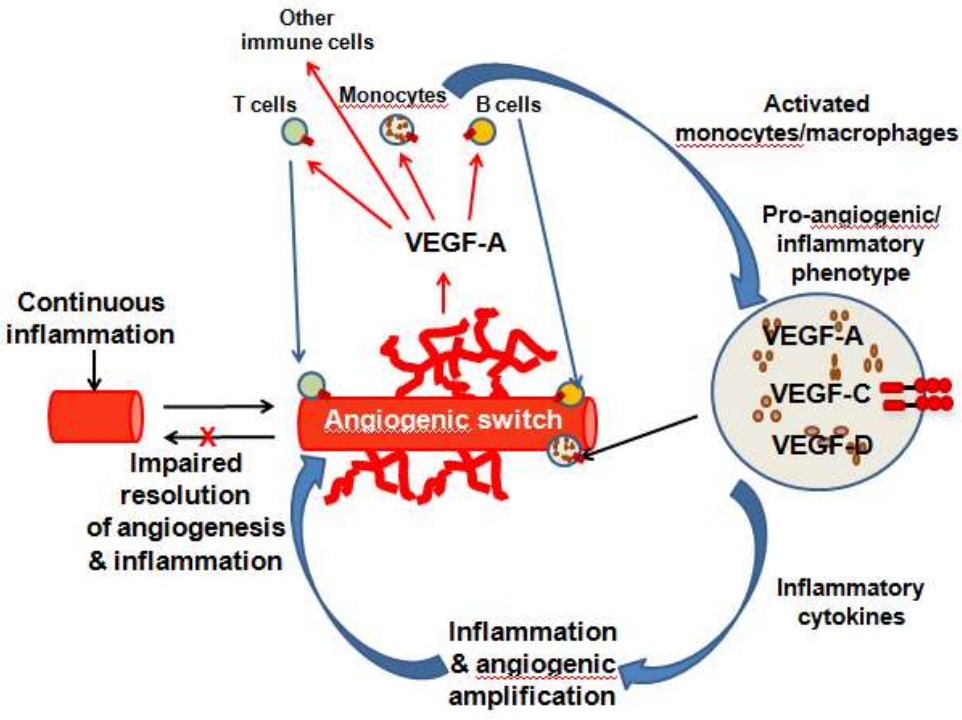

Figure 11. Simplified model of the interaction between an inflamed, angiogenic vessel and several immune cells. Persistent inflammation leads to emergence of angiogenic vessels. These vessels become adherent for immune cells, lose their angiogenic homeostasis and secrete VEGF, which mediates recruitment of immune cells such as naive T, B cells, monocytes via activation of their VEGFR1. These activated inflammatory cells migrate towards the inflamed gut, become pro-angiogenic and further differentiate into memory T cells and inflammatory/pro-angiogenic macrophages. These events result in amplification of both gut inflammation and associated pathological angiogenesis, leading to chronic IBD.

In IBD, one of the mechanisms leading to pathological angiogenesis in the inflamed gut is an increase in angiogenic or angiostatic factors, which alters the angiogenic balance. The profile of the angiogenic/angiostatic factors depends on several host- and environmental-dependent factors. For example, the angiogenic profile is distinct in dextran sodium sulfate (DSS)-induced and CD4+CD45RB^{high} T cell transfer models of colitis, two of the commonly used models to study the mechanisms in IBD. In these two models that showed an increase in gut microvessel density (MVD), a marker of pathological angiogenesis, the angiostatic factor TSP-1 was up-regulated in the inflamed colon, whereas the tissue levels of one of the most potent angiogenic factors VEGF and FGF levels were unchanged, suggesting that factors other than VEGF may contribute to increase in MVD. Interestingly, an increase in the angiostatic molecules angiostatin and endostatin in IBD might destabilize these angiogenic vessels, by preventing the pericyte stabilization and maturation[178].

Moreover, the inflammation-mediated pathological angiogenesis in IBD can be influenced by the cytokine and chemokine milieu. Several pro-inflammatory cytokines and chemokines, such as TNF-α, IL-1β, monocyte chemoattractant protein-1 (MCP-1), CXCL1 (or Gro-1, KC), can have pro-angiogenic properties in IBD, hence enhancing the pathological angiogenesis in the inflamed gut[178].

1.6.2.2. Contribution of endoglin to IBD

Under physiological and pathological conditions, it has been shown that endoglin can modulate TGF-β1-mediated signaling[28]. Thus, a deficiency in endoglin should lead to impairment in TGF-β1 signaling, excessive angiogenesis and immune response. When subjected to a single course of DSS, *Eng*$^{+/-}$ mice develop severe gut inflammation

and pathological angiogenesis, associated with increased VEGF tissue levels, suggesting that the angiogenic and immune balance were lost[179]. The mechanisms through which excessive inflammation and pathological angiogenesis occur in colitic *Eng*$^{+/-}$ mice remain to be determined.

TGF-β1 regulates initiation, resolution of inflammation and angiogenesis and fibrosis. These processes are impaired in IBD[180]. As TGF-β1 is found both in epithelial and T cells in the inflamed intestine, the amount of tissue TGF-β1 will reflect the degree of epithelial damage and regeneration and the amount of immune cells infiltrating the inflamed gut. Thus, the roles exerted by TGF-β1 in colitis are context- and cell-dependent[155].

Interestingly, cultured fibroblasts from the strictures of patients with Crohn's disease showed increased cell-surface and whole-cell expression of endoglin relative to control cells. In addition, siRNA silencing of endoglin in these fibroblasts led to enhanced TGF-β1-mediated Smad3 phosphorylation, suggesting that endoglin is a negative regulator of TGF-β1 signalling in the intestinal fibroblast and modulates Smad3 phosphorylation in IBD[181]. However, in the active lesions of the inflamed gut mucosa, the ratio of phosphorylated/total Smad3 was reduced, possible due to increase in Smad7 inhibitor levels in the inflamed mucosal and T cells[182]. Importantly, TGF-β1 signaling impairment led to loss on inhibition of the pro-inflammatory cytokines in isolated lamina propria mononuclear cells from patients with Crohn's disease. These findings indicate that impaired TGF-β1 signaling in IBD leads to increase gut inflammation.

Moreover, it appears that endoglin has a role in tissue repair. Protein levels of endoglin (CD105) start to rise one to two days after human skin wounding, further increase to 3-8 fold higher than the baseline values and remained high for up to 28 days,

when they begin to fall. Maximal endoglin expression was noted at days 7 to 10, coinciding with the peak of T cell extravasation and the point of maximum EC proliferation, thus with peak of inflammation and angiogenesis. Throughout the wound healing, endoglin was primarily detected in EC and myofibroblasts, not in SMC or macrophages, the other tissue cells that can express endoglin. In contrast, tissue CD31 protein expression barely changed between days 0 to 7 of healing, even though CD31 is considered a pan-endothelial marker[49]. These findings imply that endoglin is an accurate marker of tissue remodeling during wound healing.

Furthermore, $Eng^{+/-}$ mice subjected to skin injury, showed a delay in wound closure when compared to $Eng^{+/+}$ mice, especially in the first 2 to 8 days after the injury, demonstrating that endoglin is necessary for tissue repair[183]. The progression of tissue endoglin expression during the wound healing is shown in Figure 12.

1.7 The role of vascular-targeted therapy in angiogenic diseases

1.7.1 Overview of role of anti-angiogenic therapy

Since Dr. Folkman demonstrated that targeting the tumor-dependent vasculature can reduce the size of the tumor[2], the field of "anti-angiogenic" therapy evolved considerably. Initially, it was thought that targeting the activated but genetically stable EC that comprise the tumor vasculature avoided the acquired drug resistance, often seen with the genetically unstable tumor cells[111]. However, this was not the case, particularly when the anti-angiogenic agents were used as mono-therapy in cancer treatment, as genetic alterations occur in tumor vasculature[184]. It has also become clear that VEGF is one of the major driving factor in angiogenesis, including in tumors.

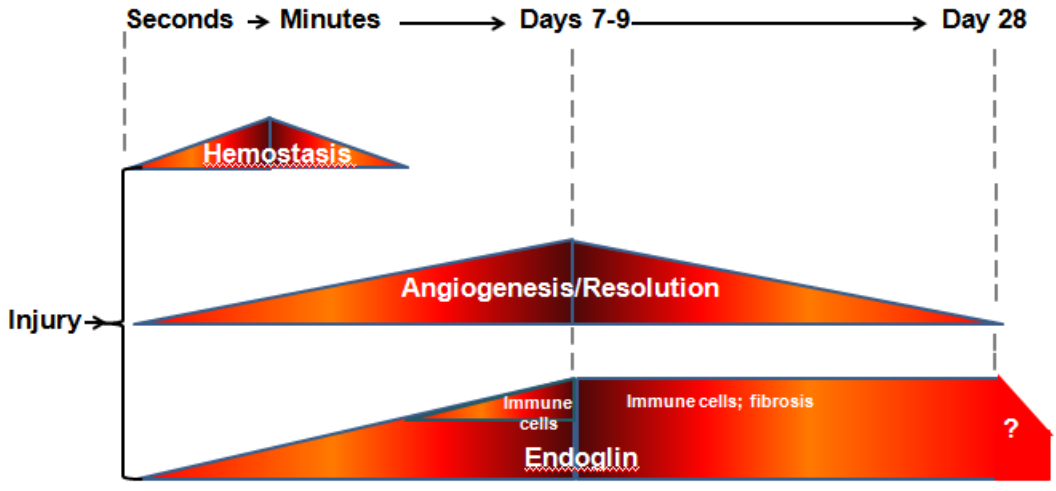

Figure 12. Temporal progression of endoglin expression during wound healing. Endoglin is expressed on quiescent and activated EC, and some immune and stromal cells. Hemostasis is the immediate response to injury, followed rapidly by angiogenesis, influx of immune cells and beginning of the repair process. Tissue endoglin expression peaks between days 7 to 9 of injury, persists until day 28 after injury, after which it starts to decrease (adapted from[49]).

Importantly, in contrast to endogenous angiostatic proteins that are directly anti-angiogenic, the anti-VEGF agents act as indirect anti-angiogenic factors when used in tumors, as they inhibit the products of tumor cells[185].

The first anti-human VEGF monoclonal antibody approved by FDA to treat colon cancer in combination with standard chemotherapy was bevacizumab[186]. Later, encouraging results were reported in a number of cancers, including metastatic non-small cell lung[187], renal[188] and ovarian[189] cancers. Yet in breast cancer, the results were inconclusive. Irrespective of the type of cancer, the benefits of this therapy in patients were small, a few months gain in the overall survival. Several reasons could explain these results: acquired or inherited drug resistance, short duration of therapy, facilitation of tumor and vascular re-growth after discontinuation of anti-angiogenic therapy, compensation by other alternative angiogenic factors, incomplete disruption of basement membrane and pericytes etc[112,190,191]. Moreover, the increased use of anti-angiogenic therapy in the last decade revealed that side effects can occur, serious ones being systemic hypertension, gastrointestinal perforations, strokes, wound dehiscence, severe proteinuria, bleeding episodes etc[192].

Interestingly, several studies have shown that anti-endoglin DNA oral vaccines exert anti-metastatic and anti-angiogenic effects in a mouse model of breast carcinoma cells[193] and aggressive melanoma over-expressing endoglin[194].

Moreover, VEGF inhibitors have proven useful in diseases in which VEGF is the principal pathogenic angiogenic factor, as is the case for retinal vascular disorders, including ROP, glaucoma, and even inflammatory choroidal neovascularization disorders[191,195].

1.7.2 Anti-VEGF therapy in HHT

The use of anti-angiogenic therapies in vascular dysplastic disorders has been sporadic at best, in part because the mechanisms of dysregulated angiogenesis in these disorders are still not deciphered. However, since VEGF emerged as one of the factors that potentially plays a role in the pathogenesis of HHT, several studies have now reported the effects of anti-VEGF therapy in patients with HHT. The first case report described the dramatic decrease in the frequency of required blood transfusions and an improvement in the cardiac output in a patient with HHT who received bevacizumab in addition to standard chemotherapy for his mesothelioma[196]. Impressively, a second case reported that six courses of bevacizumab (5 mg/kg) given over 12 weeks reversed the need for liver transplantation and the cardiac failure due to severe and extensive HHT[197]. Lately, several studies have reported the use of intranasal bevacizumab by submucosal injection, in doses varying from 3.75 mg[198] to 100 mg[199], with good results in reducing nosebleeds. Similarly, 1mg/nostril of bevacizumab added in hypertonic saline succeeded to stop the nasal bleeding for 3 months after a total dose of 8 mg[200]. Importantly, a single-center non-randomized phase 2 trial of bevacizumab (5 mg/kg every 14 days for a total of 6 injections), in patients with severe liver involvement and high cardiac index secondary to HHT demonstrated normalization of cardiac output, pulmonary hypertension (in 5/8 patients) and improvement in some hepatic hemodynamic parameters at 6 months of follow-up. However, given the short duration of treatment, the long-term safety of this therapy could not be established[201].

Moreover, use of the direct anti-angiogenic inhibitor thalidomide in several patients with HHT1 and HHT2 demonstrated that 100 mg/day of thalidomide lowered the frequency of epistaxis within 1 month and that the average circulating hemoglobin

concentration increased without additional dietary iron supplementation. In addition, *Eng*$^{+/-}$ mice treated with thalidomide displayed an increase in mural SMC cell recruitment to the defective arteries, without changes in their vessel size, patterning or microvessel density and without altering vascular growth.

1.7.3 Anti-VEGF therapy in inflammatory disorders

Immune-mediated inflammatory diseases, despite their treatment with a plethora of anti-inflammatory, immunosuppressant and biological therapies, often progress, relapse and lead to severe regional and systemic complications, some of which are lethal. As pathological angiogenesis is intertwined with inflammation, it is critical to determine if anti-angiogenic agents can reduce both the abnormal tissue vascularisation and alleviate the inflammatory process.

Human data about efficacy of anti-angiogenic therapy in chronic inflammatory diseases is scarce and originate from sporadic case reports. Recently it was shown that treatment with bevacizumab (5 mg/kg every 2 weeks for a total of 4 and 14 cycles respectively), in combination with standard chemotherapy in two patients with metastatic colon cancer, was associated with remission of the underlying IBD[113]. Moreover, remission of psoriasis following bevacizumab therapy (5 mg/kg every 2 week) in addition to chemotherapy for colon cancer was noted 45 days after commencing the anti-angiogenic treatment[202]. However, it remains to be determined if these effects are bevacizumab or chemotherapy-dependent.

Promising results have emerged from several experimental studies that investigated the effects of anti-angiogenic therapy in psoriasis[35], IBD[203] and experimental autoimmune encephalomyelitis[204]. These studies have demonstrated that in addition to anti-angiogenic effects, the anti-VEGF agents can decrease the number

and/or function, migration and transmigration of some immune cells involved in the pathogenesis of these chronic inflammatory diseases, thus may have an additional anti-inflammatory effect.

1.8 Thesis objectives

1.8.1 Rationale

Dysregulated angiogenesis plays a critical role in the pathogenesis of HHT and IBD. A major angiogenic factor is VEGF that might play a pathogenic role in these diseases.

Elevated circulatory and nasal tissue VEGF levels were reported in patients diagnosed with HHT[205, 206]. Moreover, it was shown that VEGF injected intracranially in either *Eng*$^{+/-}$ or *Alk1*$^{+/-}$ mice increased the cerebral MVD and led to the development of abnormal AVM-like structures, demonstrating that VEGF can trigger the abnormal angiogenesis in these mouse models of HHT[172]. However, it is unknown if dysregulated angiogenesis is organ-specific and if VEGF is the major contributor to abnormal vesselsformation in HHT.

Furthermore, recent human studies showed that bevacizumab reduced the frequency of epistaxis and requirements for blood transfusions[196], decreased the hyperdynamic cardiac output secondary to intrahepatic arteriovenous shunting, improved PAH in several patients[201] and even eliminated the need for liver transplantation in one case[197]. These observations suggest that anti-VEGF therapy may have beneficial effects in HHT patients. However, the mechanisms through which anti-VEGF therapy might exert beneficial effects in HHT are unknown.

In IBD, alteration in TGF-β1-mediated initiation and resolution of inflammation, angiogenesis and fibrosis contributes to pathogenesis of disease[180]. Moreover, an increase in intestinal endoglin levels, the co-receptor for TGF-β1, was reported in patients[49, 181] and mouse models of IBD[207]. In addition, the ratio of phosphorylated/total Smad3 was reduced in the active intestinal lesions of patients with Crohn's disease, suggesting that the downstream TGF-β1-mediated signaling is impaired[182]. Furthermore, *Eng*$^{+/-}$ mice subjected to a single course of the chemical irritant DSS, developed severe gut inflammation and pathological angiogenesis, indicating that endoglin might play a role[179]. However, the endoglin-mediated mechanisms responsible for excessive inflammation and pathological angiogenesis in IBD are unknown.

VEGF is a major angiogenic factor that can modulate the response of several immune cells in inflammation. Increased serum and colonic VEGF levels were reported in patients diagnosed with IBD[208-210]. Moreover, DSS-induced colitic *Eng*$^{+/-}$ mice had elevated colonic VEGF levels[179]. Yet, the role of VEGF in pathogenesis of IBD is poorly understood. Furthermore, one case report[113] and an experimental study showed that the anti-VEGF therapy might have beneficial effects in IBD[211]. However, the mechanisms of anti-VEGF therapy in IBD are largely unexplored.

1.8.2 Hypothesis

VEGF plays a pathogenic role in HHT and IBD and VEGF-targeted treatment will improve the dysregulated angiogenesis in *Eng*$^{+/-}$ and *Alk1*$^{+/-}$ models of HHT, attenuate inflammation and restore the angiogenic balance in the DSS-induced colitic *Eng*$^{+/-}$ mice.

1.8.3 Specific objectives

1) To investigate the organ-specific angiogenic phenotype, determine if VEGF plays a major role in the pathogenesis of HHT and investigate the effects of anti-VEGF therapy on dysregulated angiogenesis in $Eng^{+/-}$ and $Alk1^{+/-}$ models of HHT.

2) To determine if anti-VEGF therapy has beneficial effects on pathological angiogenesis and chronic inflammation and restored the angiogenic balance in the DSS-induced colitic $Eng^{+/-}$ mice.

The results from objectives 1 and 2 are reported in Chapters Two and Three of this thesis.

Chapter Two

Endoglin and Activin receptor-like kinase 1 heterozygous mice have a distinct pulmonary and hepatic angiogenic profile and response to anti-VEGF treatment

Daniela S. Ardelean[1,2,3], Mirjana Jerkic[1,4], Melissa Yin[5], Madonna Peter[1,3], Bo Ngan[6], Robert S. Kerbel[5,7], F. Stuart Foster[5,7], Michelle Letarte[1,3,4,7]

[1]Molecular Structure and Function Program, Hospital for Sick Children, Toronto; [2]Division of Rheumatology, the Hospital for Sick Children, Toronto; [3]Department of Immunology, University of Toronto; [4] Heart and Stroke Richard Lewar Centre of Excellence, University of Toronto; [5]Biological Sciences, Sunnybrook Health Sciences Center, Toronto; [6]Division of Pathology, Hospital for Sick Children and Department of Laboratory Medicine and Pathobiology, University of Toronto; [7]Department of Medical Biophysics, University of Toronto, Toronto, Ontario, Canada

In this Chapter Two, I developed the treatment protocol, performed all mouse experiments, monitored the mice for the entire duration of the experiments and treated the mice with G6-31 antibody and PBS vehicle. I performed the blood pressure, heart rate and proteinuria measurements, in collaboration with Dr. Mirjana Jerkic. I measured the weight of all hearts; Dr. Mirjana Jerkic assisted and participated in weight measurements of several hearts. In addition, I developed a new ultrasound hepatic protocol, in collaboration with Ms. Melissa Yin from Dr. Stuart Foster's laboratory. Ms. Melissa Yin performed all ultrasound experiments and I participated in these

experiments. I collected all the tissues used in these experiments, quantified the MVD and the alveolae in the lungs, and also measured the colonic MVD. Dr. Mirjana Jerkic assisted in the repeated assessment of the lung MVD. In collaboration with the team from the Pathology Core Centre from Modeling Human Disease Toronto Centre for Phenogenomics (TCP) in Toronto, I developed a new hepatic and cardiac computerised protocol for immunohistochemical MVD quantification in these organs. I performed all the protein extractions, TGF-β1 and VEGF ELISA measurements, and western blot for all lung and liver proteins tested in this chapter. Dr. Mirjana Jerkic did western blot duplicates for lungs and performed the endothelial cell experiments. I carried out all statistical analysis for these experiments. This project was supervised by Dr. Michelle Letarte.

2.1 Abstract

Hereditary hemorrhagic telangiectasia (HHT) is a vascular dysplasia associated with dysregulated angiogenesis and arteriovascular malformations. The disease is caused by mutations in *endoglin* (*ENG;* HHT1) or *activin receptor-like kinase 1* (*ALK1;* HHT2) genes, coding for transforming growth factor β (TGF-β) superfamily receptors. Vascular endothelial growth factor (VEGF) has been implicated in HHT and beneficial effects of anti-VEGF treatment were recently reported in HHT patients. To investigate the systemic angiogenic phenotype of *Endoglin* and *Alk1* mutant mice and their response to anti-VEGF therapy, we assessed microvessel density (MVD) in multiple organs after treatment with an antibody to mouse VEGF or vehicle. Lungs were the only organ showing an angiogenic defect, with reduced peripheral MVD and secondary right ventricular hypertrophy (RVH), yet distinctly associated with a 4-fold increase in thrombospondin-1 (TSP-1) in $Eng^{+/-}$ versus a rise in angiopoietin-2 (Ang-2) in $Alk1^{+/-}$ mice. Anti-VEGF treatment did reduce lung VEGF levels but interestingly, led to an increase in peripheral pulmonary MVD and attenuation of RVH; it also normalized TSP-1 and Ang-2 expression. Hepatic MVD, unaffected in mutant mice, was reduced by anti-VEGF therapy in heterozygous and wild type mice, indicating a liver-specific effect of treatment. Contrast-enhanced micro-ultrasound demonstrated a reduction in hepatic microvascular perfusion after anti-VEGF treatment only in $Eng^{+/-}$ mice. Our findings indicate that the mechanisms responsible for the angiogenic imbalance and the response to anti-VEGF therapy differ between *Eng* and *Alk1* heterozygous mice and raise the need for systemic monitoring of anti-angiogenic therapy effects in HHT patients.

2.2 Introduction

Hereditary hemorrhagic telangiectasia (HHT) is a systemic vascular dysplastic disorder affecting 1/5,000-8,000 people worldwide[3,212]. HHT is characterized by the development of arteriovenous malformations (AVMs) in lungs, liver, gut, brain, mucosae and skin[213]. These abnormal vascular structures can cause severe recurrent bleeding episodes, stroke, or cardiac failure secondary to hyperdynamic hepatic circulation.

Mutations in *endoglin (ENG)* and *activin receptor-like kinase 1* (*ACVRL1* or *ALK1*) genes lead to HHT1 and HHT2 respectively, and haploinsufficiency is the underlying mechanism of disease[214]. Although the manifestations vary from patient to patient, the frequency of pulmonary and cerebral AVMs is higher in HHT1 than HHT2, whereas hepatic and gastrointestinal involvement is more often diagnosed in HHT2 than HHT1 patients[212]. This indicates some heterogeneity in the response of different organs to a reduction in functional *ENG* or *ALK1* levels in HHT patients. Moreover, *ALK1* mutations (more often than *ENG* mutations) are associated with pulmonary arterial hypertension (PAH), even in the absence of classical signs of HHT[215,216]. These observations suggest that different signaling pathways may be altered in the lung vasculature of *ENG* and *ALK1* deficient individuals.

Endoglin and ALK1 are predominantly expressed in endothelial cells and are receptors of the transforming growth factor β (TGF-β) superfamily that mediate responses to bone morphogenetic protein-9 (BMP9) and TGF-β1/β3[217, 218]. Endoglin and ALK1 both bind BMP9 with high affinity and in association with BMPR2, signal via Smad1,5,8 pathways. For TGF-β1/β3 responses, endoglin acts as a co-receptor and interacts with TβRII and ALK5 to activate Smad2,3 dependent pathways, or with TβRII

and ALK1 to signal via the Smad1,5,8 pathways. Endoglin was reported to influence mostly ALK1-dependent pathways, while mutations in ALK1 lead to activation of the ALK5 cascade[82, 219, 220]. Therefore, both ALK1 and ALK5-mediated pathways will be affected in HHT1 and HHT2, albeit with different outcomes. In general, ALK5 signaling is involved in the early phase of angiogenesis, whereas the ALK1 pathway contributes to the vessel maturation phase[221]. TGF-β1 and BMP9 have been implicated in angiogenesis and extracellular matrix remodeling, in a context-dependent manner[222]. Yet, the regulation of angiogenesis through these ligands and signaling pathways and their relevance to HHT is poorly understood.

Genetically-modified mice lacking either *Endoglin* or *ALK1* die at mid-gestation of cardiovascular and angiogenic defects[60,76]. In agreement with the haploinsufficiency model of disease, *Eng*$^{+/-}$ [60,223] and *Alk1*$^{+/-}$ [224] mice survive but may develop strain-dependent vascular malformations. For example, *Eng*$^{+/-}$ mice on the 129/Ola background develop AVMs in multiple organs, including liver and lungs[165], and endothelial-specific deletion of *ENG* or *ALK1* can cause AVM-like structures in several organs[75, 225]. On the other hand, adult *Eng*$^{+/-}$ and *Alk1*$^{+/-}$ mice on the C57BL/6 background show oxidative stress-dependent endothelial dysfunction in several organs and impaired vasomotor tone [226], but rarely develop AVMs. The major phenotype observed in these mutant mice is spontaneous pulmonary arterial hypertension (PAH), associated with rarefaction of the peripheral lung vasculature and secondary right ventricular hypertrophy (RVH)[227,228]. Overall, these findings have led to the concept that mutations in *ENG* and *ALK1* genes are associated with dysregulated angiogenesis, predisposing to HHT and/or PAH[164, 222].

Angiogenesis, the formation of new vessels from the preexisting vascular bed, under physiological or pathological conditions, causes increase in tissue microvessel

density (MVD), an established angiogenic parameter and a prognostic marker in patients diagnosed with cancer and treated with anti-angiogenic agents[229]. In HHT patients and animal models, tissue- and context-dependent excessive or reduced angiogenesis have been observed. Increase in peripheral retinal MVD in mice with an *Eng* conditional deletion[225] and in skin MVD in *Eng*$^{+/-}$ mice on the 129/Ola background[230] have been reported. Our laboratory, using x-ray micro-CT imaging and histological microvessel quantitation, demonstrated that adult *Eng*$^{+/-}$ and *Alk1*$^{+/-}$ mice on the C57BL/6 background have a selective reduction in the peripheral pulmonary vascular bed[227,228]. Moreover, retinal hypo-vascularization was also recently shown in several HHT2 patients[231].

Vascular endothelial growth factor (VEGF), a major pro-angiogenic protein, has been implicated in HHT. Circulating and nasal tissue VEGF levels were higher in HHT patients[205,206]. Intracranial injection of an adenovirus expressing VEGF to either *Eng*$^{+/-}$ or *Alk1*$^{+/-}$ mice led to an increase in cerebral MVD and development of abnormal AVM-like structures, demonstrating that VEGF induces abnormal angiogenesis in a genetically predisposed host[232]. However, no comprehensive analysis of MVD and VEGF levels in various organs of *Eng*$^{+/-}$ or *Alk1*$^{+/-}$ mice has been undertaken to assess if systemic pathological angiogenesis is associated with HHT.

Anti-angiogenic therapy, often in combination with chemotherapy, has been used in preclinical tumor models and patients with metastatic cancers[233]. In HHT patients, case reports showed that bevacizumab (monoclonal antibody to VEGF) reduced the frequency of epistaxis and blood transfusions and even eliminated the need for liver transplantation[234,235]. In a recent phase II clinical trial of bevacizumab in HHT patients with severe liver disease, it was reported that hyperdynamic cardiac output secondary to

intrahepatic arteriovenous shunting was significantly improved in treated patients, at 6 months follow-up. Interestingly, several patients also showed normalization of their systolic pulmonary arterial pressure[236]. These observations suggest that anti-VEGF therapy may have beneficial effects in HHT patients. As the growth of blood vessels is promoted by VEGF[237], it is expected that anti-VEGF treatment will decrease MVD in HHT. We therefore tested the effects of systemic anti-VEGF therapy in multiple organs in *Eng*$^{+/-}$ and *Alk1*$^{+/-}$ mice, using the monoclonal antibody G6-31 to mouse VEGF-A. In these murine models, we measured MVD in histological sections of lungs, heart, distal colon and liver and *in vivo* hepatic microvascular perfusion, using contrast-enhanced micro-ultrasound (CE-US). We also compared tissue levels of several angiogenic/angiostatic factors in *Eng*$^{+/-}$ and *Alk1*$^{+/-}$ mice, relative to wild type[119] mice, after anti-VEGF or vehicle treatment.

We show a distinct increase in thrombospondin-1 (TSP-1) and angiopoietin-2 (Ang-2) expression in the lungs of *Eng*$^{+/-}$ and *Alk1*$^{+/-}$ mice respectively, and restitution to normal levels by anti-VEGF therapy. Surprisingly, but in keeping with a reduction in angiostatic factors, the anti-angiogenic treatment rescued the rarefied peripheral pulmonary microvasculature and attenuated the secondary RVH in both models. We also noted a significant *in vivo* functional response of the hepatic microvasculature of *Eng*$^{+/-}$ mice to anti-VEGF treatment. Overall, our findings show that *Eng* and *Alk1* heterozygous mice have a somewhat distinct, organ-specific angiogenic profile and response to anti-VEGF treatment and suggest that systemic monitoring of HHT1 and HHT2 patients undergoing anti-angiogenic therapy is needed.

2. 3 Materials and Methods

2. 3. 1 Mice and anti-angiogenic treatment

Congenic *Eng*$^{+/-}$ and *Alk1*$^{+/-}$ mice and their respective littermate controls were generated by successive backcrosses (N26-N30 for *Eng* mice and N10-N15 for *Alk1* mice) to C57BL/6 mice[60,68]. Mice were kept in ventilated racks, in a specific pathogen-free facility at the Toronto Center for Phenogenomics (TCP), and were fed standard chow and DietGel 76A **(**ClearH_2O, Portland, ME, USA) during the antibody treatment. 15 week-old male and female *Eng*$^{+/-}$ and *Alk1*$^{+/-}$ mice were randomized to treatment and control groups. The treated group received G6-31 monoclonal antibody, which has high affinity and specificity for murine and human VEGF-A[238], and was kindly provided by Genentech Inc, South San Francisco, CA, USA. The control groups were injected with PBS vehicle or with control IgG2a isotype antibody. *Eng*$^{+/-}$ and *Alk1*$^{+/-}$ mice were injected i.p. with 5 mg/kg of G6-31 antibody, weekly, for a total of 4 injections and were sacrificed 5-8 days after the last injection. In all experiments, *Eng*$^{+/+}$ or *Alk1*$^{+/+}$ mice were also included for reference. A minimum of 5 mice/group was tested in each experiment.

2.3.2 Blood pressure, heart rate and proteinuria

The average of ten consecutive tail systolic blood pressure (BP) and heart rate (HR) measurements/mouse, taken with a tail cuff attached to the Hatteras MC4000 Multichannel Blood Pressure analysis System (Hatteras Instruments Inc. Cary, NC, USA), was calculated. Proteinuria was assessed with the Multistix 8 SG strips for urinalysis (Siemens Heathcare Diagnostics Inc, Burlington, ON, Canada). Measurements

were done on PBS and anti-VEGF treated mice, at the end of treatment. Data were reported as mean ± SEM for each parameter.

2.3.3 Ultrasound imaging

Hepatic contrast-enhanced micro-ultrasound (CE-US) imaging was performed with the Vevo2100 high-frequency ultrasound system (VisualSonics Inc., Toronto, ON), in a blinded fashion, by an experienced investigator. Five to eight days after the last G6-31 injection, mice were anesthetized with 2% isoflurane **(**Abbott Laboratories Limited**,** Saint-Laurent, QC), delivered in combination with 1L/min oxygen (n = 7-10/group). Each mouse was placed in supine position on a heated stage; HR was maintained above 400 beats/min and body temperature monitored throughout the imaging session. A 27G butterfly needle was inserted into a tail vein for i.v. injection of the ultrasound contrast agent (UCA). The bubble-free ultrasound gel (Parker Laboratories, Inc., Fairfield, NJ) was applied on the upper abdomen, after the fur was removed. A solid-state array transducer (MS-250) was used at a centre frequency of 18MHz. Dual-mode presentation of a grayscale image side-by-side with a contrast-enhanced image, facilitated the selection of the region of interest in real-time. The imaging plane, displaying the clearest image of the inferior vena cava and abdominal aorta, was selected on the axial axis of the liver. The following settings were kept consistent throughout the study: 4% power, wide beam width, 35 dB contrast gain, zero persistence and 35 dB dynamic range.

The Vevo MicroMarker Ultrasound contrast agent (UCA (VisualSonics Inc., Toronto, ON) was reconstituted as previously described[239], then further diluted 10-fold prior to each injection and given as a 50 µL i.v. bolus to each tested mouse. For image analysis, a ROI encompassing the upper segment of the liver was drawn and matched for

each mouse. The time-intensity curve (TIC) was obtained by plotting the average intensity of pixels over time, within the ROI. Peak enhancement (PE) or the tissue blood volume, the *in vivo* equivalent of MVD, represents the difference between the maximum amplitude of the TIC and the baseline intensity. Wash-in-rate or the blood flow rate, is the maximum slope of the TIC.

2.3.4 Tissue collection, processing and vessel staining

Mice were anesthetized with ketamine (100 mg/kg) and xylazine (10 mg/kg) i.p. and blood collected by intracardiac puncture five to eight days after the 4th injection. The heart was perfused with PBS and tissues were snapped-frozen in liquid nitrogen for subsequent biochemical measurements. Other samples were washed in PBS and immersed in 4% paraformaldehyde for histological analysis. After harvesting the heart, RV was dissected from LV and septum (S) and the RV/LV + S weight ratio (Fulton index) was calculated as reported previously[227, 228].

For microvessel density (MVD) measurements, tissues were cut as follows: hearts were sectioned horizontally immediately under the atriae; lungs and liver- transversally through the hilum; distal colon - along the mesenteric border. These sections were subsequently processed, paraffin-embedded and sectioned (5 μm).

To visualize accurately the pulmonary microvasculature, lung sections were stained with Movat's pentachrome, a technique frequently used to study lung PAH-related microvascular changes in animal models[241]. We previously used the Movat's staining in the *Eng* and *Alk1* lungs, and confirmed the histological findings using x ray-micro-CT imaging[227,228]. Cardiac, hepatic and colonic sections were stained for the endothelial marker CD31. These sections were incubated overnight at 4°C with a rabbit

antibody to CD31 (ABCAM Cambridge, MA, USA; 1:100 dilution) followed by biotinylated goat anti-rabbit IgG (Vector Labs Inc, Burlington, ON, Canada; 1:200 dilution) and using an ABC detection kit (Vector Labs Inc, 1:50 dilution). Color development was done for 10 min with diaminobenzidine tetrahydrochloride. Slides were then counterstained with Harris Hematoxylin.

2.3.5 Quantification of microvessel density (MVD)

Lung MVD was measured in a blinded fashion by two independent investigators, using the Olympus BX60 microscope (Carsen Group Inc, Center Valley, PA, USA), equipped with a digital camera QImaging RETIGA 2000R (software QCapture 3-1.1.1) and analyzed with OpenLab software 3.1.4 version (Improvision Inc. Lexington MA, USA). The most vascularized area from 3 to 5 well-inflated pulmonary lobes was selected at 100x magnification. Four to nine consecutive fields/lobe, from a minimum of 3 lobes/lung (total of 15-25 independent fields/lung) were then imaged at 400x magnification. A minimum of 10 complete pulmonary peripheral small vessels per lobe (outer average diameter $\leq 40\mu m$) was counted for a minimum of 5 mice per group. To demonstrate the integrity of the pulmonary lobes, alveolae were counted in 7 consecutive fields, in the most vascularized area of the left medial pulmonary lobe, at 400x magnification.

In distal colon, the most vascularized area was first selected at 100x magnification. $CD31^+$ vessels (≤ 40 μm in outer average diameter) were counted in a blinded fashion by two independent investigators, on 5 consecutive fields, at 400x magnification. A minimum of 5 mice/group was analyzed.

For heart and liver MVD, anti-CD31 stained slides were first scanned with a Hamamatsu Nanozoomer 2 ORS. Digital automatic MVD quantitation of the entire cross-sectional cardiac area and of three randomly selected well-preserved hepatic sections was performed in a blinded manner, with the Visiopharm Integrator System image analysis software (Visiopharm A/S, Hoersholm, Denmark), module Visomorph DP^{TM} 4.3 1.0 VIS, at 200x magnification. The cut-off for computerized small vessel quantitation was established at ≤ 306 μm^2 area (≤ 20 μm diameter) and ≥ 5 μm^2 area (2.5 μm diameter). MVD was reported as the total number of small vessels/mm^2.

2.3.6 Endothelial cell experiments

Eng$^{+/+}$*, Eng*$^{+/-}$ *and Eng*$^{-/-}$ endothelial cells were generated from E9.0 murine embryos, grown and protein extracts prepared as previously described[242].

2.3.7 Protein extraction and measurements

Tissue and plasma samples were collected 5 to 8 days after the last injection. Frozen tissues were homogenized in 50 mM Tris-HCl, pH 7.4 buffer, containing 1% Triton X-100 plus protease/phosphatase inhibitors (Roche, Canada, Mississauga, ON, Canada), and centrifuged at 13,000 *g* for 30 min, at 4°C. Protein concentration in lysates or plasma was determined with the Bradford assay.

2.3.8 ELISA assays

Tissue and plasma VEGF levels were quantified using the mouse Duoset ELISA kit (R&D Systems, Minneapolis, MN, USA). Total plasma and tissue VEGF levels, measured 5 to 8 days after the last injection of G6-31 antibody, included antibody-bound VEGF and free VEGF. Free residual plasma and tissue VEGF levels were measured

after immunodepletion, performed as previously described[243]. Briefly, GammaBind G Sepharose beads (GE Healthcare, Baie D'Urfe, QC, Canada) were washed with PBS and incubated with tissue lysates or plasma. One and two-step immunodepletion were found optimal and used for tissue lysate and plasma free VEGF measurements, respectively.

Tissue levels of endogenously active and total TGF-β1 (endogenously active plus acid-treated) were determined with the mouse ELISA kit (R&D Systems). To measure total TGF-β1 levels, samples were first acidified with 1N HCl for 10 minutes at room temperature and then neutralized with 1.2 N NaOH/0.5 M HEPES. All samples were measured in duplicate.

2.3.9 Western blots

Equivalent amounts of proteins from lung or liver extracts were fractionated on 4-12% gradient SDS/PAGE under reducing or non- reducing conditions as specified in the figure legends and immunoblotted with the following primary antibodies and their appropriate dilutions: mouse anti-TSP-1, 1:1000, Thermo Fisher Scientific, Fremont, CA, USA; goat anti-Ang-2, anti-CD31, and anti-ALK1, 1:500, Santa Cruz Biotechnology Inc, Santa Cruz, CA, USA; rabbit anti-Ang-1, 1:1000, Millipore Termecula,CA,USA;rabbitanti-phosphor Smad1(Ser463/465)/Smad5(Ser463/465) /Smad8(Ser426/428)(#9511), 1:1,000, rabbit anti-phoshor-Smad2 (Ser465/467) (#3101), 1:1,000, mouse anti-Smad2 (L16D3) (#3103), 1:1,000, mouse anti-phoshor-AKT (Ser473), 1:1,000, rabbit anti-AKT, 1:1,000, Cell Signaling Technology Inc, Danvers, MA, USA; mouse anti-Smad1/5/8 (sc-81378), 1:1,000, Santa Cruz Biotechnology Inc, Santa Cruz, CA, USA; rat anti-Eng (clone MJ7/18), 1:500, Southern Biotech, Birmingham, AL, USA; mouse anti-VEGFR2, 1:500, R&D Systems, Minneapolis, MN,

USA; mouse anti-β-actin, 1:10,000, Sigma, St. Louis, MO, USA. Appropriate secondary antibodies conjugated with horseradish peroxidase (1:10,000 dilution) and enhanced chemiluminescence reagent (ECL, Perkin Elmer, Shelton, Connecticut, USA) were used for detection. Band intensities were quantified, expressed relative to β-actin (or total proteins in the case of phosphorylated proteins), and normalized to values corresponding to the mean of WT samples, for comparison between gels.

2.3.10 Statistical analysis

Statistical analysis was performed with *t*-test (for 2 groups) and one-way ANOVA (for ≥3 groups), using GraphPad Prism 5 software (GraphPad Software, La Jolla, CA, USA). If one-way ANOVA comparison led to a statistically significant result, post-hoc analysis was performed using Tukey's test. Results are expressed as mean ± SEM; $P < 0.05$ was considered statistically significant.

Ethical approval

All protocols were approved by the Animal Care Committees of the Hospital for Sick Children, the Toronto Center for Phenogenomics and the Sunnybrook Research Institute, in accordance with the Canadian Council on Animal Care guidelines and regulations.

2. 4 Results

2. 4. 1 Anti-VEGF treatment normalizes pulmonary peripheral microvessel density and attenuates right ventricular hypertrophy in adult *Eng* and *Alk1* heterozygous null mice

To elucidate the effects of anti-VEGF therapy on pulmonary microvasculature in *Eng* and *Alk1* mutant mice, we quantified peripheral MVD (≤ 40 μm outer diameter) on Movat-stained lung sections. This technique was proven reliable for such measurements in our previous studies and an independent publication[227, 228, 241]. Representative Movat-stained peripheral lung images of the PBS-treated control and mutant mice and anti-VEGF-treated *Eng* and *Alk1* heterozygous mice are shown in Figure 13. We confirmed previous reports[227, 228] of a significant decrease in lung peripheral MVD in $Eng^{+/-}$ and $Alk1^{+/-}$ mice, relative to their respective wild type[119] controls (Figure 14). Unexpectedly, anti-VEGF treatment caused an increase in pulmonary peripheral MVD, restoring it to normal levels in both $Eng^{+/-}$ and $Alk1^{+/-}$ mice (Figure 14 a, b). This response was G6-31-dependent, as IgG2a (isotype control) treatment had no effects on MVD in *Eng* mutant lungs (Figure 14 a). The G6-31 antibody did not have a significant effect on the MVD in WT $Eng^{+/+}$ lungs; however, Tukey's posthoc analysis showed a trend towards lower MVD in the anti-VEGF- versus PBS-treated $Eng^{+/+}$ mice (27.6 ± 1.6 versus 32.5 ± 2.2 vessels/mm^2; n = 5-8/group; P = 0.09). Such a reduction in MVD would be the expected result of anti-VEGF treatment, further highlighting the specificity of this agent in reversing the abnormal vascular phenotype in mutant lungs (Figure 14 a).

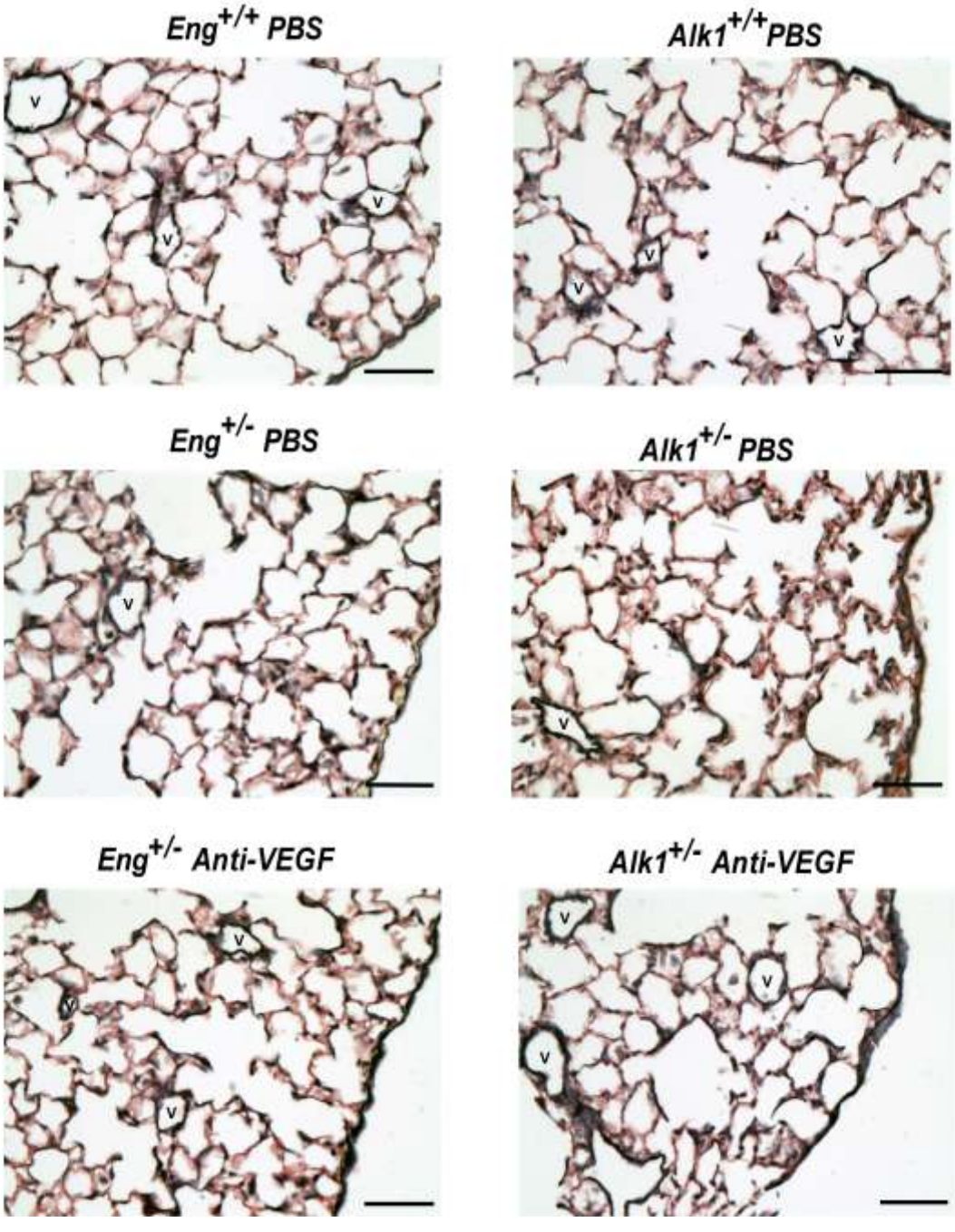

Figure 13. Representative images from peripheral lungs of PBS (vehicle) and anti-VEGF-treated mice. Lung sections from PBS-treated WT and mutant mice and from anti-VEGF-treated heterozygous mice were stained with Movat's pentachrome. Intact pulmonary small vessels in the periphery (outer average diameter ≤ 40μm) are illustrated (v) and were counted in nine fields per lobe for a minimum of three lobes per mouse at 400x magnification. Scale bars: 40 μm.

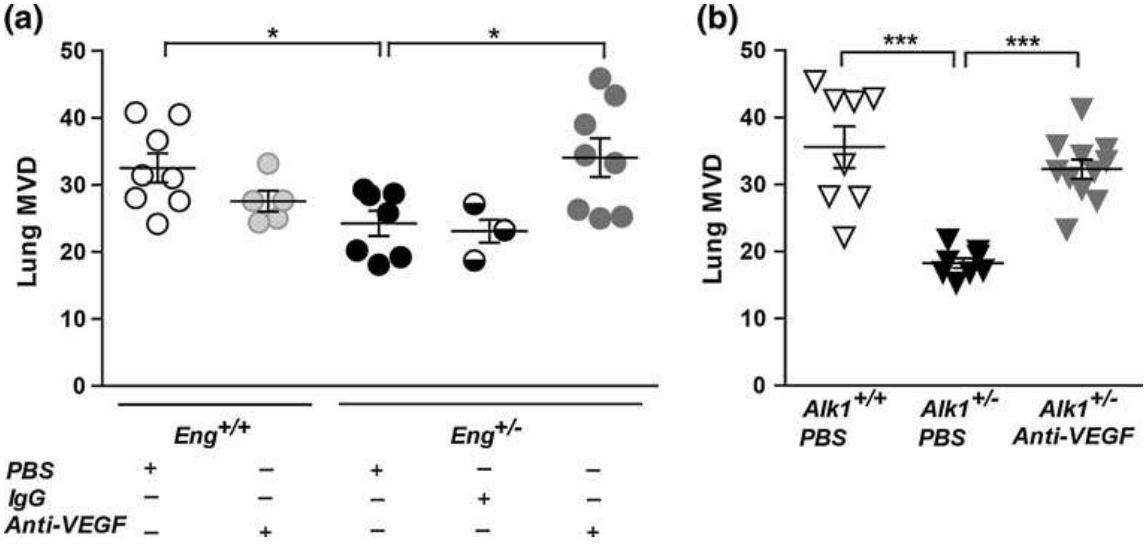

Figure 14. Anti-VEGF treatment normalizes pulmonary microvessel density (MVD) in *Endoglin* and *Alk1* mutant mice. Quantitation of pulmonary peripheral MVD was done on Movat's pentachrome stained sections, in a blinded manner (400x magnification) on **a)** *Eng* and **b)** *Alk1* mice treated with PBS and G6-31 antibody; n = 3-11/group. Circles and inverted triangles represent individual *Eng* and *Alk1* mice, respectively. ○ ▽ (wild type, PBS-treated); ◌ (wild tye, G6-31 antibody-treated); ● ▼ (mutant, PBS-treated); ◒ (mutant, IgG-treated); ● ▼ (mutant, G6-31 antibody-treated). Mean ± SEM are shown. **P*<0.05; ****P*<0.001 by one-way ANOVA, followed by Tukey's post-hoc test.

Furthermore, integrity of lung tissues was demonstrated by a similar number of alveolae in G6-31 antibody versus PBS-treated mutant mice, equivalent to that observed in WT controls (Figure 15). Thus, anti-VEGF treatment rescued the peripheral lung MVD in $Eng^{+/-}$ and $Alk1^{+/-}$ mice to levels observed in WT controls.

To exclude a primary cardiac anti-angiogenic effect of G6-31 antibody therapy, which could be responsible for the improvement in pulmonary MVD, we quantified the number of $CD31^{+}$ vessels on heart cross-sections in both $Eng^{+/-}$ and $Alk1^{+/-}$ mice, using an automated computerized system. Under basal conditions, cardiac MVD was normal in both heterozygous and WT mice. No significant change in cardiac MVD was observed in $Eng^{+/-}$ or $Alk1^{+/-}$ mice treated with anti-VEGF antibody versus PBS vehicle (Figure 16 a).

We previously showed that pulmonary peripheral rarefaction of vessels led to RVH in $Eng^{+/-}$ and $Alk1^{+/-}$ mice [227, 228]. Therefore, we analyzed the effect of anti-VEGF therapy on the RV/LV+S weight ratio (Fulton's index) in our models. In the present study, PBS-treated $Eng^{+/-}$ and $Alk1^{+/-}$ mice showed a 43% and 55% increase in Fulton's index respectively, relative to WT littermates. This increase was independent of body mass and was caused by an augmentation in RV mass, as LV+S mass was similar in PBS-treated mutant and WT mice (data not shown). Strikingly, anti-VEGF treatment also normalized the Fulton's index in both mutant mice (Figure 16 b). Collectively, we conclude that anti-VEGF treatment restored pulmonary MVD by targeting the abnormal lung peripheral microvasculature and consequently decreased secondary RVH in both $Eng^{+/-}$ and $Alk1^{+/-}$ mice.

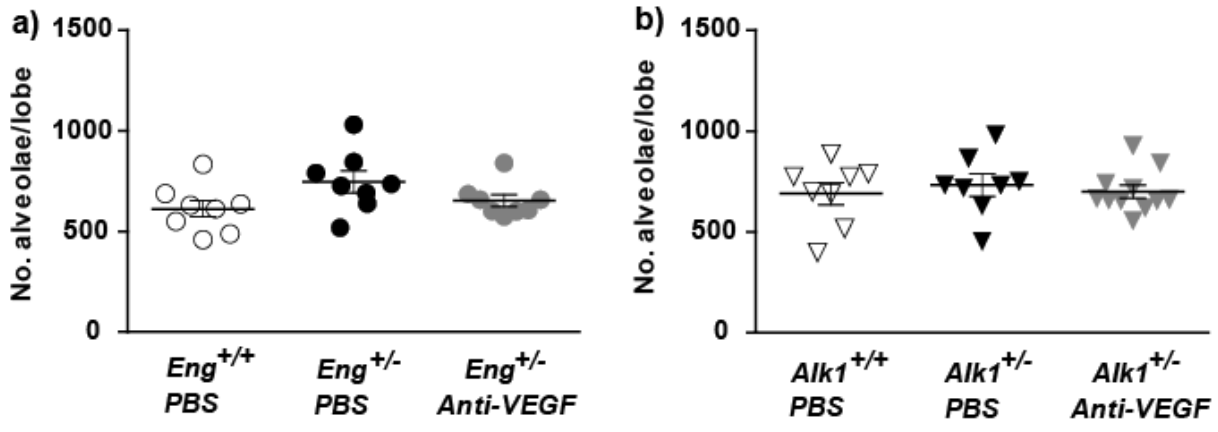

Figure 15. The number of alveolae is not altered by anti-VEGF treatment. Lung sections derived from **a)** *Eng* and **b)** *Alk1* mice were stained with Movat's pentachrome. Alveolae were counted on seven consecutive fields/lobe/mouse. Circles and inverted triangles depict individual *Eng* and *Alk1* mice, respectively: ○ ▽ (wild type, PBS-treated); ● ▼ (mutant, PBS-treated); ● ▼ (mutant, G6-31 antibody-treated); n = 8-11 mice/group. Horizontal bars represent the mean ± SEM. Three-group comparison was done using one-way ANOVA.

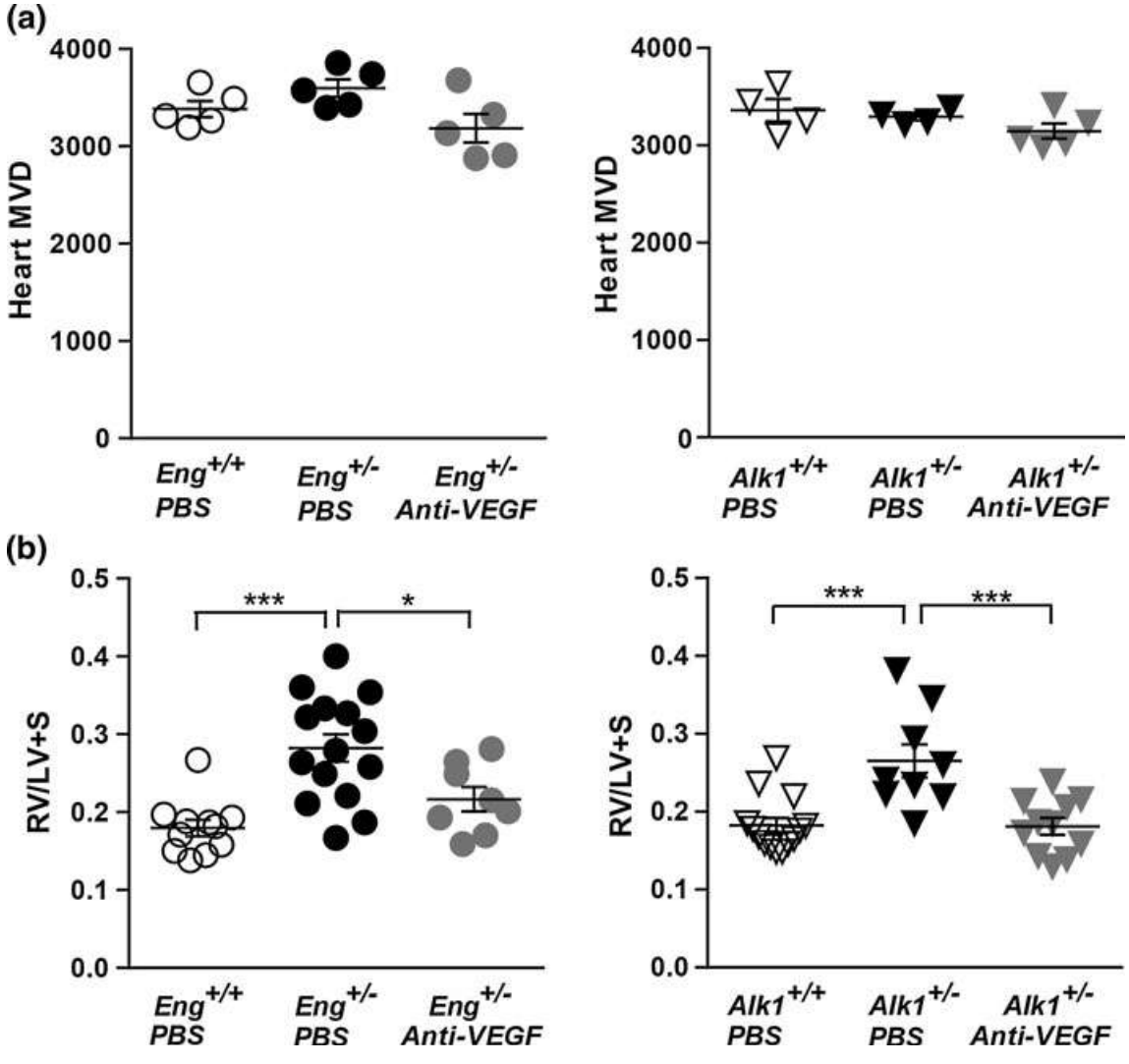

Figure 16. Anti-VEGF treatment attenuates right ventricular hypertrophy and has no effect on cardiac microvascular density (MVD) in *Eng* and *Alk1* heterozygous mice. a) Computerized quantitation of cardiac MVD was performed on CD31-stained sections (200x magnification); n = 4-5/group; **b)** Measurement of right ventricle (RV) to left ventricle (LV) plus septum (S) weights (RV/LV+S) in *Eng* and *Alk1* mice treated with PBS and G6-31 antibody; n = 8-15/group. Circles and inverted triangles represent individual *Eng* and *Alk1* mice, respectively. ○ ▽ (wild type, PBS-treated); ● ▼ (mutant, PBS-treated); ● ▼ (mutant, G6-31 antibody-treated). Mean ± SEM are shown. *P<0.05; ***P<0.001 by one-way ANOVA, followed by Tukey's post-hoc test.

2. 4. 2 Blocking VEGF restores the angiogenic balance in *Endoglin* and *Alk1* mutant lungs

To assess whether G6-31 antibody was efficient in binding VEGF, we measured VEGF levels in plasma, lungs and heart of anti-VEGF-treated *Eng* and *Alk1* mutant mice at time of sacrifice, and compared to those observed in PBS-treated heterozygous and WT mice (Table 5). Total circulating VEGF (antibody-bound + free) significantly rose from ~ 10 pg/ml at baseline in PBS-treated WT and mutant mice, to approximately 5 ng/ml in both *Eng* and *Alk1* mutant mice. This represents a 500-fold increase in circulating total VEGF levels, demonstrating that the G6-31 antibody was still present in circulation and bound to VEGF, one week after cessation of treatment. Following immunodepletion, circulating VEGF levels returned to baseline values at <10 pg/ml, in anti-VEGF-treated *Eng* and *Alk1* mutant mice. Table 5 also illustrates that G6-31 antibody targeted multiple organs, as shown by the total VEGF levels in several tissues. Lung and heart VEGF levels were similar at baseline in PBS-treated mutant versus WT mice. Importantly, pulmonary VEGF levels were decreased by ~ 40% in both $Eng^{+/-}$ and $Alk1^{+/-}$ mice after immunodepletion of antibody-bound VEGF. On the other hand, cardiac VEGF levels were reduced by34% only in G6-31 antibody-treated $Eng^{+/-}$ but not in $Alk1^{+/-}$ mice, indicating a stronger response in the heart of anti-VEGF-treated $Eng^{+/-}$ mice. This decrease in heart VEGF levels did not alter cardiac MVD nor systemic blood pressure in *Eng* mutant mice treated with anti-VEGF therapy (Fig. 16; Table 5).

Table 5. VEGF levels in *Eng* and *Alk1* mutant mice

Mice & treatment	*n*/group	Plasma (pg/ml)	Lungs (pg/mg)	Heart (pg/mg)	Colon (pg/mg)	Liver (pg/mg)
$Eng^{+/+}$ PBS-treated	5-10	5 ± 1	481 ± 15	328 ± 39	71 ± 6	1469 ± 133
$Eng^{+/-}$ PBS-treated	5-10	5 ± 1	549 ± 46	336 ± 42	93 ± 13	1696 ± 103
$Eng^{+/-}$ G6-31-treated	6-22	*4488 ± 369	*709 ± 70	*516 ± 54	*191 ± 36	1753 ± 69
$Eng^{+/-}$ G6-31-treated (after immuno-depletion)	5-8	11 ± 3	*334 ± 33	*223 ± 14	100 ± 23	†1462 ± 74
$Alk1^{+/+}$ PBS-treated	5-9	4 ± 2	469 ±16	309 ± 29	88 ± 3	1424 ± 77
$Alk1^{+/-}$ PBS-treated	5-10	7 ± 2	510 ±18	338 ± 53	98 ± 7	1604 ± 75
$Alk1^{+/-}$ G6-31-treated	5-11	*5085 ± 1184	*629 ± 40	380 ± 24	*213 ± 15	*2025 ± 140
$Alk1^{+/-}$ G6-31-treated (after immuno-depletion)	5-8	5 ± 3	*341 ± 10	223 ± 15	107 ± 9	1541 ± 169

*indicates statistically significant results ($P< 0.05$ by one-way ANOVA, followed by Tukey's post-hoc test for all G6-31 treated versus PBS-treated $Eng^{+/-}$ or $Alk1^{+/-}$ mice respectively). † indicates a trend towards significance, when compared to PBS-treated $Eng^{+/-}$ mice ($P = 0.08$).

Given the significant microvascular rarefaction observed in peripheral lungs in mutant mice, we investigated whether factors involved in vascular regression may play a role in this abnormal lung phenotype. Protein levels of the angiostatic factor TSP-1 and the vascular destabilizing protein Ang-2 were measured by Western blot in $Eng^{+/-}$ and $Alk1^{+/-}$ lungs of PBS and G6-31-antibody treated mice (Fig. 17a, b). The most noticeable change was a near 4-fold increase in basal TSP-1 levels in PBS-treated $Eng^{+/-}$ lungs relative to controls (Figure 17 c, left). In contrast, PBS-treated $Alk1^{+/-}$ lungs had normal TSP-1 levels, but showed a 36% increase in Ang-2 levels (Figure 17 c, right).

To exclude a possible interference of the number of C57BL/6 backcrosses on TSP-1 and Ang-2 levels in total lungs of $Eng^{+/+}$ and $Alk1^{+/+}$ mice, we compared these samples directly on the same gels. A representative gel and the quantitation of two independent experiments revealed no difference in the basal levels of either TSP-1 or Ang-2 in these samples (Figure 18 a, b). To further explore the changes in TSP-1 in *Eng* deficient samples, we used extracts from cultured $Eng^{+/+}$, $Eng^{+/-}$ *and* $Eng^{-/-}$ (E9.0) embryonic endothelial cells (Figure 18 c). We report that $Eng^{+/-}$ and $Eng^{-/-}$ cells have 3.3 and 6.6 fold higher TSP-1 levels than $Eng^{+/+}$ cells, and that TSP-1 is inversely correlated with endoglin levels in endothelial cells.

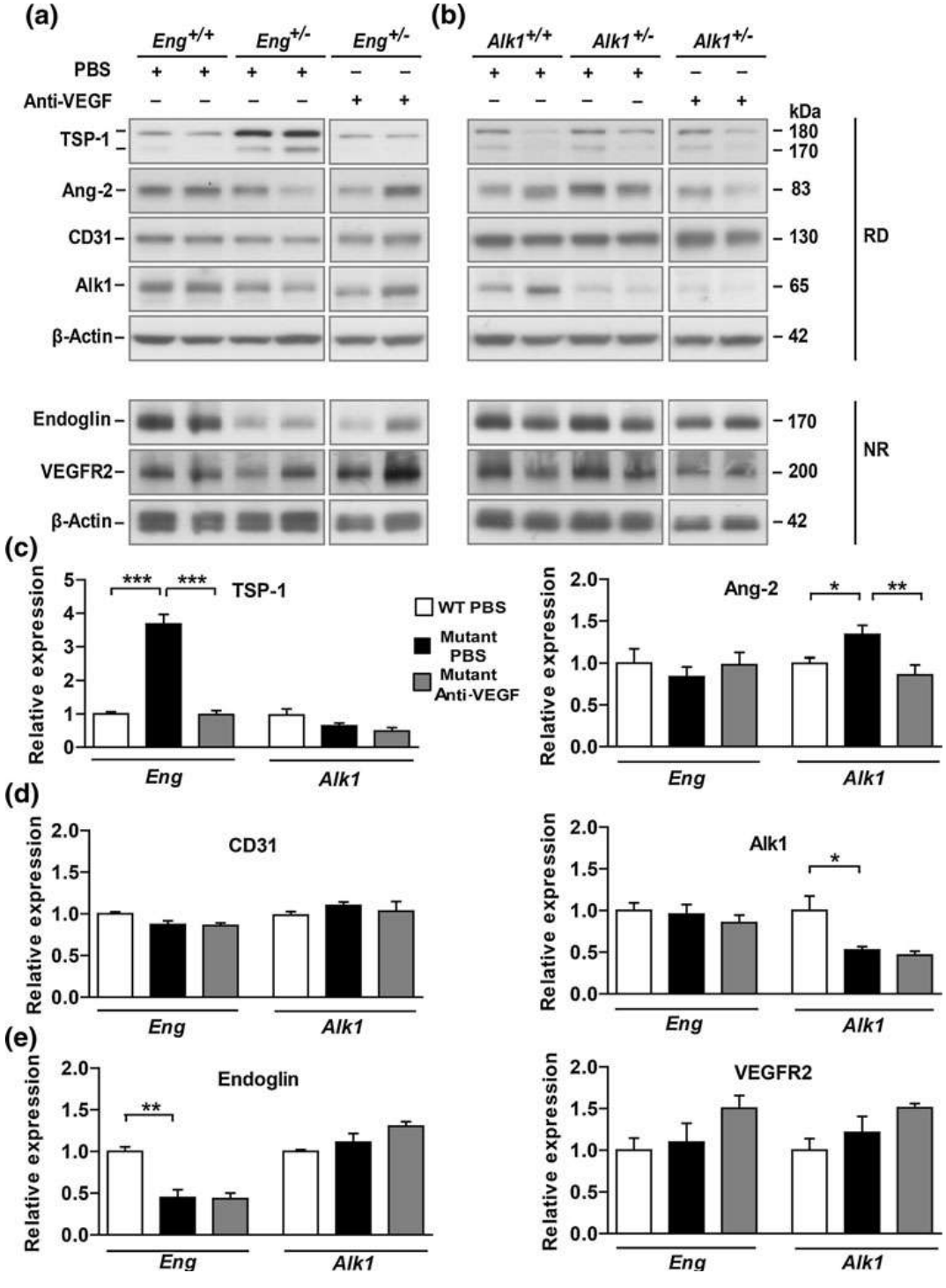
(a)
(b)
Eng+/+
Eng+/-
Eng+/-
Alk1+/+
Alk1+/-
Alk1+/-
PBS
Anti-VEGF
kDa
TSP-1
Ang-2
CD31
Alk1
β-Actin
180
170
83
130
65
42
RD
Endoglin
VEGFR2
β-Actin
170
200
42
NR
(c)
TSP-1
Ang-2
WT PBS
Mutant PBS
Mutant Anti-VEGF
Relative expression
Eng
Alk1
(d)
CD31
Alk1
(e)
Endoglin
VEGFR2

Figure 17. Pulmonary angiogenic profile differs between *Endoglin* and *Alk1* mutant mice and is restored by anti-VEGF treatment. Expression of TSP-1, Ang-2, CD31 and Alk1 (under reducing conditions, RD), and of Endoglin and VEGFR2 proteins (under non-reducing conditions, NR) was measured by Western blot in total lung extracts of **a)** *Eng* and **b)** *Alk1* mice treated with *PBS* or G6-31 antibody (for mutant mice). Representative blots are shown; *Eng* and *Alk1* gels were run in different experiments. **c)** Quantitation of protein expression relative to corresponding β-actin (RD or NR), and normalized to mean values for WT samples; n = 3-8/group. *P< 0.05, **P< 0.01, *** P< 0.005 as determined by one-way ANOVA, followed by Tukey's post-hoc test.

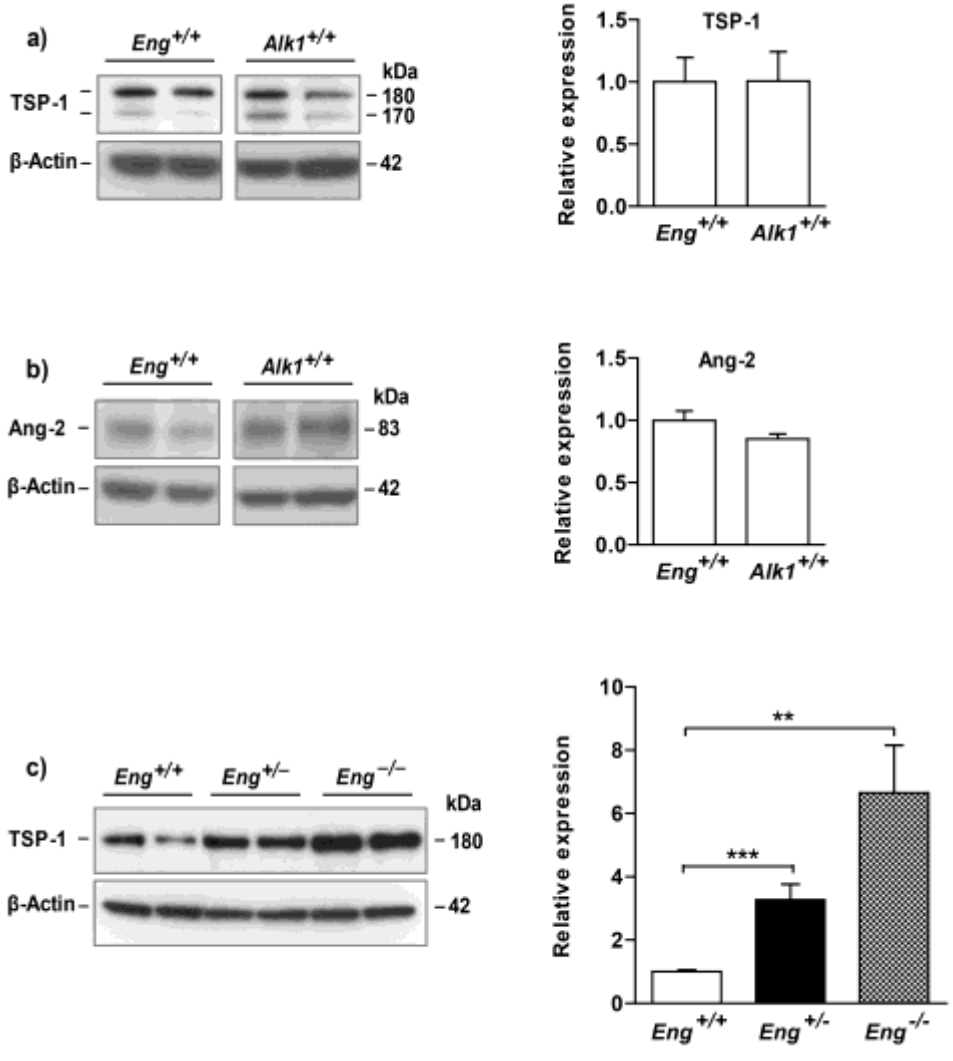

Figure 18. Similar levels of TSP-1 and Ang-2 in *Eng*$^{+/+}$ and *Alk1*$^{+/+}$ mice and increased TSP-1 expression in *Eng*- deficient endothelial cells. a) Representative Western blots (run under reducing conditions) are shown for TSP-1 and Ang-2 protein expression, measured in total lung extracts of *Eng*$^{+/+}$ and *Alk1*$^{+/+}$ mice; samples were run on the same gels and in two different experiments. Quantitation of protein expression relative to β-actin, and normalized to mean values for *Eng*$^{+/+}$ samples; n = 5-6/group. **b)** Expression of TSP-1 proteins in endothelial cells derived from *Eng*$^{+/+}$, *Eng*$^{+/-}$ *and Eng*$^{-/-}$ embryos (E8.5). A representative blot of 3 different gels is shown. Quantitation of TSP-1 expression relative to β-actin, and normalized to mean values for *Eng*$^{+/+}$ cells; n = 7-9/group. Data are shown as mean ± SEM. $^{**}P< 0.01$, *** $P< 0.005$ as determined by one-way ANOVA, followed by Tukey's post-hoc test.

These data suggest that the primary source of the increase in TSP-1 in the lungs of *Eng*$^{+/-}$ mice is the dysfunctional endothelium.

Our findings demonstrate that *Eng*$^{+/-}$ and *Alk1*$^{+/-}$ mice may have a distinct pulmonary angiogenic molecular signature associated with reduced peripheral lung microvasculature. Furthermore, elevated basal pulmonary TSP-1 and Ang-2 expression were reduced to normal levels by anti-VEGF treatment in *Eng*$^{+/-}$ and *Alk1*$^{+/-}$ mice, respectively (Figure 17 c). Overall, our data suggest that anti-VEGF treatment normalized the peripheral rarefied lung vasculature in *Eng* and *Alk1* mutant mice by restoring the pulmonary angiogenic/angiostatic balance in a VEGF-mediated and mutant-dependent manner.

Next, to establish the effect of anti-VEGF therapy on several endothelial markers [244], we measured the protein levels of CD31, Alk1, endoglin and VEGFR2 in total lung extracts in both murine models (Figure 17 a, b, d, e). We showed that CD31 levels in PBS-treated mutant lungs were comparable to those of WT mice (Fig. 17 a, b, d). Alk1 levels were unchanged in *Eng*$^{+/-}$ mice and as expected, were decreased by 50% in lungs of *Alk1*$^{+/-}$ mice (Figure 17 a, b, d). Endoglin levels were reduced by half in *Eng*$^{+/-}$ lungs and were normal in *Alk1*$^{+/-}$ mice (Figure 17 a, b, e).

VEGFR2 expression was similar in mutant and WT mice (Figure 17 a, b, e). Furthermore, pulmonary levels of CD31, Alk1, endoglin and VEGFR2 were not altered after anti-VEGF treatment in either mutant group. These data indicate that the total lung levels of these endothelial markers were not affected by the changes in peripheral pulmonary microvascularization in *Eng*$^{+/-}$ and *Alk1*$^{+/-}$ mice, even after anti-VEGF treatment (Figure 17 d, e).

To determine if the effects of anti-VEGF therapy in the mutant lungs were targeting VEGFR2-mediated pathways, we measured the phosphorylation of AKT, a downstream target of VEGFR2 signaling, involved in apoptosis, cell proliferation and migration. Our data show that AKT phoshorylation was not altered in lungs of *Eng* or *Alk1* heterozygous mice prior to and after anti-VEGF treatment (Figure 19). These data suggest that other VEGF-mediated pathways are implicated in the reversal of the dysregulated pulmonary microvascular phenotype in mutant mice treated with G6-31 antibody.

We then tested if mutant lungs had an intrinsic defect in TGF-β1 levels and if anti-VEGF treatment affected those levels. Total (endogenously active and acid-treated) TGF-β1 levels were similar in both PBS-treated mutant versus WT lungs (Table 6). Furthermore, total TGF-β1 levels remained stable after treatment with G6-31 antibody in both mutant mice, showing that targeting pulmonary VEGF did not trigger a negative feedback on TGF-β1 production in these lungs. Knowing that TSP-1 can activate latent TGF-β1[245], we then measured endogenously active pulmonary TGF-β1 levels and found them similar in $Eng^{+/-}$ and $Eng^{+/+}$ mice (26.7 ± 2.4 pg/mg protein versus 28.6 ± 3.1 pg/mg protein; n = 10-13/group). Analysis of downstream targets for ALK1 and ALK5 signaling pathways showed no difference in pulmonary Smad 1/5/8 nor Smad 2 phosphorylation relative to total Smads, nor in total Smads, in *Eng* and *Alk1* heterozygous mice, relative to WT controls (Figure 20). Thus, the elevation in lung TSP-1 levels did not induce further activation of the endogenous TGF-β1 nor downstream signaling via ALK1 or ALK5 in $Eng^{+/-}$ mice.

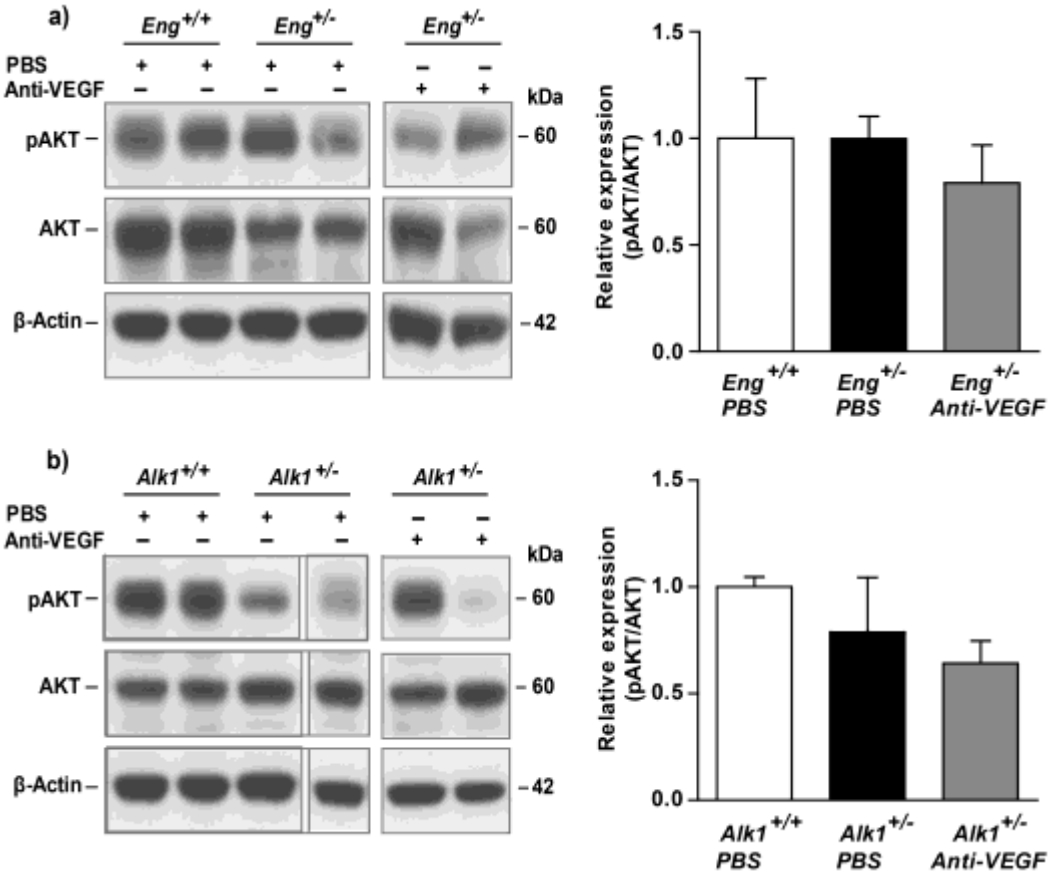

Figure 19. Phosphorylation of AKT is not altered in lungs of PBS- and anti-VEGF-treated mice. Representative Western blots (2 experiments/genotype) are shown for phosphor-AKT and total AKT proteins (run under reducing conditions), measured in total lung extracts of **a)** *Eng* and **b)** *Alk1* mice. Quantitation of phosphor-AKT relative to total AKT proteins, and normalized to mean values for the respective WT samples; n = 3-4/*Eng* groups and n = 5-7/*Alk1* groups. Data are shown as mean ± SEM.

Table 6. TGF-β1 levels are not altered by anti-VEGF treatment

Mice & treatment	*n*/group	Lungs (pg/mg)	Heart (pg/mg)	Colon (pg/mg)	Liver (pg/mg)
Eng$^{+/+}$	8-14	926 ± 168	262 ± 57	76 ± 8	625 ± 97
Eng$^{+/-}$	6-13	789 ± 121	598 ± 116	74 ± 5	817 ± 93
Eng$^{+/-}$ G6-31 treated	5-8	976 ± 197	562 ± 195	66 ± 8	730 ± 102
Alk1$^{+/+}$	7-11	1221 ± 238	164 ± 12	71 ± 7	754 ± 87
Alk1$^{+/-}$	5-10	1053 ± 173	143 ± 29	78 ± 9	700 ± 133
Alk1$^{+/-}$ G6-31 treated	4-6	808 ± 219	270 ± 109	54 ± 5	812 ± 198

Total tissue TGF-β1 (endogenously active plus acid-treated) levels were measured by ELISA in anti-VEGF and PBS-treated *Eng* and *Alk1* mutant mice and PBS-treated WT mice. Mean ± SEM are reported for each group. Results were not statistically different in the G6-31 antibody-treated mutant versus PBS-treated mutant and WT mice (by one-way ANOVA).

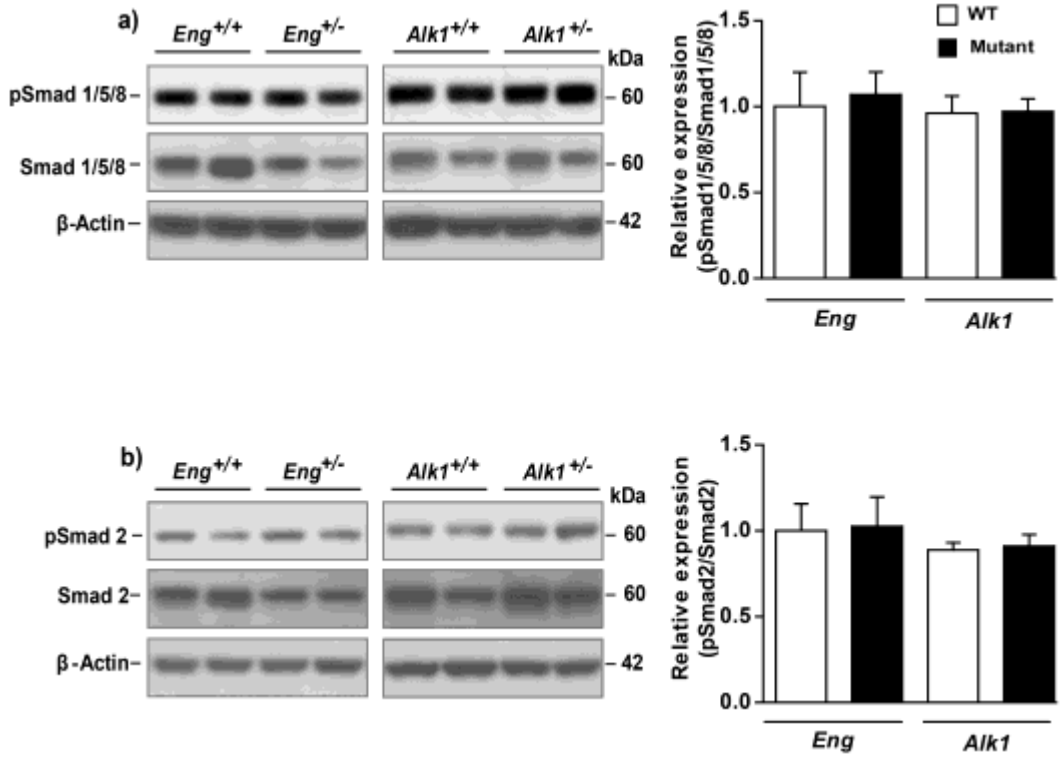

Figure 20. Smad phosphorylation is not altered in lungs of *Eng*$^{+/-}$ and *Alk1*$^{+/-}$ mice. Representative Western blots for a) pSmad 1/5/8, total Smad 1/5/8, β-actin, and b) pSmad 2, total Smad 2 and β-actin in heterozygous and control *Eng*$^{+/+}$ and *Alk1*$^{+/+}$ mice respectively. *Eng* and *Alk1* samples were run on the same gel (under reduced conditions) and processed at the same time. Quantitation of phosphor-Smads relative to corresponding total Smads, normalized to mean values for *Eng*$^{+/+}$ samples; n = 5-6/group. Data are expressed as mean ± SEM.

2. 4. 3. Anti-VEGF therapy has no anti-angiogenic effect in the colon of *Endoglin* and *Alk1* mutant mice

The colon harbors multiple telangiectasiae in HHT patients. It was therefore of interest to quantify the number of $CD31^+$ microvessels in colonic sections of $Eng^{+/-}$ and $Alk1^{+/-}$ mice, and to test the effects of anti-VEGF treatment. We report that colonic MVD was similar in heterozygous versus WT mice and remained unchanged after treatment with G6-31 antibody (Figure 21 a, b). Furthermore, basal colonic VEGF levels were comparable in PBS-treated mutant versus WT mice (Table 5). Even though G6-31 antibody targeted the colon, as demonstrated by the increase in total VEGF intestinal levels, residual free VEGF was unchanged in *Eng* and *Alk1* mutant mice (Table 5). TSP-1 protein levels were undetectable by Western blot in PBS-treated *Eng* mutant and WT mice (data not shown). In addition, total TGF-β1 levels were similar in the colon of both PBS-treated mutant versus WT mice and remained unaltered after G6-31 antibody treatment (Table 6). Therefore, we conclude that colon has a normal angiogenic phenotype in both mutant models and is not affected by anti-VEGF treatment.

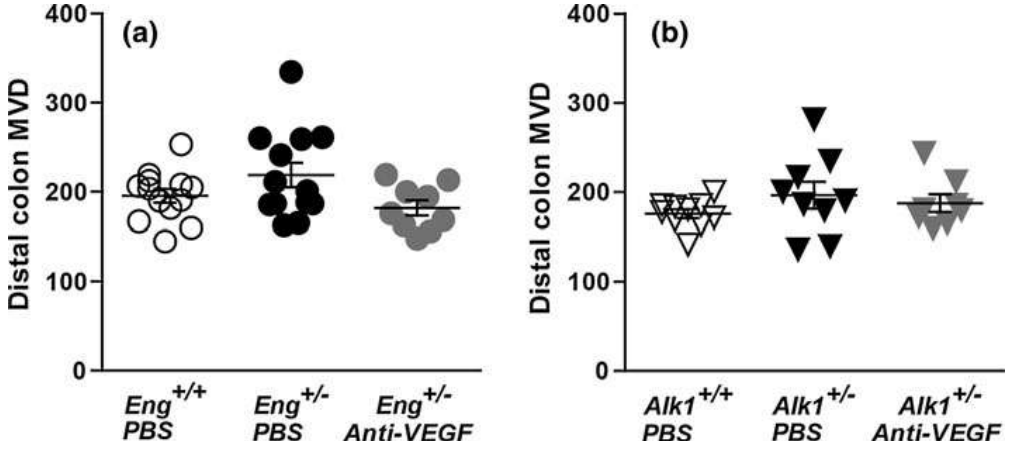

Figure 21. Anti-VEGF treatment has no effect of microvascular density (MVD) in distal colon in *Eng* and *Alk1* heterozygous mice. a) Colonic sections from PBS-treated $Eng^{+/+}$ and $Eng^{+/-}$ mice and G6-31 antibody-treated $Eng^{+/-}$ mice were stained for CD31 and MVD quantified at 400x magnification; n = 9-13/group**. b)** Equivalent samples from *Alk1* mice were processed similarly; n = 8-10/group. Circles and inverted triangles represent individual *Eng* and *Alk1* mice, respectively. ○ ▽ (wild type, PBS-treated); ● ▼ (mutant, PBS-treated); ● ▼ (mutant, G6-31 antibody-treated). Mean ± SEM are shown.

2. 4. 4 Anti-VEGF treatment has a strong anti-angiogenic effect on liver tissue in mutant and WT mice

Liver is commonly affected in patients with HHT, leading to severe complications[236]. To evaluate this highly vascularized tissue, we quantified the number of $CD31^+$ microvessels in several hepatic lobes of *Eng* and *Alk1* mice, using a digital imaging system and an automated computerized method. Representative images of a portal vein surrounded by sinusoidal vessels are shown for PBS and anti-VEGF-treated WT, $Eng^{+/-}$ and $Alk1^{+/-}$ mice in Figure 22 a-c respectively. The digitized images revealed that the number of red painted $CD31^+$ microvessels ($\leq$ 20 μm in diameter) was similar in mutant and WT livers, but showed a striking decrease in all 3 groups following anti-VEGF treatment. Data quantitation demonstrated a similar hepatic MVD in heterozygous and WT mice (Figure 22 d, e) and 28%, 39% and 46% reduction in liver MVD after G6-31 treatment in $Eng^{+/+}$, $Eng^{+/-}$ and $Alk1^{+/-}$ mice, respectively. This effect was G6-31-specific, as control IgG2a isotype treatment did not change liver MVD in $Eng^{+/-}$ mice, when compared to PBS-treated controls (Figure 22 d). The number of vessels >20 μm in diameter remained unaffected by anti-VEGF treatment in all groups (data not shown). Thereby, the reduction in hepatic MVD observed after anti-VEGF treatment appears to be liver microvasculature-specific rather than HHT-specific.

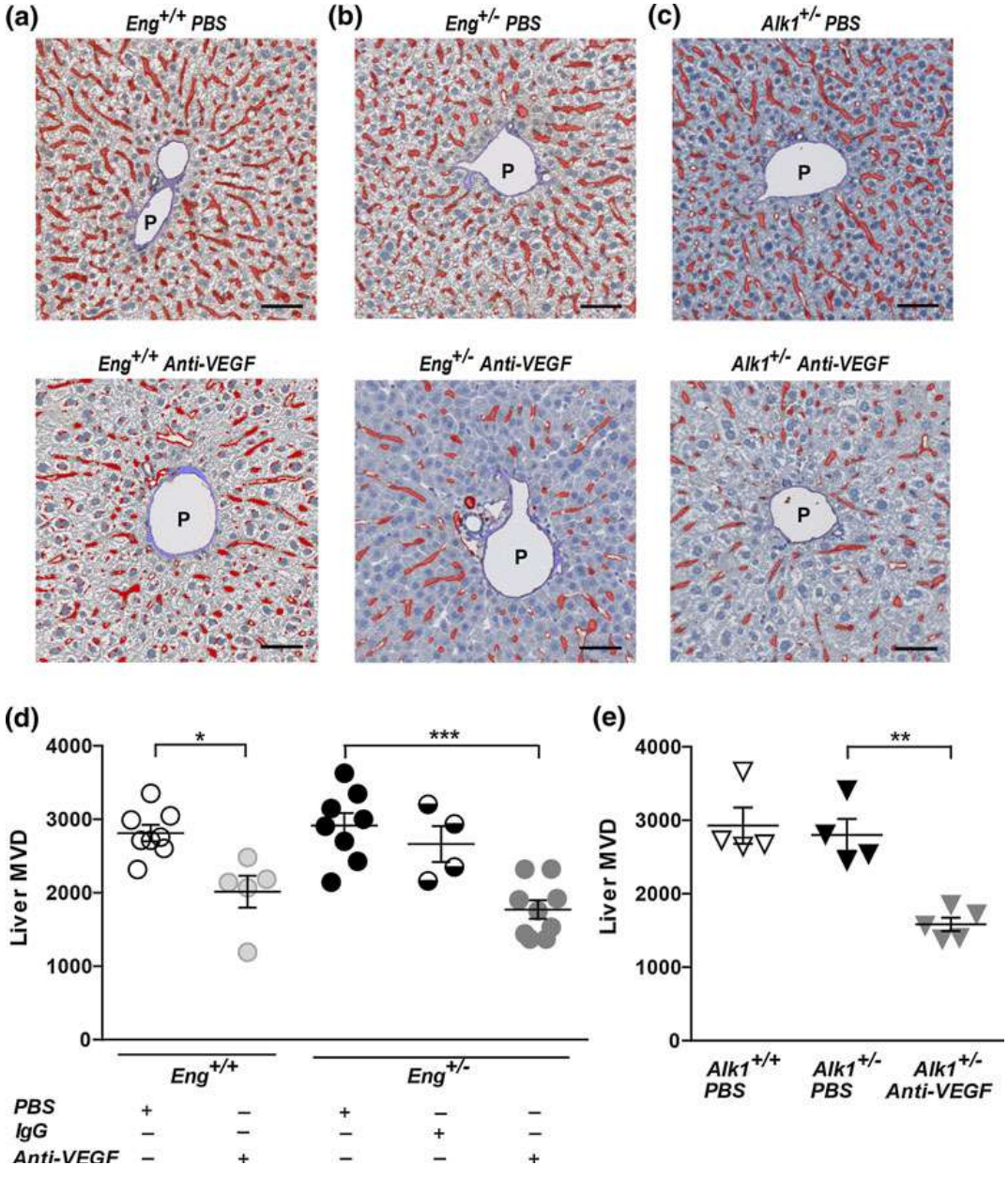
(a)
Eng+/+ PBS
(b)
Eng+/- PBS
(c)
Alk1+/- PBS
Eng+/+ Anti-VEGF
Eng+/- Anti-VEGF
Alk1+/- Anti-VEGF
P
(d)
Liver MVD
4000
3000
2000
1000
0
*
***
Eng+/+
Eng+/-
PBS
IgG
Anti-VEGF
(e)
**
Alk1+/+ PBS
Alk1+/- PBS
Alk1+/- Anti-VEGF

Figure 22. Anti-VEGF treatment reduces liver microvascular density (MVD) in mutant and WT mice. Representative computerized images of hepatic microvessels from **a)** *Eng*$^{+/+}$, **b)** *Eng*$^{+/-}$ and **c)** *Alk1*$^{+/-}$ mice treated with PBS or G6-31 antibody are shown (200x magnification; scale bar = 40 μm). Vessels < 20 μm in diameter are painted red and quantified. An area focused on a portal vein (P) was selected for each group. Quantitation of hepatic MVD on **d)** *Eng* and **e)** *Alk1* mice treated with PBS and G6-31 ntibody; *n* = 4-9/group. Circles and inverted triangles represent individual *Eng* and *Alk1* mice, respectively. ○ ▽ (wild type, PBS-treated); ◌ (wild type, G6-31 antibody-treated); ● ▼ (mutant, PBS-treated); ◒ (mutant, IgG-treated); ● ▼ (mutant, G6-31 antibody-treated). Mean ± SEM are shown. **P*<0.05; ***P*<0.01; ****P*<0.001 by one-way ANOVA, followed by Tukey's post-hoc test.

2. 4. 5 *Endoglin* and *Alk1* mutant mice have a distinct hepatic response to anti-VEGF therapy

To ascertain if G6-31 antibody was efficient in binding hepatic VEGF, we measured the VEGF levels in liver of mutant mice treated with anti-VEGF treatment and PBS. Basal hepatic VEGF levels were comparable in heterozygous versus WT mice and remained unaffected after G6-31 antibody treatment in both groups, as quantified by ELISA (Table 5). Furthermore, total hepatic VEGF was unchanged in $Eng^{+/-}$ mice, 5-8 days after the 4th injection of G6-31 antibody (Table 5). Residual VEGF, measured in the liver of anti-VEGF-treated $Eng^{+/-}$ mice and after immunodepletion, showed a trend towards reduced levels, when compared to those of PBS-treated $Eng^{+/-}$ mice (1462 ± 74 versus 1696 ± 103 pg/mg of tissue; P = 0.08; n = 7-8/group). Although total hepatic VEGF levels rose significantly in liver of *Alk1* mutant mice after anti-VEGF therapy, implying that the liver was indeed targeted by the antibody, VEGF levels returned to baseline values after immunodepletion (Table 5). It should be said that endogenous hepatic VEGF levels are very high and require extensive dilution of samples for measurements, which may contribute to the lack of detection of a significant reduction after anti-VEGF treatment.

To establish whether the hepatic angiogenic profile was differentially affected by anti-VEGF therapy, we measured the protein levels of TSP-1, CD31,VEGFR2 (Figure 23) and Ang-2 in $Eng^{+/-}$ and $Alk1^{+/-}$ mice treated with G6-31 antibody or PBS vehicle. We demonstrate that hepatic TSP-1 was 66% higher in PBS-treated $Eng^{+/-}$ versus $Eng^{+/+}$ mice (Figure 23 a), whereas no change was observed in PBS-treated $Alk1^{+/-}$ versus $Alk1^{+/+}$ mice (Figure 23 c).

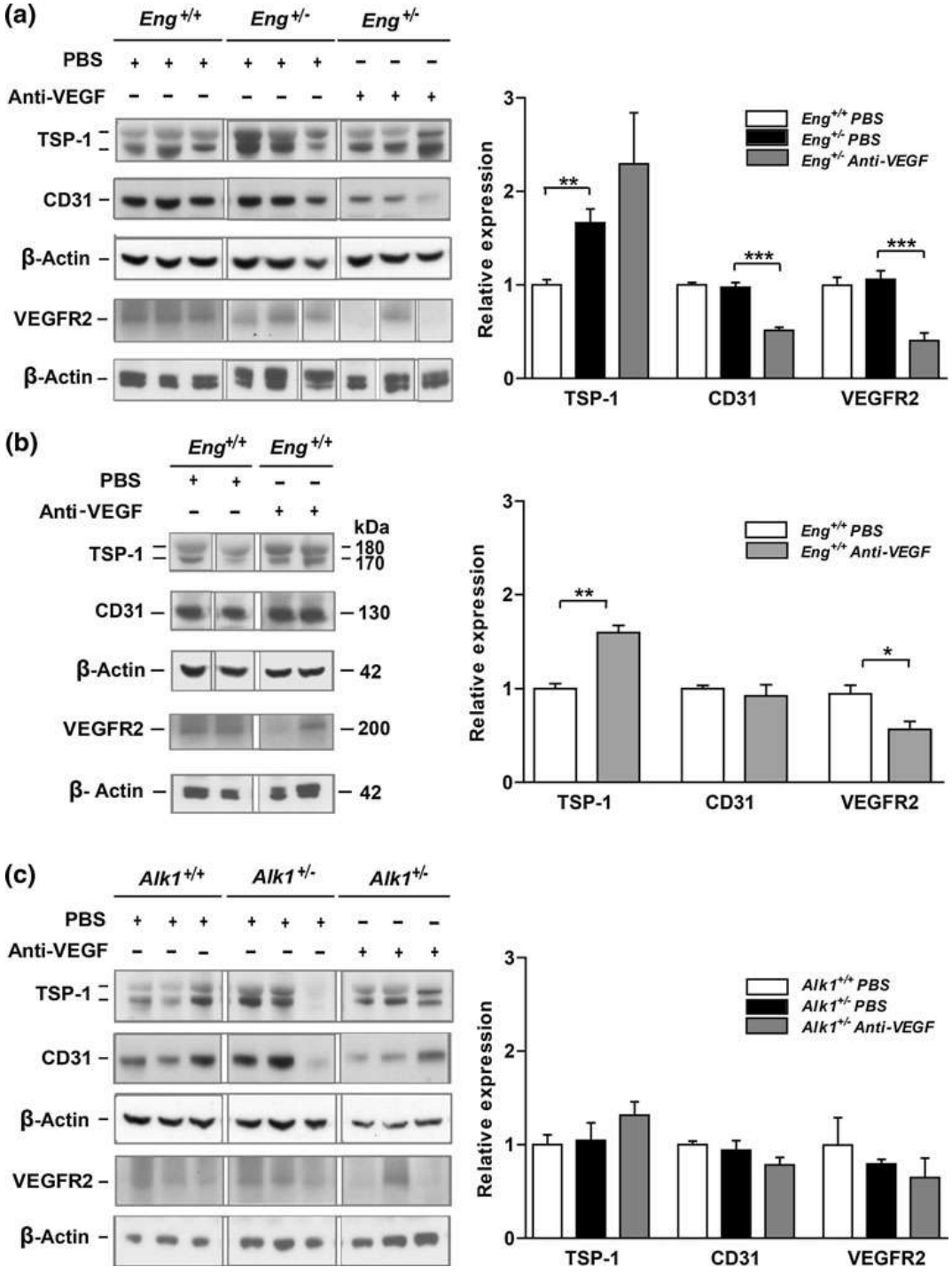
(a)
Eng+/+
Eng+/-
Eng+/-
PBS
Anti-VEGF
TSP-1
CD31
β-Actin
VEGFR2
β-Actin
Relative expression
Eng+/+ PBS
Eng+/- PBS
Eng+/- Anti-VEGF
TSP-1
CD31
VEGFR2
(b)
Eng+/+
Eng+/+
PBS
Anti-VEGF
kDa
TSP-1
180
170
CD31
130
β-Actin
42
VEGFR2
200
β- Actin
42
Relative expression
Eng+/+ PBS
Eng+/+ Anti-VEGF
TSP-1
CD31
VEGFR2
(c)
Alk1+/+
Alk1+/-
Alk1+/-
PBS
Anti-VEGF
TSP-1
CD31
β-Actin
VEGFR2
β-Actin
Relative expression
Alk1+/+ PBS
Alk1+/- PBS
Alk1+/- Anti-VEGF
TSP-1
CD31
VEGFR2

Figure 23. Hepatic angiogenic profile differs in *Endoglin* and *Alk1* mutant mice and is differentially targeted by anti-VEGF treatment. Expression of TSP-1, CD31 and VEGFR2 in total liver extracts from **a)** $Eng^{+/-}$, **b)** $Eng^{+/+}$ and **c)** $Alk1^{+/-}$ mice treated with PBS or G6-31 antibody. Representative Western blots are shown. Quantitation of protein expression was done relative to β-actin and normalized to mean values for WT samples (PBS-treated $Eng^{+/+}$ mice n = 5-10; PBS-treated $Eng^{+/-}$ mice n = 5-12; G6-31-treated $Eng^{+/-}$ mice n = 5-7; G6-31-treated $Eng^{+/+}$ mice n = 3-4; PBS-treated $Alk1^{+/+}$ mice n = 3-6; PBS-treated $Alk1^{+/-}$ mice n = 4-6; G6-31-treated $Alk1^{+/-}$ mice n = 4-7); *P< 0.05, **P< 0.01, *** P< 0.005 as determined by one-way ANOVA, followed by Tukey's post-hoc test.

After anti-VEGF treatment, we observed a 59% increase in TSP-1 in the WT *Eng*$^{+/+}$ mice (Figure 23 b) and a rising trend in *Eng* and *Alk1* mutant mice (Figure 23 a, c). These changes in hepatic TSP-1 levels after anti-VEGF treatment appear to correlate with the observed decrease in liver MVD. CD31 protein levels were similar in both PBS-treated heterozygous and WT mice (Figure 23 a, c). G6-31 antibody treatment decreased CD31 levels by 50% in *Eng*$^{+/-}$ mice, but seemingly had no effect in *Eng*$^{+/+}$ mice (Figure 23 a-b), despite reduction in MVD. This could be due to the smaller sample size in treated *Eng*$^{+/+}$(n = 4) versus *Eng*$^{+/-}$ (n=7) group. In the case of *Alk1*$^{+/-}$ mice, Tukey's post-hoc comparison showed a trend towards reduced CD31 levels in anti-VEGF compared to PBS-treated mice (0.78 ± 0.1 versus 0.94 ± 0.1; n = 6-7 /group; P = 0.16). Hepatic VEGFR2 levels were comparable in both PBS-treated heterozygous groups versus their WT littermates but were significantly reduced after anti-VEGF therapy in *Eng*$^{+/-}$ (n=5; 62% decrease) and *Eng*$^{+/+}$ mice (n=3; 46% decrease) (Figure 23 a, b). However, we could not detect a significant change in VEGFR2 in G6-31-treated *Alk1*$^{+/-}$ mice, likely due to more variability among these samples (0.65 ± 0.21; n = 4) and the semi-quantitative nature of Western blots (Figure 23 c). Overall, the effects of anti-VEGF treatment on these angiogenic/angiostatic factors were more pronounced in *Eng* than in *Alk1* mutant and *Eng*$^{+/+}$ mice. Lastly, hepatic Ang-2 levels were similar in both PBS-treated mutant and WT mice and were not altered after anti-VEGF treatment, as measured by Western blot (data not shown). To investigate further the hepatic molecular profile, we analyzed the total TGF-β1 protein levels in both heterozygous groups. Total TGF-β1 was not different in PBS-treated mutant and WT mice, and remained at baseline after anti-VEGF treatment (Table 6).

In summary, our findings suggest differences in the angiogenic/angiostatic profile of *Eng* and *Alk1* heterozygous mice that may influence their response to anti-VEGF treatment.

2. 4. 6 Distinct in vivo hepatic hemodynamic response of *Endoglin* and *Alk1* mutant mice after anti-VEGF therapy

To determine the functional hepatic microvascular effects of anti-VEGF therapy in both mutant groups, we measured liver microvascular perfusion *in vivo*, using contrast-enhanced micro-ultrasound (CE-US) imaging. We evaluated two parameters: wash-in rate, an indicator of blood flow rate and peak enhancement (PE), a measure of tissue blood volume[239]. Representative images are shown for antibody-treated and PBS-treated WT and mutant mice in Figure 24 a, b. The PE colored parametric maps showed that mutant and WT mice have comparable hepatic microvascular perfusion (red and orange-colored areas). G6-31 antibody treatment significantly reduced hepatic PE (blood volume) in the illustrated $Eng^{+/-}$ mouse, when compared to PBS treatment, as indicated by the number of hypo-perfused (blue-colored) regions (Figure 24 a). The depicted G6-31-treated *Alk1* mutant mouse had only a minor decreased in liver PE and fewer corresponding blue-colored areas (Figure 24 b). Next, dynamic changes in hepatic microvascular perfusion were plotted as a time intensity curve for each PBS and G6-31-treated *Eng and Alk1* mouse (Figure 24 c, d). Hepatic blood flow rate was comparable in the PBS-treated mutant and WT mice, but reduced only in the anti-VEGF treated *Eng* mutant mice (Fig. 24 c). Data quantitation revealed a significant (50%) decrease in WiR values in the anti-VEGF versus PBS-treated $Eng^{+/-}$ mice (Figure 24 e). In contrast, WiR was not altered in G6-31-treated *Alk1* mutant mice, compared to controls (Figure 24 f).

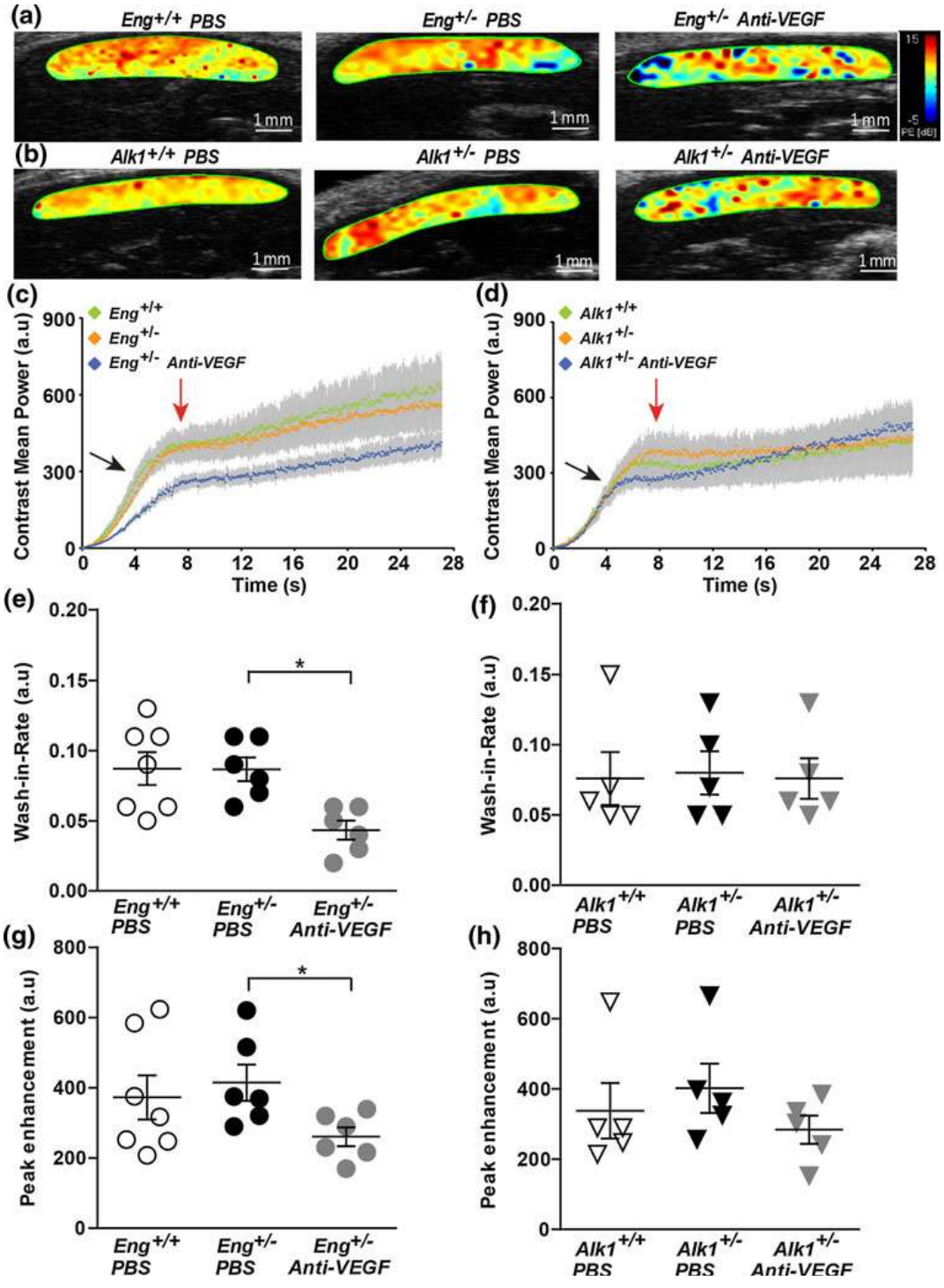
(a)
Eng+/+ PBS
Eng+/- PBS
Eng+/- Anti-VEGF
1 mm
15
-5
PE [dB]
(b)
Alk1+/+ PBS
Alk1+/- PBS
Alk1+/- Anti-VEGF
(c)
Eng+/+
Eng+/-
Eng+/- Anti-VEGF
Contrast Mean Power (a.u)
Time (s)
(d)
Alk1+/+
Alk1+/-
Alk1+/- Anti-VEGF
(e)
Wash-in-Rate (a.u)
Eng+/+ PBS
Eng+/- PBS
Eng+/- Anti-VEGF
(f)
Alk1+/+ PBS
Alk1+/- PBS
Alk1+/- Anti-VEGF
(g)
Peak enhancement (a.u)
(h)

Figure 24. *In vivo* functional hepatic microvascular effects of anti-VEGF treatment in *Endoglin* and *Alk1* mutant mice. Representative contrast-enhanced ultrasound (CE-US) parametric images of peak enhancement (PE) in liver of **a)** PBS-treated *Eng* and G6-31-treated $Eng^{+/-}$ mice and **b)** PBS-treated *Alk1* and G6-31-treated $Alk1^{+/-}$ mice. Scale bar = 1 mm; color map scale: -5 to 15 decibels [237]. Graph illustrating the time-intensity curve measured for **c)** *Eng* and **d)** *Alk1* mice treated with PBS and anti-VEGF therapy. The black arrow points to the slope or wash-in-rate [240], a parameter of blood flow rate, and the red arrow, to the plateau or PE, an index of blood volume or functional MVD. Quantitation of WiR and PE in **e), g)** *Eng* and **f), h)** *Alk1* mice treated with PBS and G6-31 antibody; n = 5-7/group. Circles and inverted triangles represent individual *Eng* and *Alk1* mice, respectively. ○ ▽(wild type, PBS-treated); ● ▼ (mutant, PBS-treated); ● ▼ (mutant, G6-31 antibody-treated) . Mean ± SEM are shown. *P< 0.05

The hepatic microvascular blood volume (PE) estimated by perfusion was similar in PBS-treated heterozygous and WT mice, confirming the computerized histologic MVD measurements (Figure 24 g, h). Interestingly, PE was reduced by 37% in anti-VEGF- versus PBS-treated $Eng^{+/-}$ mice (P = 0.02; n = 6/group) (Figure 24 g), in keeping with the significant reduction in histological MVD. In the case of anti-VEGF-treated $Alk1^{+/-}$ mice, a trend towards lower PE was noted but no significant difference was reached (Figure 24 h), despite the reduction in MVD estimated by CD31 immunostaining (Figure 22 c, e). This difference between the estimated in vivo blood volume and the histological tissue MVD in the anti-VEGF-treated heterozygous mice suggests that the flow rate contributes to the functional blood volume measurements (Figure 24 e-f). Lower hepatic blood flow rate observed in the anti-VEGF-treated $Eng^{+/-}$ but not in the $Alk1^{+/-}$ mice, may explain the difference in the total blood volume measured in these mutant mice. Importantly, the liver/body weight ratio was not affected by G6-31 antibody treatment in any of *Eng* and *Alk1* mutant mice (0.04 in all groups of mice; n = 6-24 mice/group). Thereby, we conclude that anti-VEGF treatment has a stronger *in vivo* effect on hepatic microvascular perfusion in $Eng^{+/-}$ than $Alk1^{+/-}$ mice.

2. 4. 7 Anti-VEGF treatment is well tolerated and has no apparent side effects in murine models of HHT

To determine if a total of 4 i.p. injections of G6-31 antibody (5 mg/kg weekly) had any side effects, we measured blood pressure (BP), heart rate (HR) and proteinuria at baseline (data not shown) and at the end of treatment in PBS and anti-VEGF treated $Eng^{+/-}$ and $Alk1^{+/-}$ mice (Table 7). None of these parameters were altered by treatment.

Table 7. Blood pressure, heart rate and proteinuria are not affected by G6-31 antibody treatment in *Eng* and *Alk1* heterozygous mice

Mice & treatment	*n*/group	Systolic blood pressure (mmHg)	Heart rate (beats/min)	Proteinuria (g/l)
$Eng^{+/+}$ PBS treated	7	100 ± 2	630 ± 37	0.3 ± 0.0
$Eng^{+/-}$ PBS treated	7	101 ± 4	685 ± 42	0.4 ± 0.0
$Eng^{+/-}$ G6-31 treated	5	110 ± 7	669 ± 42	0.4 ± 0.1
$Alk1^{+/+}$ PBS treated	10	110 ± 3	590 ± 9	0.4 ± 0.0
$Alk1^{+/-}$ PBS treated	3	102 ± 3	649 ± 11	0.4 ± 0.0
$Alk1^{+/-}$ G6-31 treated	4	114 ± 5	617 ± 14	0.4 ± 0.1

$Eng^{+/-}$ and $Alk1^{+/-}$ mice were injected with G6-31 antibody at 5mg/kg, weekly, for a total of 4 injections; WT and mutant mice were also treated i.p. with PBS. Blood pressure (BP), heart rate (HR) and proteinuria were measured at the end of treatment. Mean ± SEM are reported for each group. Three-group comparison was done using one-way ANOVA.

In addition, kidney, liver and lung tissue sections showed no signs of toxicity, as assessed by careful pathological examination.

2. 5 Discussion

We report that dysregulated angiogenesis was observed only in the lungs of *Eng* and *Alk1* heterozygous mice, and was characterized by rarefied peripheral microvasculature and secondary RVH. This reduced vascularization was associated with increased expression of the angiostatic protein TSP-1 in $Eng^{+/-}$ lungs and of the destabilizing factor Ang-2 in $Alk1^{+/-}$ lungs. Strikingly, systemic anti-VEGF therapy increased the peripheral lung microvascularization, restoring it to normal and eliminating RVH in both models. The treatment effectively decreased lung VEGF levels but normalized TSP-1 and Ang-2 levels in *Eng* and *Alk1* mutant mice respectively. The G6-31 monoclonal antibody treatment decreased hepatic MVD in mutant and WT mice, suggesting a liver-specific rather than an HHT-specific effect. However, *in vivo* CE-US imaging revealed that $Eng^{+/-}$ mice have a stronger hepatic hemodynamic microvascular response to anti-angiogenic therapy than $Alk1^{+/-}$ or WT mice, possibly due to the increase in basal liver TSP-1 levels. This is the first report showing that *Eng* and *Alk1* heterozygous mice may have a distinct molecular angiogenic/angiostatic profile in different organs, which may explain some of the heterogeneity observed in HHT1 versus HHT2 phenotype. Our findings provide new insight into the angiogenic imbalance associated with *ENG* and *ALK1* mutations and raise the need to assess the organ-specific effect of anti-angiogenic therapy in systemic vascular dysplastic diseases such as HHT.

Emerging data suggest that anti-VEGF therapy is beneficial in patients diagnosed with HHT. However, little is known about the mechanisms responsible for the effects of

this therapy. Published data on VEGF levels in HHT are scarce and contradictory. In adult HHT patients, mean plasma VEGF levels were higher (331 pg/ml) than in controls (20 pg/ml)[205], suggesting an overall increased angiogenesis. Retinal endothelial cells obtained from immorto/*Eng*$^{+/-}$ pups secreted higher VEGF levels than controls, in agreement with increased vascular proliferation noted in these mutant mice[246]. In *Alk1*$^{+/-}$ versus WT mice, higher VEGF mRNA and protein levels were reported in lungs, liver and intestine[247]. In the current study, we found no differences in the basal levels of VEGF in different organs of congenic *Eng* and *Alk1* mutants versus their C57BL/6 WT counterparts. These discrepancies might be explained by different genetic backgrounds, as suggested by our previous data in 129/Ola versus C57BL/6 backcrosses[165]. Our models show reduced angiogenesis in the peripheral lung microvasculature, which was not associated with decreased VEGF levels but rather with an increase in the angiostatic TSP-1 protein and in the destabilizing factor Ang-2 in *Eng*$^{+/-}$ and *Alk1*$^{+/-}$ mice respectively. In patients with HHT, it was suggested that a "second hit", an angiogenic stimulus such as VEGF, might be the trigger for AVM formation in a host with an inherited predisposition for endothelial dysfunction[248]. In this respect, conditional knockout mice with tissue-specific *Eng* or *Alk1* gene deletion[225, 249] are more appropriate to study the effects of anti-VEGF therapy on regression of AVMs.

Despite no difference in basal VEGF levels, *Eng*$^{+/-}$ and *Alk1*$^{+/-}$ mice were responsive to anti-VEGF treatment and the rarefied peripheral lung MVD, generally associated with spontaneous PAH, was normalized by antagonizing VEGF. Our findings, obtained in normoxic conditions, are in contrast with those observed in a chronic hypoxia rat model, where the anti-VEGFR2 inhibitor SU5416 induced severe PAH [250]. In agreement with our observations, another group demonstrated that the multi-

kinase inhibitor sorafenib, at low concentration, had pro-angiogenic effects[251]. Our present study suggests that the reduced peripheral lung microvasculature is due to a substantial rise in TSP-1 protein in adult *Eng*$^{+/-}$ mice. The source of this marked TSP-1 elevation in *Eng*$^{+/-}$ mice, appears to be the dysfunctional endothelium, as indicated by in vitro studies with *Eng* deficient endothelial cells. Recently, it was reported that Immorto/*Eng*$^{+/-}$ pups have lower TSP-1 levels in retinal endothelial cells, when compared to WT pups, in agreement with the observed increased in vascular proliferation[246]. Thus, TSP-1 appears to be implicated in the modulation of angiogenesis in *Eng*$^{+/-}$ mice in an organ- and context-dependent manner. TSP-1 is an angiostatic extracellular matrix factor secreted by stromal fibroblasts and endothelial cells. When TSP-1 is produced in excess, it can induce apoptosis and vessel regression[252]. TSP-1 induced apoptosis was shown to occur through binding to the CD36 receptor, a rise in caspase-3, and phosphorylation of p38 mitogen-activated protein kinase (p38MAPK) in a lung metastatic tumor mouse model[253]. Furthermore, mice deficient in TSP-1 were protected against chronic hypoxia-induced PAH[254]. These findings suggest that excessive pulmonary TSP-1 may be responsible for the peripheral MVD rarefaction observed in the *Eng*$^{+/-}$ lungs, possibly through an apoptotic mechanism.

High baseline TSP-1 levels did not correlate with normal VEGF and TGF-β1 levels measured in the total lung extracts of *Eng* mutant mice. TSP-1 can block VEGF mobilization from the extracellular matrix and disrupt VEGFR2 signaling[255, 256], mainly through CD47 receptor, thereby inhibiting vessel proliferation. In the *Eng*$^{+/-}$ lungs, we cannot exclude the possibility that VEGF levels are lower in periphery, and that this difference was not detected in the total lung extracts. Moreover, TSP-1 can activate latent TGF-β1, leading to increased signaling. However, *Eng*$^{+/-}$ mice had normal lung

levels of endogenously active TGF-β1 levels, indicating that this mechanism was likely not implicated in the mutant *Eng* mice. These results are consistent with published data showing that TSP-1 induced apoptosis is independent of activation of latent TGF-β[257]. In agreement with this observation, downstream Smad 2 and Smad 1/5/8 phosphorylation was not affected in these mutant mice. Moreover, our findings suggest that a TSP-1 dependent, VEGF-mediated mechanism is responsible for the microvascular restoration noted in the peripheral *Eng*$^{+/-}$ lungs in anti-VEGF-treated mice. In support of this hypothesis, the decrease in endogenous lung VEGF levels following anti-VEGF treatment was accompanied by normalization of pulmonary TSP-1 levels, indicating that VEGF can also regulate TSP-1. AKT phosphorylation, downstream of VEGFR2 activation, was not altered in *Eng* or *Alk1* heterozygous mice prior to and after the anti-VEGF treatment. These results suggest that other VEGF-mediated pathways are implicated in the reversal of the dysregulated lung microvascular phenotype in mutant mice treated with G6-31 antibody.

In contrast, *Alk1*$^{+/-}$ lungs showed normal TSP-1 levels and were characterized by increased Ang-2 levels. These results are compatible with the observation that *Alk1*$^{-/-}$ embryos have higher Ang-2 mRNA levels than controls[220]. Furthermore, patients diagnosed with idiopathic PAH showed an increase in Ang-2 mRNA and protein levels in their plexiform lesions[258]. Ang-2, found almost exclusively in the activated endothelium, is the functional antagonist of the Ang-1-Tie2 pathway involved in the maintenance of vascular quiescence[259]. In the absence of angiogenic stimuli, local Ang-2 over-expression results in vascular destabilization and subsequent vessel regression[260, 261]. Thus, excessive pulmonary Ang-2 may have induced the reduction in peripheral pulmonary microvasculature observed in *Alk1* mutant lungs. Furthermore, it has been

reported that Ang-2 and VEGF interact closely. VEGF can directly up-regulate Ang-2 in the vascular endothelium and modify Ang-2 transcriptional activation, as demonstrated in a murine tumor model[262]. In *Alk1* mutant mice, anti-VEGF therapy reversed the abnormal lung phenotype through an Ang-2 mediated mechanism, suggesting a direct link between VEGF and Ang-2 in tissues undergoing active vascular remodeling.

Overall, our data indicate that TSP-1 and Ang-2 may be, at least in part, responsible for some of the phenotypic heterogeneity observed in HHT1 and HHT2 patients. Importantly, irrespective of the distinct angiogenic profile of *Eng* and *Alk1* mutant lungs, the response to anti-VEGF treatment was similar in both mouse models - decreased lung VEGF levels and normalized peripheral pulmonary microvasculature. These results suggest a VEGF-mediated regulation of both TSP-1 and Ang-2 in *Eng* and *Alk1* mutant lungs, respectively.

Liver is a well-vascularized organ, rich in VEGF mRNA[263]. We report that in our mouse models, liver had the highest VEGF protein levels (~1400-1700 pg/mg tissue) among all organs. Interestingly, hepatic TSP-1 levels were also increased in $Eng^{+/-}$ mice, indicating an inverse correlation between endoglin and TSP-1 in more than one organ. This increase in hepatic TSP-1 in $Eng^{+/-}$ mice may predispose to a heightened *in vivo* hemodynamic response to anti-VEGF treatment.

Liver MVD was substantially decreased after anti-VEGF therapy in WT and both *Eng* and *Alk1* mutant mice, suggesting that the effect of G6-31 antibody was liver- rather than HHT-specific. This effect would likely be reversible after discontinuation of anti-VEGF treatment, as previously reported for several organs[264,265]. The reduction in liver MVD after G6-31 antibody treatment was associated with a significant rise in angiostatic TSP-1 in *Eng* WT mice and a further increase in TSP-1 in the $Eng^{+/-}$ mice.

There was also a significant decrease in hepatic VEGFR2 levels in the anti-VEGF-treated *Eng*$^{+/-}$ and *Eng*$^{+/+}$ mice, arguing in favor of decreased VEGF signaling in the liver microvasculature in these mice. In addition, CD31 levels were reduced in total liver extracts of anti-VEGF-treated *Eng*$^{+/-}$ mice, indicating a stronger response of these mice to G6-31 antibody treatment. The effect of the anti-angiogenic treatment on hepatic MVD appears to be on the sinusoidal endothelium, as the hepatocytes remained unaffected, as assessed by careful histopathologic examination.

To confirm the anti-angiogenic effects and assess the feasibility of *in vivo* monitoring anti-VEGF therapy in liver, we used CE-US imaging technique[239]. We observed that G6-31 antibody treatment induced ~ 40% decrease in hepatic microvascular blood flow rate and volume in *Eng*$^{+/-}$ mice, but not in *Alk1*$^{+/-}$ mice, in agreement with the stronger effects noted on angiogenic/angiostatic factors. Recently, CE-US was used to monitor the effects of bevacizumab treatment in HHT patients with severe liver disease. Transit time between hepatic artery and vein was improved in the anti-VEGF-treated group[236]. No significant change in liver enzymes was reported in these patientsafter anti-angiogenic treatment. In our mouse models, we demonstrated the effects of anti-VEGF therapy on liver microvascular perfusion by measuring the hepatic blood volume in microvessels. In addition, we observed a reduction in blood flow rate in G6-31-treated *Eng*$^{+/-}$ mice, possibly contributing to the ~ 40% decrease in liver blood volume. This significant reduction in hepatic microvascular perfusion in *Eng* mutant mice would compensate for any potential changes in hepatic vascular resistance after anti-VEGF treatment. In fact, anti-VEGF agents had beneficial effects in mouse and rat models of portal hypertension[266,267]. Taken together, CE-US represents an excellent

non-invasive modality to monitor *in vivo* the hepatic functional microvascular parameters and their response to anti-angiogenic treatment in mice and man.

G6-31 monoclonal antibody, which binds to all VEGF-A isoforms, has a strong anti-angiogenic effect in tumor models[238]. G6-31 antibody, administered i.p. at 5 mg/kg once a week for 3-6 weeks, had no significant toxicity in a murine tumor model[268]. However, long-term treatment with G6-31 antibody (up to 52 weeks) can induce diffuse glomerulosclerosis in these models[268]. In our studies, injecting G6-31 antibody at 5mg/kg i.p. once a week for a total of 4 doses, induced no changes in BP, HR or proteinuria, nor any histological signs of toxicity. A recent study reported the cardiac and systemic effects of high dose G6-31 antibody treatment (10 mg/kg, twice weekly, for a total of 5 weeks) in C57BL/6 mice and a murine model of pre-atherosclerotic hyperlipidemia[269]. This regimen induced systemic hypertension (both systolic and diastolic), LV hypertrophy and abnormal renal function, changes that could be attenuated by co-administration of the angiotensin-converting enzyme inhibitor ramipril. It is therefore essential to avoid using higher than necessary doses of anti-VEGF treatment and to monitor and treat hypertension in patients, if necessary.

In conclusion**,** we demonstrated that the anti-VEGF therapy is effective in normalizing the lung peripheral MVD, attenuating the secondary RVH and restoring TSP-1 and Ang-2 levels to normal in $Eng^{+/-}$ and $Alk1^{+/-}$ mice, respectively. Future studies will address the underlying mechanisms of this beneficial anti-angiogenic therapy that appears to reverse signs of PAH in these models and determine if TSP-1 and Ang-2 are differentially expressed in HHT1 and HHT2 patients. In addition, the G6-31 antibody treatment had a liver-specific effect on MVD in both *Eng* and *Alk1* mutants and in WT mice, with a stronger *in vivo* microvascular effect in $Eng^{+/-}$ mice. Unless the

effect observed is strictly related to the particular antibody used, our data could indicate that patients with an *ENG* mutation will have a more significant hepatic response to anti-VEGF therapy than patients with an *ALK1* mutation. Such a response could be monitored accurately *in vivo* by CE-US and would contribute to evaluation of functional angiogenesis during follow-up and to the optimization of intermittent anti-angiogenic treatment regimens in HHT patients.

2. 6 Acknowledgements

We thank Genentech for kindly providing the G6-31 anti-VEGF mouse antibody; Dr. Lee Adamson (University of Toronto) for providing the blood pressure measurement instrument and software; Lily Morikawa, MLT Manager, Pathology Core Centre from Modeling Human Disease Toronto Centre for Phenogenomics (TCP) for expert design of the hepatic and cardiac computerized protocols; Qiang Xu and Napoleon Law (CMHD Pathology Core, TCP, Toronto) for expert computerized measurements of the cardiac and hepatic MVD and for CD31 staining, respectively; Dr. Susan Newbigging (Director, CMHD Pathology Core, Toronto Center for Phenogenomics, Toronto) for facilitating the usage of the Visiopharm Integrator System; Dr. Herman Yeger, for the use of the Olympus microscope; Clinton Hupper (VisualSonics, Toronto) for performing the pilot hepatic ultrasound measurements. We thank Dr. S. Paul Oh, University of Florida, for providing the *Alk1* heterozygous mice. This work was supported by grants from the Canadian Institute of Health Research (CIHR) (MOP-6247) and the Heart and Stroke Foundation of Canada to ML (T5598), and from the Terry Fox Foundation, Visual Sonics Inc. and CIHR (MOP–12164) to FSF. D. Ardelean is the recipient of a CIHR/CAG/Abbott fellowship award.

Chapter Three

Anti-VEGF therapy reduces intestinal inflammation in Endoglin heterozygous mice subjected to experimental colitis

Daniela S. Ardelean[1,2,3], Melissa Yin[4], Mirjana Jerkic[1,5], Madonna Peter[1,3], Bo Ngan[6], Robert S. Kerbel[4,7], F. Stuart Foster[4,7], Michelle Letarte[1,3,5,7]

[1]Molecular Structure and Function Program, Hospital for Sick Children, Toronto; [2]Division of Rheumatology, the Hospital for Sick Children, Toronto; [3]Department of Immunology, University of Toronto; [4]Biological Sciences, Sunnybrook Health Sciences Center, Toronto; [5]Heart and Stroke Richard Lewar Centre of Excellence, University of Toronto; [6]Division of Pathology, Hospital for Sick Children and Department of Laboratory Medicine and Pathobiology, University of Toronto; [7]Department of Medical Biophysics, University of Toronto, Toronto, Ontario, Canada

In this Chapter Three, I developed the treatment protocol, performed all colitis experiments, monitored all colitic mice for the entire duration of the experiments and treated the mice with G6-31 antibody and PBS vehicle. I developed a new colonic ultrasonic protocol, in collaboration with Ms. Melissa Yin from Dr. Stuart Foster's laboratory. Ms. Melissa Yin performed all ultrasonic experiments; I participated in these imaging experiments. I collected all the tissues used in these experiments and quantified the colonic MVD. I performed all the protein extractions, the TGF-β1 and VEGF ELISA and the Milliplex multi-analyte quantifications and the western blots presented in this

chapter. Dr. Mirjana Jerkic participated in the Milliplex multi-analyte testing. Lastly, I carried out the statistical analysis in all experiments. This project was supervised by Dr. Michelle Letarte.

3. 1 Abstract

Chronic intestinal inflammation is associated with pathological angiogenesis that further amplifies the inflammatory response. Vascular endothelial growth factor, VEGF, is a major angiogenic cytokine that has been implicated in chronic colitis and inflammatory bowel diseases. Endoglin (CD105), a TGF-β superfamily co-receptor expressed on endothelial and some myeloid cells, is a modulator of angiogenesis involved in wound healing and potentially in resolution of inflammation. We showed previously that *Endoglin* heterozygous ($Eng^{+/-}$) mice subjected to dextran sodium sulfate developed severe colitis, abnormal colonic vessels and high tissue VEGF. We therefore tested in the current study if treatment with a monoclonal antibody to VEGF could ameliorate chronic colitis in $Eng^{+/-}$ mice. Tissue inflammation and microvessel density (MVD) were quantified on histological slides. Colonic wall thickness, microvascular hemodynamics and targeted MAdCAM-1^{+} inflamed vessels were assessed *in vivo* by ultrasound. Mediators of angiogenesis and inflammation were measured by Milliplex and ELISA assays. Colitic $Eng^{+/-}$ mice showed an increase in intestinal inflammation, MVD, colonic wall thickness, microvascular hemodynamics and the number of MAdCAM-1^{+} microvessels relative to colitic $Eng^{+/+}$ mice; these parameters were all attenuated by anti-VEGF treatment. Of all factors up-regulated in the inflamed gut, G-CSF and amphiregulin were further increased in colitic $Eng^{+/-}$ versus $Eng^{+/+}$ mice. Anti-VEGF therapy decreased tissue VEGF and inflammation-induced endoglin, IL-1β and G-CSF in colitic $Eng^{+/-}$ mice. Our results suggest that endoglin modulates intestinal angiogenic and inflammatory responses in colitis. Furthermore, contrast-enhanced ultrasound provides an excellent non-invasive imaging modality to monitor gut angiogenesis, inflammation and responses to anti-angiogenic treatment.

3. 2 Introduction

Chronic inflammatory bowel diseases, such as Crohn's disease and ulcerative colitis, are characterized by severe gut inflammation[4] and are accompanied by the formation of new, excessive and persistent abnormal blood vessels from pre-existing ones[178]. This intestinal pathological angiogenesis enhances gut inflammation by allowing a higher influx of immune cells into the affected tissue. In addition, these newly formed vessels become inflamed and can directly secrete pro-inflammatory cytokines and chemokines that attract more immune cells, further amplifying the gut inflammation[178]. Thus, targeting intestinal pathological angiogenesis may reduce chronic gut inflammation.

Vascular endothelial growth factor (VEGF), a key pro-angiogenic protein secreted by most parenchymal and endothelial cells and by several activated immune cells, has a major role in physiological and pathological angiogenesis[42]. Moreover, VEGF is an important chemotactic factor for the $VEGFR1^+$ monocytes/macrophages[270, 271], can alter the function and maturation of dendritic cells[151] and at pathophysiologic concentrations, can inhibit T cell development and function by affecting early hematopoietic progenitor cells[152]. Yet, the role of VEGF in chronic inflammatory diseases is less understood. In patients diagnosed with inflammatory bowel diseases (IBD), VEGF is increased in serum and colonic tissues[208-210], suggesting that it might contribute to the pathogenesis of these diseases. Hence, VEGF-targeted therapies could ameliorate chronic colitis. Recently, it was shown that treatment with bevacizumab, a humanized monoclonal antibody to VEGF, used in conjunction with standard chemotherapy in two patients with metastatic colon cancer, was accompanied by remission of the underlying IBD[113].

Moreover, in the iodoacetamide-induced colitis rat model, a monoclonal antibody against VEGF-A isoforms (Ab-3) improved colitis[211]. However, the mechanisms through which VEGF-targeted therapies could attenuate colitis need to be determined.

Endoglin (CD105), a co-receptor for several transforming growth factor (TGF-β) superfamily ligands, including TGF-β1 and bone morphogenic protein BMP9, is predominantly expressed in endothelial cells (EC), but is also found in activated monocytes and macrophages, some hematopoietic cells, vascular smooth muscle cells and fibroblasts[53-55,158,272]. Endoglin is a crucial angiogenic modulator, as *Eng* null mice die at mid-gestation of angiogenic and cardiovascular defects[60]. Moreover, endoglin has a key role in tissue repair and wound healing[49], by promoting TGF-β1-mediated extracellular matrix production. The role of endoglin in inflammation is mostly unknown. It has been reported that tissue endoglin is up-regulated in chronic inflammatory disorders, such as IBD[49] and psoriasis[86], where it is often associated with macrophage and T cell infiltrates[49]. In addition, increased endoglin expression was noted in cultured fibroblasts from the intestinal strictures of patients with Crohn's disease[181]. Thus, endoglin may be involved in chronic inflammatory diseases such as IBD.

In a previous study, we showed that *Endoglin* heterozygous *($Eng^{+/-}$)* mice exposed to a single five-day course of dextran sodium sulphate (DSS) developed severe, chronic gut inflammation and prominent abnormal intestinal vessels, associated with increased tissue VEGF, while colitic $Eng^{+/+}$ mice recovered[179]. Therefore, we hypothesized that VEGF plays a pathogenic role in abnormal blood vessel formation and chronic inflammation in colitic $Eng^{+/-}$ mice and that a targeting VEGF will attenuate colitis in these mice.

In the present study, using *in vivo* and *in vitro* methods, we demonstrate that colitic *Eng*$^{+/-}$ mice have more gut inflammation and pathological angiogenesis, when compared to colitic wild type mice, despite showing comparable tissue VEGF levels. These findings suggest that factors other than VEGF contribute to the severe inflammatory and angiogenic phenotype observed in the colitic *Eng*+/- mice. Among several cytokines/chemokines elevated in the inflamed gut, the granulocyte colony-stimulating factor G-CSF and the regenerative protein amphiregulin were higher in colitic *Eng*$^{+/-}$ than *Eng*$^{+/+}$ mice. Anti-VEGF treatment decreased gut inflammation including tissue IL-1β and G-CSF, pathological angiogenesis and the number of MAdCAM-1^{+} inflamed vessels in colitic *Eng*$^{+/-}$ mice, suggesting that this anti-angiogenic therapy might have anti-inflammatory properties.

3. 3 Material and methods

3. 3. 1 Mice, DSS-induced colitis and anti-VEGF treatment

Mice. *Eng*$^{+/-}$ mice were generated by successive backcrosses (N26-N30) to C57BL/6 mice[60]. Mice were kept at the Toronto Center for Phenogenomics, a pathogen-free facility, and were fed standard chow. DietGel® Recovery **(**ClearH_2O, Portland, ME, USA) was added to all groups of mice at day 6, after completion of DSS induction, and continued for the rest of the experiment.

DSS-induced colitis. Colonic inflammation was induced with a single 5-day course of 3% DSS (m.w. 36–50 kDa; MP Biomedicals, Solon, OH, USA) added to the acidified drinking water, according to an established protocol[179]; mice were then returned to acidified water. Mice were monitored for a total of 25 days and the following

parameters were recorded daily: body weight, oral fluid intake, activity, stool consistency and fecal bleeding (using ColoScreen Hemocult kit, Helena Labs, Beaumont, TX).

Anti-VEGF treatment. 12-18 week-old *Eng*$^{+/-}$ mice of both genders were randomized to anti-VEGF- versus phosphate-buffered saline (PBS) vehicle treatment. The anti-VEGF-treated groups received G6-31 monoclonal antibody, kindly provided by Genentech Inc, South San Francisco, CA, USA. This antibody has high affinity and specificity for murine and human VEGF-A Colitic *Eng*$^{+/-}$ mice received 5 mg/kg of G6-31 antibody, i.p., starting at day 9 of colitis and then every 5 days, for a total of 3 injections. Mice were sacrificed between days 20-25 of colitis. The same regimen was applied to PBS-treated mice. A minimum of 5 mice/group was tested per each experiment. Data were reported as mean ± SEM for each group of mice.

3. 3. 2 Ultrasound imaging of the distal colon

In vivo imaging of the distal colon was completed using the Vevo®2100 high-frequency ultrasound system (VisualSonics Inc., ON, Canada). PBS-treated colitic *Eng*$^{+/+}$ and *Eng*$^{+/-}$ mice and G6-31-treated colitic *Eng*$^{+/-}$ mice were imaged 1-4 days after the 3rd injection (n = 5-12/group). Mice were anesthetized with 2% isoflurane (Abbott Laboratories Limited**,** QC, Canada) delivered in combination with 1L/min O_2, then placed in supine position on a heated stage. The heart rate was maintained above 400 beats/minute and body temperature monitored throughout the imaging session. A 27G butterfly needle was inserted into a lateral tail vein for intravenous injection of the ultrasound contrast agent. The fur on the lower abdomen was removed, and a bubble-free ultrasound gel was applied (Parker Laboratories, Inc., NJ, USA). A solid-state array

transducer (MS-250) was used at a centre frequency of 18 MHz with axial and lateral resolutions of 75 μm and 165 μm, respectively. Ultrasound gel was evenly introduced into the distal colon with a straightened gavage needle, to enhance the lumen-to-wall contrast. The distal colon was first imaged under B-mode for selection of the region of interest, followed by contrast mode. The imaging plane on the sagittal axis of the colon displayed the clearest image of distal colon walls. Non-linear contrast-enhanced images were collected after a 50 μL bolus injection of MicroMarker ultrasound contrast agent (VisualSonics Inc., CA, USA). All 3D data were acquired by moving the transducer with a stepper motor, at a step size of 50 μm. The following image acquisition settings were kept consistent throughout the study: 4% power, 37 dB contrast gain, and wide beam width.

Image analysis was completed offline on the VevoCQ™. B-mode images were collected as a 3D image stack, covering the length of the distal colon. For colonic wall thickness, ten measurements per mouse were taken from the top and bottom distal colon walls, by drawing lines across the intestinal wall of multiple B-mode images from the 3D stack; these values were then averaged. To determine the intestinal wall hemodynamic changes in each mouse, two ROIs, encompassing the top and bottom distal colonic walls, were drawn with reference to the respective B-mode image. Contrast data was extracted from the time-intensity curves (TIC) generated from the wash-in of microbubbles (MBs), and quantified using VevoCQ™ software. Two parameters were extracted from the TIC: 1) peak enhancement (PE), the difference between maximum amplitude and the baseline intensity of the curve, as an indication of the tissue blood volume; 2) wash-in rate (WinR), the maximum slope of the curve, used as a measurement of blood flow rate. Data from three different experiments, each

including at least 5 mice/group, were then quantified. Mean and SEM are shown.

3. 3. 3 MAdCAM-1-targeted contrast -enhanced ultrasound imaging of the inflamed colon

Molecular imaging of the inflamed colon was performed using mucosal addressin cell adhesion molecule-1 (MAdCAM-1)-targeted microbubbles (MBs) ultrasound (US) contrast agents. We used the Vevo MicroMarker target-ready contrast MBs (VisualSonics Inc, Toronto), composed of a perfluorocarbon gas core encapsulated in a streptavidin-coated phospholipid shell. The targeting ligand was the biotinylated rat anti-mouse MAdCAM-1antibody (clone MECA-367, Southern Biotech, Birmingham, AL, USA), attached to MBs through the biotinstreptavidin conjugation. Prior to injection, MBs were incubated with the MAdCAM-1 antibody at a ratio of 8 μg ofantibody per 107 MBs[273]. One 50 μL bolus of targeted MBs per mouse was administered via the tail vein in PBStreated colitic $Eng^{+/+}$, $Eng^{+/-}$ mice and G6-31-treated colitic $Eng^{+/-}$ mice, placed in random order. Thirty seconds after each bolus, contrast US images were collected to verify MBs wash-in rate (WinR), followed by a 2 minute pause to allow the binding of MAdCAM-1-targeted MBs to the inflamed intestinal microvessels. After the accumulation of MBs in the distal colon and image collection for 15 seconds, a high-power destruction pulse sequence was applied to disrupt all MBs in the field of view. The following 30 seconds of imaging were used to observe the recirculation of free MBs into the field of view. Quantification of the adherent targeted MBs to the intestinal MAdCAM-1^{+} microvessels was performed with the VevoCQTM software. The differential targeted enhancement, the dTE parameter, representing the difference in contrast signal intensity between the pre- and

postdestruction image frame[273, 239] was used to measure the relative amount of bound targeted MBs to the intestinal MAdCAM-1^{+} microvessels in all three groups of colitic mice.

3. 3. 4 Colonic histologic evaluation

Mice were anesthetised with ketamine (100 mg/kg) and xylazine (10 mg/kg) i.p, and blood collected by intracardiac puncture 1-6 days after the last injection. Heart was perfused with PBS through the left ventricle, for organ harvesting. Distal colon was cut longitudinally, washed in PBS and immersed in 4% paraformaldehyde. Tissues were processed, paraffin-embedded, sectioned (5 μm) and stained with hematoxylin-eosin (H&E).

Inflammation score. The severity of colonic inflammation was scored for all samples, by an experienced pathologist, in a blinded fashion. The most affected colonic area was first selected at 100x magnification. The histological inflammatory score was obtained for this most affected area at 400x magnification, and quantified in three power fields per section, using a previously published system[274], with slight modifications. To indicate the decrease in goblet cell number, a scale from 0-minus 4 was used. All other scores were expressed as positive numbers: mucosal thickening (0-4) (0 = no increase; 1 = 25% increase; 2 = 50% increase; 3 = 75% increase; 4 = 100 % mucosa thickened); presence of mucosal inflammatory cells (0-4) (0 = difficult to find; 1 = minor increase in cell number, but not clustered or invading the glands; 2 = significant increase in neutrophils (PMN), invading the glands; 3 = groups of PMN in near every field; 4 = PMN in every field); presence of submucosal inflammatory cell infiltrate scored by a similar method (0-4); destruction of architecture (0-4); ulcers (0-4, corresponding to 0, 25%, 50%, 75%, 100% loss of epithelium); crypt abscesses (containing PMN) (0-4,

corresponding to 0, 25%, 50%, 75%, 100% involvement of the epithelium). The inflammatory score, ranging from 0-30, was calculated for each mouse by adding the score for each component. The average inflammatory socre per each group of mice was reported.

Other colonic sections were stained for the endothelial cell marker CD31. Tissue sections were incubated overnight at 4°C with a rabbit antibody to CD31 (ABCAM Cambridge, MA, USA; 1:100 dilution) followed by biotinylated goat anti-rabbit IgG (Vector Labs Inc, Burlington, ON, Canada; 1:200 dilution) and an ABC detection kit (Vector Labs Inc, 1:50 dilution). Color development was done for 10 minutes with diaminobenzidine tetrahydrochloride. Slides were then counterstained with Harris Hematoxylin.

3. 3. 5 Quantification of microvessel density (MVD)

Colonic MVD was quantified using the Olympus BX60 microscope (Carsen Group Inc, Center Valley, PA, USA), equipped with a digital camera QImaging RETIGA 2000R (software QCapture 3-1.1.1) and analyzed with OpenLab software 3.1.4 version (Improvision Inc. Lexington MA, USA). The most vascularised colonic area was selected at 100x magnification and the $CD31^+$ vessels were counted in 5 consecutive fields, at 400x magnification. A minimum of 5 mice/group was analyzed. MVD was reported as the total number of vessels/mm^2.

3. 3. 6 Protein measurements

Tissue and plasma samples were collected at days 20-25 of colitis. The frozen tissues were homogenized in 0.05 M Tris-HCl, pH 7.4 supplemented with 1% Triton X-

100 and protease/phosphatase inhibitors (Roche, Canada, Mississauga, ON, Canada), and centrifuged at 13,000 g for 30 minutes, at 4°C. Protein concentration in lysates or plasma was measured with the Bradford assay.

3. 3. 7 ELISA assays

Tissue levels of TGF-β1 were determined with the mouse ELISA kit (R&D Systems). To measure total TGF-β1 levels, samples were first acidified with 1N HCl for 10 minutes at room temperature and then neutralized with 1.2 N NaOH/0.5 M HEPES. All samples were measured in duplicate.

Tissue and plasma VEGF levels were quantified using the mouse Duoset ELISA kit (R&D Systems, Minneapolis, MN, USA). Total plasma and tissue VEGF levels, measured at time of sacrifice, included antibody-bound VEGF and free VEGF. Free residual plasma and tissue VEGF levels were measured after immunodepletion, performed as previously described[243]. Briefly, GammaBind G Sepharose beads (GE Healthcare, Baie D'Urfe, QC, Canada) were washed with PBS and incubated with tissue lysates or plasma. One and two-step immunodepletion were used for the tissue lysates and plasma free VEGF measurements, respectively.

Quantification of colonic angiogenic and growth factors was performed using the 27-plex MILLIPLEX map for multi-analyte profiling of mouse angiogenesis/growth factors using the magnetic bead panel kit MAGPMAG-24K, kindly provided by EMD Millipore Corporation, Billerica, MA USA. Samples were analyzed using the Luminex xMAP instrument.

3. 3. 8 Western blots

Colonic protein extracts were fractionated on 4-12% gradient gels by SDS/PAGE under reducing or non-reducing conditions and immunoblotted with the following primary antibodies at appropriate dilutions: rabbit anti-phosphorSmad1 (Ser463/465)/Smad5(Ser463/465)/Smad8(Ser426/428) (#9511), 1:1,000, rabbit anti-phoshor-Smad2 (Ser465/467) (#3101), 1:1,000, mouse anti-Smad2 (L16D3) (#3103), 1:1,000 (all from Cell Signaling Technology Inc, Danvers, MA, USA); mouse anti-Smad1/5/8 (sc-81378), 1:1,000, Santa Cruz Biotechnology Inc, Santa Cruz, CA, USA; mouse anti-VEGFR2, (clone # 91201, catalog MAB443), 1:500 (R&D Systems, Minneapolis, MN, USA); mouse anti-β-actin, 1:10,000 (Sigma, St. Louis, MO, USA). Appropriate secondary antibodies conjugated with horseradish peroxidase (1:10,000 dilution) and the enhanced chemiluminescence reagent (ECL, Perkin Elmer, Shelton, Connecticut, USA) were used for detection. Band intensity was quantified, expressed relative to β-actin, and normalized to values corresponding to the mean of WT samples, for comparison between experiments.

3. 3. 9 Statistical analysis

Statistical analysis was performed with t-test (for 2 groups), one-way ANOVA (for ≥ 3-group comparison), using GraphPad Prism 5 software (GraphPad Software, La Jolla, CA, USA). If ANOVA comparison led to a statistically significant result, post-hoc analysis was performed using Tukey's test for one-way ANOVA. Results are expressed as mean ± SEM; $P \leq 0.05$ was considered statistically significant.

Ethical approval

All protocols were approved by the Animal Care Committees of the Hospital for Sick Children, the Toronto Center for Phenogenomics and the Sunnybrook Research Institute, in accordance with the Canadian Council on Animal Care guidelines and regulations.

3. 4 Results

3. 4. 1 Colitic *Eng*$^{+/-}$ mice have higher and persistent colonic CD31^{+} microvessel density (MVD) than colitic *Eng*$^{+/+}$ mice

Our laboratory showed previously that congenic *Eng*$^{+/-}$ mice subjected to a single five-day course of 3% DSS developed severe, chronic colitis and abnormal intestinal blood vessels, while colitic wild type (WT or *Eng*$^{+/+}$) mice recovered[179]. We also demonstrated that the peak of disease and tissue inflammation occurred at day 9 in both groups of mice and that both inflammation and abnormal vascular protusions remained high till days 18-26 in colitic *Eng*$^{+/-}$ mice, while decreasing in colitic WT mice[179].

In the present study, to investigate the changes over time in colonic pathological angiogenesis, we quantified CD31^{+} microvessel density (MVD) at day 0 (prior to DSS), day 9 (peak of inflammation) and days 20-25 of colitis (normally expected recovery phase) in colitic *Eng*$^{+/-}$ and *Eng*$^{+/+}$ mice (Figure 25). CD31^{+} MVD is an established angiogenic parameter that has been used to evaluate the response to anti-angiogenic therapy in several experimental and human studies (Figure 25). CD31^{+} MVD is an established angiogenic parameter that has been used to evaluate the response to anti-angiogenic therapy in several experimental and human studies [275].

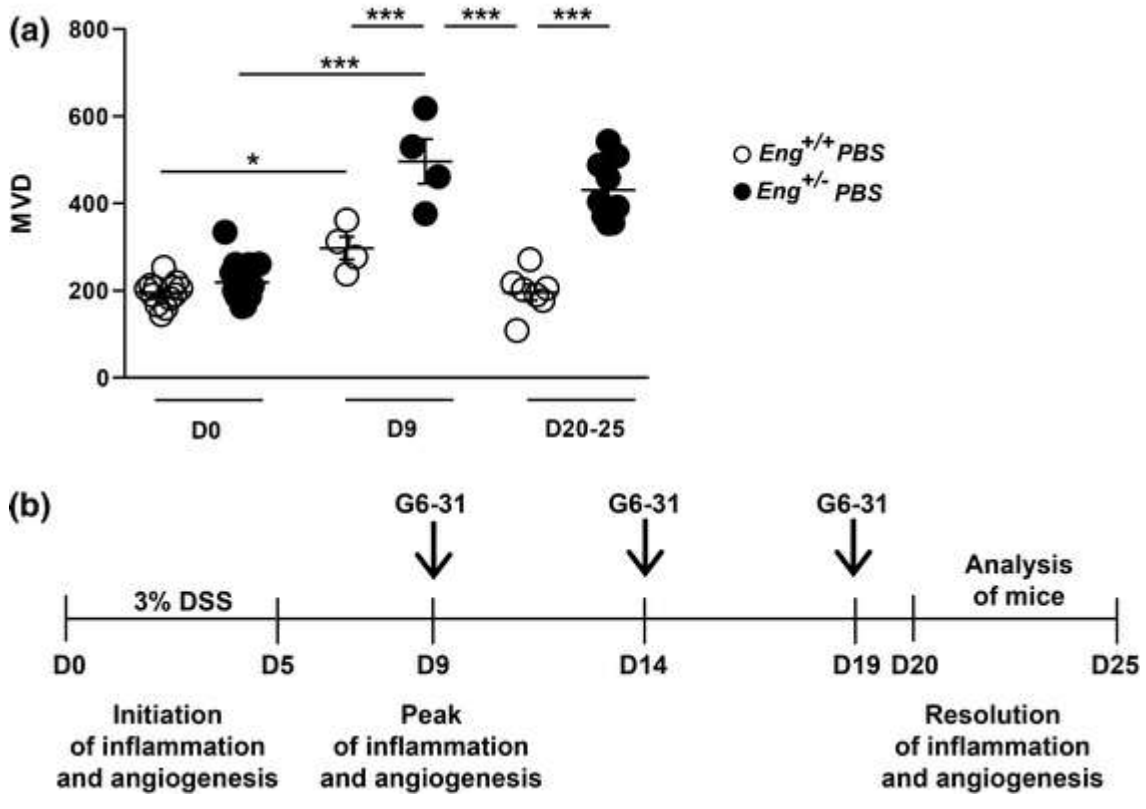

Figure 25. Colitic *Eng*$^{+/-}$ mice have persistent higher intestinal microvessel density (MVD), but the same peak of disease as colitic *Eng*$^{+/-}$ mice. a) Colitic *Eng*$^{+/-}$ mice had higher colonic MVD, compared to colitic WT mice (n = 13/group at day 0; n = 4/group at day 9 of colitis; n = 7-9/group at days 20-25 of colitis**)**; **b)** Schematic of DSS induction of colitis and anti-VEGF treatment regimen in *Eng*$^{+/-}$ mice. DSS was administrated for 5 days in drinking water, followed by return to normal water. G6-31 monoclonal antibody was injected i.p at 5 mg/kg, at days 9, 14 and 19 of colitis. Mice were monitored daily and sacrificed between days 20 and 25 of colitis. Black arrows indicate the timing of injections. Circles depict: (wild type, PBS-treated); (mutant, PBS-treated). Mean ± SEM are shown. *P<0.05; ***P<0.001 by one-way ANOVA, followed by Tukey's post-hoc test.

Here we confirm our recent observations that colonic MVD is similar in WT and *Eng*$^{+/-}$ mice at baseline, under non-inflammatory conditions, as shown in Chapter Two. At day 9 of colitis, colonic MVD was significantly higher (2.2-fold) in colitic *Eng*$^{+/-}$ than WT mice (1.5-fold), and compared to day 0 (pre-DSS). At days 20-25 of colitis, colonic MVD remained higher in *Eng*$^{+/-}$ mice (1.9-fold) compared to day 0, whereas in colitic WT mice, MVD returned to baseline or non-inflammatory value. These results suggest that colitic *Eng*$^{+/-}$ mice had a higher intestinal angiogenic response in the initial phase corresponding to maximum inflammation and a delayed or impaired resolution of tissue angiogenesis, as demonstrated by the persistence of high MVD in the recovery phase of colitis, when compared to colitic WT mice (Figure 25 a).

In Chapter Two, we ruled out an effect of G6-31 antibody on intestinal MVD in *Eng*$^{+/+}$ and of IgG isotype control on several organs including the gut, in *Eng*$^{+/+}$ and *Eng*$^{+/-}$ mice, under non-inflammatory conditions[276]. We therefore started the anti-VEGF treatment on day 9, at the peak of inflammation and angiogenesis. G6-31 antibody treatment was given at 5 mg/kg i.p, at days 9, 14 and 19, for a total of 3 injections. Mice were then analyzed at days 20-25 of colitis (expected time of resolution of inflammation and angiogenesis) (Figure 25 b).

3. 4. 2 Anti-VEGF therapy decreases colonic inflammation and microvessel density (MVD) in colitic *Endoglin* heterozygous mice

To investigate the effects of anti-VEGF treatment on tissue inflammation, colonic sections obtained from PBS-treated *Eng*$^{+/+}$, *Eng*$^{+/-}$ and anti-VEGF-treated *Eng*$^{+/-}$ mice sacrificed at days 20-25 of the DSS-induced colitis, were examined by an experienced pathologist. Representative images of H&E-stained colonic sections

obtained from these mice are shown in Figure 26 a. Sections from a PBS-treated colitic *Eng*$^{+/+}$ mouse showed minimal inflammatory infiltrate, normal tissue architecture and submucosal thickness, indicating resolution of inflammation. In contrast, colonic sections from a PBS-treated colitic *Eng*$^{+/-}$ mouse revealed significant inflammatory infiltrate in the mucosa, loss of tissue architecture and submucosal edema, suggesting ongoing inflammation. Sections from the colon of the G6-31-treated colitic *Eng*$^{+/-}$ mouse displayed reduced inflammatory infiltrates, thinner submucosal layer and restoration of normal tissue architecture, pointing towards recovery from inflammation and tissue regeneration.

To determine the effects of G6-31 antibody on intestinal angiogenesis, MVD was quantified in colonic sections of anti-VEGF-treated colitic *Eng*$^{+/-}$ mice and compared to that of PBS-treated colitic *Eng*$^{+/-}$ and *Eng*$^{+/+}$ mice. Representative images of CD31-stained colonic vessels are shown for all three groups of mice in Figure 26 b. Sections from the PBS-treated colitic *Eng*$^{+/+}$ mouse revealed several microvessels in the inflamed tissue, whereas the colon from the PBS-treated colitic *Eng*$^{+/-}$ mouse showed multiple microvessels in the mucosal and submucosal layers, predominantly clustered within the inflammatory infiltrates. A colonic CD31^{+} microvascular staining pattern similar to that of a PBS-treated colitic WT mouse was observed in the G6-31-treated colitic *Eng*$^{+/-}$ mouse, suggesting that the treatment had reduced tissue MVD.

Data quantification demonstrated that PBS-treated colitic *Eng*$^{+/-}$ mice had a ~ 2-fold higher inflammation score than colitic WT mice. Importantly, inflammation score was reduced in G6-31-treated colitic *Eng*$^{+/-}$ mice to levels comparable to those seen in colitic *Eng*$^{+/+}$ mice (Figure 26 c).

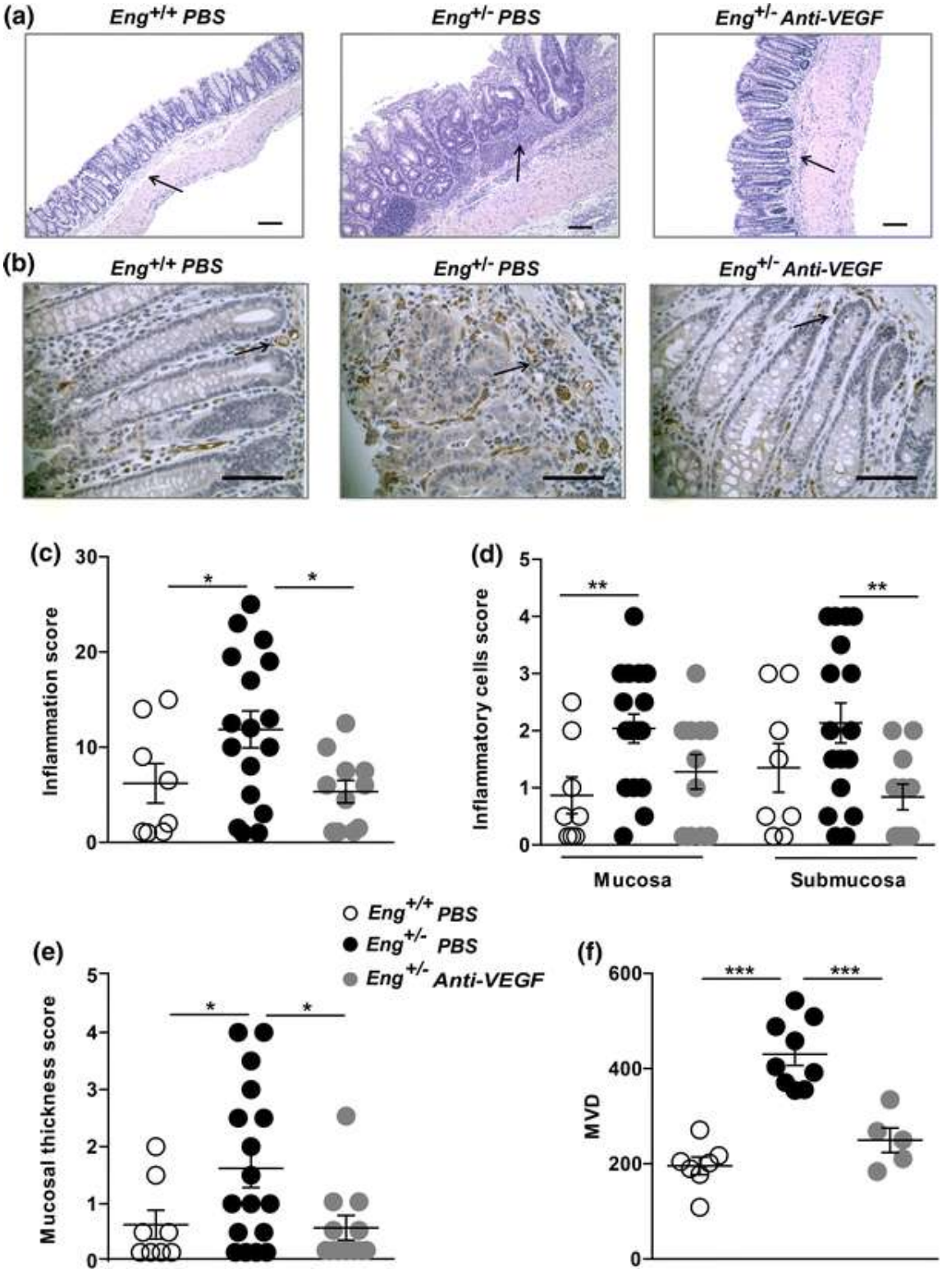
(a)
Eng+/+ PBS
Eng+/- PBS
Eng+/- Anti-VEGF
(b)
Eng+/+ PBS
Eng+/- PBS
Eng+/- Anti-VEGF
(c)
Inflammation score
30
20
10
0
*
*
(d)
Inflammatory cells score
5
4
3
2
1
0
**
**
Mucosa
Submucosa
Eng+/+ PBS
Eng+/- PBS
Eng+/- Anti-VEGF
(e)
Mucosal thickness score
5
4
3
2
1
0
*
*
(f)
MVD
600
400
200
0
***
***

Figure 26. Anti-VEGF treatment reduces scores for colonic inflammation, mucosal thickness, submucosal inflammatory cell infiltrate and microvascular density (MVD) in colitic *Eng*+/- mice. a) Representative images of H&E-stained colonic sections (100 x magnification) from PBS-treated colitic *Eng*+/+, *Eng*+/- and G6-31-treated colitic *Eng*+/- mice, sacrificed between days 20 and 25 of colitis. Black arrows point towards the inflammatory infiltrates. Scale bars: 10 μm. **b)** Colonic sections from PBS-treated colitic *Eng*+/+, *Eng*+/- and G6-31 antibody-treated colitic *Eng*+/- mice were stained for CD31, and MVD quantified in 5 consecutive fields at 400x magnification. Black arrows point towards CD31+ vessels (depicted in brown). Scale bars: 40 μm. **c)** Colonic inflammation score **d)** Scores for inflammatory cell infiltrates in intestinal mucosa and submucosa and **e)** mucosal thickness score for all 3 groups of mice were quantified on H&E-stained sections (n = 8-11/group); **f)** Quantification of CD31+ vessels in colitic mice (n = 5-9/group). Circles represent individual mice. (WT, PBS-treated); (mutant, PBS-treated); (mutant, G6-31-treated). Mean ± SEM are shown. *P<0.05; **P<0.01; ***P<0.001 by one-way ANOVA, followed by Tukey's post-hoc test.

Moreover, the estimated inflammatory cell score was ~ 2-fold higher in the intestinal mucosa of PBS-treated colitic *Eng*$^{+/-}$ than in *Eng*$^{+/+}$ mice, and reduced to WT values in the submucosa of anti-VEGF-treated colitic *Eng*$^{+/-}$ mice (Figure 26 d). Analysis of colonic mucosal thickness showed a 2.8-fold higher score in PBS-treated colitic *Eng*$^{+/-}$ versus *Eng*$^{+/+}$ mice, value which was normalized by anti-VEGF treatment (Figure. 26 e). Furthermore, anti-VEGF therapy had a strong anti-angiogenic effect on the inflamed colon of G6-31-treated colitic *Eng*$^{+/-}$ mice, decreasing the number of vessels from 430 ± 24 to 250 ± 26 vessels/mm^2, close to pre-DSS levels or non-inflammatory conditions (~ 200 vessels/mm^2) (Figure 26 f). These findings demonstrate that G6-31 antibody treatment led to resolution of histological colonic inflammation, mucosal thickness and pathological angiogenesis in colitic *Eng*$^{+/-}$ mice.

3. 4. 3 Antibodies to VEGF reduces *in vivo* colonic wall thickness, microvascular hemodynamics and the number of Mad-CAM-1+ inflamed vessels in colitic *Eng*$^{+/-}$ mice

To determine the *in vivo* the effects of anti-VEGF therapy on chronic gut inflammation, we measured colonic thickness along the upper and lower distal colon walls, in G6-31-treated colitic *Eng*$^{+/-}$ versus PBS-treated colitic *Eng*$^{+/-}$ and *Eng*$^{+/+}$ mice, using B-mode ultrasound. Representative images of multiple successive colonic wall measurements are shown in Figure 27 a. The PBS-treated colitic *Eng*$^{+/-}$ mouse had a thicker gut wall than the colitic WT mouse. Importantly, the G6-31-treated colitic *Eng*$^{+/-}$ mouse showed a marked reduction in intestinal wall thickness, when compared to the PBS-treated colitic *Eng*$^{+/-}$ mouse.

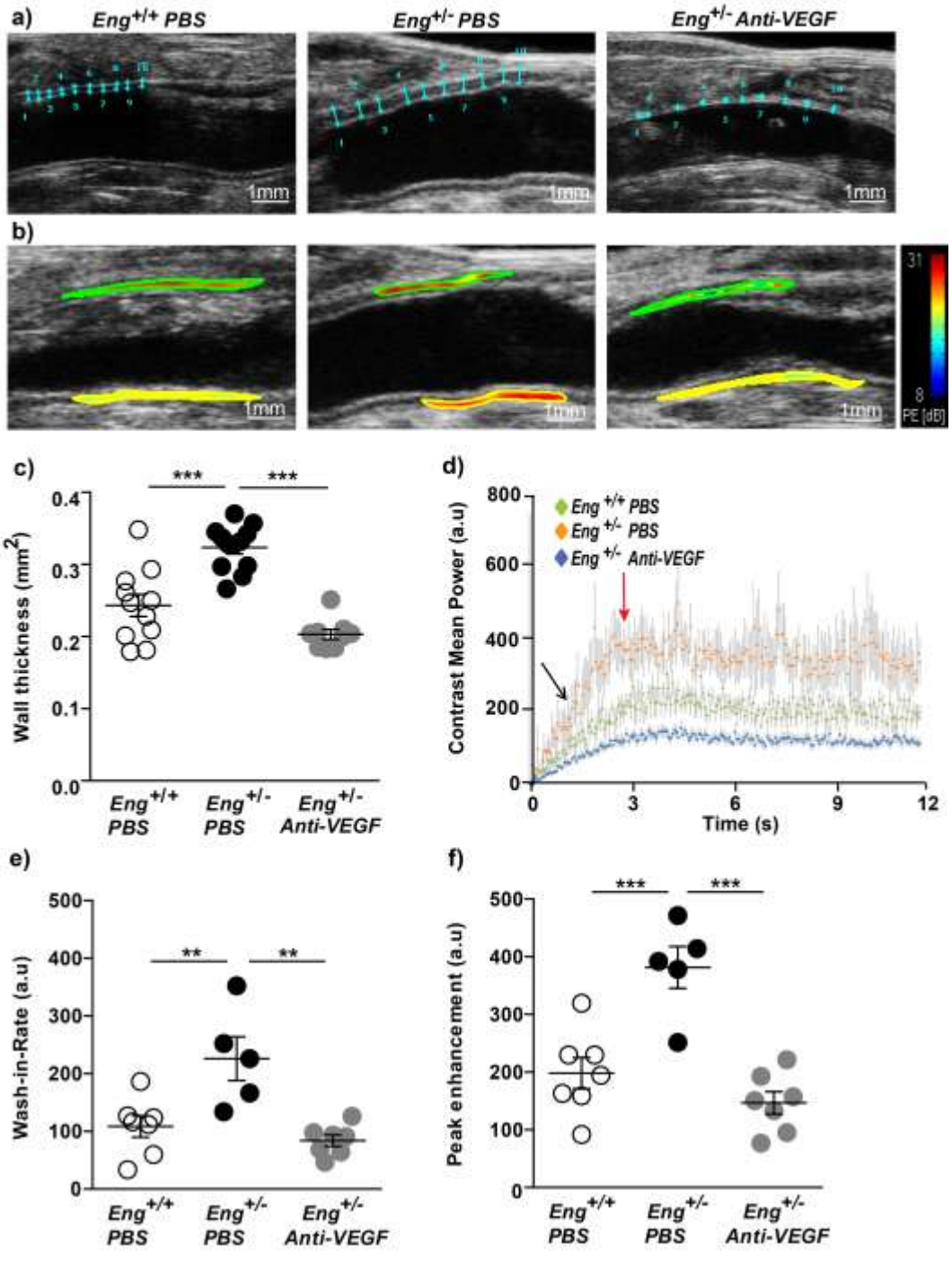
a)
Eng+/+ PBS
Eng+/- PBS
Eng+/- Anti-VEGF
1mm
b)
31
8
PE [dB]
c)
***
***
Wall thickness (mm2)
0.4
0.3
0.2
0.1
0.0
Eng+/+ PBS
Eng+/- PBS
Eng+/- Anti-VEGF
d)
Eng +/+ PBS
Eng +/- PBS
Eng +/- Anti-VEGF
Contrast Mean Power (a.u)
800
600
400
200
0
0
3
6
9
12
Time (s)
e)
**
**
Wash-in-Rate (a.u)
500
400
300
200
100
0
Eng+/+ PBS
Eng+/- PBS
Eng+/- Anti-VEGF
f)
***
***
Peak enhancement (a.u)
500
400
300
200
100
0
Eng+/+ PBS
Eng+/- PBS
Eng+/- Anti-VEGF

Figure 27. *In vivo* effects of anti-VEGF treatment on intestinal wall thickness and microvascular hemodynamics of colitic *Eng*+/- mice. Representative **a)** colonic wall thickness and **b)** contrast-enhanced ultrasound (CE-US) parametric images of peak enhancement (PE) blood flow in PBS-treated colitic $Eng^{+/+}$, $Eng^{+/-}$ and G6-31-treated colitic $Eng^{+/-}$ mice. Scale bar = 1 mm; color map scale: 8 to 31 decibels[237]; **c)** Quantification of intestinal wall thickness in colitic mice; *n* = 8-11/group; **d)** Graph illustrating the time-intensity curves measured for PBS-treated colitic $Eng^{+/+}$, $Eng^{+/-}$ and G6-31-treated colitic *Eng*+/- mice. Black arrow points to the slope or wash-in-rate, WiR, a parameter of blood flow rate, and the red arrow, to the plateau or peak enhancement, PE, an index of blood volume. Data generated in 3 experiments were plotted for each individual mice. Quantification of **e)** WiR and **f)** PE for PBStreated colitic $Eng^{+/+}$, $Eng^{+/-}$ and G6-31-treated colitic $Eng^{+/-}$ mice; *n* = 5-7/group. Circles represent individual mice. (wild type, PBS-treated); (mutant, PBS-treated); (mutant, G6-31 antibody-treated). Mean ± SEM are shown. **P*<0.05; ***P*<0.01; ****P*<0.001 by one-way ANOVA, followed by Tukey's post-hoc test.

To investigate *in vivo* the effect of anti-VEGF therapy on small vessel hemodynamics (blood kinetics and volume), we quantified microvascular perfusion in the intestinal wall, using non-targeted contrast-enhanced ultrasound (CE-US) imaging. Two parameters were determined: wash-in rate (WinR), a measure of blood flow rate, and peak enhancement (PE), an *in vivo* ultrasonic surrogate of tissue blood volume[239]. Representative images of colonic PE measurements are shown in Figure 27 b. The PBS-treated colitic $Eng^{+/-}$ mouse had higher (more red-colored areas) intestinal wall PE than the PBS-treated colitic WT mouse. Furthermore, colonic PE was lower in the anti-VEGF-treated colitic $Eng^{+/-}$ versus the PBS-treated colitic $Eng^{+/-}$ mouse (less red- and appearance of blue-colored areas, representing regions of lower blood volume).

Data quantification confirmed the increase in wall thickness in colitic $Eng^{+/-}$ versus WT mice and the significant reduction in this parameter in anti-VEGF treated colitic $Eng^{+/-}$ mice (Figure 27 c). Importantly, the *in vivo* quantitation of intestinal wall thickness correlated with the histological measurements (Figure 26 e), indicating that B-mode ultrasound is a valid non-invasive method for determining the effect of inflammation on the gut wall.

To visualize the dynamic changes in intestinal microvascular perfusion in the inflamed gut of PBS-treated $Eng^{+/+}$, $Eng^{+/-}$ and anti-VEGF- treated colitic $Eng^{+/-}$ mice, we plotted for each mouse the changes in the ultrasound contrast signal (Figure 27 d). Colonic blood flow rate (WiR, slope of the curve) and blood volume (PE, plateau of the curve) were higher in PBS-treated colitic mutant versus WT mice, and reduced by anti-VEGF treatment. Data quantification confirmed that PBS-treated colitic $Eng^{+/-}$ mice had a 2-fold higher WiR than colitic WT mice, and that anti-VEGF-treatment significantly decreased WiR in colitic $Eng^{+/-}$ mice (Figure 27 e). Moreover, colonic blood volume

(PE) was ~2-fold higher in PBS-treated colitic *Eng*$^{+/-}$ versus *Eng*$^{+/+}$ mice and significantly reduced by anti-VEGF treatment (Figure 27 f). These findings indicate that the G6-31 treatment was effective in reducing *in vivo* both colonic wall thickness and microvascular hemodynamics in our experimental model of colitis.

Mucosal addressin cell adhesion molecule-1 (MAdCAM-1) is an endothelial adhesion protein that selectively recruits leukocytes expressing α4β7 integrin to sites of intestinal inflammation[277]. To determine *in vivo* the intestinal MAdCAM-1 expression in colitic mice, we used a targeted contrast-enhanced ultrasound (CE-US) technique. The following parameters were measured in PBS-treated colitic *Eng*$^{+/-}$ and *Eng*$^{+/+}$ mice and anti-VEGF-treated colitic *Eng*$^{+/-}$ mice: WiR (bloof flow rate), PE (tissue blood volume) and the differential targeted enhancement or dTE that quantifies binding of targeted MBs to MAdCAM-1 expressed on the inflamed intestinal microvasculature[239].

We demonstrate that the elevated MAdCAM-1-targeted WiR observed in PBS-treated colitic *Eng*$^{+/-}$ versus colitic WT mice is reduced by the anti-VEGF-treatment (Figure 28 a). Moreover, the heightened colonic blood volume (PE) noted in PBS-treated colitic *Eng*$^{+/-}$ versus *Eng*$^{+/+}$ mice was significantly reduced by G6-31 antibody treatment (Figure 28 b). These observations confirm the colonic microvascular hemodynamic data obtained with the non-targeted MBs (Figure 27 e, f). Importantly, dTE, measuring the binding of targeted MBs to the MAdCAM-1^{+} inflamed intestinal microvessels, was higher in PBS-treated colitic *Eng*$^{+/-}$ versus *Eng*$^{+/+}$ mice and reduced after G6-31 antibody treatmentt (Figure 28 c). A diagram depicting the three parameters measured with the targeted MBs CE-US technique is shown in Figure 28 d.

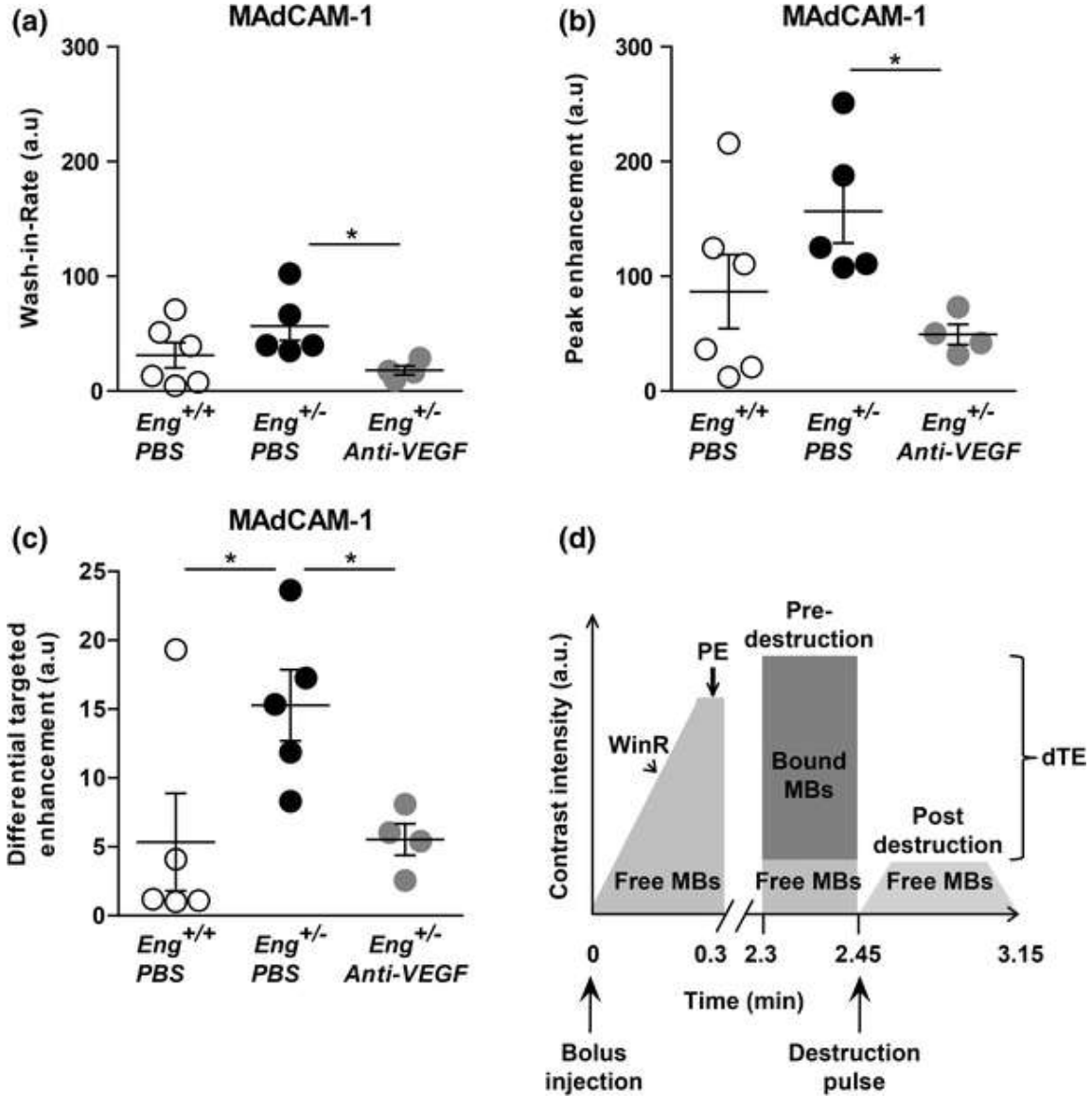

Figure 28. ***In vivo*** **effects of anti-VEGF treatment on MAdCAM-1+ inflamed vessels of colitic** ***Eng+/-*** **mice.** Quantitation of MAdCAM-1-targeted contrast-enhanced ultrasound (CE-US) signals of **a)** wash-in-rate, WiR (blood flow rate**);** *n* = 4-6/group, **b)** peak enhancement, PE (colonic blood volume); *n* = 4-6/group, and **c)** differential targeted enhancement, dTE, the difference between the mean MBs signals before and after the high impulse burst, measuring the binding of targeted MBs to MAdCAM-1+ inflamed vessels; *n* = 4-5/group. Circles represent individual mice. (wild type, PBS-treated) (mutant, PBS-treated); (mutant, G6-31 antibody-treated). Mean ± SEM are shown. **P*<0.05, followed by Tukey's post-hoc test; d) Diagram of the molecular CE-

US imaging experiment. A bolus of targeted MBs is injected at 0 second, followed by a 30 second acquisition of images to assess WinR and PE. The signal due to binding of targeted MBs to tissue MAdCAM-1+ microvessels increases. Imaging is resumed after 2 minutes, and 15 seconds recorded (from 2.3 to 2.45 sec) to obtain pre-destruction reference frames. A high impulse disruption burst is then applied, followed by 30 seconds of post-destruction imaging. The postdestruction contrast signal is then subtracted from the pre-destruction signal to give the dTE (MAdCAM-1 binding) value. Diagram adapted from reference[273]

These results suggest that the higher number of inflamed MAdCAM-1^{+} intestinal microvessels observed in colitic *Eng*$^{+/-}$ mice could have bound more incoming leukocytes, leading to more inflammation in the affected tissue. Anti-VEGF treatment reduced the number of targeted inflamed small vessels and consequently could have decreased the number of leukocytes adhering to these vessels and invading the inflamed gut. This is supported by Figure 26 d showing less infiltrating cells in the inflamed intestinal submucosa after G6-31 treatment.

Overall, these *in vivo* imaging data indicate that anti-VEGF treatment reduced the inflamed colonic wall thickness, the excessive microvascular perfusion in the gut, the number of intestinal MAdCAM-1^{+} microvessels leading to less infiltration of immune cells in the submucosa in colitic *Eng*$^{+/-}$ mice**.**

3. 4. 4 Anti-VEGF therapy decreases the colonic levels of inflammation-induced endoglin, IL-1β and G-CSF in colitic *Eng*$^{+/-}$ mice

To elucidate the mechanisms responsible for the effects of G6-31 therapy, we measured the colonic levels of 27 angiogenic (including endoglin), inflammatory and chemotactic factors at days 20-25 of colitis (Figure 29 and Table 8). As expected, the colon of *Eng*$^{+/-}$ mice had ~ 50% less endoglin before DSS induction of colitis, compared to WT mice (Figure 29 a). Inflammation significantly increased (by 1.7-fold) colonic endoglin levels in PBS-treated colitic *Eng*$^{+/+}$ and *Eng*$^{+/-}$ mice, when compared to their respective controls at day 0, pre-DSS induction (Figure 29 a), confirming previous observations made in patients with IBD and mouse models of chronic colitis[49,181,207].

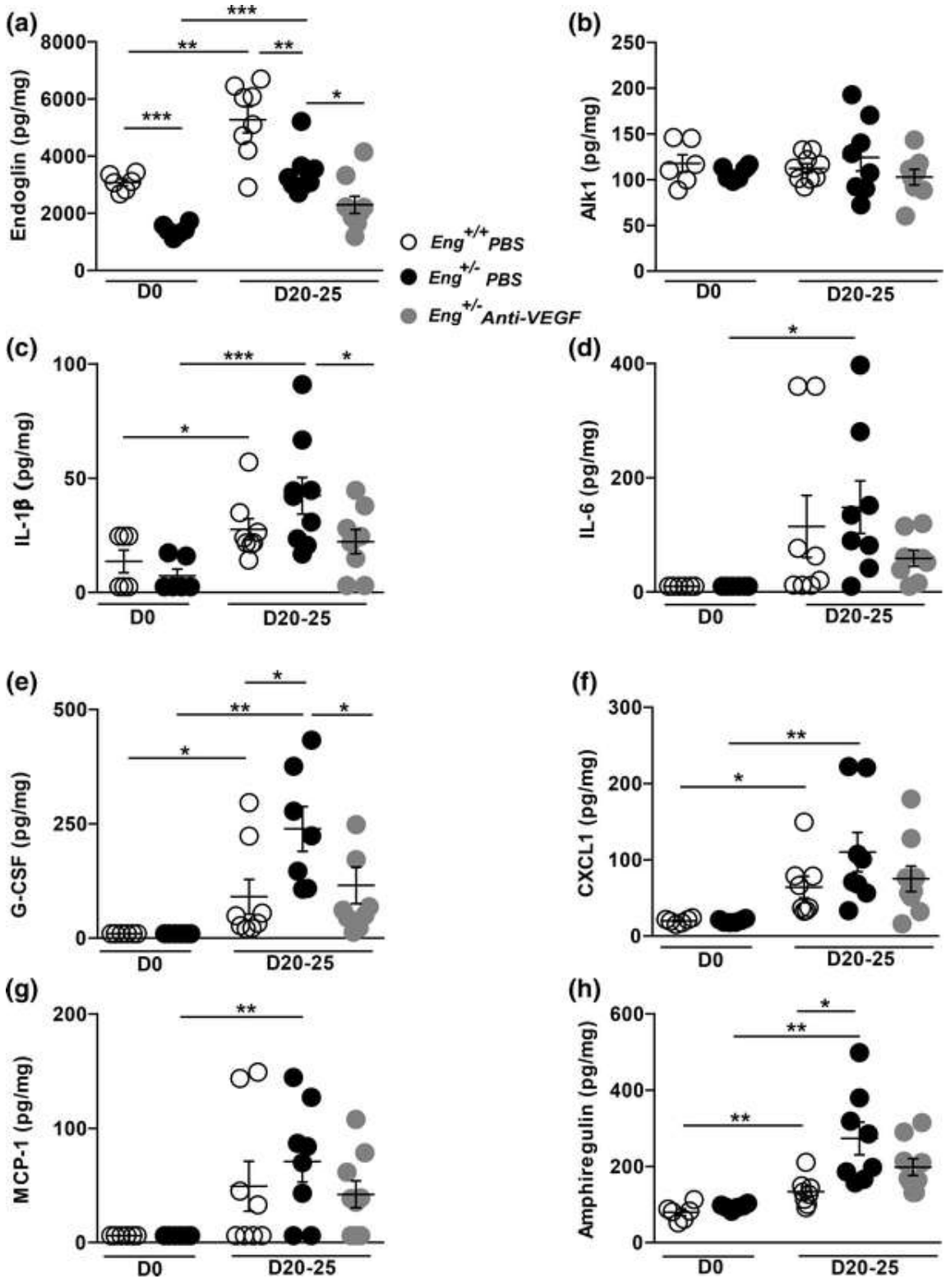
(a)
Endoglin (pg/mg)
8000
6000
4000
2000
0
***
**
**
***
*
D0
D20-25
(b)
Alk1 (pg/mg)
250
200
150
100
50
0
D0
D20-25
Eng+/+ PBS
Eng+/- PBS
Eng+/- Anti-VEGF
(c)
IL-1β (pg/mg)
100
50
0
***
*
*
D0
D20-25
(d)
IL-6 (pg/mg)
400
200
0
*
D0
D20-25
(e)
G-CSF (pg/mg)
500
250
0
*
**
*
*
D0
D20-25
(f)
CXCL1 (pg/mg)
300
200
100
0
**
*
D0
D20-25
(g)
MCP-1 (pg/mg)
200
100
0
**
D0
D20-25
(h)
Amphiregulin (pg/mg)
600
400
200
0
*
**
**
D0
D20-25

Figure 29. Changes in colonic levels of pro-inflammatory and myeloid chemotactic factors in colitic *Eng*$^{+/+}$ and *Eng*$^{+/-}$ mice and G-6-31 antibody-treated mice. Colonic levels of **a)** endoglin, **b)** Alk1, **c)** IL-1β, **d)** IL-6, **e)** GCSF, **f)** CXCL1, **g)** MCP-1 and **h)** amphiregulin in PBS-treated WT and *Eng*$^{+/-}$ mice at day 0 (pre-DSS, noninflammatory conditions and in PBS-treated colitic *Eng*+/+ and *Eng*+/- mice and in G6-31 antibody-treated colitic *Eng*$^{+/-}$ mice at days 20-25 of colitis (n = 6-9/group). Circles represent individual mice. (wild type, PBS-treated); (mutant, PBS-treated); (mutant, G6-31 antibody-treated). Mean ± SEM are shown. *P<0.05; **P<0.01; ***P<0.001 by one-way ANOVA, followed by Tukey's post-hoc test.

Table 8. Colonic molecular profile in *Eng*$^{+/+}$ and *Eng*$^{+/-}$ mice under basal conditions and in PBS-treated colitic *Eng*$^{+/+}$, *Eng*$^{+/-}$ and G6-31-treated *Eng*$^{+/-}$ mice.

	Day 0		Day 20-25		
Protein (pg/mg)	*Eng*$^{+/+}$ PBS-treated	*Eng*$^{+/-}$ PBS-treated	*Eng*$^{+/+}$ PBS-treated	*Eng*$^{+/-}$ PBS-treated	*Eng*$^{+/-}$ G6-31-treated
Endoglin	3080 ± 120	¶1422 ± 88	‡5278 ± 458	*‡3431 ± 277	†2297 ± 300
IL-1β	0 ± 0	0 ± 0	‡28 ± 5	‡42 ± 8	†21 ± 6
IL-6	0 ± 0	0 ± 0	114 ± 54	‡168 ± 48	66 ± 15
G-CSF	0 ± 0	0 ± 0	‡91 ± 38	*‡239 ± 49	† 85 ± 29
Amphiregulin	80 ± 9	94 ± 3	‡134 ± 13	*‡273 ± 43	198 ± 22
CXCL1 [52]	20 ± 1	20 ± 1	‡64 ± 16	‡111 ± 26	75 ± 17
MCP-1 (CCL2)	0 ± 0	0 ± 0	46 ± 23	‡69 ± 19	41 ± 13
HGF	3764 ± 255	4184 ± 266	‡9292 ± 686	‡9152 ± 781	8238 ± 1148
PLGF	1 ± 1	1 ± 1	‡12 ± 3	‡12 ± 2	10 ± 2
Betacellulin	13 ± 1	14 ± 1	‡5 ± 2	‡4 ± 2	7 ± 2
SDF-1	451± 11	483 ± 30	364 ± 48	321 ± 40	294 ± 30
Leptin	128 ± 12	109 ± 4	80 ± 9	124 ± 27	155 ± 11
FGF-2	3347 ± 185	4044 ± 163	3347 ± 380	4079 ± 541	3865 ± 559
Alk1	118 ± 10	107 ± 3	110 ± 5	124 ± 15	103 ± 9
Angiopoietin-2	110 ± 3	107 ± 5	107 ± 4	106 ± 9	82 ± 8
Endothelin-1	6 ± 0	8 ± 0	6 ± 0	6 ± 1	6 ± 1

Five-group analysis was done by one-way ANOVA, followed by Tukey post-hoc analysis. * statistically significant versus PBS-treated colitic *Eng*$^{+/+}$ mice; † statistically significant versus PBS-treated colitic *Eng*$^{+/-}$ mice; ‡ statistically significant compared to corresponding *Eng*$^{+/+}$ or *Eng*$^{+/-}$ groups respectively, under basal conditions; ¶ statistically significant compared to *Eng*$^{+/+}$ group, under basal conditions; ; n = 6-9/group.

This increase was likely related to activation of the vascular endothelium, known to be associated with higher levels of endoglin. However, some of the rise in tissue endoglin might be due to an increase in endoglin^{+} myeloid cells[53] in the inflammatory infiltrates, as the PBS-treated colitic *Eng*$^{+/-}$ mice showed more tissue inflammation than colitic WT mice, or to higher endoglin expression in intestinal stromal cells[55]. In support of this hypothesis, our laboratory recently showed that the colonic lamina propria of colitic *Eng*$^{+/-}$ mice has an increased number of infiltrating myeloid cells (Peter et al, unpublished data). Interestingly, anti-VEGF treatment decreased the colonic inflammation-induced rise in endoglin levels in colitic *Eng*$^{+/-}$ mice (Figure 29 a), suggesting that the treatment could have targeted different cell types expressing endoglin. Moreover, the levels of Alk1, a receptor for BMP9 of the TGF-β1 superfamily of ligands, almost exclusively expressed on endothelial cells, did not rise with inflammation in either colitic *Eng*$^{+/-}$ or *Eng*$^{+/+}$ mice, and remained unchanged after G6-31treatment (Figure 29 b), indicating that endoglin might be a more accurate marker of inflammation-induced activation of the vascular endothelium.

Furthermore, the colonic pro-inflammatory cytokine interleukin 1-β (IL-1β) was significantly increased in PBS-treated colitic *Eng*$^{+/+}$ and *Eng*$^{+/-}$ mice versus day 0 values. Importantly, IL-1β levels in PBS-treated colitic *Eng*$^{+/-}$ mice were reduced by G6-31 antibody treatment (Figure 29 c). Intestinal IL-6 levels were higher in PBS-treated colitic *Eng*$^{+/-}$ ($P = 0.01$) when compared to levels at day 0, and unchanged in the G6-31-treated mutant mice ($P = 0.1$) (Figure 29 d). These data support the observation that colitic *Eng*$^{+/-}$ mice manifest more colonic inflammation than WT mice and that the anti-VEGF-therapy had a beneficial effect in reducing the tissue inflammation in colitic *Eng*$^{+/-}$ mice, possibly by targeting IL-1β-producing cells.

G-CSF is produced primarily by monocytes and macrophages, and regulates the production, migration, differentiation and function of neutrophils (PMN)[278,279]. We show that the rise in colonic G-CSF is significantly higher in colitic $Eng^{+/-}$ than WT mice, suggesting that more PMN may be present in the inflamed colon of $Eng^{+/-}$ mice, as recently confirmed in our laboratory (Peter et al, unpublished data). Importantly, G6-31 treatment reduced tissue G-CSF in colitic $Eng^{+/-}$ mice (P = 0.02) (Peter et al, unpublished data). Importantly, G6-31 treatment reduced tissue G-CSF in colitic $Eng^{+/-}$ mice (P = 0.02) (Figure 29 e).

Moreover, CXCL1 (or KC, keratinocyte-derived cytokine), a potent PMN-activating and chemotactic factor produced by macrophages, fibroblasts, endothelial and intestinal epithelial cells, was increased in both PBS-treated colitic $Eng^{+/+}$ and $Eng^{+/-}$ mice, when compared to day 0 levels, but was not affected in G6-31-treated colitic $Eng^{+/-}$ mice (P = 0.2) (Figure 29 f).

MCP-1 (or CCL2), produced by dendritic cells, macrophages, endothelial cells and fibroblasts, is a key chemokine that regulates migration of monocytes/macrophages and differentiation of monocytes into functional intestinal macrophages in colitis[280, 281]. Intestinal MCP-1 was markedly elevated in the inflamed colon of PBStreated colitic $Eng^{+/-}$ mice (P = 0.01) when compared to levels measured at day 0, but remained unaffected after G6-31 treatment (P = 0.2) (Figure 29 g). This suggests an enhanced migration of monocytes/macrophages to the inflamed gut of colitic $Eng^{+/-}$ mice, potentially leading to increased colonic infiltration by macrophages, as recently demonstrated in our laboratory (Peter et al, unpublished data).

Amphiregulin is a ligand for the epidermal growth factor receptor. Amphiregulin promotes intestinal epithelial regeneration, TGF-β1-induced fibroblast proliferation, and

enhances and sustains the suppressive function of regulatory T cells, thus exerting an indirect anti-inflammatory effect[282-284]. We report that colonic amphiregulin was significantly higher at days 20-25 of colitis in PBS-treated colitic *Eng*$^{+/-}$ than *Eng*$^{+/+}$ mice, pointing towards a local compensatory protective mechanism. However, anti-VEGF treatment did not alter the amphiregulin levels (Figure 29 h).

Hepatocyte-growth factor (HGF) is an angiogenic and anti-inflammatory cytokine secreted by stromal cells and promoting colonic epithelial regeneration[285-287]. In our study, HGF was significantly increased in the expected recovery phase of colitis in both PBS-treated colitic *Eng*$^{+/+}$ and *Eng*$^{+/-}$ mice and not altered by anti-VEGF therapy (Table 8). Similarly, placental growth factor (PLGF), a pro-angiogenic member of the VEGF family, was elevated in the colonic tissues of both PBS-treated colitic *Eng*$^{+/+}$ and *Eng*$^{+/-}$ mice, but unchanged by G6-31 treatment (Table 8). Lastly, betacellulin, an angiogenic protein and ligand for the epidermal growth factor receptor, predominantly expressed in goblet cells and intestinal epithelium[288], was reduced in both PBS-treated colitic *Eng*$^{+/+}$ and *Eng*$^{+/-}$ mice and remained unaltered in the anti-VEGF-treated colitic *Eng*$^{+/-}$ mice (Table 8). The intestinal levels of stromal cell-derived factor 1 (SDF-1), the angiogenic fibroblast growth factor 2 (FGF-2), leptin, angiopoietin-2 and endothelin-1 did not change under inflammatory conditions in the PBS-treated colitic *Eng*$^{+/+}$ and *Eng*$^{+/-}$ mice and were not changed by anti-VEGF treatment (Table 8). The colonic Fas ligand, a cell surface molecule for the tumor necrosis factor (TNF) family, TNF-α, epidermal growth factor, follistatin, IL-17, prolactin, macrophage inflammatory protein-1α (or CCL3), VEGF-C and-D were undetectable in non-inflammatory and inflammatory conditions in all groups of mice (data not shown). Thereby, we concluded that only the inflammation-induced rise in G-CSF, amphiregulin and IL-1β were

associated with endoglin deficiency. Importantly, anti-VEGF treatment targeted specifically G-CSF and IL-1β in colitic *Eng*$^{+/-}$ mice.

3. 4. 5. Total Smad2 and Smad1/5/8 levels are increased in colitic mice and anti-VEGF-targeted therapy reduces colonic VEGF levels

TGF-β1 plays an important role in inflammation, angiogenesis and IBD[180]. Without TGF-β1, mice die at 3 weeks of age due to overwhelming systemic inflammation, including in the gut [289]. However, the intestinal TGF-β1 levels reported in experimental models of colitis vary in a model and context-dependent manner[182, 207, 209]. To investigate the effect of G6-31 antibody therapy on TGF-β1 in the *Endoglin* heteroyzgous model of chronic colitis, we measured total TGF-β1 levels in colonic lysates from PBS-treated colitic *Eng*$^{+/+}$, *Eng*$^{+/-}$ and anti-VEGF-treated *Eng*$^{+/-}$ mice. Colonic TGF-β1 levels were similar in PBS-treated colitic *Eng*$^{+/-}$ and *Eng*$^{+/+}$ mice, likely due to local, tissue regulatory mechanisms (Figure 30 a). Importantly, intestinal TGF-β1 levels were not affected after anti-VEGF therapy in colitic *Eng*$^{+/-}$ mice (Figure 30 a), as also observed under non-inflammatory conditions (Chapter Two).

To determine if antibodies targeting VEGF were effective in binding VEGF in tissue and in circulation, we quantified total (G6-31 antibody-bound VEGF+free, unbound VEGF) and free residual VEGF (left after removal of antibody-bound VEGF from samples assessed for total VEGF levels) in all three groups of mice, at days 20-25 of colitis. Total circulating VEGF levels rose 50-fold (311 ± 165 pg/ml versus ~ 6 pg/ml) in G6-31- versus PBS-treated colitic *Eng*$^{+/-}$ mice, demonstrating that the monoclonal antibody was still present in circulation, one to six days after the last injection.

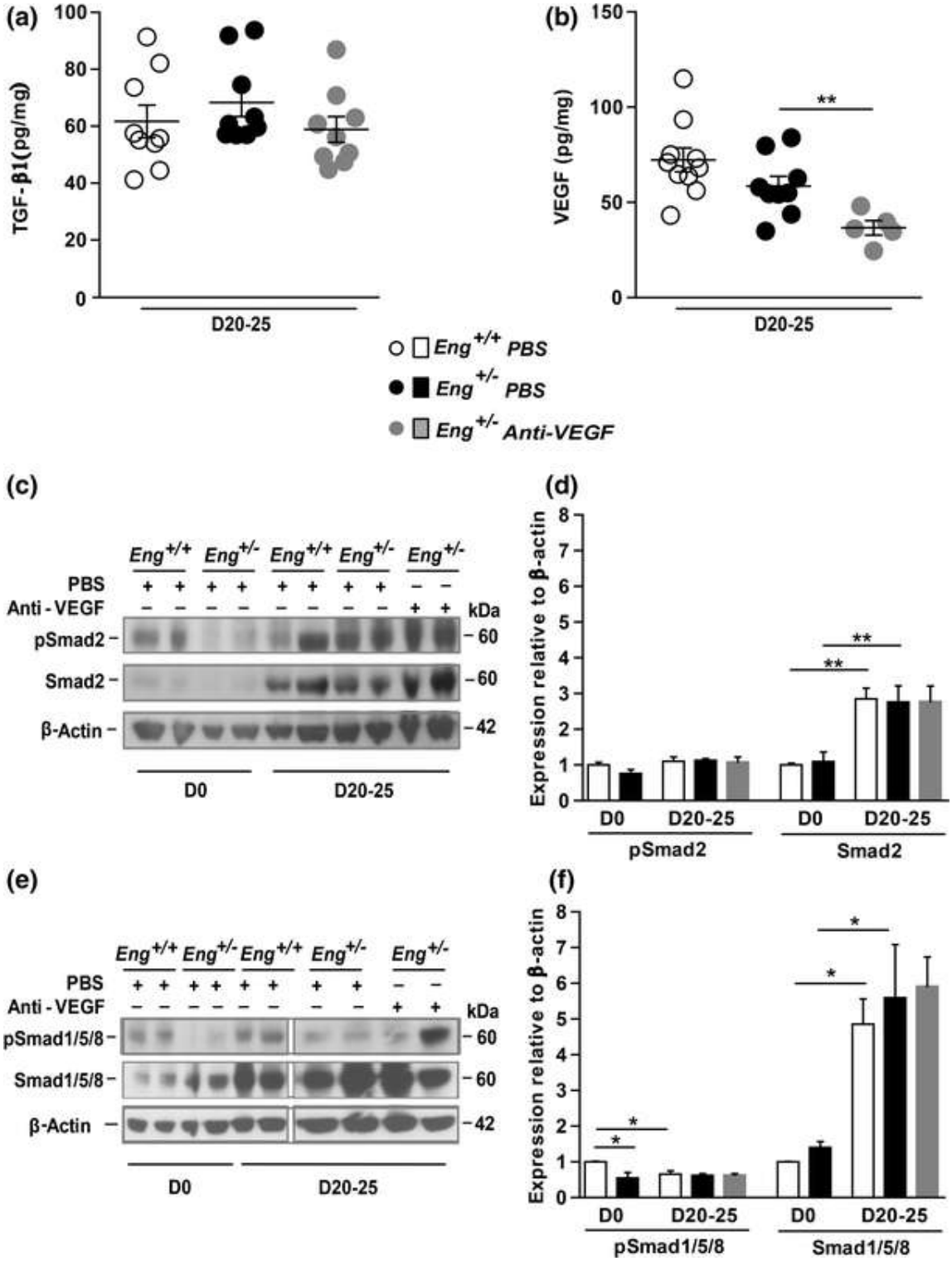
(a)
TGF-β1(pg/mg)
100
80
60
40
20
0
D20-25
(b)
VEGF (pg/mg)
150
100
50
0
**
D20-25
Eng+/+ PBS
Eng+/- PBS
Eng+/- Anti-VEGF
(c)
Eng+/+ Eng+/- Eng+/+ Eng+/- Eng+/-
PBS
Anti-VEGF
kDa
pSmad2
Smad2
β-Actin
60
60
42
D0
D20-25
(d)
Expression relative to β-actin
**
**
D0 D20-25 D0 D20-25
pSmad2
Smad2
(e)
Eng+/+ Eng+/- Eng+/+ Eng+/- Eng+/-
PBS
Anti-VEGF
kDa
pSmad1/5/8
Smad1/5/8
β-Actin
60
60
42
D0
D20-25
(f)
Expression relative to β-actin
*
*
*
*
D0 D20-25 D0 D20-25
pSmad1/5/8
Smad1/5/8

Figure 30. Anti-VEGF treatment did not alter colonic TGF-β1 levels nor Smad2 and Smad1/5/8/ signaling, but reduced VEGF levels in colitic *Eng*$^{+/-}$ mice. Quantification of **a)** total (acid-treated) intestinal TGF-β1 in PBStreated colitic *Eng*$^{+/+}$ and *Eng*$^{+/-}$ mice and in G6-31-treated colitic *Eng*$^{+/-}$ mice (n = 9/group), and **b)** colonic VEGF free residual levels (after immunodepletion) in PBS-treated colitic *Eng*$^{+/+}$, *Eng*$^{+/-}$ and G6-31 antibody treated colitic *Eng*$^{+/-}$ mice (n =5-10/group), as measured by ELISA. Circles represent individual mice. (wild type, PBS-treated); (mutant, PBS-treated); (mutant, G6-31 antibody-treated). Representative Western blots for **c)** pSmad2, total Smad2 and β-actin and **e)** pSmad1/5/8, total Smad1/5/8 and β-actin in PBS-treated *Eng*$^{+/+}$ and *Eng*$^{+/-}$ mice at day 0 (pre-DSS, non-inflammatory conditions) and in PBS-treated colitic *Eng*$^{+/+}$, *Eng*$^{+/-}$ and G6-31-treated colitic *Eng*$^{+/-}$ mice at days 20-25 of colitis. All 5 groups of samples were run on the same gel (under reducing conditions) in each experiment; the results from two independent gels for Smad2 and Smad1/5/8 respectively, were then quantified and averaged for each protein. Quantification of **d)** pSmad2 and total Smad2 relative to β-actin and **f)** pSmad1/5/8 and total Smad1/5/8 relative to β-actin, and normalized to mean values for their respective *Eng*$^{+/+}$ samples at day 0; n = 4-5/group. Data are expressed as mean ± SEM. *P<0.05; **P<0.01; by one-way ANOVA, followed by Tukey's post-hoc test.

After immunodepletion, circulating VEGF levels returned to pre-DSS, non-inflammatory levels (6 ± 1 pg/ml). These results suggest that G6-31 antibody was efficacious in binding plasma VEGF. Furthermore, colonic VEGF levels were similar in PBS-treated colitic $Eng^{+/+}$ and $Eng^{+/-}$ mice (72 ± 6 versus 59 ± 5 pg/mg of tissue, respectively; P = 0.1, by Tukey's post-hoc test), and significantly reduced after immunodepletion in anti-VEGF-treated colitic $Eng^{+/-}$ mice (P = 0.005), as measured at days 20-25 of colitis (Figure 30 b). The VEGF levels in PBS-treated colitic $Eng^{+/+}$ and $Eng^{+/-}$ mice were confirmed by western blot (n = 6-8/group) and by multi-analyte profiling assay (n = 8/group; data now shown). Thus, VEGF does not appear to play a major role in the increased inflammation and pathological angiogenesis observed in colitic $Eng^{+/-}$ mice. We also measured the protein levels of VEGFR2, the major signalling receptor for VEGF, in total colonic lysates. Data quantification demonstrated that VEGFR2 levels were comparable in PBS-treated colitic $Eng^{+/-}$ versus WT mice and unchanged after G6-31 therapy (data not shown).

Endoglin modulates the signals for TGF-β1 and BMP9 ligands, by regulating membrane receptors ALK1 and ALK5 and downstream Smad activation. TGF-β1 stimulation generally leads to ALK5-mediated phosphorylation of intracytoplasmic Smad2/3, while BMP9 activates ALK1 and Smad1/5/8 signaling[80]. To investigate the consequences of endoglin deficiency on TGF-β1/BMP9 downstream pathways in IBD and the effects of anti-VEGF therapy on these signaling routes, we measured the phosphorylated and total colonic levels of receptor-regulated Smad2 and Smad1/5/8 in PBS-treated colitic $Eng^{+/+}$, $Eng^{+/-}$ mice and G6-31-treated colitic $Eng^{+/-}$ mice. Representative western blot images showed comparable phospho-Smad2 at day 0 and days 20-25 of colitis in $Eng^{+/-}$ and $Eng^{+/+}$ mice; total Smad2 levels were similar in $Eng^{+/-}$

and $Eng^{+/+}$ mice, low at day 0 and higher at days 20-25 of colitis (Figure 30 c). Data quantification confirmed that pSmad2 levels relative to β-actin were similar in PBStreated $Eng^{+/+}$ and $Eng^{+/-}$ mice at day 0 and remained unchanged at days 20-25 of colitis in PBS-treated colitic $Eng^{+/+}$, $Eng^{+/-}$ and G6-31-treated colitic $Eng^{+/-}$ mice. Total Smad2 levels relative to β-actin were comparable in PBS-treated $Eng^{+/+}$ and $Eng^{+/-}$ mice at day 0, yet increased by ~ 3-fold in both PBS-treated groups and remained unaffected in the anti-VEGF-treated colitic $Eng^{+/-}$ mice (Figure 30 d).

Representative western blot images of Smad1/5/8 showed lower pSmad1/5/8 in $Eng^{+/-}$ versus $Eng^{+/+}$ mice at day 0 and comparable low levels at days 20-25 of colitis in PBS-treated $Eng^{+/-}$, $Eng^{+/+}$ and G6-31-treated $Eng^{+/-}$ mice. Total Smad1/5/8 levels appeared similar in *Eng*+/- versus *Eng*+/+ mice, low at day 0 and elevated in all 3 groups at days 20-25 of colitis (Figure 30 e). Data quantification demonstrated a lower pSmad1/5/8 relative to β-actin in $Eng^{+/-}$ versus $Eng^{+/+}$ mice at day 0, prior to DSS-induced colitis. Interestingly, colitis induced a decrease in pSmad1/5/8 in PBS-treated colitic WT mice, whereas it was unchanged in PBS- and G6-31-treated colitic $Eng^{+/-}$ mice at days 20-25 of colitis. Moreover, total Smad1/5/8 relative to β-actin was similar in $Eng^{+/-}$ and $Eng^{+/+}$ mice atday 0, and ~ 5 -fold increased during colitis in both PBS-treated colitic $Eng^{+/+}$ and $Eng^{+/-}$ mice; anti-VEGF treatment did not alter colonic total Smad1/5/8 in colitic $Eng^{+/-}$ mice (Figure 30 f). We conclude that chronic gut inflammation induces an increase in both total Smad2 and Smad1/5/8 in PBS-treated colitic *Eng*+/+ and *Eng*+/- mice, without affecting their corresponding phosphorylated levels. However, anti-VEGF therapy did not alter these TGF-β/BMP9-activated signaling proteins, suggesting that VEGF might act downstream of these pathways or on

other VEGF-mediated routes, some of which are shared with the non-canonical TGF-β/BMP9 pathways.

3. 5 Discussion

Our findings demonstrate that the severe gut inflammation observed in the *Endoglin* heterozygous mouse model of chronic colitis is associated with excessive and persistent pathological angiogenesis, as demonstrated by increased colonic MVD. *In vivo* ultrasound studies revealed a higher inflammation-induced colonic wall thickness, an increase in intestinal microvascular hemodynamics, and more MadCAM-1^{+} inflamed microvessels that would allow more leukocytes trafficking in colitic $Eng^{+/-}$ than WT mice. Interestingly, at the tissue level, gut inflammation triggered an increase in the expression of endoglin in colitic WT and $Eng^{+/-}$ mice, the latter only partially compensating for the constitutively lower level of endoglin. A higher rise in G-CSF and the regenerative protein amphiregulin was observed in colitic $Eng^{+/-}$ mice, suggesting that endoglin might play a role in regulating these factors The intestinal G-CSF and IL-1β levels were reduced after G6-31 treatment. Overall, the anti-VEGF therapy showed both *in vivo* and *in vitro* anti-angiogenic and anti-inflammatory effects on the inflamed gut of colitic $Eng^{+/-}$ mice.

We demonstrate that intestinal pathological angiogenesis in colitic $Eng^{+/-}$ mice is characterized by a persistent increase in gut MVD associated with severe inflammation, in agreement with other experimental colitis studies[100,178,207]. We further defined the colonic pathological angiogenic phenotype in the $Eng^{+/-}$ mouse model of colitis by using *in vivo* non-targeted and targeted CE-US, and showed that colitic $Eng^{+/-}$ mice have excessive inflammation-induced tissue angiogenesis, accompanied by increased

microvascular blood flow rate and volume. CE-US uses microbubbles with diameters between 1-3 μm, allowing the assessment in real-time of functional microvascular hemodynamics[239]. Thus, it provides a more accurate evaluation of the changes in the inflamed microvasculature during progression of colitis and in response to anti-angiogenic treatment. The targeted MBs evaluation of the hemodynamic parameters WiR and PE confirmed the non-targeted CE-US data, further supportingthe utility of CE-US imaging technique in evaluating blood kinetics and volume in the inflamed intestinal small vessels. In addition, MAdCAM-1-targeted CE-US imaging allowed *in vivo* quantification not only of the colonic microcirculation, but specifically of the inflamed microvessels. Thus, MAdCAM-1-targeted CE-US is a reliable method to determine *in vivo* the microvascular angiogenic response during gut inflammation. MAdCAM-1 is an adhesion molecule selectively expressed on endothelial cells in the lamina propria of the intestine, high endothelial venules of Peyer's patches, gut-associated lymphoid tissue and mesenteric lymph nodes[290]. Importantly, MAdCAM-1 expression is up-regulated at sites of intestinal inflammation[291, 292]. As MAdCAM-1 acts as a gut specific recruiting factor for leukocytes expressing α4β7 integrin[290], it is regarded as a marker of leukocyteendothelial adhesion in the inflamed gut. Recently, experimental and human studies showed that targeted MAdCAM-1 therapy had promising results in controlling gut inflammation[291,293]. In our model of chronic colitis, anti-VEGF therapy reduced *in vivo* the inflammation-associated rise in colonic MAdCAM-1 levels in $Eng^{+/-}$ mice, potentially accounting for decreased leukocyte-endothelial adhesion and trafficking to the inflamed gut. Furthermore, colitic $Eng^{+/-}$ mice had thicker intestinal walls than WT mice, as assessed non-invasively by ultrasound, reflecting the higher inflammation and mucosal thickness noted on histological sections.

Thereby, B-mode and CE-US are reliable methods to evaluate *in vivo* the effect of inflammation on colonic wall thickness, tissue microcirculatory hemodynamics and quantifying inflamed vessels and response to therapy.

Despite the recognition that pathological angiogenesis contributes to pathogenesis of chronic inflammatory diseases, little is known about the role of anti-VEGF treatment in colitis. In addition, the few experimental studies that used anti-VEGF agents showed opposite results, likely due to differences in the genetic background of the models used and various interventional approaches[203, 211, 294, 295]. As tissue damage and repair occur concomitantly and are associated with angiogenesis, consideration of the degree of angiogenic suppression during the antiangiogenic treatment is critical in chronic inflammatory diseases. Furthermore, in some patients diagnosed with cancer, bevacizumab treatment has been associated with rare, but potential severe side effects, such as intestinal perforation[192,296]. These observations indicate that the effects of anti-angiogenic treatment in chronic colitis need to be diligently evaluated.

We show that the G6-31 therapy started at day 9 of colitis, at the peak of tissue inflammation, reduced both inflammation and pathological angiogenesis in colitic $Eng^{+/-}$ mice. Chronic colitis led to an increase in tissue IL-1β, G-CSF and CXCL1 in both colitic $Eng^{+/-}$ and $Eng^{+/+}$ mice, while IL-6 and MCP-1 were significantly augmented only in colitic mutant mice. These factors have been shown previously to be up-regulated in human and experimental colitis[178, 207, 280, 281, 297-305]. Interestingly, higher intestinal levels of G-CSF were observed in colitic $Eng^{+/-}$ versus $Eng^{+/+}$ mice, suggesting that endoglin haploinsufficiency is potentially associated with higher myeloid cell infiltration in the

inflamed gut of colitic *Eng*+/- mice, as was recently confirmed in our laboratory (Peter et al, unpublished data).

In the present study, we noted similar VEGF levels in colitic $Eng^{+/-}$ and $Eng^{+/+}$ mice in the expected recovery phase of colitis, as opposed to the higher levels observed previously in colitic $Eng^{+/-}$ mice. This discrepancy is possibly due to housing of mice in a different facility, variations in their health status, and differences in sensitivity of the ELISA assays used in the two studies. These findings imply that VEGF does not play a major role in the persistence of severe inflammation and pathological angiogenesis in our model. Yet, the reduction in tissue VEGF levels after G6-31 antibody treatment could have affected the tissue angiogenic balance and indirectly contributed to the effects of therapy in our model of colitis, as we observed previously that under non-inflammatory conditions, G6-31 therapy targeted the colon, without affecting free VEGF levels[276]. However, the absence of other methods of blocking VEGF and of other control groups in the present study precludes the confirmation of a direct contribution of reduced intestinal VEGF levels to the effects of G6-31 therapy. We propose that G-CSF and possibly IL-1β might have contributed to the severe inflammatory and angiogenic phenotype observed in colitic $Eng^{+/-}$ mice, particularly when the pro-angiogenic factors HGF and PlGF were similar and betacellulin and FGF low in both colitic $Eng^{+/-}$ and $Eng^{+/+}$ mice. Interestingly, in addition to their role in inflammation, G-CSF and IL-1β, as well as IL-6, MCP-1 and CXCL1, have additional pro-angiogenic properties[306,307-310].

Little is known about the effects of G-CSF on gut inflammation. An experimental and two pilot clinical studies showed that treatment with G-CSF might improve colitis[311-313]. However, in the setting of endoglin deficiency, the increase in colonic G-CSF appears to be associated with excessive inflammation and pathological

angiogenesis, hence with worse colitis. Higher colonic G-CSF levels observed in colitic *Eng*$^{+/-}$ mice could have contributed to the severity of colitis: a) directly, as G-CSF can have pro-angiogenic effects; b) indirectly, via GCSF- induced migration of myeloid cells that can acquire pro-angiogenic properties in the inflamed gut; c) via GCSF- induced myeloid cell secretion of Bv8, a pro-angiogenic and pro-inflammatory peptide. Bv8 (prokineticin-2), induced by G-CSF in circulating monocytes, neutrophils, and dendritic cells[314]further mediates the G-CSF effects on $CD11b^{+}Gr1^{+}$myeloid cells and contributes to refractoriness to anti-VEGF treatment in tumor mouse models[315]. The potential role of Bv8 in our model of colitis requires further investigation. Moreover, it has been recently demonstrated that combination of anti-G-CSF and anti-VEGF antibodies had additive effect on reducing myeloid cell mobilization and angiogenesis in tumor models[315]. These observations support the possibility that the decrease in G-CSF after G6-31 antibody treatment could have led to anti-immune and anti-angiogenic effects. A model depicting the inflammatory and angiogenic phenotype in colitic *Eng*+/- mice and the effects of G6-31 therapy are shown in Figure 31.

The colonic endoglin levels rose with progression of inflammation and pathological angiogenesis in both colitic *Eng*$^{+/-}$ and *Eng*$^{+/+}$ mice. Thus, endoglin is a general marker of inflammation, angiogenesis and tissue remodelling in colitis. Moreover, the increase in total Smad2 and Smad1/5/8 in both colitic *Eng*$^{+/-}$ and *Eng*$^{+/+}$ mice is related to the tissue inflammatory and angiogenic response in colitis. However, anti-VEGF treatment did not alter phospho- or total Smad2 and Smad1/5/8 levels, suggesting that its targets are downstream of Smads or in other VEGF-mediated pathways. The intestinal regenerative factor amphiregulin was increased in both colitic *Eng*$^{+/-}$ and *Eng*$^{+/+}$ mice, as shown in other models of colitis[282, 283].

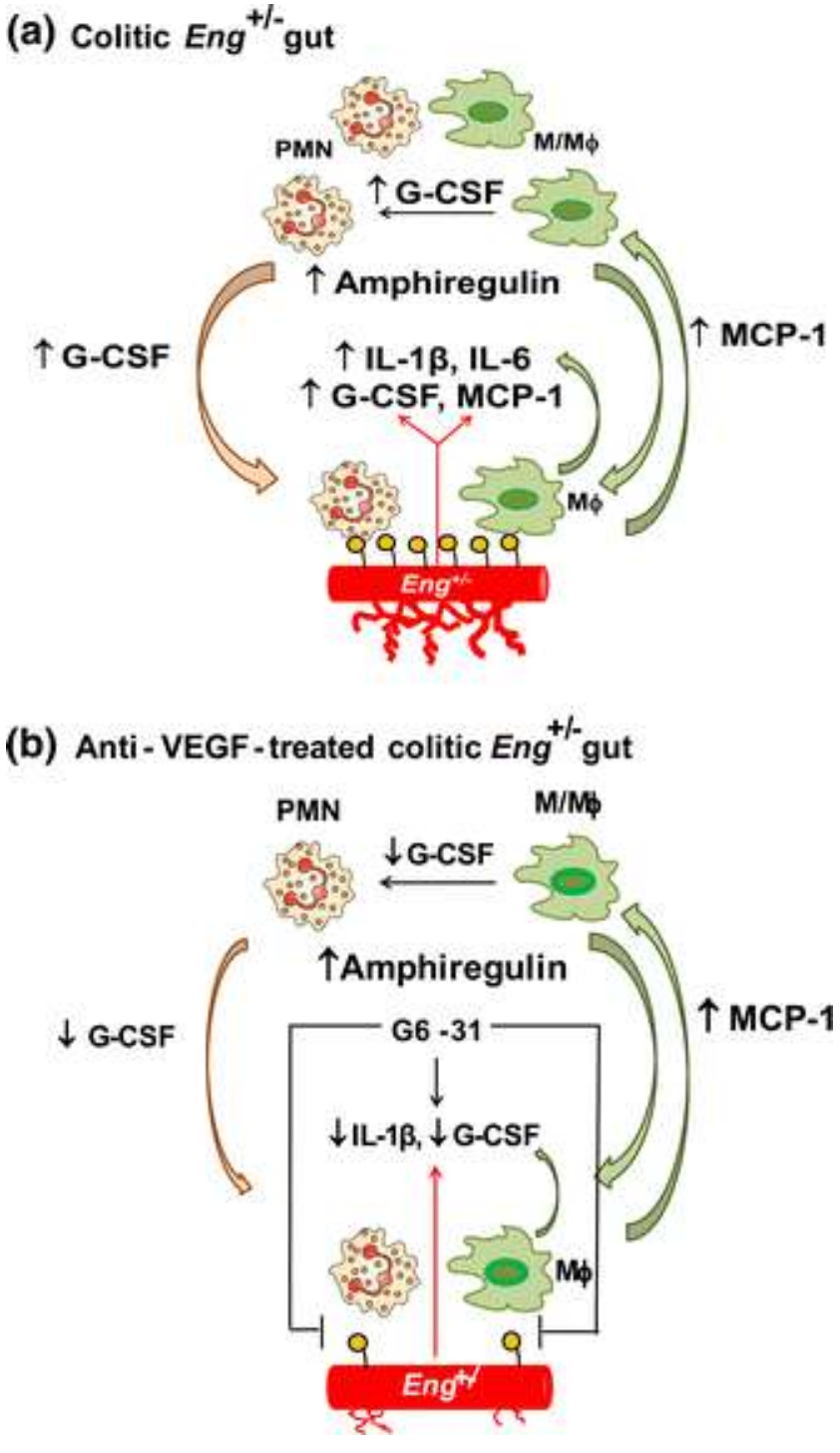
(a) Colitic Eng+/- gut
PMN
M/Mϕ
↑ G-CSF
↑ Amphiregulin
↑ G-CSF
↑ IL-1β, IL-6
↑ G-CSF, MCP-1
↑ MCP-1
Mϕ
Eng+/-
(b) Anti-VEGF-treated colitic Eng+/- gut
PMN
M/Mϕ
↓ G-CSF
↑ Amphiregulin
↓ G-CSF
G6 -31
↓ IL-1β, ↓ G-CSF
↑ MCP-1
Mϕ
Eng+/-

Figure 31. Model depicting the colitic *Eng*$^{+/-}$ gut before and after treatment with G6-31 antibody. a) Colitic *Eng*$^{+/-}$ mice express higher colonic G-CSF, secreted by monocyte/macrophages (M/Mϕ) and the inflamed endothelium. GCSF promotes migration and activity of neutrophils (PMN). Activated Mϕ and endothelium also produce MCP-1 that stimulates migration and differentiation of monocytes into macrophages. All these activated cells secrete high levels of IL-1β and IL-6, leading to amplification of inflammation and pathological angiogenesis. In addition, colitic *Eng*$^{+/-}$ mice have more amphiregulin in their gut and show higher microvessel density (MVD) than colitic *Eng*$^{+/+}$ mice. These inflamed intestinal microvessels express more MAdCAM-1( ). Thus, colitic *Eng*$^{+/-}$ mice manifest higher intestinal inflammation, myeloid cell infiltration and pathological angiogenesis, leading to impairment of resolution of these parameters; **b)** G6-31 antibody treatment decreased tissue G-CSF and IL-1β without affecting MCP-1 and amphiregulin. In addition, anti-VEGF treatment reduced microvessel density (MVD) and the number of MAdCAM-1^{+} ( ) inflamed vessels, leading to reduced angiogenesis and less gut inflammation.

Surprisingly, colitic *Eng*$^{+/-}$ mice had a further elevation in intestinal amphiregulin, when compared to colitic WT mice. As amphiregulin exerts TGF-β1-mediated fibrotic and T regulatory cell-dependent anti-inflammatory effects[282-284], it suggests that the higher increase in colonic amphiregulin in colitic *Eng*$^{+/-}$ mice is an additional compensatory mechanism for endoglin deficiency, known to be accompanied by reduced fibrosis[316].

In conclusion, the excessive colonic inflammation, increased MVD and enhanced intestinal microvascular hemodynamics observed in colitic *Eng*$^{+/-}$ mice suggest that tissue endoglin, beyond its rise with inflammation and angiogenesis during the wound healing process, might have additional angiogenic and inflammatory modulatory roles, possibly by interfering with myeloid cell migration and secretion of pro-inflammatory and pro-angiogenic cytokines. Hence, we propose that constitutive endoglin has a protective role in chronic colitis. The anti-VEGF treatment may have additional anti-inflammatory effects, by decreasing the MAdCAM-1^{+} inflamed microvessels which should lead to reduced leukocyte-endothelial adhesion and transmigration. These findings have implications for understanding of the pathogenic mechanisms and the effects of VEGF-targeted therapies in chronic inflammatory diseases, including colitis. The B-mode US and CE-US imaging techniques enable accurate *in vivo* monitoring of gut inflammation, intestinal microvascular hemodynamics and molecular aspects of inflammation in the inflamed colonic vessels, providing the foundation for translation of these findings to patients with IBD, for early and optimal monitoring of disease activity and response to treatment.

3. 5 Acknowledgements

We thank Genentech for kindly providing the G6-31 anti-VEGF mouse antibody; Dr. Wen-Rong Lie from EMD Millipore for the mouse angiogenesis/growth factor magnetic bead panel kit*;* Lily Morikawa and Napoleon Law from the Pathology Core Centre of the Modeling Human Disease Toronto Centre for Phenogenomics, Toronto, for help with the CD31 staining; Dr. Herman Yeger, for the use of the Olympus microscope; John Sun (VisualSonics, Toronto) for performing the pilot ultrasound measurements in colitic mice. We also thank the reviewers for their insightful comments. This work was supported by grants from the Canadian Institute of Health Research (CIHR) (MOP-6247) and the Heart and Stroke Foundation of Canada(T5598) to ML, and from the Terry Fox Foundation, VisualSonics Inc. and CIHR (MOP–12164) to FSF. D. S. Ardelean was the recipient of a CIHR/Canadian Association of Gastroenterology/Abbott fellowship award.

Chapter Four

Discussion and Conclusions

4.1 Summary of contribution to knowledge

The main objectives of this thesis were 1) to determine if *Eng* and *Alk1* heterozygous mice have a systemic dysregulated angiogenesis; 2) to investigate the effects of anti-VEGF therapy in these models of HHT and 3) to test the efficacy of anti-VEGF therapy in the DSS-induced *Eng* heterozygous model of chronic colitis.

We demonstrated that *Eng* and *Alk1* heterozygous mice have a localized, pulmonary dysregulated angiogenesis, due to an organ-dependent angiogenic imbalance. Pulmonary endoglin deficiency was associated with a rise in TSP-1, whereas Alk1 insufficiency correlated with a rise in Ang-2. Systemic administration of anti-VEGF treatment led to restoration of a normal angiogenic phenotype in the lungs of *Eng* and *Alk1* heterozygous mice, by modulating the organ-dependent angiogenic balance. In liver of $Eng^{+/-}$ and $Alk1^{+/-}$ mice, anti-VEGF treatment led to a non-specific decrease in tissue MVD. However, *in vivo* assessment of hepatic functional angiogenesis by US demonstrated that the effects of anti-VEGF therapy were significant on liver of $Eng^{+/-}$ but not $Alk1^{+/-}$ mice, suggesting a distinct, genotype-specific response to anti-angiogenic therapy.

Furthermore, we showed that the pathological angiogenesis associated with severe colitis in $Eng^{+/-}$ mice is characterized by excessive, persistent MVD, as assessed *in vitro*. High intestinal microvascular hemodynamics and increased MAdCAM-1 expression were noted *in vivo* by US. Moreover, severe tissue inflammation led to increase in colonic endoglin and other pro-inflammatory and angiogenic factors in both

WT and *Eng*$^{+/-}$ mice. Interestingly, we observed a genotype-dependent higher rise in G-CSF, amphiregulin and likely IL-1β, suggesting the endoglin deficiency might be responsible for these changes. Anti-VEGF therapy decreased *in vitro* and *in vivo* tissue inflammation and pathological angiogenesis, as determined by US data and potentially reduced leukocyte-endothelial adhesion in the inflamed vessels of colitic *Eng*$^{+/-}$ mice. In addition, anti-VEGF diminished the tissue levels of endoglin, G-CSF and IL-1β, indicating that it might have an anti-inflammatory effect, in addition to its known anti-angiogenic properties.

4. 2 *Eng*$^{+/-}$ and *Alk1*$^{+/-}$ mice have a distinct pulmonary angiogenic profile

Our hypothesis was that *Eng*$^{+/-}$ and *Alk1*$^{+/-}$ mouse models of HHT have a systemic dysregulated angiogenesis, that VEGF plays a role in this dysregulated angiogenesis and that the anti-VEGF therapy will be beneficial in attenuating the pathological angiogenic phenotype in these models.

While examining the microvasculature of several organs in these mice, we observed that only the lungs showed an abnormal microvascular phenotype, with reduced peripheral microvascular density (MVD) leading to secondary right ventricular hypertrophy (RVH). Heart, liver and colon of both *Eng*$^{+/-}$ and *Alk1*$^{+/-}$ mice had normal MVD when compared to wild type controls. Interestingly, the rarefied peripheral pulmonary MVD in *Eng*$^{+/-}$ mice was associated with a four-fold increase in the levels of TSP-1 and no change in VEGF, suggesting that the pulmonary angiogenic balance was shifted towards an angiostatic phenotype. Moreover, *Eng*$^{+/-}$ and *Eng*$^{-/-}$ endothelial cells had 3.3 and 6.6 fold higher TSP-1 levels than *Eng*$^{+/+}$ cells, indicating an inverse correlation between the endoglin expression and TSP-1 production in the dysfunctional

endothelium. These data suggest that a deficiency in the angiogenic modulator endoglin may lead to an up-regulation of the angiostatic factor TSP-1 in the lung vasculature.

Despite showing a reduction in pulmonary peripheral MVD similar to that observed in *Eng*$^{+/-}$ mice, *Alk1*$^{+/-}$ mice had normal TSP-1 levels in their lungs, yet an increase in the vascular destabilizing factor Ang-2, pointing towards a distinct Alk1-dependent pulmonary angiogenic imbalance. Local Ang-2 over-expression likely resulted in vascular destabilization and subsequent vessel regression, as shown previously[261,317]. Thus, excessive pulmonary Ang-2 may be responsible for the reduction in peripheral pulmonary microvasculature observed in *Alk1* mutant lungs. Importantly, the pulmonary VEGF levels in *Alk1*$^{+/-}$ mice were similar to those observed in WT mice.

To elucidate how these differences might have occurred in the abnormal lungs of *Eng*$^{+/-}$ and *Alk1*$^{+/-}$ mice, we assessed the activation of the canonical TGF-β1/BMP9-mediated pathways. No difference was observed in either phosphorylated or total Smad2 and Smad1/5/8 levels respectively, in the lung extracts from *Eng*$^{+/-}$ and *Alk1*$^{+/-}$ mice relative to their corresponding controls. These results suggest that these signaling pathways were not impaired in the affected lungs. Moreover, not only were VEGF levels not affected but the phosphorylated and total levels of Akt, downstream of VEGFR2, were similar in *Eng*$^{+/-}$ and *Alk1*$^{+/-}$ mice, indicating that this pathway was not altered.

We speculate that other TGF-β1/BMP9-mediated and VEGF-dependent pathways might be activated in the abnormal lungs of *Eng*$^{+/-}$ and *Alk1*$^{+/-}$ mice. For example, TSP-1-induced apoptosis can occur through binding to its CD36 receptor, leading to a rise in caspase-3 and phosphorylation of the p38 mitogen-activated protein kinase (p38MAPK) in a lung metastatic tumor mouse model[253]. This potential mechanism and the interaction between TSP-1, endoglin and VEGF are shown in Figure

32. Moreover, Ang-2 can alter several pathways via Tie-2 activation, including p38 MAPK, leading to apoptosis, thus vascular regression[318]. This suggested mechanism and the interaction between Ang-2, endoglin and VEGF are shown in Figure 33. This common pathway for TGF-β1/BMP9, VEGF, TSP-1 and Ang-2-mediated signaling might explain why the lungs of *Eng*$^{+/-}$ and *Alk1*$^{+/-}$ mice, despite their distinct angiogenic protein profile, display the same angiogenic phenotype, a reduction in peripheral pulmonary MVD.

Our laboratory showed previously that both *Eng*$^{+/-}$ and *Alk1*$^{+/-}$ mice developed an age-dependent PAH due to increased endothelial oxidative stress[227, 319]. Here we propose that TSP-1 and Ang-2 might have a role of in pathogenesis of PAH in *Eng*$^{+/-}$ and *Alk1*$^{+/-}$ mice. In support of this statement, it has been shown that mice deficient in TSP-1 were protected against chronic hypoxia-induced PAH[254]. Moreover, *Alk1*$^{-/-}$ embryos have higher Ang-2 mRNA levels than controls[69]. Furthermore, patients diagnosed with idiopathic PAH showed an increase in Ang-2 mRNA and protein levels in their plexiform lesions[320].

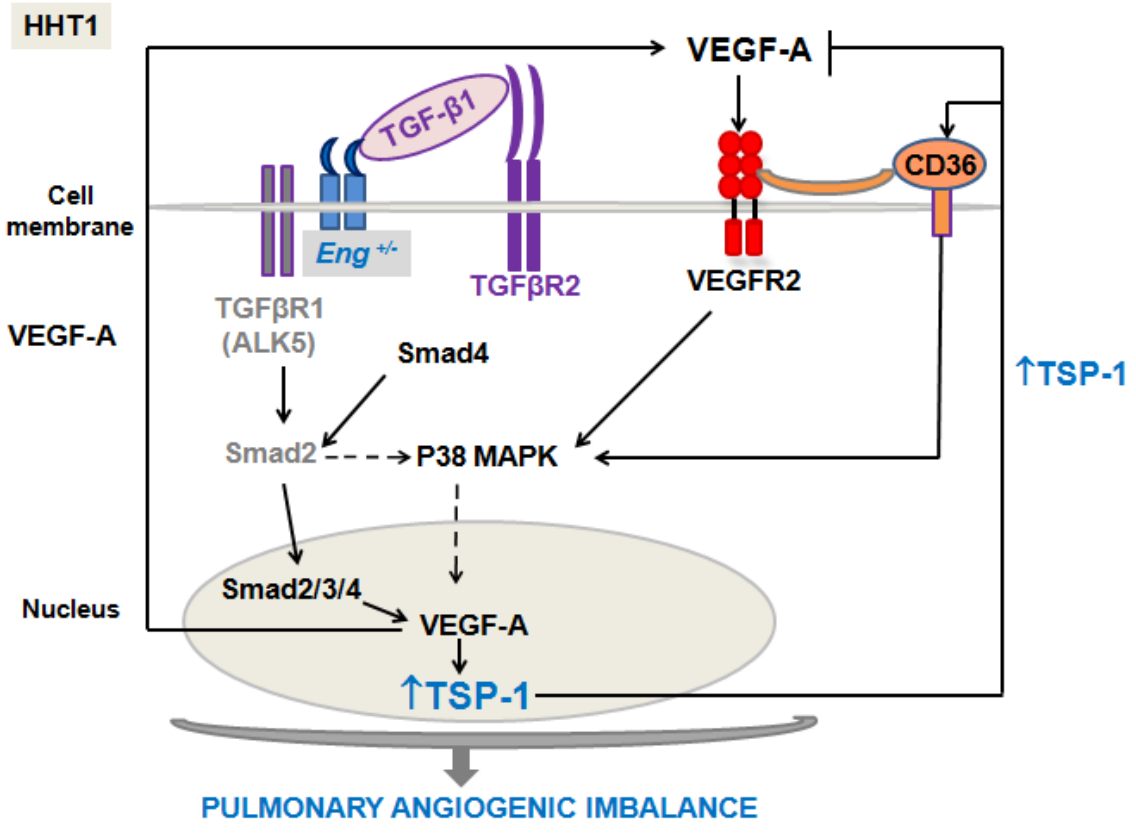

Figure 32. A working model of interaction between TSP-1, VEGF and endoglin. Dysregulated pulmonary angiogenesis in the lungs of *Eng*$^{+/-}$ mice is associated with an increase in TSP-1 levels. TSP-1 binds VEGF directly in the ECM, decreasing its levels[96]. In addition, TSP-1 can signal via CD36 through several pathways, including p38 MAPK, leading to apoptosis, hence vascular regression[321]. Interestingly, p38 MAPK is also a route for TGF-β1 and VEGF downstream signaling (not tested in our model; the hypothetic signaling pathway is depicted by dash lines). Here we demonstrate that the lungs of *Eng*$^{+/-}$ mice have normal pSmad2 and total Smad2 levels, therefore the TGF-β1 signaling is not affected at this level. Moreover, it is known that the intranuclear Smad2/3/4 complex can bind VEGF promotor and regulate its transcription. The fact that the reduction in lung VEGF after anti-VEGF therapy normalizes TSP-1 levels in *Eng*$^{+/-}$ mice, indicates that VEGF can also alter TSP-1 directly, in an unknown manner.

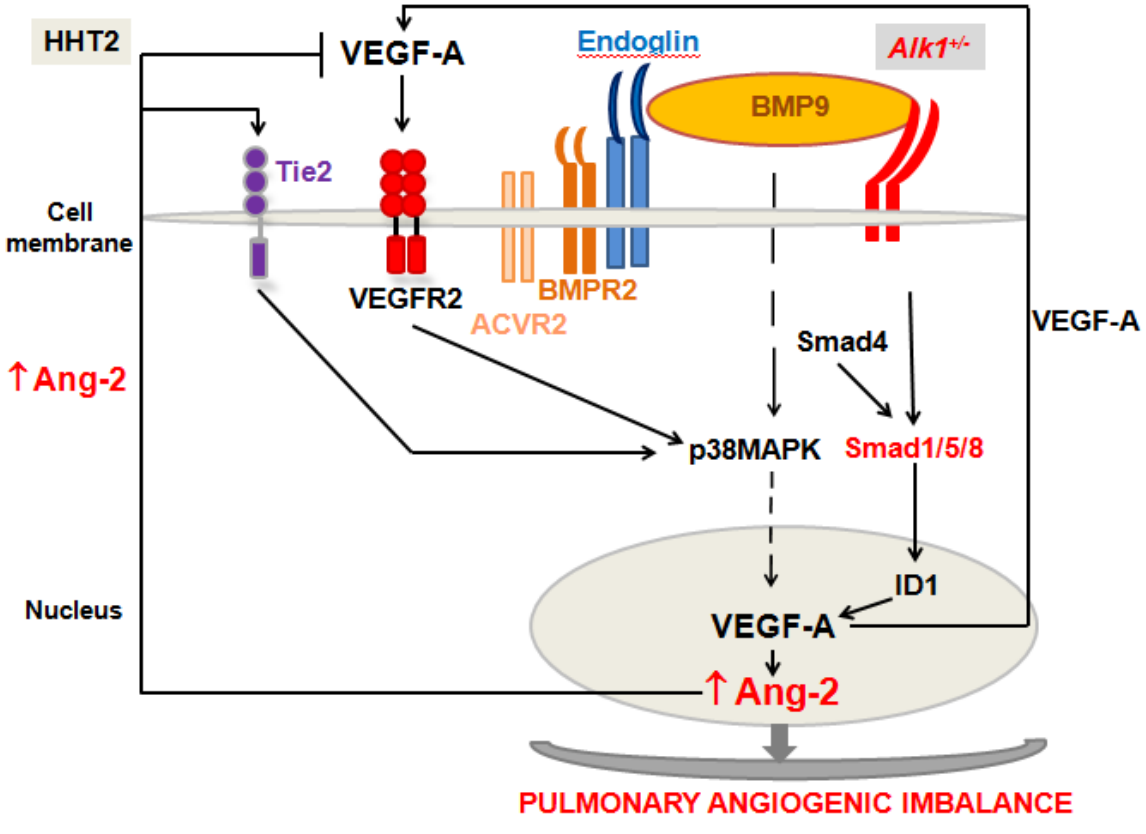

Figure 33. A working model of interaction between Ang-2, VEGF and ALK1. Dysregulated pulmonary angiogenesis in the lungs of *Alk1*$^{+/-}$ mice is characterized by an increase in pulmonary Ang-2 levels. Ang-2 inhibits directly VEGF. In addition, Ang-2 activation of Tie-2 receptor can alter several pathways, including p38 MAPK, leading to apoptosis, thus vascular regression[318] (not tested in our model; the hypothetic signaling pathway is depicted by dash lines). Moreover, VEGF induces the transcription and secretion of Ang-2. Here we report that the lungs of *Alk1*$^{+/-}$ mice have normal pSmad1/5/8 and total Smad1/5/8 levels, therefore the BMP9 signaling is not affected at this level. ID1, the target of the BMP9 downstream signaling can activate VEGF at the mRNA and protein levels. The fact that the reduction in lung VEGF after G6-31 antibody therapy normalizes the Ang-2 levels in *Alk1*$^{+/-}$ mice, suggest that VEGF can modulate Ang-2 directly.

4. 3 The hepatic angiogenic profile differs in *Eng*$^{+/-}$ and *Alk1*$^{+/-}$ mice

We also demonstrated that the hepatic TSP-1 levels were increased by 60% in *Eng*$^{+/-}$ versus WT mice, indicating an inverse correlation between endoglin and TSP-1 in more than one organ. In contrast, Ang-2 levels were unchanged in *Alk1*$^{+/-}$ mice, compared to *Alk1*$^{+/+}$ mice. It is howeover possible that a subset of liver microvessels is producing more Ang2 in *Alk1*$^{+/-}$ mice but that this is not detectable in total liver extracts.

4.4 Beneficial effects of anti-VEGF therapy in *Eng*$^{+/-}$ and *Alk1*$^{+/-}$ mice

4.4.1 Anti-VEGF therapy restores a normal pulmonary microvascular phenotype in *Eng*$^{+/-}$ and *Alk1*$^{+/-}$ mice

Surprisingly, anti-VEGF treatment, despite decreasing VEGF levels, increased the peripheral pulmonary MVD in *Eng*$^{+/-}$ and *Alk1*$^{+/-}$ mice. This led to attenuation of RVH in both mouse models. Moreover, G6-31 antibody normalized the pulmonary TSP-1 and Ang-2 levels in *Eng*$^{+/-}$ and *Alk1*$^{+/-}$ mice respectively. These effects of anti-VEGF therapy were secondary to the reduction in pulmonary VEGF levels. In addition, antbodies to VEGF bound not only to lung tissue but also to circulatory VEGF, demonstrating that this treatment was efficacious in targeting VEGF systemically. Overall, our results suggest that targeting VEGF can restore the pulmonary angiogenic balance, by normalizing TSP-1 and Ang-2 in *Eng* and *Alk1* mutant lungs, respectively. Thus, VEGF may act as a regulator of the angiogenic balance in tissues, by modulating several pathways and proteins involved in angiogenic modulation.

4.4.2 Anti-VEGF therapy decreases hepatic functional angiogenesis in *Eng*$^{+/-}$ but not in *Alk1*$^{+/-}$ mice

The effect of anti-VEGF treatment on liver was non-specific, as the therapy reduced MVD in both *Eng*$^{+/-}$ and *Eng*$^{+/+}$ mice. A significant reduction in hepatic MVD was also noted in anti-VEGF-treated *Alk1*$^{+/-}$ mice. However, hepatic VEGF levels remained unaltered after anti-VEGF treatment in both *Eng*$^{+/-}$ and *Alk1*$^{+/-}$ mice, likely due to high endogenous VEGF levels prior to onset of therapy. Furthermore, a 59% increase in hepatic TSP-1 was observed in the anti-VEGF-treated *Eng*$^{+/+}$ mice and a rising trend in the anti-VEGF-treated *Eng* and *Alk1* mutant mice. These changes in hepatic TSP-1 levels after anti-VEGF treatment appear to correlate with the observed decrease in liver MVD.

The *in vivo* assessment of hepatic functional angiogenesis or hemodynamics, showed that anti-VEGF therapy significantly reduced blood flow rate and volume in *Eng*$^{+/-}$ mice. In contrast, hepatic functional angiogenesis was not affected in *Alk1*$^{+/-}$ mice, despite the significant decrease in MVD after treatment, suggesting that the *in vivo* hepatic response to anti-VEGF therapy is distinct in *Eng*$^{+/-}$ mice and *Alk1*$^{+/-}$ mice. The difference in the total blood volume measured in these mutant mice could be due to lower hepatic blood flow rate observed in the anti-VEGF-treated *Eng*$^{+/-}$ but not in the *Alk1*$^{+/-}$ mice.

Overall, these findings indicate that the systemic anti-VEGF therapy also targets tissues with normal MVD, such as liver. We propose that *in vivo* quantification of the blood flow rate and volume by CE-US is a more accurate and functionally relevant method to determine the effects of anti-angiogenic therapy on organs than histological measurements of tissue MVD. CE-US represents an excellent non-invasive modality to

monitor *in vivo* the hepatic functional angiogenesis and response to anti-angiogenic treatment, allowing the optimization of intermittent anti-angiogenic treatment regimens in preclinical models of HHT.

4. 5 The emergent role of VEGF-targeted therapies in HHT

The first single-center, phase 2 clinical trial of systemic bevacizumab given at 5 mg per kg, every 14 days for a total of 6 injections in HHT patients with severe liver involvement had some encouraging results[201]. A partial reduction in the excessive cardiac output was seen in the majority of patients (17/24 or 70%), a complete response in 3/24 and no response in 4/24 patients. The duration and frequency of epistaxis were improved after treatment. Elevated systolic pulmonary pressures were attenuated in 5/8 patients. Even though the presence of vascular spots (the ultrasonic image for hepatic AVM) was unchanged after treatment, their hemodynamic parameters were better, which might explain the improvement in cardiac output. The treatment was tolerated; only 2 patients developed severe hypertension and required anti-hypertensive medication. However, the optimal biological dose, the duration and frequency of treatment, the long-term and multi-organ effects of systemic anti-VEGF therapy need to be determined in future studies. In the last 2 years, four more clinical trials of topical intranasal bevacizumab were commenced in HHT patients, two of which are completed. The release of their results is pending.

4. 6 The emergent role of endoglin and Alk1-targeted therapies in cancer

Anti-angiogenic therapy can target various factors implicated in the angiogenic balance, including angiogenic modulators such as endoglin and ALK1.

Recently, several studies have shown that targeting endoglin and ALK1 led to

anti-angiogenic effects in tumor models. Several anti-endoglin DNA oral vaccines have demonstrated anti-metastatic and anti-angiogenic effects in a mouse model of breast carcinoma cells[193] and aggressive melanoma[194]. Moreover, chimeric ALK1-Fc inhibited the growth of B16 melanoma explants and decreased the tumor growth in mice grafted with MCF7 mammary adenocarcinoma cells[72]. Furthermore, antibodies to ALK1 delayed tumor growth in a human melanoma model resistant to a VEGF receptor kinase inhibitor[73]. In addition, systemic treatment with the ALK1-Fc fusion protein RAP-041 reduced tumor growth and progression in the RIP1-Tag2 transgenic tumor mouse model [71].

Overall, these results confirm that endoglin and ALK1 are implicated in the angiogenic regulation of vessel growth and that targeted therapies of endoglin and ALK1 offer new avenues in oncology.

4.7 Colitic *Eng*$^{+/-}$ mice have high colonic MVD and pro-inflammatory cytokines and an intestinal angiogenic imbalance

Our laboratory showed previously that *Eng*$^{+/-}$ mice subjected to a single course of DSS develop severe colitis and increased number of abnormal vessels in the inflamed gut[179]. Moreover, colitic *Eng*$^{+/-}$ mice had high tissue VEGF levels[179]. Thus, we hypothesized that VEGF plays a pathogenic role in the abnormal blood vessel formation and in chronic inflammation in colitic *Eng*$^{+/-}$ mice and that targeted VEGF therapy will reduce pathological angiogenesis and inflammation in these mice.

In Chapter Three, we demonstrated that colitic *Eng*$^{+/-}$ mice have persistent, exaggerated colonic MVD, when compared to colitic WT mice. The time point of maximal tissue angiogenesis corresponded to the peak of inflammation in colitic *Eng*$^{+/-}$

and *Eng*$^{+/+}$ mice (day 9). We confirmed that colitic *Eng*$^{+/-}$ mice had more tissue inflammation and inflamamtory cells then colitic WT mice. *In vivo* ultrasound studies revealed that colitic *Eng*$^{+/-}$ mice have higher colonic wall thickness and microvascular hemodynamics versus colitic *Eng*$^{+/+}$ mice. In the present study, tissue VEGF levels were similar in colitic *Eng*$^{+/-}$ and *Eng*$^{+/+}$ mice. These results differ from the previously published data[179], likely due to differences in ELISA assay sensitivity and housing of mice in a different animal facility. Tissue TGF-β1 levels were similar in colitic *Eng*$^{+/-}$ and *Eng*$^{+/+}$ mice. Moreover, total Smad2 and Smad1/5/8 were increased in both colitic *Eng*$^{+/-}$ and *Eng*$^{+/+}$ mice, and related to the tissue inflammatory and angiogenic responses in colitis. Several cytokines and angiogenic factors were increased with inflammation in the gut of both colitic *Eng*$^{+/-}$ and *Eng*$^{+/+}$ mice: endoglin, IL-1β, whereas IL-6 and MCP-1 were significantly augmented only in colitic mutant mice. However, only the neutrophil chemotactic factor G-CSF and the regenerative protein amphiregulin were further increased in colitic *Eng* heterozygous mice, suggesting that the endoglin deficiency might play a modulating role in tissue production of these inflammation-induced factors. A summary of changes in intestinal microvasculature and inflammatory parameters in colitic *Eng*$^{+/-}$ mice and their response to G6-31 antibody treatment is shown in Figure 31.

Taken together, it appears that the loss of endoglin leads to severe colitis, thus endoglin might have a protective role in IBD. As endoglin is expressed in endothelial and stromal cells and in macrophages, its rise with inflammation suggests that endoglin is also a potential marker of tissue remodeling in chronic inflammatory diseases.

4.8 Anti-VEGF therapy reduces chronic intestinal inflammation in the endoglin heterozygous mouse model of inflammatory bowel disease

Anti-VEGF treatment reduced the exaggerated gut inflammation observed in colitic *Eng*$^{+/-}$ mice. Moreover, targeted VEGF therapy decreased the excessive intestinal MVD. Importantly, we showed that anti-VEGF therapy attenuated *in vivo* the intestinal wall thickness and microvascular hemodynamics, confirming the histological data.

The reduction in gut VEGF levels after anti-VEGF therapy did not alter the intestinal TGF-β1 levels. In addition, anti-VEGF treatment did not alter phospho- or total Smad2 and Smad1/5/8 levels, suggesting that its targets are downstream of Smads or in other VEGF-mediated pathways.

Overall, these findings suggest that the anti-VEGF therapy has some beneficial effects in colitis. We propose that ultrasound is an effective non-invasive method to monitor the progression of colitis and the response to anti-VEGF therapy in mice and potentially in man.

4.9 The emergent role of anti-VEGF therapy in chronic inflammatory diseases

Only recently has anti-VEGF therapy been recognized as having direct anti-inflammatory effects in animal models. Several preclinical cancer studies have shown that anti-VEGF therapies can alter the immune infiltration in tumors by reducing the number of macrophages[322], accumulation of myeloid-derived suppressor cells (MDSCs) and plasmacytoid DC, when compared to control mice[323].

In experimental inflammation models, an antibody to VEGF administered to G-CSF-R$^{-/-}$RAG2$^{-/-}$ mice decreased neutrophil mobilization[324]. Moreover, 50μg of G6–31

antibody given every two days for a total of 4 injections reduced the number of neutrophils, macrophages and granulocytes and their transmigration through the epidermis in a mouse model of psoriasis[35]. These findings suggest that anti-VEGF treatment might have a preferential effect on immune cells of myeloid origin.

We have shown that G6-31 monoclonal antibody given to colitic *Eng*$^{+/-}$ mice reduced the intestinal wall thickness, inflammatory score and number of inflammatory cells in the gut submucosa, IL-1β and G-CSF, indicating that anti-VEGF therapy had an anti-inflammatory effect in our model of IBD. However, it is unclear if this effect is due to direct targeting of immune cells or to indirect targeting of inflammed vessels, that would lead to decreased infiltration in the affected areas. The potential anti-inflammatory effects of anti-VEGF therapy could be beneficial and open new avenues for treatment of chronic inflammatory diseases.

In summary, endoglin, ALK1 and VEGF play an angiogenic modulatory role in HHT. We demonstrated that endoglin is inversely correlated with the level of angiostatic TSP-1 in the abnormal lung phenotype, while ALK1 deficiency is characterized by a rise in the vascular destabilizing factor Ang-2. These findings might explain some of the heterogeneity between HHT1 and HHT2. We also propose that changes in TSP-1 and Ang-2 might also contribute to the pathogenesis of PAH in *Eng*$^{+/-}$ and *Alk1*$^{+/-}$ mice and perhaps in patients diagnosed with HHT1 and HHT2. Anti-VEGF therapy may have a beneficial role in restoring the angiogenic balance in HHT and PAH-associated with endoglin and ALK1 mutations. In addition, we report that endoglin and VEGF have a regulatory role in inflammation and pathological angiogenesis in chronic colitis, with endoglin likely being protective.

Anti-VEGF treatment decreases *in vitro* and *in vivo* colonic inflammation and pathological angiogenesis, as assessed by MAdCAM-1 tagged CE-US, in colitic $Eng^{+/-}$ mice. Moreover, anti-VEGF therapy reduced the elevated tissue endoglin, IL-1β and G-CSF, suggesting that it has anti-inflammatory properties. We show that CE-US is an excellent non-invasive imaging modality to assess functional angiogenesis in liver and colon. We also demonstrate that MAdCAM-1-targeted-CE-US offers new avenues for investigating *in vivo* the molecular aspects of inflammation in chronic inflammatory diseases.

References

1. Voronov E, Shouval DS, Krelin Y, et al. IL-1 is required for tumor invasiveness and angiogenesis. Proc Natl Acad Sci U S A. 2003;100:2645-2650

2. Folkman J. Tumor angiogenesis: therapeutic implications. N Engl J Med. 1971;285:1182-1186

3. Shovlin CL. Hereditary haemorrhagic telangiectasia: pathophysiology, diagnosis and treatment. Blood Rev. 2010;24:203-219

4. Abraham C, Cho JH. Inflammatory bowel disease. N Engl J Med. 2009;361:2066-2078

5. Carmeliet P. Angiogenesis in health and disease. Nat Med. 2003;9:653-660

6. Avraham-Davidi I, Yona S, Grunewald M, et al. On-site education of VEGF-recruited monocytes improves their performance as angiogenic and arteriogenic accessory cells. J Exp Med. 2013

7. Risau W, Flamme I. Vasculogenesis. Annu Rev Cell Dev Biol. 1995;11:73-91

8. Figg WD, Folkman MJ, SpringerLink (Online service). Angiogenesis An Integrative Approach From Science to Medicine. Boston, MA: Springer Science+Business Media, LLC; 2008

9. Ribatti D, Vacca A, Nico B, et al. Postnatal vasculogenesis. Mech Dev. 2001;100:157-163

10. Reisinger K, Baal N, McKinnon T, et al. The gonadotropins: tissue-specific angiogenic factors. Mol Cell Endocrinol. 2007;269:65-80

11. Collin O, Bergh A. Leydig cells secrete factors which increase vascular permeability and endothelial cell proliferation. Int J Androl. 1996;19:221-228

12. LeCouter J, Lin R, Tejada M, et al. The endocrine-gland-derived VEGF homologue Bv8 promotes angiogenesis in the testis: Localization of Bv8 receptors to endothelial cells. Proc Natl Acad Sci U S A. 2003;100:2685-2690

13. Yano K, Brown LF, Lawler J, et al. Thrombospondin-1 plays a critical role in the induction of hair follicle involution and vascular regression during the catagen phase. J Invest Dermatol. 2003;120:14-19

14. Folkman J, Klagsbrun M. Angiogenic factors. Science. 1987;235:442-447

15. Vailhe B, Vittet D, Feige JJ. In vitro models of vasculogenesis and angiogenesis. Lab Invest. 2001;81:439-452

16. Pepper MS, Vassalli JD, Orci L, et al. Biphasic effect of transforming growth factor-beta 1 on in vitro angiogenesis. Exp Cell Res. 1993;204:356-363

17. Chang JH, Gabison EE, Kato T, et al. Corneal neovascularization. Curr Opin Ophthalmol. 2001;12:242-249

18. Motz GT, Coukos G. The parallel lives of angiogenesis and immunosuppression: cancer and other tales. Nat Rev Immunol. 2011;11:702-711

19. Martinez A. A new family of angiogenic factors. Cancer letters. 2006;236:157-163

20. Clapp C, Thebault S, Jeziorski MC, et al. Peptide hormone regulation of angiogenesis. Physiol Rev. 2009;89:1177-1215

21. Belotti D, Foglieni C, Resovi A, et al. Targeting angiogenesis with compounds from the extracellular matrix. Int J Biochem Cell Biol. 2011;43:1674-1685

22. Folkman J. Angiogenesis. Annu Rev Med. 2006;57:1-18

23. Olsson AK, Dimberg A, Kreuger J, et al. VEGF receptor signalling - in control of vascular function. Nat Rev Mol Cell Biol. 2006;7:359-371

24. Varey AH, Rennel ES, Qiu Y, et al. VEGF 165 b, an antiangiogenic VEGF-A isoform, binds and inhibits bevacizumab treatment in experimental colorectal carcinoma: balance of pro- and antiangiogenic VEGF-A isoforms has implications for therapy. Br J Cancer. 2008;98:1366-1379

25. Kerbel RS. Tumor angiogenesis: past, present and the near future. Carcinogenesis. 2000;21:505-515

26. Castonguay R, Werner ED, Matthews RG, et al. Soluble endoglin specifically binds bone morphogenetic proteins 9 and 10 via its orphan domain, inhibits blood vessel formation, and suppresses tumor growth. J Biol Chem. 2011;286:30034-30046

27. Quackenbush EJ, Letarte M. Identification of several cell surface proteins of non-T, non-B acute lymphoblastic leukemia by using monoclonal antibodies. J Immunol. 1985;134:1276-1285

28. Duff SE, Li C, Garland JM, et al. CD105 is important for angiogenesis: evidence and potential applications. Faseb J. 2003;17:984-992

29. Augustin HG, Koh GY, Thurston G, et al. Control of vascular morphogenesis and homeostasis through the angiopoietin-Tie system. Nat Rev Mol Cell Biol. 2009;10:165-177

30. Bidart M, Ricard N, Levet S, et al. BMP9 is produced by hepatocytes and circulates mainly in an active mature form complexed to its prodomain. Cell Mol Life Sci. 2012;69:313-324

31. Arcondeguy T, Lacazette E, Millevoi S, et al. VEGF-A mRNA processing, stability and translation: a paradigm for intricate regulation of gene expression at the post-transcriptional level. Nucleic Acids Res. 2013;41:7997-8010

32. Lee S, Chen TT, Barber CL, et al. Autocrine VEGF signaling is required for vascular homeostasis. Cell. 2007;130:691-703

33. Ferrara N, Carver-Moore K, Chen H, et al. Heterozygous embryonic lethality induced by targeted inactivation of the VEGF gene. Nature. 1996;380:439-442

34. Ozawa CR, Banfi A, Glazer NL, et al. Microenvironmental VEGF concentration, not total dose, determines a threshold between normal and aberrant angiogenesis. J Clin Invest. 2004;113:516-527

35. Schonthaler HB, Huggenberger R, Wculek SK, et al. Systemic anti-VEGF treatment strongly reduces skin inflammation in a mouse model of psoriasis. Proc Natl Acad Sci U S A. 2009;106:21264-21269

36. Koch S, Claesson-Welsh L. Signal transduction by vascular endothelial growth factor receptors. Cold Spring Harb Perspect Med. 2012;2:a006502

37. Kendall RL, Thomas KA. Inhibition of vascular endothelial cell growth factor activity by an endogenously encoded soluble receptor. Proc Natl Acad Sci U S A. 1993;90:10705-10709

38. Ebos JM, Bocci G, Man S, et al. A naturally occurring soluble form of vascular endothelial growth factor receptor 2 detected in mouse and human plasma. Mol Cancer Res. 2004;2:315-326

39. Singh N, Tiem M, Watkins R, et al. Soluble vascular endothelial growth factor receptor 3 is essential for corneal alymphaticity. Blood. 2013;121:4242-4249

40. Sarrazin S, Lamanna WC, Esko JD. Heparan sulfate proteoglycans. Cold Spring Harb Perspect Biol. 2011;3

41. Dvorak HF. Vascular permeability factor/vascular endothelial growth factor: a critical cytokine in tumor angiogenesis and a potential target for diagnosis and therapy. J Clin Oncol. 2002;20:4368-4380

42. Kerbel RS. Tumor angiogenesis. N Engl J Med. 2008;358:2039-2049

43. Moustakas A, Heldin CH. Non-Smad TGF-beta signals. J Cell Sci. 2005;118:3573-3584

44. Kulkarni AB, Karlsson S. Transforming growth factor-beta 1 knockout mice. A mutation in one cytokine gene causes a dramatic inflammatory disease. Am J Pathol. 1993;143:3-9

45. Wu X, Ma J, Han JD, et al. Distinct regulation of gene expression in human endothelial cells by TGF-beta and its receptors. Microvasc Res. 2006;71:12-19

46. David L, Mallet C, Keramidas M, et al. Bone morphogenetic protein-9 is a circulating vascular quiescence factor. Circ Res. 2008;102:914-922

47. Larrivee B, Prahst C, Gordon E, et al. ALK1 signaling inhibits angiogenesis by cooperating with the Notch pathway. Dev Cell. 2012;22:489-500

48. Suzuki Y, Ohga N, Morishita Y, et al. BMP-9 induces proliferation of multiple types of endothelial cells in vitro and in vivo. J Cell Sci. 2010;123:1684-1692

49. Torsney E, Charlton R, Parums D, et al. Inducible expression of human endoglin during inflammation and wound healing in vivo. Inflamm Res. 2002;51:464-470

50. Burrows FJ, Derbyshire EJ, Tazzari PL, et al. Up-regulation of endoglin on vascular endothelial cells in human solid tumors: implications for diagnosis and therapy. Clin Cancer Res. 1995;1:1623-1634

51. Buhring HJ, Muller CA, Letarte M, et al. Endoglin is expressed on a subpopulation of immature erythroid cells of normal human bone marrow. Leukemia. 1991;5:841-847

52. Kestendjieva S, Kyurkchiev D, Tsvetkova G, et al. Characterization of mesenchymal stem cells isolated from the human umbilical cord. Cell Biol Int. 2008;32:724-732

53. Lastres P, Bellon T, Cabanas C, et al. Regulated expression on human macrophages of endoglin, an Arg-Gly-Asp-containing surface antigen. Eur J Immunol. 1992;22:393-397

54. Adam PJ, Clesham GJ, Weissberg PL. Expression of endoglin mRNA and protein in human vascular smooth muscle cells. Biochem Biophys Res Commun. 1998;247:33-37

55. St-Jacques S, Cymerman U, Pece N, et al. Molecular characterization and in situ localization of murine endoglin reveal that it is a transforming growth factor-beta binding protein of endothelial and stromal cells. Endocrinology. 1994;134:2645-2657

56. Chen CZ, Li M, de Graaf D, et al. Identification of endoglin as a functional marker that defines long-term repopulating hematopoietic stem cells. Proc Natl Acad Sci U S A. 2002;99:15468-15473

57. Gougos A, St Jacques S, Greaves A, et al. Identification of distinct epitopes of endoglin, an RGD-containing glycoprotein of endothelial cells, leukemic cells, and syncytiotrophoblasts. Int Immunol. 1992;4:83-92

58. Caniggia I, Taylor CV, Ritchie JW, et al. Endoglin regulates trophoblast differentiation along the invasive pathway in human placental villous explants. Endocrinology. 1997;138:4977-4988

59. Qu R, Silver MM, Letarte M. Distribution of endoglin in early human development reveals high levels on endocardial cushion tissue mesenchyme during valve formation. Cell Tissue Res. 1998;292:333-343

60. Bourdeau A, Dumont DJ, Letarte M. A murine model of hereditary hemorrhagic telangiectasia. J. Clin. Invest. 1999;104:1343-1351

61. Arthur HM, Ure J, Smith AJ, et al. Endoglin, an ancillary TGFbeta receptor, is required for extraembryonic angiogenesis and plays a key role in heart development. Dev Biol. 2000;217:42-53

62. Cho SK, Bourdeau A, Letarte M, et al. Expression and function of CD105 during the onset of hematopoiesis from Flk1(+) precursors. Blood. 2001;98:3635-3642

63. Perlingeiro RC. Endoglin is required for hemangioblast and early hematopoietic development. Development. 2007;134:3041-3048

64. Nomura-Kitabayashi A, Anderson GA, Sleep G, et al. Endoglin is dispensable for angiogenesis, but required for endocardial cushion formation in the midgestation mouse embryo. Dev Biol. 2009;335:66-77

65. Bellon T, Corbi A, Lastres P, et al. Identification and expression of two forms of the human transforming growth factor-beta-binding protein endoglin with distinct cytoplasmic regions. Eur J Immunol. 1993;23:2340-2345

66. Velasco S, Alvarez-Munoz P, Pericacho M, et al. L- and S-endoglin differentially modulate TGFbeta1 signaling mediated by ALK1 and ALK5 in L6E9 myoblasts. J Cell Sci. 2008;121:913-919

67. Llorca O, Trujillo A, Blanco FJ, et al. Structural model of human endoglin, a transmembrane receptor responsible for hereditary hemorrhagic telangiectasia. J Mol Biol. 2007;365:694-705

68. Seki T, Yun J, Oh SP. Arterial endothelium-specific activin receptor-like kinase 1 expression suggests its role in arterialization and vascular remodeling. Circ Res. 2003;93:682-689

69. Oh SP, Seki T, Goss KA, et al. Activin receptor-like kinase 1 modulates transforming growth factor-beta 1 signaling in the regulation of angiogenesis. Proc Natl Acad Sci U S A. 2000;97:2626-2631

70. Goumans MJ, Valdimarsdottir G, Itoh S, et al. Balancing the activation state of the endothelium via two distinct TGF-beta type I receptors. Embo J. 2002;21:1743-1753

71. Cunha SI, Pietras K. ALK1 as an emerging target for antiangiogenic therapy of cancer. Blood. 2011;117:6999-7006

72. Mitchell D, Pobre EG, Mulivor AW, et al. ALK1-Fc inhibits multiple mediators of angiogenesis and suppresses tumor growth. Mol Cancer Ther. 2010;9:379-388

73. Hu-Lowe DD, Chen E, Zhang L, et al. Targeting activin receptor-like kinase 1 inhibits angiogenesis and tumorigenesis through a mechanism of action complementary to anti-VEGF therapies. Cancer Res. 2011;71:1362-1373

74. Corti P, Young S, Chen CY, et al. Interaction between alk1 and blood flow in the development of arteriovenous malformations. Development. 2011;138:1573-1582

75. Park SO, Wankhede M, Lee YJ, et al. Real-time imaging of de novo arteriovenous malformation in a mouse model of hereditary hemorrhagic telangiectasia. J Clin Invest. 2009;119:3487-3496

76. Urness LD, Sorensen LK, Li DY. Arteriovenous malformations in mice lacking activin receptor-like kinase-1. Nat Genet. 2000;26:328-331

77. Roman BL, Pham VN, Lawson ND, et al. Disruption of acvrl1 increases endothelial cell number in zebrafish cranial vessels. Development. 2002;129:3009-3019

78. Seki T, Hong KH, Oh SP. Nonoverlapping expression patterns of ALK1 and ALK5 reveal distinct roles of each receptor in vascular development. Lab Invest. 2006;86:116-129

79. Park SO, Lee YJ, Seki T, et al. ALK5- and TGFBR2-independent role of ALK1 in the pathogenesis of hereditary hemorrhagic telangiectasia type 2. Blood. 2008;111:633-642

80. Miyazono K, Kusanagi K, Inoue H. Divergence and convergence of TGF-beta/BMP signaling. J Cell Physiol. 2001;187:265-276

81. Pardali E, Goumans MJ, ten Dijke P. Signaling by members of the TGF-beta family in vascular morphogenesis and disease. Trends Cell Biol. 2010;20:556-567

82. Goumans MJ, Valdimarsdottir G, Itoh S, et al. Activin receptor-like kinase (ALK)1 is an antagonistic mediator of lateral TGFbeta/ALK5 signaling. Mol Cell. 2003;12:817-828

83. Ray BN, Lee NY, How T, et al. ALK5 phosphorylation of the endoglin cytoplasmic domain regulates Smad1/5/8 signaling and endothelial cell migration. Carcinogenesis. 2010;31:435-441

84. Tian H, Mythreye K, Golzio C, et al. Endoglin mediates fibronectin/alpha5beta1 integrin and TGF-beta pathway crosstalk in endothelial cells. Embo J. 2012;31:3885-3900

85. Zhang YE. Non-Smad pathways in TGF-beta signaling. Cell Res. 2009;19:128-139

86. van de Kerkhof PC, Rulo HF, van Pelt JP, et al. Expression of endoglin in the transition between psoriatic uninvolved and involved skin. Acta Derm Venereol. 1998;78:19-21

87. Thurston G, Daly C. The complex role of angiopoietin-2 in the angiopoietin-tie signaling pathway. Cold Spring Harb Perspect Med. 2012;2:a006550

88. Fiedler U, Augustin HG. Angiopoietins: a link between angiogenesis and inflammation. Trends Immunol. 2006;27:552-558

89. Huang YQ, Li JJ, Karpatkin S. Identification of a family of alternatively spliced mRNA species of angiopoietin-1. Blood. 2000;95:1993-1999

90. Dumont DJ, Gradwohl G, Fong GH, et al. Dominant-negative and targeted null mutations in the endothelial receptor tyrosine kinase, tek, reveal a critical role in vasculogenesis of the embryo. Genes Dev. 1994;8:1897-1909

91. Lemieux C, Maliba R, Favier J, et al. Angiopoietins can directly activate endothelial cells and neutrophils to promote proinflammatory responses. Blood. 2005;105:1523-1530

92. Puri MC, Rossant J, Alitalo K, et al. The receptor tyrosine kinase TIE is required for integrity and survival of vascular endothelial cells. Embo J. 1995;14:5884-5891

93. D'Amico G, Korhonen EA, Waltari M, et al. Loss of endothelial Tie1 receptor impairs lymphatic vessel development-brief report. Arterioscler Thromb Vasc Biol. 2010;30:207-209

94. Jones N, Voskas D, Master Z, et al. Rescue of the early vascular defects in Tek/Tie2 null mice reveals an essential survival function. EMBO Rep. 2001;2:438-445

95. Gamble JR, Drew J, Trezise L, et al. Angiopoietin-1 is an antipermeability and anti-inflammatory agent in vitro and targets cell junctions. Circ Res. 2000;87:603-607

96. Lopez-Dee Z, Pidcock K, Gutierrez LS. Thrombospondin-1: multiple paths to inflammation. Mediators Inflamm. 2011;2011:296069

97. Krishna SM, Golledge J. The role of thrombospondin-1 in cardiovascular health and pathology. Int J Cardiol. 2013;168:692-706

98. Zhang X, Kazerounian S, Duquette M, et al. Thrombospondin-1 modulates vascular endothelial growth factor activity at the receptor level. Faseb J. 2009;23:3368-3376

99. Takahashi T, Takahashi K, Mernaugh RL, et al. A monoclonal antibody against CD148, a receptor-like tyrosine phosphatase, inhibits endothelial-cell growth and angiogenesis. Blood. 2006;108:1234-1242

100. Danese S, Sans M, de la Motte C, et al. Angiogenesis as a novel component of inflammatory bowel disease pathogenesis. Gastroenterology. 2006;130:2060-2073

101. Walsh DA. Angiogenesis and arthritis. Rheumatology (Oxford). 1999;38:103-112

102. Palladino M, Gatto I, Neri V, et al. Angiogenic Impairment of the Vascular Endothelium: A Novel Mechanism and Potential Therapeutic Target in Muscular Dystrophy. Arterioscler Thromb Vasc Biol. 2013;33:2867-76.

103. Powe CE, Ecker J, Rana S, et al. Preeclampsia and the risk of large-for-gestational-age infants. Am J Obstet Gynecol. 2011;204:425 e421-426

104. Chung NA, Lydakis C, Belgore F, et al. Angiogenesis in myocardial infarction. An acute or chronic process? Eur Heart J. 2002;23:1604-1608

105. Krupinski J, Kaluza J, Kumar P, et al. Role of angiogenesis in patients with cerebral ischemic stroke. Stroke. 1994;25:1794-1798

106. Folkman J. Angiogenesis in cancer, vascular, rheumatoid and other disease. Nat Med. 1995;1:27-31

107. Sabba C, Cirulli A, Rizzi R, et al. Angiogenesis and hereditary hemorrhagic telangiectasia. Rendu-Osler-Weber disease. Acta Haematol. 2001;106:214-219

108. Martin A, Komada MR, Sane DC. Abnormal angiogenesis in diabetes mellitus. Med Res Rev. 2003;23:117-145

109. Rupnick MA, Panigrahy D, Zhang CY, et al. Adipose tissue mass can be regulated through the vasculature. Proc Natl Acad Sci U S A. 2002;99:10730-10735

110. Khurana R, Simons M, Martin JF, et al. Role of angiogenesis in cardiovascular disease: a critical appraisal. Circulation. 2005;112:1813-1824

111. Kerbel RS. Inhibition of tumor angiogenesis as a strategy to circumvent acquired resistance to anti-cancer therapeutic agents. Bioessays. 1991;13:31-36

112. Shojaei F. Anti-angiogenesis therapy in cancer: current challenges and future perspectives. Cancer letters. 2012;320:130-137

113. Coriat R, Mir O, Leblanc S, et al. Feasibility of anti-VEGF agent bevacizumab in patients with Crohn's disease. Inflamm Bowel Dis. 2011;17:1632

114. McCuskey RS. The hepatic microvascular system in health and its response to toxicants. Anatomical record. 2008;291:661-671

115. Garlanda C, Dejana E. Heterogeneity of endothelial cells. Specific markers. Arterioscler Thromb Vasc Biol. 1997;17:1193-1202

116. Miskinyte S, Butler MG, Herve D, et al. Loss of BRCC3 deubiquitinating enzyme leads to abnormal angiogenesis and is associated with syndromic moyamoya. Am J Hum Genet. 2011;88:718-728

117. Whitehead KJ, Smith MC, Li DY. Arteriovenous malformations and other vascular malformation syndromes. Cold Spring Harb Perspect Med. 2013;3:a006635

118. Hartley J, Westmacott R, Decker J, et al. Childhood-onset CADASIL: clinical, imaging, and neurocognitive features. J Child Neurol. 2010;25:623-627

119. Bharatha A, Faughnan ME, Kim H, et al. Brain arteriovenous malformation multiplicity predicts the diagnosis of hereditary hemorrhagic telangiectasia: quantitative assessment. Stroke. 2012;43:72-78

120. Desai BS, Schneider JA, Li JL, et al. Evidence of angiogenic vessels in Alzheimer's disease. J Neural Transm. 2009;116:587-597

121. Desai Bradaric B, Patel A, Schneider JA, et al. Evidence for angiogenesis in Parkinson's disease, incidental Lewy body disease, and progressive supranuclear palsy. J Neural Transm. 2012;119:59-71

122. Kirk S, Frank JA, Karlik S. Angiogenesis in multiple sclerosis: is it good, bad or an epiphenomenon? J Neurol Sci. 2004;217:125-130

123. Heimann H, Damato B. Congenital vascular malformations of the retina and choroid. Eye (Lond). 2010;24:459-467

124. Rinaldi M, Buscarini E, Danesino C, et al. Ocular manifestations in hereditary hemorrhagic telangiectasia (Rendu-Osler-Weber disease): a case-series. Ophthalmic Genet. 2011;32:12-17

125. Hartnett ME, Penn JS. Mechanisms and management of retinopathy of prematurity. N Engl J Med. 2012;367:2515-2526

126. Johnson D, Sharma S. Ocular and systemic safety of bevacizumab and ranibizumab in patients with neovascular age-related macular degeneration. Curr Opin Ophthalmol. 2013;24:205-212

127. Qi JH, Ebrahem Q, Moore N, et al. A novel function for tissue inhibitor of metalloproteinases-3 (TIMP3): inhibition of angiogenesis by blockage of VEGF binding to VEGF receptor-2. Nat Med. 2003;9:407-415

128. Guttmacher AE, Marchuk DA, White RI, Jr. Hereditary hemorrhagic telangiectasia. N Engl J Med. 1995;333:918-924

129. El-Melegy NT, Mohamed NA. Angiogenic biomarkers in children with congenital heart disease: possible implications. Ital J Pediatr. 2010;36:32

130. Stalmans I, Lambrechts D, De Smet F, et al. VEGF: a modifier of the del22q11 (DiGeorge) syndrome? Nat Med. 2003;9:173-182

131. Shiojima I, Sato K, Izumiya Y, et al. Disruption of coordinated cardiac hypertrophy and angiogenesis contributes to the transition to heart failure. J Clin Invest. 2005;115:2108-2118

132. Humbert M, Trembath RC. Genetics of pulmonary hypertension: from bench to bedside. Eur Respir J. 2002;20:741-749

133. Ribatti D, Puxeddu I, Crivellato E, et al. Angiogenesis in asthma. Clin Exp Allergy. 2009;39:1815-1821

134. Fabris L, Cadamuro M, Fiorotto R, et al. Effects of angiogenic factor overexpression by human and rodent cholangiocytes in polycystic liver diseases. Hepatology. 2006;43:1001-1012

135. Buscarini E, Leandro G, Conte D, et al. Natural history and outcome of hepatic vascular malformations in a large cohort of patients with hereditary hemorrhagic teleangiectasia. Dig Dis Sci. 2011;56:2166-2178

136. Fernandez M, Semela D, Bruix J, et al. Angiogenesis in liver disease. J Hepatol. 2009;50:604-620

137. Heidenreich R, Rocken M, Ghoreschi K. Angiogenesis drives psoriasis pathogenesis. Int J Exp Pathol. 2009;90:232-248

138. Bello-Reuss E, Holubec K, Rajaraman S. Angiogenesis in autosomal-dominant polycystic kidney disease. Kidney Int. 2001;60:37-45

139. Maeshima Y, Makino H. Angiogenesis and chronic kidney disease. Fibrogenesis Tissue Repair. 2010;3:13

140. LeCouter J, Lin R, Ferrara N. Endocrine gland-derived VEGF and the emerging hypothesis of organ-specific regulation of angiogenesis. Nat Med. 2002;8:913-917

141. Potente M, Gerhardt H, Carmeliet P. Basic and therapeutic aspects of angiogenesis. Cell. 2011;146:873-887

142. Aird WC. Phenotypic heterogeneity of the endothelium: II. Representative vascular beds. Circ Res. 2007;100:174-190

143. Stewart PA, Wiley MJ. Developing nervous tissue induces formation of blood-brain barrier characteristics in invading endothelial cells: a study using quail--chick transplantation chimeras. Dev Biol. 1981;84:183-192

144. Shukunami C, Oshima Y, Hiraki Y. Chondromodulin-I and tenomodulin: a new class of tissue-specific angiogenesis inhibitors found in hypovascular connective tissues. Biochem Biophys Res Commun. 2005;333:299-307

145. Molema G. Heterogeneity in endothelial responsiveness to cytokines, molecular causes, and pharmacological consequences. Semin Thromb Hemost. 2010;36:246-264

146. Girerd B, Montani D, Coulet F, et al. Clinical outcomes of pulmonary arterial hypertension in patients carrying an ACVRL1 (ALK1) mutation. Am J Respir Crit Care Med. 2010;181:851-861

147. Taichman NS, Young S, Cruchley AT, et al. Human neutrophils secrete vascular endothelial growth factor. J Leukoc Biol. 1997;62:397-400

148. Delgoffe GM, Woo SR, Turnis ME, et al. Stability and function of regulatory T cells is maintained by a neuropilin-1-semaphorin-4a axis. Nature. 2013;501:252-256

149. Rehman J, Li J, Orschell CM, et al. Peripheral blood "endothelial progenitor cells" are derived from monocyte/macrophages and secrete angiogenic growth factors. Circulation. 2003;107:1164-1169

150. Freeman MR, Schneck FX, Gagnon ML, et al. Peripheral blood T lymphocytes and lymphocytes infiltrating human cancers express vascular endothelial growth factor: a potential role for T cells in angiogenesis. Cancer Res. 1995;55:4140-4145

151. Gabrilovich D, Ishida T, Oyama T, et al. Vascular endothelial growth factor inhibits the development of dendritic cells and dramatically affects the differentiation of multiple hematopoietic lineages in vivo. Blood. 1998;92:4150-4166

152. Ohm JE, Gabrilovich DI, Sempowski GD, et al. VEGF inhibits T-cell development and may contribute to tumor-induced immune suppression. Blood. 2003;101:4878-4886

153. Vallejo AN, Mugge LO, Klimiuk PA, et al. Central role of thrombospondin-1 in the activation and clonal expansion of inflammatory T cells. J Immunol. 2000;164:2947-2954

154. Danese S, Dejana E, Fiocchi C. Immune regulation by microvascular endothelial cells: directing innate and adaptive immunity, coagulation, and inflammation. J Immunol. 2007;178:6017-6022

155. Li MO, Wan YY, Sanjabi S, et al. Transforming growth factor-beta regulation of immune responses. Annu Rev Immunol. 2006;24:99-146

156. Brandes ME, Mai UE, Ohura K, et al. Type I transforming growth factor-beta receptors on neutrophils mediate chemotaxis to transforming growth factor-beta. J Immunol. 1991;147:1600-1606

157. Schmidt-Weber CB, Letarte M, Kunzmann S, et al. TGF-{beta} signaling of human T cells is modulated by the ancillary TGF-{beta} receptor endoglin. Int Immunol. 2005;17:921-930

158. Rokhlin OW, Cohen MB, Kubagawa H, et al. Differential expression of endoglin on fetal and adult hematopoietic cells in human bone marrow. J Immunol. 1995;154:4456-4465

159. Rossi E, Sanz-Rodriguez F, Eleno N, et al. Endothelial endoglin is involved in inflammation: role in leukocyte adhesion and transmigration. Blood. 2013;121:403-415

160. Li C, Guo B, Ding S, et al. TNF alpha down-regulates CD105 expression in vascular endothelial cells: a comparative study with TGF beta 1. Anticancer Res. 2003;23:1189-1196

161. Govani FS, Shovlin CL. Hereditary haemorrhagic telangiectasia: a clinical and scientific review. Eur J Hum Genet. 2009;17:860-871

162. Cole SG, Begbie ME, Wallace GM, et al. A new locus for hereditary haemorrhagic telangiectasia (HHT3) maps to chromosome 5. J Med Genet. 2005;42:577-582

163. Bayrak-Toydemir P, McDonald J, Akarsu N, et al. A fourth locus for hereditary hemorrhagic telangiectasia maps to chromosome 7. Am J Med Genet A. 2006;140:2155-2162

164. Torsney E, Charlton R, Diamond AG, et al. Mouse model for hereditary hemorrhagic telangiectasia has a generalized vascular abnormality. Circulation. 2003;107:1653-1657

165. Bourdeau A, Faughnan ME, McDonald ML, et al. Potential role of modifier genes influencing transforming growth factor-beta1 levels in the development of vascular defects in endoglin heterozygous mice with hereditary hemorrhagic telangiectasia. Am J Pathol. 2001;158:2011-2020

166. Bourdeau A, Cymerman U, Paquet ME, et al. Endoglin expression is reduced in normal vessels but still detectable in arteriovenous malformations of patients with hereditary hemorrhagic telangiectasia type 1. Am J Pathol. 2000;156:911-923

167. Benzinou M, Clermont FF, Letteboer TG, et al. Mouse and human strategies identify PTPN14 as a modifier of angiogenesis and hereditary haemorrhagic telangiectasia. Nat Commun. 2012;3:616

168. Jacobson BS. Hereditary hemorrhagic telangiectasia: A model for blood vessel growth and enlargement. Am J Pathol. 2000;156:737-742

169. Li DY, Sorensen LK, Brooke BS, et al. Defective angiogenesis in mice lacking endoglin. Science. 1999;284:1534-1537

170. Braverman IM, Keh A, Jacobson BS. Ultrastructure and three-dimensional organization of the telangiectases of hereditary hemorrhagic telangiectasia. J Invest Dermatol. 1990;95:422-427

171. Fernandez LA, Sanz-Rodriguez F, Blanco FJ, et al. Hereditary hemorrhagic telangiectasia, a vascular dysplasia affecting the TGF-beta signaling pathway. Clin Med Res. 2006;4:66-78

172. Hao Q, Zhu Y, Su H, et al. VEGF Induces More Severe Cerebrovascular Dysplasia in Endoglin than in Alk1 Mice. Transl Stroke Res. 2010;1:197-201

173. Panes J, Granger DN. Leukocyte-endothelial cell interactions: molecular mechanisms and implications in gastrointestinal disease. Gastroenterology. 1998;114:1066-1090

174. Danese S, Sans M, Fiocchi C. The CD40/CD40L costimulatory pathway in inflammatory bowel disease. Gut. 2004;53:1035-1043

175. Burgio VL, Fais S, Boirivant M, et al. Peripheral monocyte and naive T-cell recruitment and activation in Crohn's disease. Gastroenterology. 1995;109:1029-1038

176. Brahme F, Hildell J. Angiography in Crohn's disease revisited. AJR Am J Roentgenol. 1976;126:941-951

177. Spalinger J, Patriquin H, Miron MC, et al. Doppler US in patients with crohn disease: vessel density in the diseased bowel reflects disease activity. Radiology. 2000;217:787-791

178. Chidlow JH, Jr., Shukla D, Grisham MB, et al. Pathogenic angiogenesis in IBD and experimental colitis: new ideas and therapeutic avenues. Am J Physiol Gastrointest Liver Physiol. 2007;293:G5-G18

179. Jerkic M, Peter M, Ardelean D, et al. Dextran sulfate sodium leads to chronic colitis and pathological angiogenesis in Endoglin heterozygous mice. Inflamm Bowel Dis. 2010;16:1859-1870

180. Feagins LA. Role of transforming growth factor-beta in inflammatory bowel disease and colitis-associated colon cancer. Inflamm Bowel Dis. 2010;16:1963-1968

181. Burke JP, Watson RW, Mulsow JJ, et al. Endoglin negatively regulates transforming growth factor beta1-induced profibrotic responses in intestinal fibroblasts. Br J Surg. 2010;97:892-901

182. Monteleone G, Kumberova A, Croft NM, et al. Blocking Smad7 restores TGF-beta1 signaling in chronic inflammatory bowel disease. J Clin Invest. 2001;108:601-609

183. Perez-Gomez E, Jerkic M, Prieto M, et al. Impaired Wound Repair in Adult Endoglin Heterozygous Mice Associated with Lower NO Bioavailability. J Invest Dermatol. 2014; 134: 247–255

184. Yu JL, Rak JW, Coomber BL, et al. Effect of p53 status on tumor response to antiangiogenic therapy. Science. 2002;295:1526-1528

185. Folkman J. Looking for a good endothelial address. Cancer Cell. 2002;1:113-115

186. Hurwitz H, Fehrenbacher L, Novotny W, et al. Bevacizumab plus irinotecan, fluorouracil, and leucovorin for metastatic colorectal cancer. N Engl J Med. 2004;350:2335-2342

187. Sandler A, Gray R, Perry MC, et al. Paclitaxel-carboplatin alone or with bevacizumab for non-small-cell lung cancer. N Engl J Med. 2006;355:2542-2550

188. Yang JC, Haworth L, Sherry RM, et al. A randomized trial of bevacizumab, an anti-vascular endothelial growth factor antibody, for metastatic renal cancer. N Engl J Med. 2003;349:427-434

189. Burger RA, Brady MF, Bookman MA, et al. Incorporation of bevacizumab in the primary treatment of ovarian cancer. N Engl J Med. 2011;365:2473-2483

190. Ebos JM, Lee CR, Cruz-Munoz W, et al. Accelerated metastasis after short-term treatment with a potent inhibitor of tumor angiogenesis. Cancer Cell. 2009;15:232-239

191. Cao Y, Arbiser J, D'Amato RJ, et al. Forty-year journey of angiogenesis translational research. Sci Transl Med. 2011;3:114rv113

192. Borofsky SE, Levine MS, Rubesin SE, et al. Bevacizumab-induced perforation of the gastrointestinal tract: clinical and radiographic findings in 11 patients. Abdom Imaging. 2013;38:265-272

193. Lee SH, Mizutani N, Mizutani M, et al. Endoglin (CD105) is a target for an oral DNA vaccine against breast cancer. Cancer Immunol Immunother. 2006;55:1565-1574

194. Jarosz M, Jazowiecka-Rakus J, Cichon T, et al. Therapeutic antitumor potential of endoglin-based DNA vaccine combined with immunomodulatory agents. Gene Ther. 2013;20:262-273

195. Al-Latayfeh M, Silva PS, Sun JK, et al. Antiangiogenic therapy for ischemic retinopathies. Cold Spring Harb Perspect Med. 2012;2:a006411

196. Flieger D, Hainke S, Fischbach W. Dramatic improvement in hereditary hemorrhagic telangiectasia after treatment with the vascular endothelial growth factor (VEGF) antagonist bevacizumab. Ann Hematol. 2006;85:631-632

197. Mitchell A, Adams LA, MacQuillan G, et al. Bevacizumab reverses need for liver transplantation in hereditary hemorrhagic telangiectasia. Liver Transpl. 2008;14:210-213

198. Rohrmeier C, Sachs HG, Kuehnel TS. A retrospective analysis of low dose, intranasal injected bevacizumab (Avastin) in hereditary haemorrhagic telangiectasia. Eur Arch Otorhinolaryngol. 2012;269:531-536

199. Simonds J, Miller F, Mandel J, et al. The effect of bevacizumab (Avastin) treatment on epistaxis in hereditary hemorrhagic telangiectasia. Laryngoscope. 2009;119:988-992

200. Davidson TM, Olitsky SE, Wei JL. Hereditary hemorrhagic telangiectasia/avastin. Laryngoscope. 2010;120:432-435

201. Dupuis-Girod S, Ginon I, Saurin JC, et al. Bevacizumab in patients with hereditary hemorrhagic telangiectasia and severe hepatic vascular malformations and high cardiac output. Jama. 2012;307:948-955

202. Akman A, Yilmaz E, Mutlu H, et al. Complete remission of psoriasis following bevacizumab therapy for colon cancer. Clin Exp Dermatol. 2009;34:e202-204

203. Chidlow JH, Jr., Glawe JD, Pattillo CB, et al. VEGF(1)(6)(4) isoform specific regulation of T-cell-dependent experimental colitis in mice. Inflamm Bowel Dis. 2011;17:1501-1512

204. MacMillan CJ, Furlong SJ, Doucette CD, et al. Bevacizumab diminishes experimental autoimmune encephalomyelitis by inhibiting spinal cord angiogenesis and reducing peripheral T-cell responses. J Neuropathol Exp Neurol. 2012;71:983-999

205. Sadick H, Riedel F, Naim R, et al. Patients with hereditary hemorrhagic telangiectasia have increased plasma levels of vascular endothelial growth factor and transforming growth factor-beta1 as well as high ALK1 tissue expression. Haematologica. 2005;90:818-828

206. Sadick H, Naim R, Gossler U, et al. Angiogenesis in hereditary hemorrhagic telangiectasia: VEGF165 plasma concentration in correlation to the VEGF expression and microvessel density. International Journal of Molecular Medicine. 2005;15:15-19

207. Chidlow JH, Jr., Langston W, Greer JJ, et al. Differential angiogenic regulation of experimental colitis. Am J Pathol. 2006;169:2014-2030

208. Bousvaros A, Leichtner A, Zurakowski D, et al. Elevated serum vascular endothelial growth factor in children and young adults with Crohn's disease. Dig Dis Sci. 1999;44:424-430

209. Kanazawa S, Tsunoda T, Onuma E, et al. VEGF, basic-FGF, and TGF-beta in Crohn's disease and ulcerative colitis: a novel mechanism of chronic intestinal inflammation. Am J Gastroenterol. 2001;96:822-828

210. Griga T, Voigt E, Gretzer B, et al. Increased production of vascular endothelial growth factor by intestinal mucosa of patients with inflammatory bowel disease. Hepatogastroenterology. 1999;46:920-923

211. Tolstanova G, Khomenko T, Deng X, et al. Neutralizing anti-vascular endothelial growth factor (VEGF) antibody reduces severity of experimental ulcerative colitis in rats: direct evidence for the pathogenic role of VEGF. J Pharmacol Exp Ther. 2009;328:749-757

212. Shovlin CL. Hereditary haemorrhagic telangiectasia: pathophysiology, diagnosis and treatment. Blood Rev. 2010;24:203-219

213. Dupuis-Girod S, Bailly S, Plauchu H. Hereditary hemorrhagic telangiectasia: from molecular biology to patient care. J Thromb Haemost. 2010;8:1447-1456

214. Abdalla SA, Letarte M. Hereditary haemorrhagic telangiectasia: current views on genetics and mechanisms of disease. J Med Genet. 2006;43:97-110

215. Girerd B, Montani D, Coulet F, et al. Clinical outcomes of pulmonary arterial hypertension in patients carrying an ACVRL1 (ALK1) mutation. Am J Respir Crit Care Med. 2010;181:851-861

216. Mache CJ, Gamillscheg A, Popper HH, et al. Early-life pulmonary arterial hypertension with subsequent development of diffuse pulmonary arteriovenous malformations in hereditary haemorrhagic telangiectasia type 1. Thorax. 2008;63:85-86

217. Blanco FJ, Santibanez JF, Guerrero-Esteo M, et al. Interaction and functional interplay between endoglin and ALK-1, two components of the endothelial transforming growth factor-beta receptor complex. J Cell Physiol. 2005;204:574-584

218. David L, Mallet C, Mazerbourg S, et al. Identification of BMP9 and BMP10 as functional activators of the orphan activin receptor-like kinase 1 (ALK1) in endothelial cells. Blood. 2007;109:1953-1961

219. Lebrin F, Goumans MJ, Jonker L, et al. Endoglin promotes endothelial cell proliferation and TGF-beta/ALK1 signal transduction. Embo J. 2004;23:4018-4028

220. Oh SP, Seki T, Goss KA, et al. Activin receptor-like kinase 1 modulates transforming growth factor-beta 1 signaling in the regulation of angiogenesis. Proc Natl Acad Sci U S A. 2000;97:2626-2631

221. Lamouille S, Mallet C, Feige JJ, et al. Activin receptor-like kinase 1 is implicated in the maturation phase of angiogenesis. Blood. 2002;100:4495-4501

222. Pardali E, Goumans MJ, ten Dijke P. Signaling by members of the TGF-beta family in vascular morphogenesis and disease. Trends Cell Biol. 2010;20:556-567

223. Bourdeau A, Faughnan ME, Letarte M. Endoglin-deficient mice, a unique model to study hereditary hemorrhagic telangiectasia. Trends Cardiovasc Med. 2000;10:279-285

224. Srinivasan S, Hanes MA, Dickens T, et al. A mouse model for hereditary hemorrhagic telangiectasia (HHT) type 2. Hum Mol Genet. 2003;12:473-482

225. Mahmoud M, Allinson KR, Zhai Z, et al. Pathogenesis of arteriovenous malformations in the absence of endoglin. Circ Res. 2010;106:1425-1433

226. Jerkic M, Sotov V, Letarte M. Oxidative stress contributes to endothelial dysfunction in mouse models of hereditary hemorrhagic telangiectasia. Oxid Med Cell Longev. 2012;2012:686972

227. Toporsian M, Jerkic M, Zhou YQ, et al. Spontaneous adult-onset pulmonary arterial hypertension attributable to increased endothelial oxidative stress in a murine model of hereditary hemorrhagic telangiectasia. Arterioscler Thromb Vasc Biol. 2010;30:509-517

228. Jerkic M, Kabir MG, Davies A, et al. Pulmonary hypertension in adult Alk1 heterozygous mice due to oxidative stress. Cardiovasc Res. 2011;92:375-384

229. Hlatky L, Hahnfeldt P, Folkman J. Clinical application of antiangiogenic therapy: microvessel density, what it does and doesn't tell us. J Natl Cancer Inst. 2002;94:883-893

230. Bourdeau A, Cymerman U, Paquet ME, et al. Endoglin expression is reduced in normal vessels but still detectable in arteriovenous malformations of patients with hereditary hemorrhagic telangiectasia type 1. Am J Pathol. 2000;156:911-923

231. Rinaldi M, Buscarini E, Danesino C, et al. Ocular manifestations in hereditary hemorrhagic telangiectasia (Rendu-Osler-Weber disease): a case-series. Ophthalmic Genet. 2011;32:12-17

232. Hao Q, Zhu Y, Su H, et al. VEGF Induces More Severe Cerebrovascular Dysplasia in Endoglin than in Alk1 Mice. Transl Stroke Res. 2010;1:197-201

233. Kerbel RS. Tumor angiogenesis. N Engl J Med. 2008;358:2039-2049

234. Mitchell A, Adams LA, MacQuillan G, et al. Bevacizumab reverses need for liver transplantation in hereditary hemorrhagic telangiectasia. Liver Transpl. 2008;14:210-213

235. Bose P, Holter JL, Selby GB. Bevacizumab in hereditary hemorrhagic telangiectasia. N Engl J Med. 2009;360:2143-2144

236. Dupuis-Girod S, Ginon I, Saurin JC, et al. Bevacizumab in patients with hereditary hemorrhagic telangiectasia and severe hepatic vascular malformations and high cardiac output. JAMA. 2012;307:948-955

237. Pettersson A, Nagy JA, Brown LF, et al. Heterogeneity of the angiogenic response induced in different normal adult tissues by vascular permeability factor/vascular endothelial growth factor. Lab Invest. 2000;80:99-115

238. Liang WC, Wu X, Peale FV, et al. Cross-species vascular endothelial growth factor (VEGF)-blocking antibodies completely inhibit the growth of human tumor xenografts and measure the contribution of stromal VEGF. J Biol Chem. 2006;281:951-961

239. Foster FS, Hossack J, Adamson SL. Micro-ultrasound for preclinical imaging. Interface Focus. 2011;1:576-601

240. Atreya R, Mudter J, Finotto S, et al. Blockade of interleukin 6 trans signaling suppresses T-cell resistance against apoptosis in chronic intestinal inflammation: evidence in crohn disease and experimental colitis in vivo. Nat Med. 2000;6:583-588

241. Guignabert C, Alvira CM, Alastalo TP, et al. Tie2-mediated loss of peroxisome proliferator-activated receptor-gamma in mice causes PDGF receptor-beta-dependent pulmonary arterial muscularization. Am J Physiol Lung Cell Mol Physiol. 2009;297:L1082-1090

242. Pece-Barbara N, Vera S, Kathirkamathamby K, et al. Endoglin null endothelial cells proliferate faster and are more responsive to transforming growth factor beta1 with higher affinity receptors and an activated Alk1 pathway. J. Biol. Chem. 2005;280:27800-27808

243. Loupakis F, Falcone A, Masi G, et al. Vascular endothelial growth factor levels in immunodepleted plasma of cancer patients as a possible pharmacodynamic marker for bevacizumab activity. J Clin Oncol. 2007;25:1816-1818

244. Baffert F, Thurston G, Rochon-Duck M, et al. Age-related changes in vascular endothelial growth factor dependency and angiopoietin-1-induced plasticity of adult blood vessels. Circ Res. 2004;94:984-992

245. Lawler PR, Lawler J. Molecular basis for the regulation of angiogenesis by thrombospondin-1 and -2. Cold Spring Harb Perspect Med. 2012;2:a006627

246. Park S, Dimaio TA, Liu W, et al. Endoglin Regulates the Activation and Quiescence of Endothelium by Participating in Canonical and Non-Canonical TGF-beta Signaling Pathways. J Cell Sci. 2013

247. Shao ES, Lin L, Yao Y, et al. Expression of vascular endothelial growth factor is coordinately regulated by the activin-like kinase receptors 1 and 5 in endothelial cells. Blood. 2009;114:2197-2206

248. Choi EJ, Walker EJ, Shen F, et al. Minimal homozygous endothelial deletion of eng with VEGF stimulation is sufficient to cause cerebrovascular dysplasia in the adult mouse. Cerebrovasc Dis. 2012;33:540-547

249. Walker EJ, Su H, Shen F, et al. Bevacizumab Attenuates VEGF-Induced Angiogenesis and Vascular Malformations in the Adult Mouse Brain. Stroke. 2012;43:1925-1930

250. Taraseviciene-Stewart L, Kasahara Y, Alger L, et al. Inhibition of the VEGF receptor 2 combined with chronic hypoxia causes cell death-dependent pulmonary endothelial cell proliferation and severe pulmonary hypertension. Faseb J. 2001;15:427-438

251. Rose A, Grandoch M, vom Dorp F, et al. Stimulatory effects of the multi-kinase inhibitor sorafenib on human bladder cancer cells. Br J Pharmacol. 2010;160:1690-1698

252. Conery AR, Cao Y, Thompson EA, et al. Akt interacts directly with Smad3 to regulate the sensitivity to TGF-beta induced apoptosis. Nat Cell Biol. 2004;6:366-372

253. Jimenez B, Volpert OV, Crawford SE, et al. Signals leading to apoptosis-dependent inhibition of neovascularization by thrombospondin-1. Nat Med. 2000;6:41-48

254. Ochoa CD, Yu L, Al-Ansari E, et al. Thrombospondin-1 null mice are resistant to hypoxia-induced pulmonary hypertension. J Cardiothorac Surg. 2010;5:32

255. Greenaway J, Lawler J, Moorehead R, et al. Thrombospondin-1 inhibits VEGF levels in the ovary directly by binding and internalization via the low density lipoprotein receptor-related protein-1 (LRP-1). J Cell Physiol. 2007;210:807-818

256. Kaur S, Martin-Manso G, Pendrak ML, et al. Thrombospondin-1 inhibits VEGF receptor-2 signaling by disrupting its association with CD47. J Biol Chem. 2010;285:38923-38932

257. Guo N, Krutzsch HC, Inman JK, et al. Thrombospondin 1 and type I repeat peptides of thrombospondin 1 specifically induce apoptosis of endothelial cells. Cancer Res. 1997;57:1735-1742

258. Kumpers P, Nickel N, Lukasz A, et al. Circulating angiopoietins in idiopathic pulmonary arterial hypertension. Eur Heart J. 2010;31:2291-2300

259. Fiedler U, Augustin HG. Angiopoietins: a link between angiogenesis and inflammation. Trends Immunol. 2006;27:552-558

260. Lobov IB, Brooks PC, Lang RA. Angiopoietin-2 displays VEGF-dependent modulation of capillary structure and endothelial cell survival in vivo. Proc Natl Acad Sci U S A. 2002;99:11205-11210

261. Cao Y, Sonveaux P, Liu S, et al. Systemic overexpression of angiopoietin-2 promotes tumor microvessel regression and inhibits angiogenesis and tumor growth. Cancer Res. 2007;67:3835-3844

262. Zhang L, Yang N, Park JW, et al. Tumor-derived vascular endothelial growth factor up-regulates angiopoietin-2 in host endothelium and destabilizes host vasculature, supporting angiogenesis in ovarian cancer. Cancer Res. 2003;63:3403-3412

263. DeLeve LD, Wang X, Hu L, et al. Rat liver sinusoidal endothelial cell phenotype is maintained by paracrine and autocrine regulation. Am J Physiol Gastrointest Liver Physiol. 2004;287:G757-763

264. Baffert F, Le T, Sennino B, et al. Cellular changes in normal blood capillaries undergoing regression after inhibition of VEGF signaling. Am J Physiol Heart Circ Physiol. 2006;290:H547-559

265. Kamba T, Tam BY, Hashizume H, et al. VEGF-dependent plasticity of fenestrated capillaries in the normal adult microvasculature. Am J Physiol Heart Circ Physiol. 2006;290:H560-576

266. Mejias M, Garcia-Pras E, Tiani C, et al. Beneficial effects of sorafenib on splanchnic, intrahepatic, and portocollateral circulations in portal hypertensive and cirrhotic rats. Hepatology. 2009;49:1245-1256

267. Fernandez M, Vizzutti F, Garcia-Pagan JC, et al. Anti-VEGF receptor-2 monoclonal antibody prevents portal-systemic collateral vessel formation in portal hypertensive mice. Gastroenterology. 2004;126:886-894

268. Korsisaari N, Kasman IM, Forrest WF, et al. Inhibition of VEGF-A prevents the angiogenic switch and results in increased survival of Apc+/min mice. Proc Natl Acad Sci U S A. 2007;104:10625-10630

269. Belcik JT, Qi Y, Kaufmann BA, et al. Cardiovascular and Systemic MicrovascularEffects of Anti-Vascular Endothelial Growth Factor Therapy for Cancer. J Am Coll Cardiol. 2012;60:618-625

270. Clauss M, Gerlach M, Gerlach H, et al. Vascular permeability factor: a tumor-derived polypeptide that induces endothelial cell and monocyte procoagulant activity, and promotes monocyte migration. J Exp Med. 1990;172:1535-1545

271. Barleon B, Sozzani S, Zhou D, et al. Migration of human monocytes in response to vascular endothelial growth factor (VEGF) is mediated via the VEGF receptor flt-1. Blood. 1996;87:3336-3343

272. Gougos A, Letarte M. Identification of a human endothelial cell antigen with monoclonal antibody 44G4 produced against a pre-B leukemic cell line. J Immunol. 1988;141:1925-1933

273. Rychak JJ, Graba J, Cheung AM, et al. Microultrasound molecular imaging of vascular endothelial growth factor receptor 2 in a mouse model of tumor angiogenesis. Mol Imaging. 2007;6:289-296

274. Van der Sluis M, De Koning BA, De Bruijn AC, et al. Muc2-deficient mice spontaneously develop colitis, indicating that MUC2 is critical for colonic protection. Gastroenterology. 2006;131:117-129

275. Hlatky L, Hahnfeldt P, Folkman J. Clinical application of antiangiogenic therapy: microvessel density, what it does and doesn't tell us. J Natl Cancer Inst. 2002;94:883-893

276. Ardelean DS, Jerkic M, Yin M, et al. Endoglin and activin receptor-like kinase 1 heterozygous mice have a distinct pulmonary and hepatic angiogenic profile and response to anti-VEGF treatment. Angiogenesis. 2014;17:129-46

277. Shigematsu T, Specian RD, Wolf RE, et al. MAdCAM mediates lymphocyte-endothelial cell adhesion in a murine model of chronic colitis. Am J Physiol Gastrointest Liver Physiol. 2001;281:G1309-1315

278. Metcalf D. The granulocyte-macrophage colony-stimulating factors. Science. 1985;229:16-22

279. Demetri GD, Griffin JD. Granulocyte colony-stimulating factor and its receptor. Blood. 1991;78:2791-2808

280. Deshmane SL, Kremlev S, Amini S, et al. Monocyte chemoattractant protein-1 (MCP-1): an overview. J Interferon Cytokine Res. 2009;29:313-326

281. Khan WI, Motomura Y, Wang H, et al. Critical role of MCP-1 in the pathogenesis of experimental colitis in the context of immune and enterochromaffin cells. Am J Physiol Gastrointest Liver Physiol. 2006;291:G803-811

282. Shao J, Sheng H. Amphiregulin promotes intestinal epithelial regeneration: roles of intestinal subepithelial myofibroblasts. Endocrinology. 2010;151:3728-3737

283. Zhou Y, Lee JY, Lee CM, et al. Amphiregulin, an epidermal growth factor receptor ligand, plays an essential role in the pathogenesis of transforming growth factor-beta-induced pulmonary fibrosis. J Biol Chem. 2012;287:41991-42000

284. Zaiss DM, van Loosdregt J, Gorlani A, et al. Amphiregulin enhances regulatory T cell-suppressive function via the epidermal growth factor receptor. Immunity. 2013;38:275-284

285. Kanayama M, Takahara T, Yata Y, et al. Hepatocyte growth factor promotes colonic epithelial regeneration via Akt signaling. Am J Physiol Gastrointest Liver Physiol. 2007;293:G230-239

286. Ido A, Numata M, Kodama M, et al. Mucosal repair and growth factors: recombinant human hepatocyte growth factor as an innovative therapy for inflammatory bowel disease. J Gastroenterol. 2005;40:925-931

287. Oh K, Iimuro Y, Takeuchi M, et al. Ameliorating effect of hepatocyte growth factor on inflammatory bowel disease in a murine model. Am J Physiol Gastrointest Liver Physiol. 2005;288:G729-735

288. Kallincos NC, Xian CJ, Dunbar AJ, et al. Cloning of rat betacellulin and characterization of its expression in the gastrointestinal tract. Growth Factors. 2000;18:203-213

289. Kulkarni AB, Huh CG, Becker D, et al. Transforming growth factor beta 1 null mutation in mice causes excessive inflammatory response and early death. Proc Natl Acad Sci U S A. 1993;90:770-774

290. Briskin M, Winsor-Hines D, Shyjan A, et al. Human mucosal addressin cell adhesion molecule-1 is preferentially expressed in intestinal tract and associated lymphoid tissue. Am J Pathol. 1997;151:97-110

291. Farkas S, Hornung M, Sattler C, et al. Blocking MAdCAM-1 in vivo reduces leukocyte extravasation and reverses chronic inflammation in experimental colitis. Int J Colorectal Dis. 2006;21:71-78

292. Bachmann C, Klibanov AL, Olson TS, et al. Targeting mucosal addressin cellular adhesion molecule (MAdCAM)-1 to noninvasively image experimental Crohn's disease. Gastroenterology. 2006;130:8-16

293. Vermeire S, Ghosh S, Panes J, et al. The mucosal addressin cell adhesion molecule antibody PF-00547,659 in ulcerative colitis: a randomised study. Gut. 2011;60:1068-1075

294. Scaldaferri F, Vetrano S, Sans M, et al. VEGF-A links angiogenesis and inflammation in inflammatory bowel disease pathogenesis. Gastroenterology. 2009;136:585-595 e585

295. Chernoguz A, Crawford K, Vandersall A, et al. Pretreatment with anti-VEGF therapy may exacerbate inflammation in experimental acute colitis. J Pediatr Surg. 2012;47:347-354

296. Goessling W, Mayer RJ. Systemic treatment of patients who have colorectal cancer and inflammatory bowel disease. Gastroenterol Clin North Am. 2006;35:713-727

297. Ina K, Kusugami K, Hosokawa T, et al. Increased mucosal production of granulocyte colony-stimulating factor is related to a delay in neutrophil apoptosis in Inflammatory Bowel disease. J Gastroenterol Hepatol. 1999;14:46-53

298. McAlindon ME, Hawkey CJ, Mahida YR. Expression of interleukin 1 beta and interleukin 1 beta converting enzyme by intestinal macrophages in health and inflammatory bowel disease. Gut. 1998;42:214-219

299. Ludwiczek O, Vannier E, Borggraefe I, et al. Imbalance between interleukin-1 agonists and antagonists: relationship to severity of inflammatory bowel disease. Clin Exp Immunol. 2004;138:323-329

300. Nemetz A, Nosti-Escanilla MP, Molnar T, et al. IL1B gene polymorphisms influence the course and severity of inflammatory bowel disease. Immunogenetics. 1999;49:527-531

301. Guimbaud R, Bertrand V, Chauvelot-Moachon L, et al. Network of inflammatory cytokines and correlation with disease activity in ulcerative colitis. Am J Gastroenterol. 1998;93:2397-2404

302. Sunderkotter C, Steinbrink K, Goebeler M, et al. Macrophages and angiogenesis. J Leukoc Biol. 1994;55:410-422

303. Mahida YR. The key role of macrophages in the immunopathogenesis of inflammatory bowel disease. Inflamm Bowel Dis. 2000;6:21-33

304. Naito Y, Takagi T, Uchiyama K, et al. Reduced intestinal inflammation induced by dextran sodium sulfate in interleukin-6-deficient mice. Int J Mol Med. 2004;14:191-196

305. Sander LE, Obermeier F, Dierssen U, et al. Gp130 signaling promotes development of acute experimental colitis by facilitating early neutrophil/macrophage recruitment and activation. J Immunol. 2008;181:3586-3594

306. Voronov E, Shouval DS, Krelin Y, et al. IL-1 is required for tumor invasiveness and angiogenesis. Proc Natl Acad Sci U S A. 2003;100:2645-2650

307. Holzinger C, Weissinger E, Zuckermann A, et al. Effects of interleukin-1, -2, -4, -6, interferon-gamma and granulocyte/macrophage colony stimulating factor on human vascular endothelial cells. Immunol Lett. 1993;35:109-117

308. Natori T, Sata M, Washida M, et al. G-CSF stimulates angiogenesis and promotes tumor growth: potential contribution of bone marrow-derived endothelial progenitor cells. Biochem Biophys Res Commun. 2002;297:1058-1061

309. Miyake M, Goodison S, Urquidi V, et al. Expression of CXCL1 in human endothelial cells induces angiogenesis through the CXCR2 receptor and the ERK1/2 and EGF pathways. Lab Invest. 2013;93:768-778

310. Niu J, Azfer A, Zhelyabovska O, et al. Monocyte chemotactic protein (MCP)-1 promotes angiogenesis via a novel transcription factor, MCP-1-induced protein (MCPIP). J Biol Chem. 2008;283:14542-14551

311. Kudo T, Matsumoto T, Nakamichi I, et al. Recombinant human granulocyte colony-stimulating factor reduces colonic epithelial cell apoptosis and ameliorates murine dextran sulfate sodium-induced colitis. Scand J Gastroenterol. 2008;43:689-697

312. Dejaco C, Lichtenberger C, Miehsler W, et al. An open-label pilot study of granulocyte colony-stimulating factor for the treatment of severe endoscopic postoperative recurrence in Crohn's disease. Digestion. 2003;68:63-70

313. Korzenik JR, Dieckgraefe BK. An open-labelled study of granulocyte colony-stimulating factor in the treatment of active Crohn's disease. Aliment Pharmacol Ther. 2005;21:391-400

314. Zhong C, Qu X, Tan M, et al. Characterization and regulation of bv8 in human blood cells. Clin Cancer Res. 2009;15:2675-2684

315. Shojaei F, Wu X, Qu X, et al. G-CSF-initiated myeloid cell mobilization and angiogenesis mediate tumor refractoriness to anti-VEGF therapy in mouse models. Proc Natl Acad Sci U S A. 2009;106:6742-6747

316. Kapur NK, Wilson S, Yunis AA, et al. Reduced endoglin activity limits cardiac fibrosis and improves survival in heart failure. Circulation. 2012;125:2728-2738

317. Lobov IB, Brooks PC, Lang RA. Angiopoietin-2 displays VEGF-dependent modulation of capillary structure and endothelial cell survival in vivo. Proc Natl Acad Sci U S A. 2002;99:11205-11210

318. Harfouche R, Hussain SN. Signaling and regulation of endothelial cell survival by angiopoietin-2. Am J Physiol Heart Circ Physiol. 2006;291:H1635-1645

319. Jerkic M, Kabir MG, Davies A, et al. Pulmonary hypertension in adult Alk1 heterozygous mice due to oxidative stress. Cardiovasc Res. 2011;92:375-384

320. Kumpers P, Nickel N, Lukasz A, et al. Circulating angiopoietins in idiopathic pulmonary arterial hypertension. Eur Heart J. 2010;31:2291-2300

321. Jimenez B, Volpert OV, Crawford SE, et al. Signals leading to apoptosis-dependent inhibition of neovascularization by thrombospondin-1. Nat Med. 2000;6:41-48

322. Roland CL, Dineen SP, Lynn KD, et al. Inhibition of vascular endothelial growth factor reduces angiogenesis and modulates immune cell infiltration of orthotopic breast cancer xenografts. Mol Cancer Ther. 2009;8:1761-1771

323. Ozao-Choy J, Ma G, Kao J, et al. The novel role of tyrosine kinase inhibitor in the reversal of immune suppression and modulation of tumor microenvironment for immune-based cancer therapies. Cancer Res. 2009;69:2514-2522

324. Phan VT, Wu X, Cheng JH, et al. Oncogenic RAS pathway activation promotes resistance to anti-VEGF therapy through G-CSF-induced neutrophil recruitment. Proc Natl Acad Sci U S A. 2013;110:6079-6084